Report A001AE

UNIVERSAL VIRUS ADSORPTION ON INERT PARTICLES UTILIZING THE COATED LATEX ADSORPTION METHOD (CLAM)

Gokaldas C. Parikh
Thomas C. Sorensen
and Gilbert C. K. Ho
South Dakota State University
Brookings, South Dakota 57006

30 June 1975

Final Technical Report for Period 1 July 1972 - 30 June 1975

Prepared for
Office of Naval Research
800 N Quincy Street
Arlington, Va. 22217

Office of Naval Research
Elliot Hall
Minneapolis, Minnesota 55455

MICROBIOLOGY DEPARTMENT
Dairy-Microbiology Bldg. (605)688-4116
South Dakota State University
Brookings, S D 57006

May 26, 1976

J. E. Candiff
Defense Documentation Center
Cameron Station
Alexandria, Virginia 22314

Dear Sir:

Thank you for your call on May 17 concerning a missing page from the ONR Report A001AE, Universal Virus Adsorption on Inert Particles Utilizing the Coated Latex Adsorption Method (CLAM), submitted by Dr. G. C. Parikh, June 30, 1975.

We were able to locate page 325, but it appears that a page 324 does not exist. Richard Fulker, Dr. Parikh's former research assistant, stated that apparently the pages were misnumbered. There does not appear to be any more missing information.

We have enclosed a copy of page 325. This should make your report complete.

Sincerely,

B. Myers

Mrs. Bunny Myers
Administrative Secretary

Enclosure

SECURITY CLASSIFICATION OF THIS PAGE (When Data Entered)

REPORT DOCUMENTATION PAGE

READ INSTRUCTIONS BEFORE COMPLETING FORM

1. REPORT NUMBER: A001AE	2. GOVT ACCESSION NO.
3. RECIPIENT'S CATALOG NUMBER	
4. TITLE (and Subtitle): UNIVERSAL VIRUS ADSORPTION ON INERT PARTICLES UTILIZING THE COATED LATEX ADSORPTION METHOD (CLAM)	5. TYPE OF REPORT & PERIOD COVERED: Final report, 1 Jul [redacted]72 - 30 Jun [redacted]975
	6. PERFORMING ORG. REPORT NUMBER
7. AUTHOR(s): Gokaldas C. Parikh, Thomas C. Sorensen, Gilbert C. K. Ho	8. CONTRACT OR GRANT NUMBER(s): N00014-73-C-0084
9. PERFORMING ORGANIZATION NAME AND ADDRESS: South Dakota State University, Brookings, South Dakota	10. PROGRAM ELEMENT, PROJECT, TASK AREA & WORK UNIT NUMBERS: NR136-952
11. CONTROLLING OFFICE NAME AND ADDRESS: Office of Naval Research, Microbiology Program / Code 443, Arlington, Virginia 22217	12. REPORT DATE: 30 Jun [redacted]975
	13. NUMBER OF PAGES: 335
14. MONITORING AGENCY NAME & ADDRESS (if different from Controlling Office): Same as Block 11	15. SECURITY CLASS. (of this report): Unclassified
	15a. DECLASSIFICATION/DOWNGRADING SCHEDULE

16. DISTRIBUTION STATEMENT (of this Report)

This document has been approved for public release; its distribution is unlimited.

17. DISTRIBUTION STATEMENT (of the abstract entered in Block 20, if different from Report)

18. SUPPLEMENTARY NOTES

19. KEY WORDS (Continue on reverse side if necessary and identify by block number)

Adsorption	Assays	CLAM Particle
Agglutination	Coated Latex Adsorption Method (CLAM)	Enterotoxin B
Antibody	Concanavalin A	Image Analysis
Antigen	Coulter Counter	Immune Response

20. ABSTRACT (Continue on reverse side if necessary and identify by block number)

Development and instrumentation of a rapid method of virus and viral antibody detection and identification utilizing the Coated Latex Adsorption Method (CLAM) is presented. Comprised of an inert latex particle "carrier", adsorbing antibody, and detected virus or antibody, the classic CLAM particle may now be classified into two major types (in vitro and in vivo).

The in vitro CLAM particle was developed because of the ability of monodispersed latex particles to adsorb, in vitro, a variety of substances (i.e. viral and bacterial antibody, enterotoxin B, virus particles, bacterial and

DD FORM 1 JAN 73 1473 EDITION OF 1 NOV 68 IS OBSOLETE S/N 0102-014-6601

SECURITY CLASSIFICATION OF THIS PAGE (When Data Entered)

Block 19 continued

Computer Model, in vitro
Computer Model, in vivo
Iodine-125
Kinetics
Latex
Particle Agglutination
Radioimmunoassay
Radioiodination
Virus
Virus Detection

Block 20 continued

subsequently react with its biologically significant counterpart (i.e. virus or bacteria, antitoxin, viral or bacterial antibody) to produce a complex which could be quickly detected within one minute using present day instrument technology. In modifying the components of the CLAM particle and using radioiodine tagging methods, detection and quantitation of the complex has been possible by radioimmunoassay techniques. Additionally, adsorption and latex aggregate formation has been monitored by a Coulter Counter model F for cross correlation with radioisotopic methods. A CLAM particle standard system using Concanavalin A (literature survey included) as adsorbant has allowed formulation of a completely defined and controllable CLAM particle, from which dynamics of adsorbant effect may be determined in either small increments of latex adsorption, or large increments, which lead to latex aggregation formation. Simulated image analysis by a closed circuit television linked with minicomputer has permitted extraction of basic information of latex aggregate area, length, perimeter, etc. with subsequent identification and classification of the aggregate. The image may be stored on magnetic tape and reconstructed for later referral. Energy kinetics of the antigen-antibody reaction as applicable to the CLAM detection system are presented, with equations defined for association, dissociation, and equilibrium phenomena of the antigen-antibody complex.

The in vivo CLAM particle retains the basic descriptive properties of the in vitro particle except that it is applied directly to a living host system by various routes of innoculation. By locating at sites of antibody production, the particle acts as tracer, locator, and quantitator of a variety of dynamic biological processes within the host and can thus permit, for example, determination of the earliest possible time of antibody detection after infection.

A history, with bibliography, in addition to appropriate equations and conceptual model building blocks based on rates of immunological phenomena are presented. Two proposed dynamic and predictive in vitro and in vivo computer-mediated models of the CLAM detection system are also introduced. Computer programs written for an 8-K read-write memory Hewlett-Packard model 9830A programmable calculator and used in the report are listed in the Appendix.

TABLE OF CONTENTS

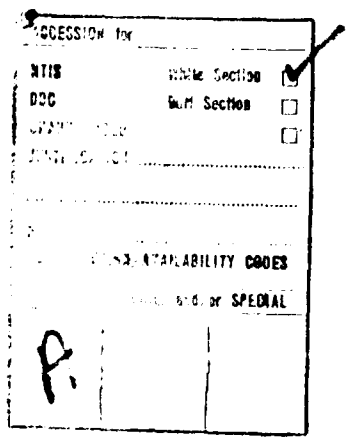

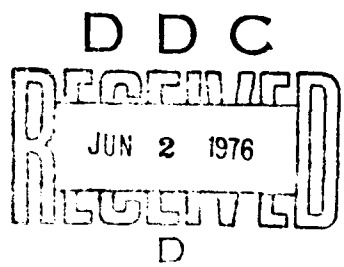

INTRODUCTION

Methods now used to detect and identify viruses, virus-specific antibodies, and concanavalin A employ tissue culture cells, laboratory animals, chemical reactions, or routine serological blood tests; these methods require extensive time for sample preparation and testing and give irregular results due to biological variability and instability associated with living systems. No universal method for detecting and identifying microorganisms exists which is rapid, sensitive, specific, and economical.

Development and instrumentation of a rapid method of virus and viral antibody detection and identification utilizing the Coated Latex Adsorption Method (CLAM) has therefore been investigated and the findings documented in this report. The report has been divided into two broad areas: (1) CLAM method employing the Coulter Counter and (2) approaches in in vivo CLAM modeling. The second area has been accepted as fulfilling the requirements for a master's thesis.

The CLAM method utilizes latex carrier particles which are inert to most chemicals and thus have a much longer shelf life than those biologicals used in existing methods. Additionally, the cost of maintaining expensive laboratory tissue cultures and biologicals, laboratory animals, and associated instruments, equipment, and rearing facilities may be eliminated. Time required for detection and identification is much shorter than with conventional methods and may be reduced to minutes as compared with days which are required for some techniques. The process is as sensitive and specific as present methods and in most cases actually surpasses acceptable sensitivity and specificity limits. Adaptation of the process to other substances which may be adsorbed to the particle surface expand the capabilities to detection and identification of such adsorbents as bacteria, bacteria-specific antibodies, hormones, enzymes, nucleic acids, toxins, and lipids.

Any carrier particle which maintains its uniform size such as bentonite, glass beads, acryl particles, other forms of latex, etc. may be substituted for the polyvinyltoluene latex particle used in the examples. Also, any particle counter which operates principally by measuring the volume of particles may be substituted for the Coulter Counter model F. Sonification of the particles to assure that the maximum number of single particles are present in a particle suspension may be substituted by any other method, provided that a major population of uniform-sized monomers may be obtained. In the examples presented, virus, antibody, and concanavalin A are adsorbed to the carrier particle surface. Other adsorbents, if they can be attached to the particle surface, may be substituted with equal success of the process. Additionally, rather than using volume displacement as a mechanism of detection, a radioisotope (I^{125}) may be used to measure the CLAM particles by radioimmunoassay.

The Coated Latex Adsorption Method (CLAM) utilized for this study was developed under the theory that monodispersed latex particles (polyvinyltoluene) would adsorb certain substances. One such substance was the viral antibody. With the antibody adsorbed to the latex, the antibody and antigen (or virus) would form a complex, causing the virus to adsorb to the latex. The antigen-antibody complex would precipitate if the antigen was soluble, or agglutinate if it was cellular. The latex particle could therefore be substituted for the red blood cell (RBC) in traditional hemagglutination tests. Not only would the integrity of the reaction be upheld, but specificity could also be included in the resulting agglutination.

The basic particle (Fig. 1) utilized virus adsorbed to an antibody-coated latex particle. The coating material of virus-specific antibody, stable at room temperature, was selected because it exerted the highest known specificity for its reaction with the virus. Furthermore, the antibody molecules enhanced rapid attachment of virus particles to latex and thus provided a system for quick read out.

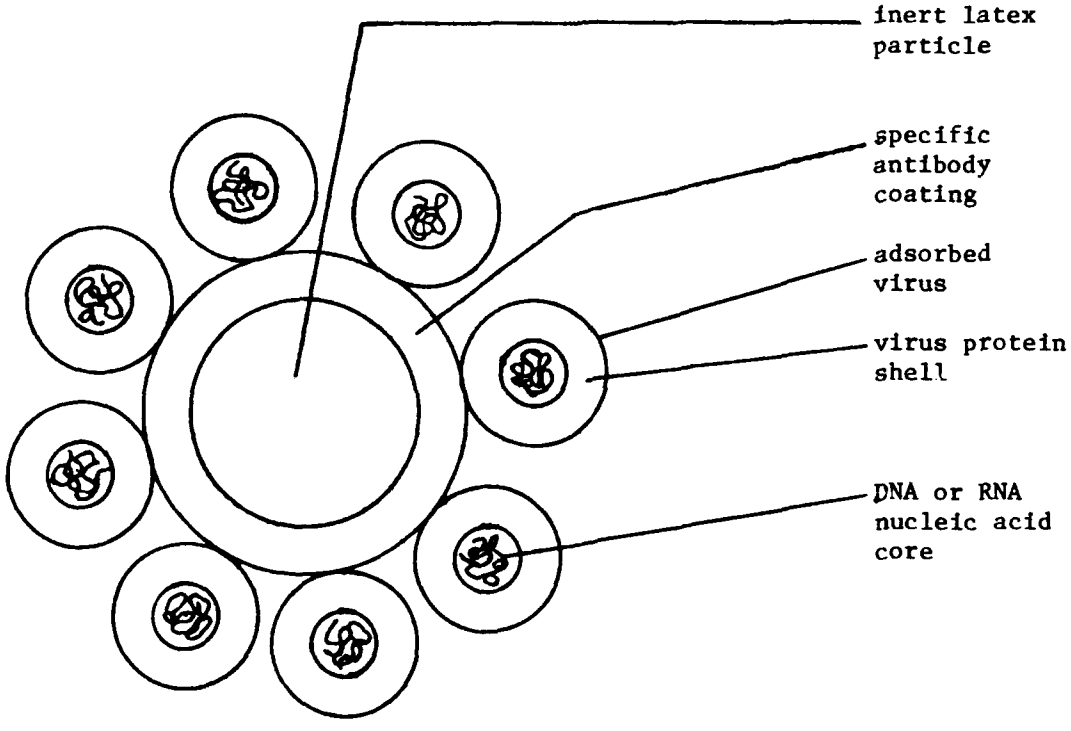

Fig. 1 . CLAM particle

Modification of the CLAM particle by using various antibody coatings and antigens in addition to tagging the components with a radioisotope allowed for identification and quantification. Radioactive iodine was chosen for the labeling of the materials to be detected and compared because of its ability to bond to tyrosine and sulfur-containing amino acids in a chemical oxidation process.

Initially, the CLAM system of virus detection showed that affective amounts of virus and/or antibody were adsorbed to the latex surface. Studies of the interaction which occurred between latex and the adsorbing material produced repeatable and consistent indications that latex was adsorbing in a predictable manner. The major approach of detecting gross change of the latex particle as induced by the adsorbing material, was to look for the production of a latex aggregate. Originally this was performed manually, using a Petroff-Hausser counting chamber.

Preliminary experimentation with approximately 2 X 10^4 pfu (plaque-forming unit) of Epizootic hemorrhagic disease, South Dakota strain, (EHD SD #10) and 2 X 10^4 pfu of Eastern-equine encephalitis (EEE) produced aggregation of 1.011 um polystyrene latex-likewise, 0.05 ml of 1 X $10^{5.3}$ pfu/0.2 ml Western equine encephalitis (WEE) agglutinated 1.011 um polystyrene latex. (2-1-72 - 6-30-72)

Indications that large numbers of samples would be required for an extensive study of the phenomenon led the investigators to utilize a Coulter Counter Coulter Electronics, Hialeah, Florida), and instrument originally designed to count red and white blood cells. After preliminary experimentation with the counter, it was concluded that this would be the best method available to us to investigate any change in the latex suspension, especially those changes which produced latex aggregation formation.

Using viruses, antibodies and latex prepared in the manner as given in a previous report (2-1-70 - 1-31-71) a characteristic principle of the agglutination phenomenon as detected with a Coulter Counter was defined.

For example plotting data (normal latex) obtained on the Coulter Counter, an expected decrease in raw count as threshold value was increased was observed (Fig. 2). However, when the difference in raw counts at succeeding threshold values was plotted, a series of "hills and valleys" occurred. The differential hills of the curve indicated various size aggregates of latex At lower threshold values, nearly all particles were counted. As the threshold value was increased, the total count decreased, but a continuation of the hills and valleys phenomen did remain. To utilize the maximum number of

Figure 2. Control Latex Coulter Counter Curve with Average Difference

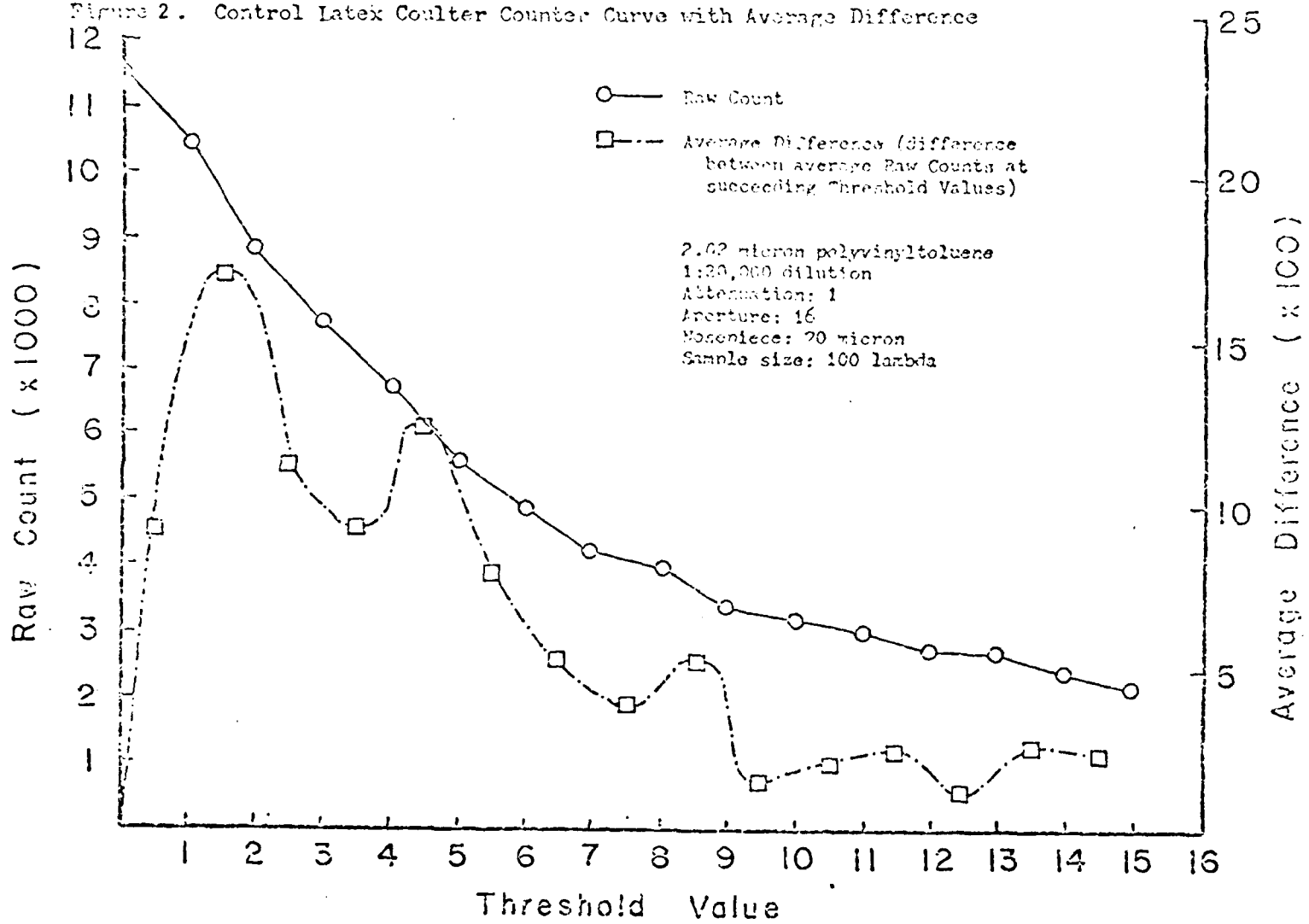

latex particles for determining total number of particles in suspension, an initial threshold value near 1 appeared preferable. Background counts produced by the "noise" of the instruments were found to be insignificant when compared to both the latex raw count and the difference between raw counts at succeeding threshold values.

Upon the addition of a known number of WEE virus ($10^{5.3}$ pfu) to a known number of latex particles, a distinct shift in the hill and valley curve occurred (Fig. 3). Not only was the curve shifted on a horizontal plane, but the amplitude of the curve was altered at various threshold values (Fig. 4) The most predominant changes occurred in the range of threshold values from 0 to 10. Still, the actual number of particles comprising an aggregate was not known, but, none the less, the virus suspension did have a profound effect on the suspension of latex.

To study further the effect that virus and antibody had upon the formation of latex aggregates, an extensive analysis of latex-virus interaction was initiated. A larger number of counts was taken at each individual threshold, thus allowing a better statistical picture of the events that occurred. Because data were still unavailable which would characterize the aggregates into finite groups of dimers, trimers, tetramers, etc., an attempt was made to analyze the data obtained in such a manner that characteristics of the virus-induced aggregates could be measured and thus allow for comparison with different concentrations of virus and antibody. Tables 28 through 30 indicate the cumulative data obtained in the Coulter Counter latex-WEE virus agglutination study. The control counts for latex (Table 28) exhibited the decrease in count as the threshold increases, as was shown earlier.

Figure 3. VEE Virus-Latex Coulter Counter Curve with Average Difference

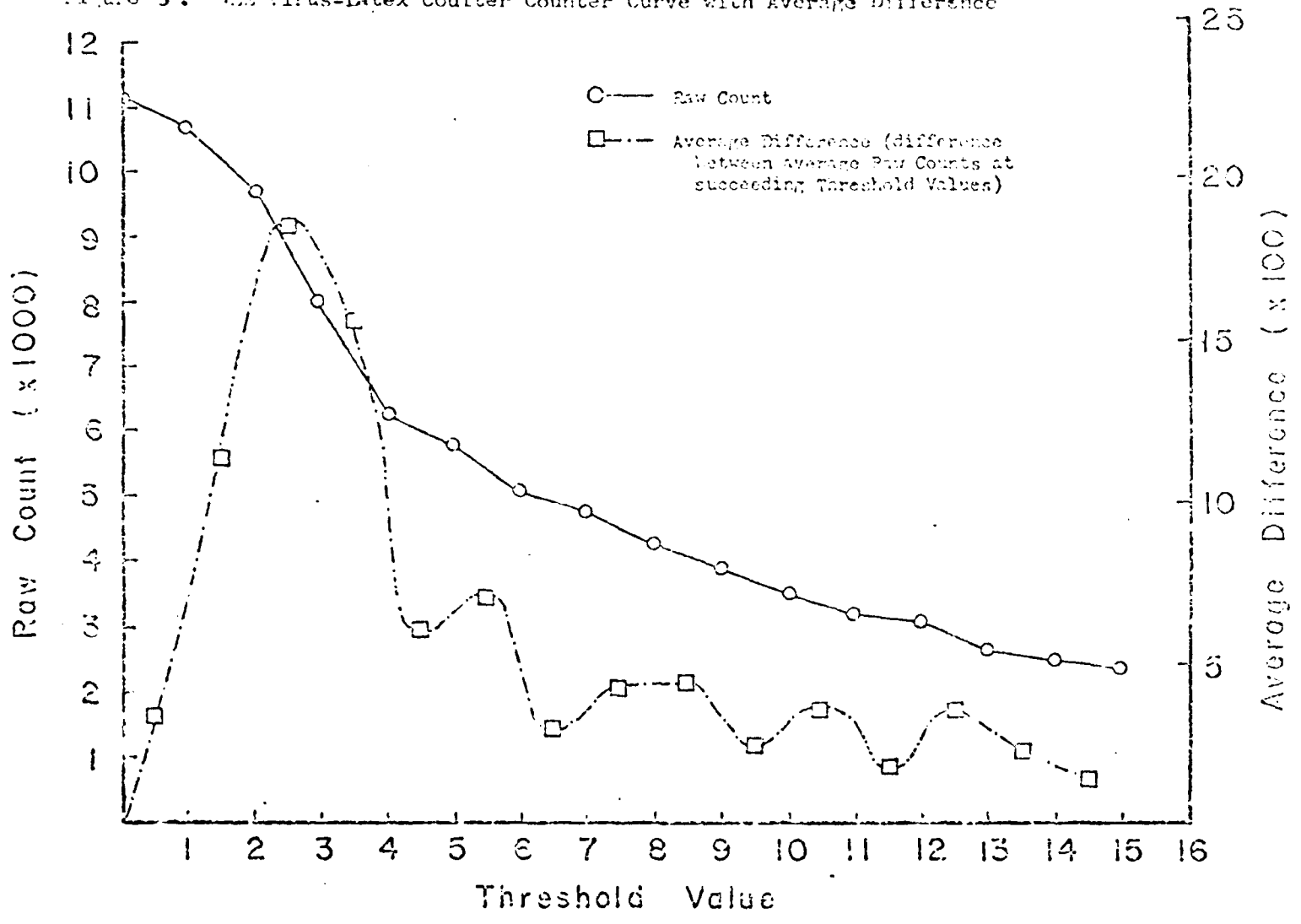

Figure 4. Comparison Average Difference Curve of VP3 Virus-Latex and Latex Control

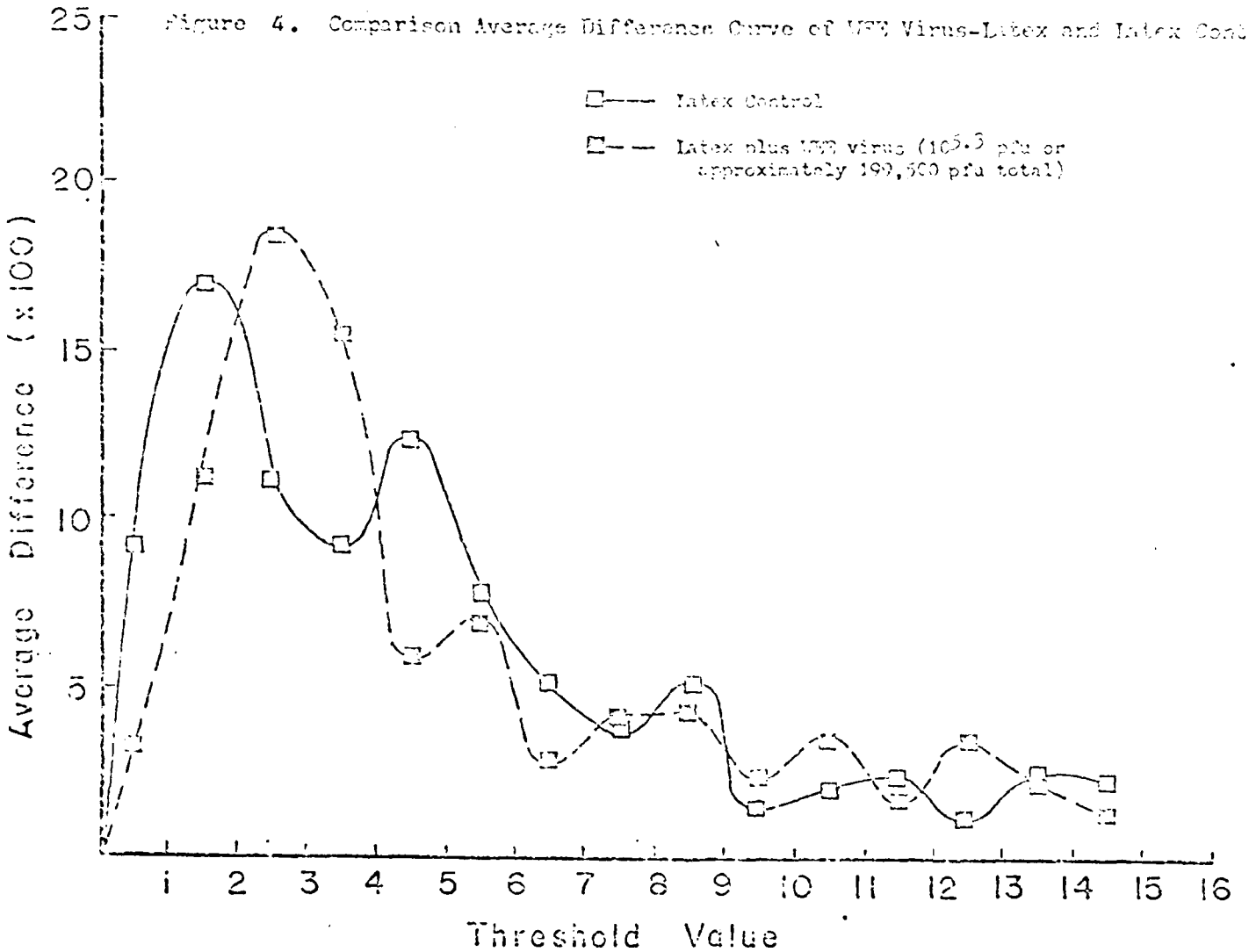

Using a methematical process defined in a previous report (2-1-72 - 6-30-72) four dilutions of WEE virus and five dilutions of WEE antibody were analyzed and defined as a mathematical expression or polynomial (Table 1). Thus, a "signature" or "fingerprint" describing the effect that WEE virus had on latex agglutination was determined. Also, the percent of variance in y was explained and the total variance of y was given. In all but one signature, the percent of explained variance in y was found to be greater than 58%.

The "signature" method of analyzing Coulter Counter data was modified to allow the detection of minute changes in latex particle volume displacement as a result of virus particles adsorbing to the latex. Calculations which allowed the determination of the latex particle volume displacement using known mathematical constants of the Coulter Counter system led to an even more sensitive method of virus detection. By "pre-programming" the Coulter Counter with uncoated and unreacted latex particles of a known volume, a known displacement was observed. When the attentuation of the Coulter Counter was decreased, the amplification of the entire eystem increased with a resultantly greater resolved peak of known volume displacement (Fig. 5).

Therefore each channel was representative of a smaller volume displacement value. Because each channel was representative of a smaller volume displacement, a shift occurred from left to right when the attenuation was decreased from 1 to .500. However, when the volume in each channel was calculated, the peak for each latex population profile occurred at similar values (see X axis on graph). In effect, this gave a greater degree of resolution in each channel, and thus created a more sensitive method of detecting any change that might be produced by virus adsorption on latex.

Further use of the relationship between constants of the system resulted in a determination of the volume displacement throughout the entire zone of detection as indicated in the following:

$$V = \frac{(K)(B)(T)}{I}$$

where "V" is volume, "K" is a constant of the entire system, "B" is the setting number of the attenuation switch, "T" is the channel number in dial diversions (equivalent to threshold setting), and "I" is the actual aperature current calibration. By measuring I across the external and internal electrodes of the Coulter Counter, and using a particle of known volume, the subsequent relationship was derived:

$$K = \frac{(V)(I)}{(B)(T)} = \frac{(4.31592\ u^3)(1.25 \times 10^{-4}\ amps)}{(B)(T)} = 5.3949 \times 10^{-4} \qquad (2)$$

When K was determined for the system, equation (1) was used for determination of the volume at specific channels or threshold settings. The volume which was detected in each channel with various settings of Aperture and Attenuation was reported earlier (9-1-67 - 6-30-73). Depending upon the size of the latex particle or aggregate to be detected setting the Attenuation and Aperture switches to the proper positions permitted detection of that volume as measured in cubic microns. Thus, the 2.02 um latex particles (volume - 4.32 um) were measured at threshold (T) setting of 6 when the Aperture was 8 and the Attenuation was 1.

Table 1 . [illegible] Virus, Antibody, and Virus-Antibody Signature Equations

10^{-1} [illegible] virus Polynomial regression of degree 3

$y = -1713.17 + x(852.53) + x^2(-115.27) + x^3(4.60)$

58.1[illegible] variance in y explained 6833163 total variance

10^{-2} [illegible] virus Polynomial regression of degree 5

$y = -1402.90 + x(-316.89) + x^2(347.18) + x^3(-69.53) + x^4(5.39)$

$+ x^5(-.15)$ 91.6[illegible] variance in y explained 4699235 total variance

10^{-3} [illegible] virus Polynomial regression of degree 5

$y = -2811.72 + x(2343.09) + x^2(-743.87) + x^3(107.45) + x^4(-7.11)$

$+ x^5(.17)$ 94.6[illegible] variance in y explained 8360457 total variance

10^{-4} [illegible] virus Polynomial regression of degree 4

$y = -2040.62 + x(1386.42) + x^2(-315.03) + x^3(28.39) + x^4(-.87)$

82.8[illegible] variance in y explained 5401401 total variance

10^{-1} [illegible] antibody Polynomial regression of degree 3

$y = -1330.90 + x(590.90) + x^2(-71.77) + x^3(2.71)$

86.2[illegible] variance in y explained 2920206 total variance

10^{-2} [illegible] antibody Polynomial regression of degree 3

$y = -2440.90 + x(984.01) + x^2(-112.96) + x^3(4.22)$

82.6[illegible] variance in y explained 9340485 total variance

10^{-3} [illegible] antibody Polynomial regression of degree 2

$y = -1874.14 + x(304.85) + x^2(-19.46)$

82.3[illegible] variance in y explained 6987729 total variance

10^{-4} [illegible] antibody Polynomial regression of degree 5

$y = -1667.62 + x(1628.16) + x^2(-605.25) + x^3(97.10) + x^4(-6.90)$

$+ x^5(.18)$ 82.2[illegible] variance in y explained 3245545 total variance

Table 1 . continued

10^{-5} [illegible] antibody Polynomial regression of degree 2

$y = -1160.60 + x(224.12) + x^2(-10.46)$

88.9% variance in y explained 2409226 total variance

10^{-1} [illegible] virus plus

10^{-1} [illegible] antibody Polynomial regression of degree 5

Not significant

10^{-2} [illegible] virus plus

10^{-2} [illegible] antibody Polynomial regression of degree 3

$y = -1818.97 + x(605.56) + x^2(-68.23) + x^3(2.49)$

91.3% variance in y explained 4604082 total variance

x = the threshold at which the Coulter Count is obtained

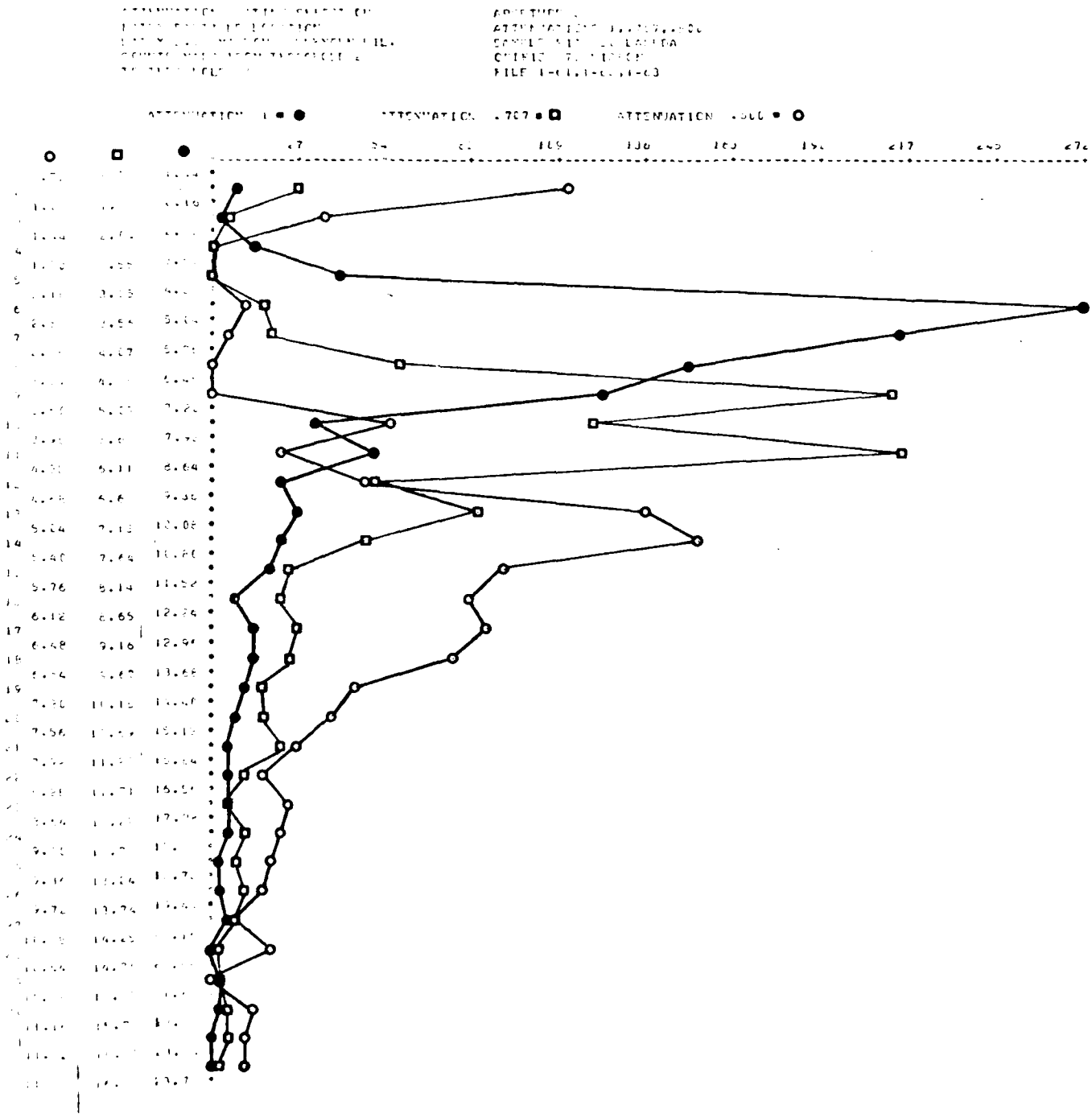

Figure 5 Latex counts in channels 2-12 for attenuations 1, .707, .500

The potential that the measurement of individual channels had to detect induced virus adsorption on latex was realized and further developed. In addition, the process of adsorption was seen to be applicable to a wide variety of substances and not strictly limited to only virus adsorption. Consequently, a number of modifications of the original CLAM particle process were attempted. Indeed, in addition to virus adsorption, viral antibody, bacterial antibody, bacteria, Staphylococcus aureus enterotoxin B, and concanavalin A have been successfully adsorbed to the surface of the latex particle (7-1-73 - 9-30-74).

After recognizing that modifications of the original CLAM particle process permitted a whole new method of detection, a new philosophy of utilizing the process had to be defined and developed. The philosophy required the addition of instrument limits as well as new concepts of the adsorption process.

When virus particles, antibody molecules, bacteria, or other adsorbents such as concanavalin A or toxin are adsorbed on latex particles of a uniform size, the adsorption causes agglutination of the latex particles which can be quantitatively and qualitatively analyzed by using a Coulter Counter. Prior to the agglutination of the latex particles, however, small increases in latex volume displacement due to increases in adsorption of adsorbent material may be qualitatively and quantitatively analyzed by using a Coulter Counter and various computational processes mediated by a computer. Also, increases in volume displacement of a growing tissue culture cell may be analyzed in a like manner.

Therefore, two broad classifications of this phenomen have been defined: non-agglutination (NAGG) and agglutination (AGG). Simply described, when an adsorbing material (adsorbent) attaches itself to the latex surface, the latex particle, which is of uniform diameter, has its total volume changed by that volume which is required by the adsorbent. The resultant complex (latex-adsorbent) continues to increase in volume as more coating occurs. This is referred to as the non-agglutination class of detection. When adsorption reaches a particular degree, a "triggering" level, the complex has a tendency towards agglutinating and the production of dimers, trimers, tetramer, etc. This is obviously referred to as the agglutination class of detection.

The agglutination detection class has been further broken down into three groups which indicate to what degree the agglutination has occurred. The production of latex dimers and trimers has, therefore, been defined as ultramicro adsorption agglutination. At this level, adsorption of the latex has progressed to the point where the "triggering" level of non-agglutination has just been surpassed and small aggregates of latex are formed. As more adsorption occurs, larger aggregates within the range of tetramers to decimers are produced, known as micro adsorption agglutination. Both of the previously noted groups are invisible to the human eye and require instrumentation to detect and amplify the phenomena. The third type, macro adsorption agglutination results in latex polymer formation, a visible reaction which may be easily seen on a slide or card. It is this type of agglutination which has been exploited in tests such as rheumatoid arthritis latex fixation test, syphilis rapid plasma reagin card test, C-reactive protein latex slide test, and pregnancy latex tests.

Various concentrations of different viruses, antibodies, bacteria, toxin, and concanavalin A, referred to as adsorbants, produce different patterns of adsorption as measured by changes in volume displacements. By predetermining the proper instrument settings based on the extent of resolution desired, known discrete volume displacements may be monitored individually, or whole zones of volume displacements may be monitored collectively. These patterns may then be rapidly analyzed by the computer which has been programmed to perform various computational and manipulative steps to derive trends of adsorption activity specific for each group and concentration of adsorbent.

The three major methods of qualifying and quantitating adsorption on latex are: (1) single channel shift, (2) multiple channel shift, and (3) centroid movement. By using the Coulter Counter, all methods utilize, to some extent, latex volume displacement as a measure of adsorbent activity. However, character-

istics unique to each method provide differing degrees of detection sensitivity.

Single channel shift provides for the detection of increases or decreases in volume displacement and the subsequent stepwise shifting of particles from one detection channel to another. Within limits of the detection instrument, adsorption on latex or tissue culture cell volume changes may be detected. Coulter counts which are representative of the number of mean particles within the key channel (i.e., channel 3 or channel 6) may be monitored. Decreases in the count are interpreted as the measurement of particles which are being changed by the adsorbant, and thus are not counted in the same channel as before, but rather move to the next immediate channel and are counted there. Therefore, the need to monitor only the channel within which the mean particle is counted, and the immediate next channel permit what is defined as single channel shift. When the proper adsorbant:latex ratio occurs, small decreases in the mean particle channel can be detected as small increases in the immediate next channel. When plotted, the trend of count decrease and the trend of count increase provide a point of overlap which represents, of course, the concentration at which an equal count is found in both channels.

Multiple channel shifts occur when ultramicro adsorption agglutination (dimer and trimer production) and micro adsorption agglutination (tetramer to decimer production) result because the adsorbant coats the latex surface; subsequently, this results in the formation of latex aggregates. Because this phenomenon results in a major shift of population groups within the entire latex population distribution, resolution of the detection system need not be as great as with single channel shift. In most cases, also, the requisite of a higher adsorbant concentration must be fulfilled to produce latex aggregates, and thus the detection system's relative sensitivity is not as great.

Threshold counts, which have been taken with the Coulter Counter, of normal latex and treated latex are channelized as before. However, the shift in count is produced by aggregate formation, as opposed to a "layering" effect of the adsorbant on the latex surface. Thus, the channel within which the mean diameter particle is detected and the channels within which aggregates of the mean diameter particle would be detected are of importance.

Assuming that aggregates would be detected in channels within which the volume measured was exact multiples of the monodispersed latex, under certain instrument conditions, monomers, dimers, trimers, and tetramers would then be detected in channels 6, 12, 18, and 24 respectively. For example, the volume range of 2.02 $\pm$0.0135 um latex was determined to be 4.229976 um^3 - 4.403043 um^3 with a mean volume of 4.315931 um^3 by the equation:

$$\text{Volume}_{\text{sphere}} = 4.189r^3$$

r = radius of sphere

It has been shown that particles of this size could be detected in channel 6 when the instrument was set at aperture 8, attenuation 1, with a 70 um aperture tube or orifice. Channel 5 was shown to detect particles of 3.5966 $\pm$ 0.3596 um^3 and channel 7 could detect particles of 5.0352 $\pm$ 0.3596 um^3. As the entire range of volume displacement of monomer latex falls within the resolution limits channel 6, it must therefore be concluded that monomers are indeed counted in only channel 6 under the above instrument conditions. Latex aggregates such as dimers, trimers, tetramers, etc. must therefore be detected in those channels

which measure the volume as a multiple of the integer values of the number of latex forming an aggregate. (Fig. 6)

Because counts were obtained in channels other than 6, 12, 18, 24, etc., in which aggregates comprised of integer-valued latex particles were found, a preliminary method of "zoning" the channels into monomer, dimer, trimer, tetramer,...decimer zones was proposed. As channel 6 was defined as the mean channel for the monomer zone, channels 5 and 7, 4 and 8, and 3 and 9 were characterized as descending in regards to their relative populations or counts. Similarly, the dimer zone was comprised of the mean channel, channel 12. In decreasing importance were channels 11 and 13, 10 and 14, and 9 and 15. Figure 6 represents the concept for the monomer, dimer, and trimer zones; however, each zone which represents an integer-valued latex aggregate channel plus associated channels, may be represented in a like fashion. The counts linking channels (9, 15, 21, etc.) are halved to permit an equitable distribution of counts within each zone at a specific data collection channel.

If a cumulative effect of adsorbant on latex is desired, centroid movement permits a qualitative determination and the establishment of trends of activity in the entire population distribution. As explained more fully later, centroid analysis may be used to measure a true shift in the total mass of particles when an adsorbant attaches to the surface of latex and subsequently causes the latex to increase their volume of displacement. Trends, projections, and extrapolations may then be computed to determine the effect of other adsorbant concentrations on latex activity.

The claimed process as represented in a flow diagram (Fig. 7) includes a number of operational steps, some of which may be modified or expanded. Additionally, both operator and instrument-mediated blocks are combined to provide a functional, step-wise procedure of the process.

Particles of uniform size, which may or may not be of the type and characteristics demonstrated in the given examples, are first sonified by an ultrasonic bath to assure that any self-induced aggregates may be dissociated and a predominant population of monodispersed particles obtained. To a portion of the particle suspension is added the adsorbant (virus, antibody, concanavalin A, or another substance capable of adsorbing to the latex surface). Similarly, a control particle suspension is treated in an identical manner except no adsorbant is added.

After the proper instrument settings which permit the desired volume displacement as well as the appropriate level of resolution are selected, multiple counts of each sample are obtained. The number of counts required for each sample must be determined in relationship to the desired significance of the end results.

The principle of operation utilized in the process employs a particle analyzer, e.g. the Coulter Counter, which measures particles in suspension, as a function of their volume displacement in an electrolyte. Figure 8 visually represents the major functional operation of the Coulter Counter as utilized in the claimed process. When a vacuum is applied to the aperture tube - monometer assembly piece, mercury within the monometer is unbalanced and flows past the start-stop contacts. This resets the counter to zero. When the stopcock is closed, the

Figure 6. Monomer, dimer, and trimer zone concept for particle classification

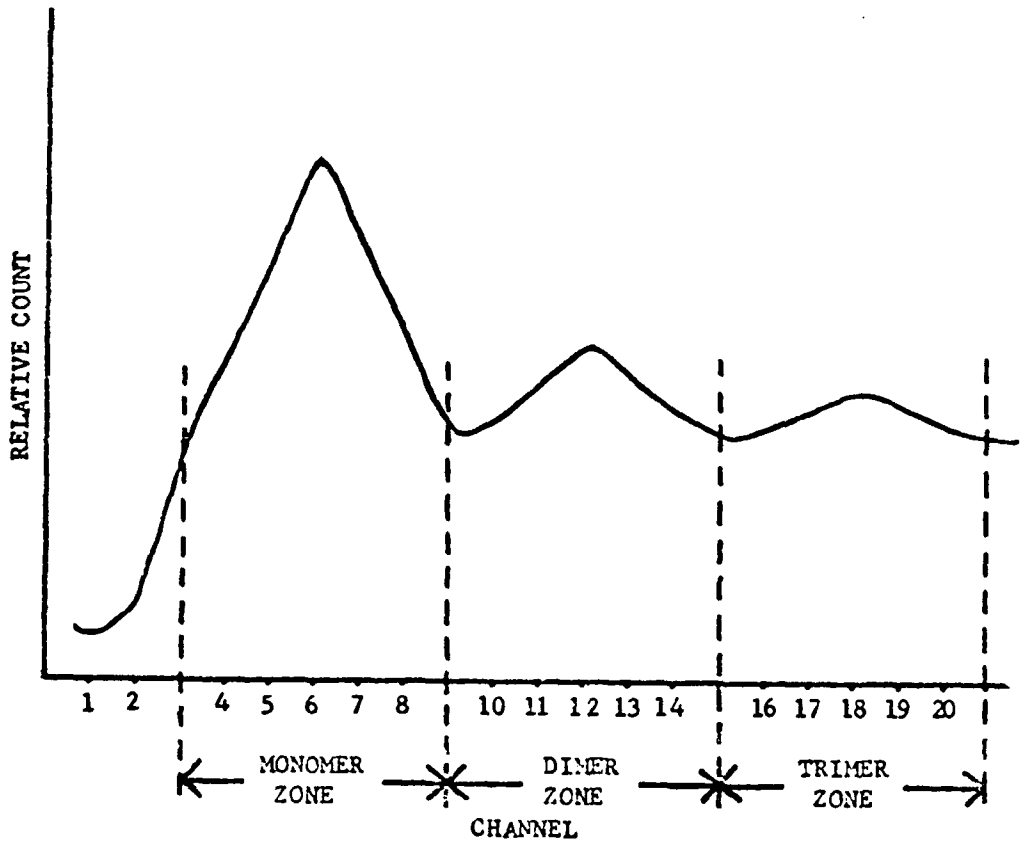

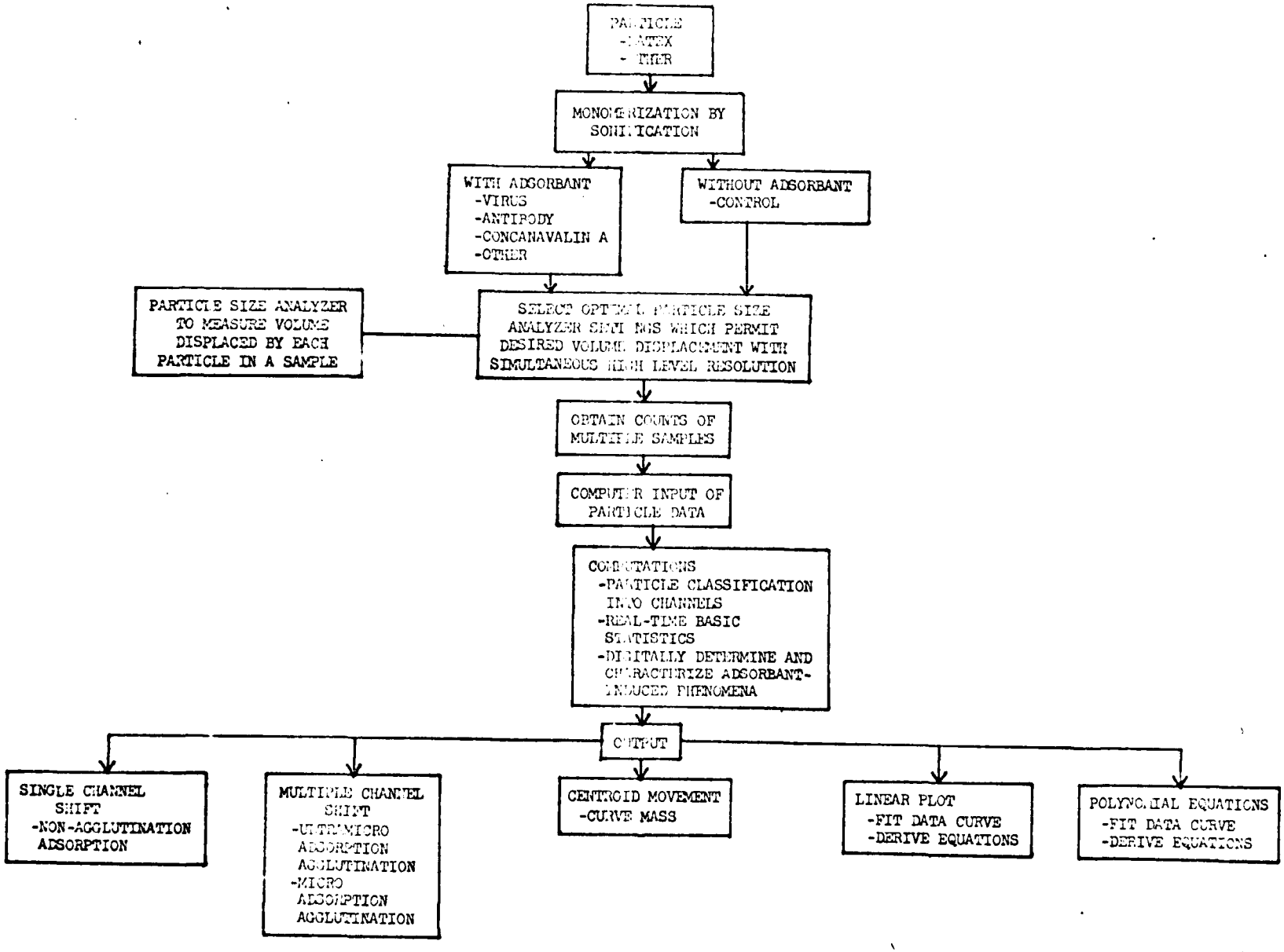

Figure 7 Flow diagram of adsorbant detection and titration system

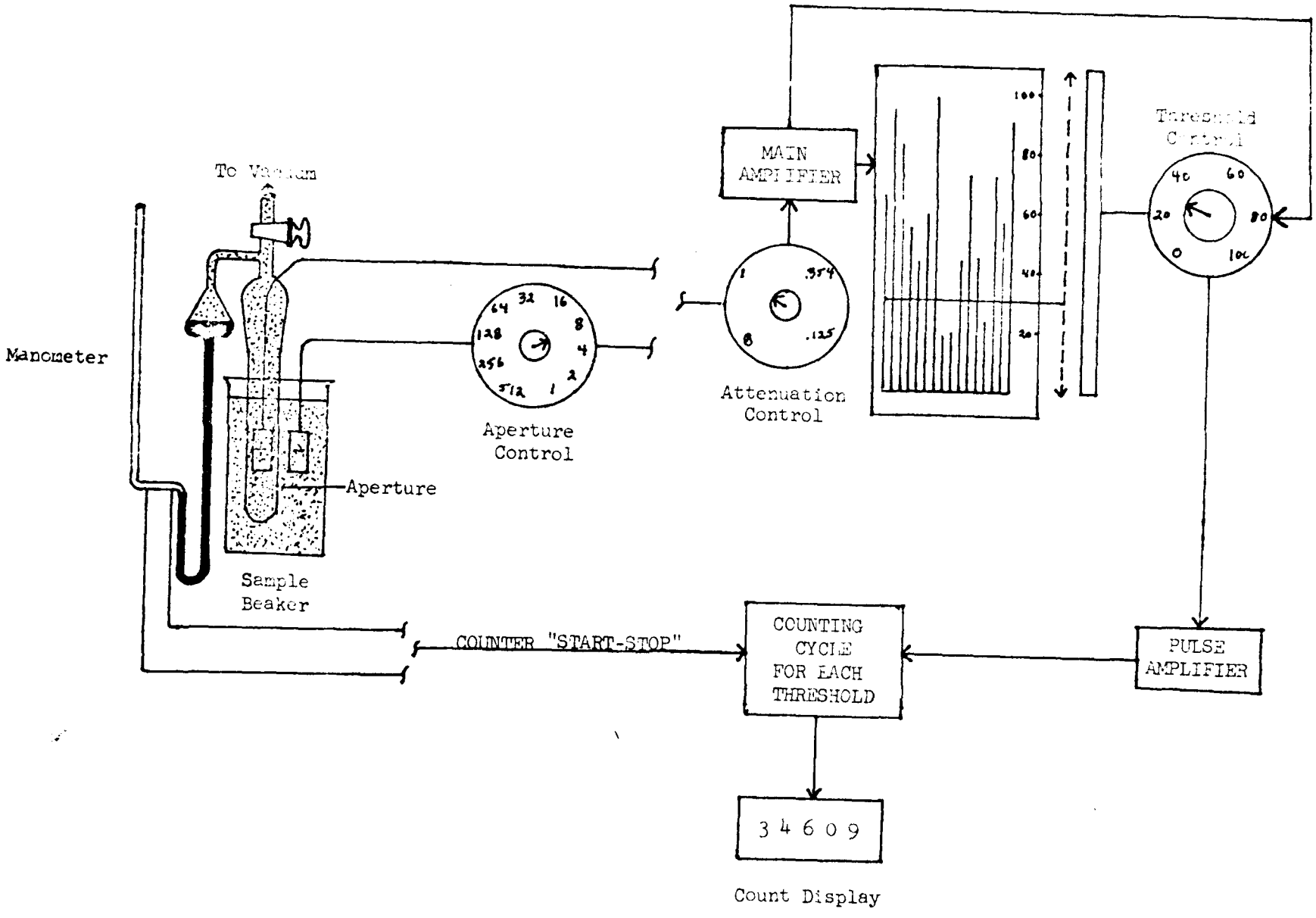

Figure 8 Functional operation of Coulter Counter model F

mercury begins to travel back to its balanced position. Simultaneously, the sample is drawn from the sample beaker, through the aperture, and into the aperture tube. When the mercury touches the start contact, the counting cycle begins. When the mercury touches the stop contact, the count is completed. Therefore a reproducible volume may be represented.

As the particles are drawn through the aperture, an amount of electrolyte is displaced which is equal to the volume of the particle. The electrolyte displacement then results in a change in the current flow between the internal (+) and external (-) electrodes. The baseline quantity of current may be limited by an aperture control which either increases or decreases the current. The change in aperture current, as a signal, may then be amplified by the attenuation control, and the subsequent signal displayed on an oscilloscope as a scan of pulses, each representative of a particle's volume displacement. As a discriminator, the threshold control permits only pulses of a determined height to be further processed. Those pulses are then amplified further, counted, and digitally displayed.

Each count is directly input either automatically or manually into the computer for analysis. Identifying and descriptive data may also be input. Through a series of computational steps, counts from the particle analyzer are channelized into representative groups of particles, each of a known volume displacement and aggregate description. Real-time basic statistics are performed on the particle analyzer counts to permit immediate determination of proper statistically significant data and the necessity for additional counts if proper limits of reliability are not attained.

The adsorbent-induced phenomena are so characterized as to permit digital representation of the adsorbent effect which may then be compared and displayed in three major methods: single-channel shift, multiple-channel shift, and centroid movement, each characteristic of the degree of sensitivity required for the specific adsorbent type and concentration in question. Single channel shift may be used to detect the smallest amount of adsorbent effect, as the principle mechanism of detection is volume displacement and, the small incremental increases or decreases in that displacement which are produced as a function of adsorption or adsorbent concentration. In effect, non-agglutination adsorption is detected by the method; this, therefore provides the most sensitive procedure by which the adsorbent-induced phenomena may be detected, identified, and characterized.

Multiple-channel shift operates in a similar manner, however, particle aggregates are detected as they shift from the channel or zone within which monomers are detected, into the channel or zone within which aggregates of the monomer are detected. The phenomenon occurs when the concentration and effect of the adsorbent exceeds a "triggering" level which results in particle aggregate formation. As this occurs with a greater amount of adsorbent, the process is not as sensitive as the single-channel shift.

Centroid movement is used when what is desired is a representation of what has occurred over the entire measured population distribution. Particles of all volume displacement channels affect the centroid location. Therefore, after the adsorption, the same volume displacement channels are used to calculate

another centroid location. The shift in centroid location, as induced by the adsorption, then represents the effect of the adsorbent on the particle. Any subsequent attachments to the particle may then be analyzed in an identical manner.

Additionally, best fit of the data by a linear plot or by a polynomial permits a unique identifying "fingerprint" of each type and concentration of adsorbent. This process may be utilized in all three methods provided the proper number of data information points is available such that a significant curve representation of the adsorbent effect may be determined. Also, classical methods of statistics which permit acceptance of only that equation which best fits the data may be used to further define the process.

STANDARD ADSORBENT SYSTEM - CONCANAVALIN A

A method that has been reported (Annual Technical Report No. 1, Contract N00014-73-C-0084, Task No. NR 136-952) in which the effect of adsorbent was measured as a function of changes in channel count, was used to analyze the effect of Con A. Although counts were obtained in the range of channels from 5-54, the most representative channels of Con A effect were those from 5-20. This was especially true when the concentration of Con A was equal to or less than 42 mg. Apparently the counts in channels 5-20 remained relatively constant, even after the addition of 30 mg Con A. However, the predominant peak in channel 6 was drastically reduced by increasing the Con A concentration to 34 mg. Additionally, a new peak was produced in channel 9 and a series of increased counts was found in channels 11-20. As the Con A concentration was increased up to 42 mg, a "moving wave" type of phenomenon was observed, as counts in the lower channels decreased, and counts in the higher channels increased. This suggested that Con A was interacting with the latex particles in such a fashion, as to decrease the number of latex particles in a channel as the Con A concentration increased. Because the suspension of latex particles was a closed system, the particles, as measured by counts, could not have simply disappeared or dissolved. Rather, they must have relocated into other channels, more specifically, those channels of greater volume displacement detection.

Because of earlier documentation (Annual Technical Report No. 1, Contract N00014-72-C-0084, Task No. NR 136-952), the distribution of counts in channels 6, 12, 18, and 24, when Con A concentration was increased, was further studied (Fig. 9). These channels represented monomers, dimers, trimers, and tetramers respectively. As the monomers decreased in count, (as Con A concentration increased) an increase in the dimer, trimer, and tetramer populations followed. This was anticipated as an indication of Con A-induced formation of aggregates. Likewise, as the dimer and trimer populations decreased, a subsequent increase in tetramer population was observed. These key channels, then, served as a quick indication of aggregate formation as a function of increased Con A concentration.

Figure 9 Monomer, dimer, trimer, and tetramer distribution as a function of Con A concentration

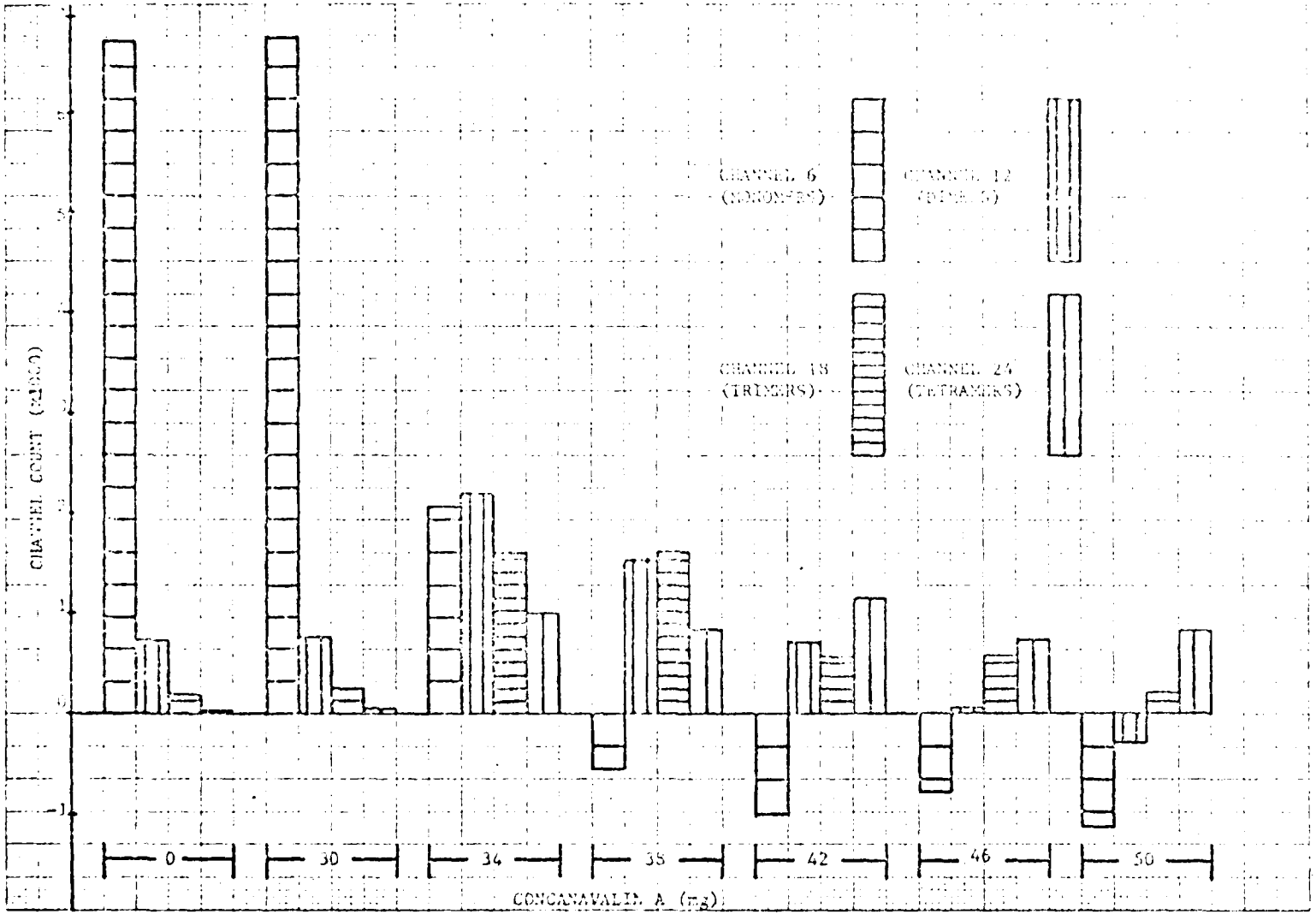

CLAM PARTICLE DETECTION OF CONCANAVALIN A BY CENTROID ANALYSIS

To test the concept of latex agglutination which was induced by an adsorbent, another study using a different adsorbent was initiated. Concanavalin A (Con A), a phytohemagglutinin with extreme agglutinating properties of erythrocytes, starch granules, yeast cells, bacteria, and viruses, was chosen as the adsorbent. By modifying the concentration of Con A relative to a constant number of latex particles, the adsorptive properties of Con A, in addition to the agglutinating properties of latex, could be monitored on the Coulter Counter.

A quantity of nearly 250 ml of an approximate 1:20,000 dilution of 2.02 um polyvinyltoluene (Dow Chemical Company, Indianapolis, Indiana) was prepared in Isoton pH 7.5-7.6 (Coulter Electronics, Hialeah, Florida). The transparency of the solution resembled water. The beaker of latex suspension was sonified in an ultrasonic water bath (Cole-Parmer, Chicago, Illinois) for 15 minutes just prior to taking counts on the Coulter Counter. Approximately 50 ml of the sonified latex suspension was placed in a small beaker and maintained for later use. After thoroughly mixing, the latex was counted on a Coulter Counter model F (Coulter Electronics, Hialeah, Florida) equipped with 70 um aperture tube and set at: Attenuation 1, Aperture 8, Sample size 50 μl. To the beaker, which then contained approximately 200 ml of latex suspension, was added 1 ml of a 30 mg/ml concentration of Con A (Pharmacia Fine Chemicals, Uppsala, Sweden) as prepared in Isoton, plus 1 ml of latex from the small beaker. Again a series of counts was obtained at the aforementioned instrument settings. Additional Con A was added in increments of 2 ml (concentration = 2 mg/ml) as prepared in Isoton. Two (2) ml of latex from the small beaker was also added. The suspension was mixed well by using a small magnetic stirrer and then counted on the Coulter Counter. For each increment, a series of latex counts was obtained for threshold 5 - 20,23,25,29 - 31, and 35 - 37 (Tables 2-8). These thresholds were chosen because they would include counts which had been produced from single latex and from aggregates of latex.) Channel counts were calculated from the threshold counts.

Because channel 6 had been previously identified as the channel within which the single latex particle (monomer) would be counted, that channel and channels 12, 18, and 24, which would be representative of dimers, trimers, and tetramers, were analyzed further. When the data was interpolated at 0.5 mg intervals (Table 9) and then plotted (Fig. 10), a graph showing the relationship between these four key channels was obtained. As was expected, the population distribution

indicated that the original 30 mg Con A-latex suspension was comprised of predominately monomers, followed by a reduced population of dimers, trimers, and tetramers. This remained effective until approximately 34 mg of Con A, when the dimer population increased above that of the monomers. Likewise, the trimer population and dimer population apparently were quite equal from 37 mg to 43 mg Con A. However, at that point, the dimer count continued to drop and the trimer count remained fairly stable. The tetramer count increased above any of the other key channels when the Con A concentration reached 41 mg and remained quite level from then on.

Because the relative rate of monomer decrease was much greater than the rate of increase for the dimers, trimers, or tetramers, when taken individually, the indication was that the monomer channel was "feeding" the production of aggregates in the dimer, trimer, and tetramer channels. Although this was especially significant up to approximately 37 mg Con A, at approximately 34.5 mg Con A the dimer population began to decrease. However, not until approximately 36.5 mg Con A did the trimer population begin to drop. The dimer drop continued smoothly, the trimer drop leveled somewhat between 42 and 47 mg Con A and then continued to fall, and the tetramer count fluctuated within about 300 counts from 34 mg to 50 mg Con A with a very gradual slope. In effect then, by monitoring the key channels, the aggregate production may be detected and the agglutinating effect of adsorbant on a carrier particle may be effectively recognized.

In a like manner as with WEE virus and WEE antibody induced centroid location shift and WEE virus induced single channel shift, the process of multiple channel shift may be expressed by linear or polynomial regression. For example, the four population groups (monomers, dimers, trimers, tetramers) may each be defined in terms of an equation which, within statistical reliability, best fits the actual experimental data and thus associates each population group with a unique polynomial identity or expression.

When polynomial regressions of degree 1-5 were determined for each population group, the apparent best fit occurred with a polynomial of degree 4 or 5, which corresponded to an R^2 of .8513 to .9998 (Tables 10-13). When compared to the actual curve (Figs. 11-14), the polynomials of each population group and each degree represented varying levels of closeness of fit. Obviously, the 1st degree polynomial offered the least best fitting curve. However, in some cases where the actual curve might approach a straight line, the 1st degree polynomial may be the best choice. Degree 2 and 3 polynomials fit the curve at some locations exactly, but in all cases did not fit best.

By using a degree 5 polynomial for all population groups, the best R^2 value was obtained and thus the best reliable polynomial to describe the observed effect was derived. Each group was defined then according to the following:

Monomer

$$Y = -734827.196 + X(102189.7509) + X^2(-5327.337526) + X^3(132.5336776) + X^4(-1.589580402) + X^5(7.39427 \times 10^{-3})$$

Dimer

$$Y = -1077154.364 + X(123176.7535) + X^2(-5567.904735) + X^3(124.8833813) + X^4(-1.393469097) + X^5(6.19693 \times 10^{-3})$$

Trimer

$$Y = 1515088.938 + X(-212135.3519) + X^2(11631.53915) + X^3(-312.6351083) + X^4(4.127682150) + X^5(-0.02145785)$$

Tetramer

$$Y = -2107428.658 + X(268133.5663) + X^2(-13567.20170) + X^3(341.3165543) + X^4(-4.26815877) + X^5(0.021219249)$$

Where Y - the particle count and X = the mg of Con A added.

By reiteration then, the amount of Con A present in an unknown may be determined by the particle count of the specific population group.

The process is not limited to only the four population groups given in the example, but may be expanded to include all particle aggregate groups within a sample, provided that corresponding known data is available to which comparisons may be made.

Whole particle aggregates are produced when the adsorbant concentration level reaches a certain point, and at that point the utilization of multiple channel shift as a process of agglutination detection can be realized. This process need not be applied only to Con A adsorption but may also be used for detecting other components such as toxin, bacteria, viral and bacterial antibody, and any other substance which may be effectively adsorbed onto the surface of the particle. When applied to tissue culture cells, the process may be utilized to detect cellular agglutination as well as large changes in cell volume which may be induced by viruses, bacteria, antibiotics, chemicals, or carcinogens and their effects.

When centroid analysis (Tables 15-25) was performed on the Con A experimental data, the Con A-induced shift in the mass of the whole latex population indicated that larger particles were formed. Shifts (Figs. 15 and 16) in the centroid location of up to 4 channels (9.2 with 30 mg Con A to 13.3 with 34 mg Con A) indicated that more than just single channel shift had occurred in that concentration range of Con A.

Figure 17 represented the centroid location as a function of Con A concentration (experimental values darkened) with a closely linear portion from 30 mg to 38 mg Con A. From 46 mg to 50 mg Con A a small drop in the centroid location occurred which indicated that the major populations (monomers and dimers) no longer were playing a significant role in the adsorption effect and that the "mass" of the curve had effectively reached a static state. Smaller shifts in centroid location were seen even with 38 mg Con A and were demonstrated as a decrease in the slope of the curve.

To represent the centroid location shift as an equation, linear regression (Table 26, Figure 18) and polynomial regression (Table 27, Figure 19) were performed on the data. Although the linear regression provided a straight line relationship between Con A concentration and centroid location, the best representation or fit of the data was found to be a 5th degree polynomial with a R^2 of 0.9982:

$$Y = -325.1472246 + X(29.39134168) + X^2(-0.965568266) + X^3(0.014340645) + X\,(-8.09754 \times 10^{-5})$$

Thus, within the statistical reliability of the data, interval of the measured data, and identical experimental conditions, the centroid location may be used to determine the concentration of Con A in an unknown sample by reiteration. The dramatic shift in centroid location, when compared to the previously noted multiple channel shift analysis, provides an exceptional method by which adsorbant effect may be detected.

Table 2 Particle Counts for Latex Control in Important Thresholds and Channels

CON A-LATEX AGGLUTINATION
LATEX 2.12 MICRON UNKNOWN DIL.
DECREASING FROM ORIG 256 ML VOL.
+2 ML CON A (2 MG/ML)

APERTURE 8
ATTENUATION 1
ORIFICE 70 MICRON
SAMPLE SIZE 50 LAMBDA
PCT OF FILE

LATEX CONTROL

5		23056	23053
		22719	132.53
		[illegible]	[illegible]
	2028		
6		[illegible]	21685
		[illegible]	[illegible]
		21645	0.18%
	6703		
7		13890	14102
		14276	195.79
		14140	1.39%
	4217		
8		9839	9865
		9895	45.50
		9930	0.46%
	2655		
9		6844	7020
		7142	155.99
		7073	2.22%
	1998		
10		5056	5022
		5015	31.10
		4995	0.62%
	668		
11		4162	4154
		4147	25.66
		4132	0.62%
	599		
12		3555	3554
		3556	2.08
		3552	0.06%
	729		
13		2746	2825
		2883	70.67
		2846	2.51%
	531		
14		2279	2294
		2241	61.33
		2361	2.67%
	665		
15		1565	1609
		1665	51.07
		1597	3.17%
	395		
16		1233	1214
		1181	26.45
		1227	2.34%
	273		
17		884	941
		997	56.50
		941	6.01%
	206		
18		728	734
		723	17.10
		754	2.33%
	188		
19		552	546
		549	7.94
		537	1.45%
	78		
20		440	468
		455	36.29
		509	7.75%
23		380	296
		269	74.28
		239	25.09%
	70		
24		247	226
		216	18.19
		215	8.05%
	28		
25		202	198
		201	6.66
		190	3.37%
29		122	127
		124	7.00
		135	5.51%
	10		
30		112	117
		117	5.51
		123	4.69%
	3		
31		122	115
		124	14.47
		98	12.62%
35		77	85
		103	15.95
		74	18.84%
	15		
36		56	70
		68	13.11
		64	16.74%
	1		
37		73	69
		69	4.51
		64	6.57%

CON A-LATEX AGGLUTINATION
LATEX 2.02 MICRON UNKNOWN DIL.
DECREASING FROM ORIG 250 ML VOL.
+2 ML CON A (2 MG/ML)
+2 ML CONTROL LATEX

APERTURE 8
ATTENUATION 1
ORIFICE 70 MICRON
SAMPLE SIZE 50 LAMBDA
NOT ON FILE

+50 MG CON A

5		23723	23575	17		1400	1410
		23438	142.96			1441	27.40
		23563	0.61%			1389	1.94%
	2500				161		
6		21189	21075	18		1264	1329
		20961	105.43			1226	51.10
		21055	0.50%			1183	4.16%
	6787				273		
7		14157	14288	19		918	956
		14510	193.53			992	37.02
		14196	1.35%			957	3.87%
	3965				65		
8		10430	10323	22		882	890
		10252	94.30			894	7.23
		10287	0.91%			895	0.81%
	2584						
9		7608	6739	23		610	616
		7772	118.01			596	23.03
		7837	1.38%			641	3.74%
	2041				60		
10		5646	5698	24		561	556
		5727	45.13			556	6.24
		5721	0.79%			549	1.12%
	921				51		
11		4753	4777	25		514	505
		4773	26.76			492	11.72
		4806	0.56%			510	2.32%
	608						
12		4204	4169	29		421	380
		4128	38.35			351	36.35
		4175	0.92%			369	9.56%
	756				20		
13		3409	3413	30		368	360
		3428	13.45			351	6.62
		3402	0.39%			362	2.39%
	553				-29		
14		2894	2860	31		373	369
		2760	69.21			409	16.33
		2905	2.42%			365	4.71%
	566						
15		2179	2194	35		289	295
		2293	92.42			306	9.81
		2110	4.21%			289	3.33%
	361				12		
16		1886	1833	36		289	282
		1774	56.19			265	15.14
		1836	3.07%			293	5.36%
	423				-4		
				37		299	296
						267	17.01
						293	5.94%

Table - Particle Counts for Latex Reacted with 34mg Con A in Important Thresholds and Channels

CON A-LATEX AGGLUTINATION
LATEX 3.02 MICRON UNKNOWN DIL.
DECREASING FROM GRID 250 ML VOL.
+2 ML CON A (2 MG/ML)
+2 ML CONTROL LATEX

APERTURE 8
ATTENUATION 1
ORIFICE 70 MICRON
SAMPLE SIZE 50 LAMBDA
NOT ON FILE

+34 MG CON A

5	42589	42808	
	43019	215.11	
	[illegible]	0.50%	
	1075		
6	41772	41753	
	41790	41.10	
	41736	0.10%	
	2096		
7	39588	39637	
	39666	42.44	
	39656	0.11%	
	1529		
8	38364	38107	
	37638	263.23	
	38120	0.69%	
	997		
9	36939	37110	
	37136	159.60	
	37255	0.43%	
	3578		
10	33668	33532	
	33564	153.96	
	33365	0.46%	
	1332		
11	32291	32200	
	32247	121.52	
	32162	0.38%	
	2046		
12	30163	30154	
	30158	11.53	
	30141	0.04%	
	2213		
13	27937	27941	
	27851	91.56	
	28134	0.33%	
	2214		
14	25630	25727	
	25783	84.10	
	25767	0.33%	
	2076		
15	23634	23651	
	23545	159.39	
	23573	0.67%	
	1738		
16	21463	21912	
	22642	637.53	
	21432	2.91%	
	1800		
17	20143	20112	
	19868	230.07	
	20325	1.14%	
	1837		
18	18128	18275	
	18366	183.78	
	18390	0.73%	
	1710		
19	16740	16564	
	16386	177.02	
	16567	1.07%	
	1130		
20	15541	15434	
	15613	249.71	
	15149	1.62%	
	1044		
23	12106	11930	
	11673	227.76	
	12012	1.91%	
	1044		
24	10911	10886	
	10692	182.79	
	11055	1.66%	
	1001		
25	9757	9885	
	10010	126.54	
	9869	1.26%	
29	7026	7091	
	7216	110.28	
	7026	1.56%	
	325		
30	6513	6766	
	7369	524.46	
	6416	7.75%	
	723		
31	5991	6043	
	5968	111.16	
	6171	1.84%	
35	4221	4330	
	4402	95.61	
	4306	2.21%	
	212		
36	4136	4117	
	4046	63.57	
	4168	1.54%	
	311		
37	3821	3806	
	3949	151.06	
	3648	3.97%	

```
[illegible]                                        [illegible]
LATEX 2.02 MICRON [illegible] DIL.                 [illegible]ATION 1
DECREASING FROM ORIG 250 ML VOL.                   ORIFICE 70 MICRON
 +2 ML CON A (2 MG/ML)                             SAMPLE SIZE 50 LAMBDA
 +2 ML CONTROL LATEX                               NOT ON FILE

          +38 MG CON A

 5          38544   39042               17            34494   34483
            39372  293.54                             34456   14.74
     [illegible] [illegible]                    [illegible] [illegible]
      -834                                      1167
 6     [illegible] [illegible]          18            33521   33316
            39733 [illegible]                         33149  166.89
            40044   0.39%                             33278   0.57%
      -550                                      1631
 7          40231   40425               19            31641   31685
            40545  109.23                             31696   39.66
            40400   0.27%                             31718   0.13%
      -132                                       949
 8          40683   40557               20            30807   30736
            40340  188.93                             30867  132.93
            40649   0.47%                             30583   0.43%
       165
 9          40349   40390               23            26968   26929
            40519  114.55                             27022  117.46
            40301   0.28%                             26797   0.44%
        36                                      1529
10          40455   40353               24            25415   25400
            40264   96.10                             25431   41.20
            40341   0.24%                             25353   0.16%
       501                                       842
11          39774   39853               25            24663   24558
            40077  197.15                             24433  116.21
            39707   0.49%                             24577   0.47%
      -215
12          39784   40067               29            22907   20881
            39350  393.36                             20120 1772.92
            41066   2.23%                             19615   8.49%
      1509                                      2168
13          38496   38558               30            18835   18713
            38342  251.98                             18553  144.66
            38835   0.65%                             18750   0.77%
       874                                      1367
14          37679   37684               31            17327   17326
            37577  168.88                             17295   30.51
            37597   0.45%                             17356   0.18%
        26
15          38512   37558               35            14017   13859
            36656 1035.93                             13606  193.63
            37507   2.86%                             13954   1.40%
      2065                                      1035
16          35611   35593               36            12729   12854
            35538   48.57                             13119  229.62
            35630   0.14%                             12714   1.79%
      1110                                       295
                                        37            12651   12559
                                                      12463   67.29
                                                      12563   0.54%
```

Table 6 Particle Counts for Latex Reacted with 42mg Con A in Important Thresholds and Channels

CON A-LATEX AGGLUTINATION
LATEX 2.02 MICRON POLYSCIN DIL.
DECREASING FROM ORIG 250 ML VOL.
+2 ML CON A (2 MG/ML)
+2 ML CONTROL LATEX

ATTENUATION 1
ORIFICE 70 MICRON
SAMPLE SIZE 50 LAMBDA
NOF ON FILE

+42 MG CON A

5		37471	37210	17		38076	36154
		36795	362.15			38209	67.98
		37303	0.98%			38175	0.18%
	-681				972		
6		37916	37891	18		37132	37162
		38183	245.98			37214	44.07
		37683	0.65%			37201	0.12%
	-1011				579		
7		38891	38902	19		36535	36603
		38783	124.86			36284	356.42
		39032	0.32%			36991	0.96%
	-508				936		
8		39232	39410	20		36489	35606
		39678	236.04			35321	714.17
		39321	0.60%			35193	2.00%
	-525						
9		40011	39936	23		32205	32267
		39707	201.83			32468	178.28
		40069	0.51%			32128	0.55%
	-156				1020		
10		40025	40094	24		31343	31247
		40326	206.74			31219	65.11
		39930	0.52%			31180	0.27%
	-69				1157		
11		39868	40163	25		30063	30090
		40379	264.35			30286	194.59
		40241	0.66%			29899	0.65%
	-371						
12		41334	40533	29		25631	25520
		40197	696.34			25350	149.31
		40169	1.72%			25578	0.59%
	717				1241		
13		39832	39816	30		24167	24279
		39786	26.00			24368	132.45
		39830	0.07%			24302	0.42%
	193				1144		
14		39514	39623	31		23168	23135
		39618	112.10			22994	123.71
		39738	0.28%			23224	0.53%
	454						
15		39352	39169	35		18732	16910
		39069	158.58			19167	228.18
		39067	0.40%			18630	1.21%
	627				849		
16		38714	38542	36		18203	18061
		38478	150.57			17850	186.34
		38434	0.39%			18130	1.03%
	388				1018		
				37		16937	17043
						17181	123.24
						17010	0.73%

CON A-LATEX FLOCCULATION
LATEX 2.6% PICRON INHIBITION OIL.
DECREASING FREQ ORIG 450 ML VOL.
+2 ML CON A (2 MG/ML)
+2 ML CONTROL LATEX

+46 MG CON A

5		36346	35775
		35700	537.44
		35279	1.50%
	-657		
6		36385	36432
		36346	114.38
		36362	0.31%
	-795		
7		37347	37226
		37745	586.35
		36587	1.58%
	-679		
8		36169	38105
		37872	268.91
		38275	0.55%
	-512		
9		38717	38617
		38545	116.55
		38489	0.30%
	-754		
10		39490	39371
		39193	157.23
		29431	0.40%
	-125		
11		39422	39496
		39767	242.21
		39800	0.61%
	-541		
12		40700	40037
		39662	575.82
		39749	1.44%
	61		
13		40057	39975
		39809	144.35
		40061	0.36%
	-362		
14		40439	40337
		40267	88.05
		40286	0.22%
	252		
15		40065	40085
		40105	20.01
		40086	0.05%
	241		
16		39900	39844
		39793	53.67
		39839	0.13%
	117		

ATTENUATION 1
ORIFICE 70 : PICRON
SAMPLE SIZE 50 LAMBDA
NOT ON FILE

17		39762	39727
		39736	30.75
		39712	0.06%
	142		
18		39518	39585
		39592	63.32
		39644	0.16%
	584		
19		39043	39000
		38902	65.41
		39056	0.22%
	419		
20		38373	38531
		38732	186.32
		38639	0.48%
23		37202	37131
		36749	582.96
		36842	1.57%
	1230		
24		35866	35901
		36009	203.43
		36027	0.57%
	743		
25		35032	35158
		35246	112.41
		35194	0.32%
29		31232	31367
		31459	119.45
		31410	0.38%
	788		
30		30579	30579
		30552	27.50
		30607	0.09%
	1183		
31		29342	29396
		29333	102.00
		29514	0.35%
35		25437	25288
		25116	161.66
		25310	0.64%
	893		
36		24319	24394
		24373	86.63
		24469	0.36%
	406		
37		23647	23969
		23813	621.46
		24706	2.59%

Table 8 Particle Counts for Latex Reacted with 50mg Con A in Important Thresholds and Channels

[illegible] A-LATEX AGGLUTINATION
LATEX 2.02 MICRON [illegible] DIL.
DECREASING FROM CRIT 250 ML VOL.
+2 ML CON A (2 MG/ML)
+2 ML CONTROL LATEX

ATTENUATION 1
ORIFICE 70 MICRON
SAMPLE SIZE 50 LAMBDA
NOW ON FILE

+50 MG CON A

5		34859	34770	17		40378	40603
		34953	189.28			40379	389.42
		34699	0.54%			41053	0.96%
	-824				465		
6		35555	35594	18		40069	40139
		35664	60.50			40078	112.96
		35564	0.17%			40269	0.28%
	-1137				208		
7		36641	36732	19		39950	39931
		36185	597.18			40084	163.86
		37369	1.63%			39756	0.41%
	-475				-89		
8		37158	37206	20		39743	40020
		37378	153.32			40329	526.44
		37083	0.41%			39687	1.32%
	-552						
9		37822	37759	23		38447	38477
		37750	59.48			38261	212.59
		37704	0.16%			38703	0.55%
	-906				693		
10		38467	38645	24		37754	37784
		35728	175.21			37843	51.97
		38800	0.45%			37745	0.14%
	-188				847		
11		38549	38853	25		37137	36937
		39012	263.09			37042	268.37
		38997	0.66%			36632	0.73%
	-716						
12		39669	39569	29		34107	34027
		39429	124.74			33952	77.62
		39608	0.32%			34022	0.23%
	-294				339		
13		39659	39862	30		33256	33666
		40023	185.71			33632	460.56
		39905	0.47%			34174	1.37%
	-527				1175		
14		39962	40389	31		32561	32513
		40027	664.07			32514	68.00
		41178	1.69%			32445	0.21%
	100						
15		40344	40289	35		28640	28646
		40493	236.35			28555	93.63
		40030	0.59%			28742	0.33%
	-218				949		
16		40527	40507	36		27578	27697
		40466	35.22			27622	169.44
		40527	0.09%			27691	0.61%
	-97				558		
				37		27161	27139
						27108	27.62
						27148	0.10%

Table 9 EFFECT OF CON A CONCENTRATION ON AGGREGATE FORMATION IN CHANNELS 6,12,18,24

CHANNEL 6				CHANNEL 12			
*** INTERPOLATED ***		****** GIVEN ******		*** INTERPOLATED ***		****** GIVEN ******	
x^a	y^b	x^a	y^b	x^a	y^b	x^a	y^b
30.00	6790.9700	30.00	6767.0000	30.00	756.0000	30.00	756.0000
30.50	6053.5700			30.50	1147.1500		
31.00	5430.1960			31.00	1436.2100		
31.50	4797.1110			31.50	1697.2000		
32.00	4194.6200			32.00	1864.1800		
32.50	3622.9700			32.50	2031.2000		
33.00	3082.4900			33.00	2132.3200		
33.50	2573.4100			33.50	2191.5600		
34.00	2095.9900	34.00	2096.0000	34.00	2213.0000	34.00	2213.0000
34.50	1650.5400			34.50	2200.6600		
35.00	1237.3100			35.00	2158.6100		
35.50	856.5820			35.50	2090.6900		
36.00	508.6240			36.00	2001.5600		
36.50	193.7140			36.50	1894.6500		
37.00	-87.8750			37.00	1774.2200		
37.50	-335.8710			37.50	1644.3200		
38.00	-550.0000	38.00	-550.0000	38.00	1509.0000	38.00	1509.0000
38.50	-696.1910			38.50	1410.2100		
39.00	-811.1970			39.00	1310.4900		
39.50	-897.9330			39.50	1210.2800		
40.00	-959.3750			40.00	1109.9900		
40.50	-998.4570			40.50	1010.0900		
41.00	-1018.1800			41.00	910.9990		
41.50	-1021.3900			41.50	813.1560		
42.00	-1011.0000	42.00	-1011.0000	42.00	716.9990	42.00	717.0000
42.50	-995.6960			42.50	624.1780		
43.00	-973.2260			43.00	533.6040		
43.50	-943.0020			43.50	446.2000		
44.00	-910.4270			44.00	361.6670		
44.50	-876.9400			44.50	280.5060		
45.00	-844.9299			45.00	203.2260		
45.50	-816.8110			45.50	129.9220		
46.00	-795.0000	46.00	-795.0000	46.00	61.0000	46.00	61.0000
46.50	-807.3730			46.50	0.2407		
47.00	-828.4620			47.00	-55.6227		
47.50	-858.2370			47.50	-107.1970		
48.00	-896.0890			48.00	-153.8910		
48.50	-943.8050			48.50	-195.9110		
49.00	-999.5720			49.00	-233.2640		
49.50	-1063.9700			49.50	-265.9560		
50.00	-1137.0000	50.00	-1137.0000	50.00	-293.9990	50.00	-294.0000

a = Con A concentration (mg), b = latex count

Table 9 (cont) EFFECT OF CON A CONCENTRATION ON AGGREGATE FORMATION IN CHANNELS 6,12,18,&24

CHANNEL 18				CHANNEL 24			
*** INTERPOLATED ***		****** GIVEN ******		*** INTERPOLATED ***		****** GIVEN ******	
x^a	y^b	x^a	y^b	x^a	y^b	x^a	y^b
30.00	273.0000	30.00	273.0000	30.00	50.9999	30.00	51.0000
30.50	554.0900			30.50	284.5040		
31.00	804.0500			31.00	479.0390		
31.50	1023.9900			31.50	637.6940		
32.00	1214.9300			32.00	763.5620		
32.50	1377.9400			32.50	859.7350		
33.00	1514.0200			33.00	929.3040		
33.50	1624.4100			33.50	975.3620		
34.00	1710.0000	34.00	1710.0000	34.00	1000.9900	34.00	1001.0000
34.50	1771.0900			34.50	1009.3000		
35.00	1811.1600			35.00	1003.3800		
35.50	1826.8600			35.50	986.3110		
36.00	1820.0500			36.00	961.1870		
36.50	1800.8100			36.50	931.1020		
37.00	1768.1700			37.00	899.1460		
37.50	1725.2900			37.50	868.4160		
38.00	1631.0000	38.00	1631.0000	38.00	841.9990	38.00	842.0000
38.50	1511.0000			38.50	820.1240		
39.00	1379.9300			39.00	923.3040		
39.50	1241.4900			39.50	969.1920		
40.00	1099.7400			40.00	1015.4300		
40.50	956.6600			40.50	1059.0900		
41.00	822.2030			41.00	1099.6000		
41.50	694.3260			41.50	1132.8200		
42.00	578.9990	42.00	579.0000	42.00	1156.9900	42.00	1157.0000
42.50	501.3100			42.50	1119.5400		
43.00	537.3260			43.00	1073.1300		
43.50	534.2440			43.50	1020.2000		
44.00	539.2500			44.00	963.1870		
44.50	549.5370			44.50	904.5240		
45.00	562.2960			45.00	846.6480		
45.50	574.7200			45.50	791.5950		
46.00	583.9990	46.00	584.0000	46.00	743.0000	46.00	743.0000
46.50	557.7370			46.50	727.8050		
47.00	525.5300			47.00	720.6910		
47.50	487.3890			47.50	721.6460		
48.00	443.3830			48.00	730.6560		
48.50	393.3420			48.50	747.7090		
49.00	337.4550			49.00	772.7930		
49.50	275.6710			49.50	805.8940		
50.00	207.9990	50.00	208.0000	50.00	846.9990	50.00	847.0000

a = Con A concentration (mg), b = latex count

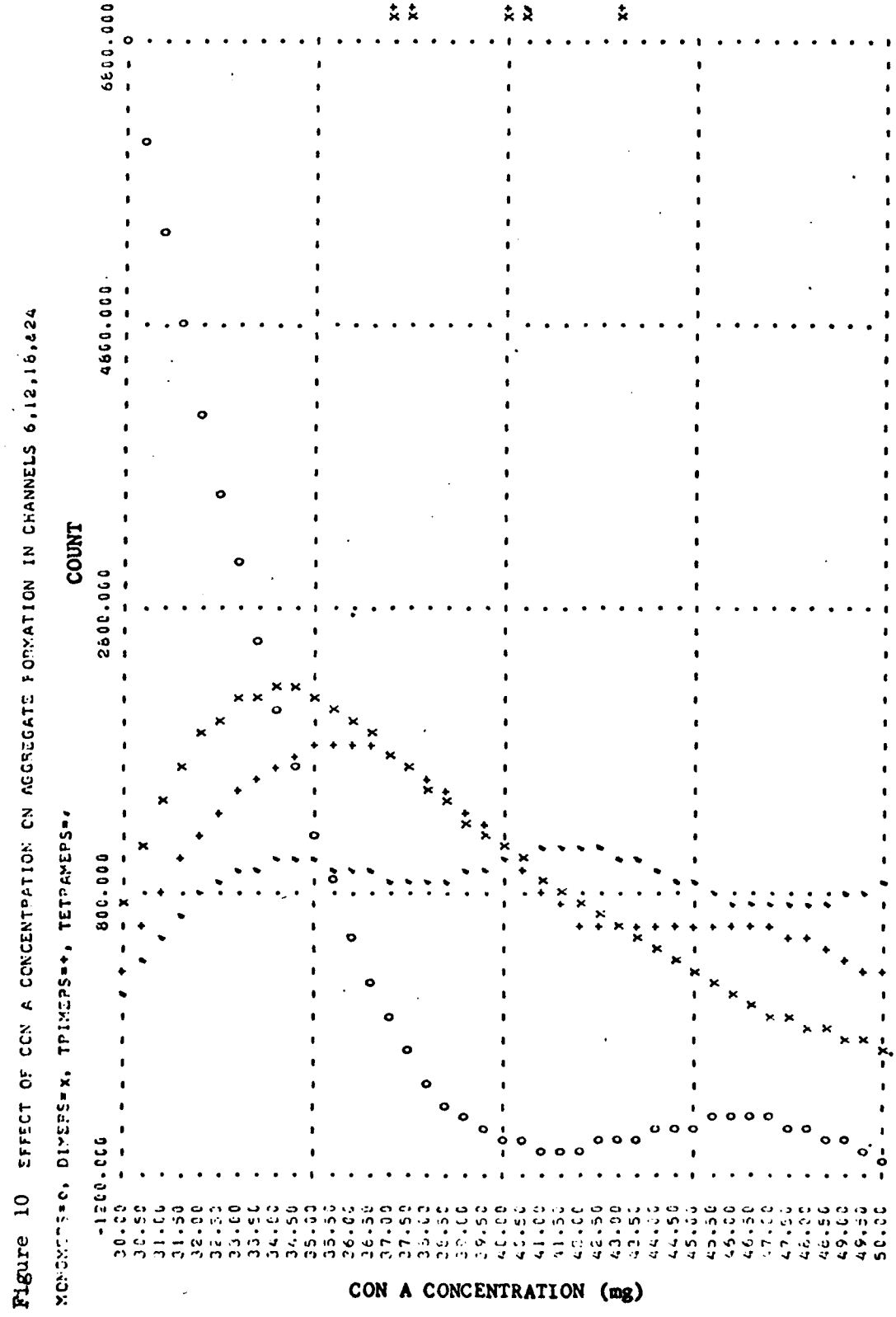
EFFECT OF CON A CONCENTRATION ON AGGREGATE FORMATION IN CHANNELS 6,12,16,424
CONCENTRATION=0, DIMERS=x, TRIMERS=+, TETRAMERS=.
COUNT
-1200.000
800.000
2600.000
4600.000
6600.000
CON A CONCENTRATION (mg)

Figure 10

Table 10 Polynomial Regression of Degrees 1-5 and Statistics for Monomer (Channel 6) Latex Particles as Affected by Con A Concentration

NO.	MONOMER (6) CHANNEL Con A concentration* X	Latex count Y
1	30.0000	6787.0000
2	34.0000	2096.0000
3	38.0000	-550.0000
4	42.0000	-1011.0000
5	46.0000	-795.0000
6	50.0000	-1137.0000

NO. POINTS = 6

X: MEAN= 40 ST.DEV.= 7.483314774
Y: MEAN= 898.3333333 ST.DEV.= 3126.147256

CORR.COEFF.=-0.833617454

POLYNOMIAL REGRESSION DEGREE 1
COEFFICIENTS

B(0)= 14828.04762
B(1)=-348.2428571

R SQUARE = 0.694918060

POLYNOMIAL REGRESSION DEGREE 2
COEFFICIENTS

B(0)= 72372.45949
B(1)=-3311.903554
B(2)= 37.04575872

R SQUARE = 0.963344231

POLYNOMIAL REGRESSION DEGREE 3
COEFFICIENTS

B(0)= 226568.6463
B(1)=-15266.67074
B(2)= 341.5406049
B(3)=-2.537457077

R SQUARE = 0.998318254

POLYNOMIAL REGRESSION DEGREE 4
COEFFICIENTS

B(0)=-40265.6319
B(1)= 12353.05979
B(2)=-719.2200854
B(3)= 15.34416997
B(4)=-0.111760473

R SQUARE = 0.999699200

POLYNOMIAL REGRESSION DEGREE 5
COEFFICIENTS

B(0)=-734827.196
B(1)= 102189.7509
B(2)=-5327.337526
B(3)= 132.5336776
B(4)=-1.589580402
B(5)= 7.39427E-03

R SQUARE = 0.999832395

*Con A concentration expressed as mg

Table 11 Polynomial Regression of Degrees 1-5 and Statistics for Dimer (Channel 12) Latex Particles as Affected by Con A Concentration

NO.	DIMER (12) CHANNEL Con A concentration* X	Latex count Y
1	30.0000	756.0000
2	34.0000	2213.0000
3	38.0000	1509.0000
4	42.0000	717.0000
5	46.0000	61.0000
6	50.0000	-294.0000

NO. POINTS = 6

X: MEAN= 40 ST.DEV.= 7.483314774
Y: MEAN= 827 ST.DEV.= 921.5918836

CORR.COEFF.=-0.724882903

POLYNOMIAL REGRESSION DEGREE 1
COEFFICIENTS

B(0)= 4397.857143
B(1)=-89.27142857

R SQUARE = 0.525455224

POLYNOMIAL REGRESSION DEGREE 2
COEFFICIENTS

B(0)=-10975.98205
B(1)= 702.5142808
B(2)=-9.897321367

R SQUARE = 0.745912680

POLYNOMIAL REGRESSION DEGREE 3
COEFFICIENTS

B(0)=-125108.8207
B(1)= 9565.990090
B(2)=-235.2781292
B(3)= 1.678173418

R SQUARE = 0.966388587

POLYNOMIAL REGRESSION DEGREE 4
COEFFICIENTS

B(0)=-495062.3197
B(1)= 47687.20988
B(2)=-1705.974217
B(3)= 26.67022989
B(4)=-0.154950775

R SQUARE = 0.996932823

POLYNOMIAL REGRESSION DEGREE 5
COEFFICIENTS

B(0)=-1077154.364
B(1)= 123176.7535
B(2)=-5567.904735
B(3)= 124.6833813
B(4)=-1.393469097
B(5)= 6.19693E-03

R SQUARE = 0.998009268

*Con A concentration expressed as mg

Table 12 Polynomial Regression of Degrees 1-5 and Statistics for Trimer (Channel 18) Latex Particles as Affected by Con A Concentration

NO.	TRIMER (18) CHANNEL Con A concentration* X	Latex count Y
1	30.0000	273.0000
2	34.0000	1710.0000
3	38.0000	1631.0000
4	42.0000	579.0000
5	46.0000	584.0000
6	50.0000	208.0000

NO. POINTS = 6

X: MEAN= 40 ST.DEV.= 7.483314774
Y: MEAN= 830.8333333 ST.DEV.= 668.8266585

CORR.COEFF.=-0.380016798

POLYNOMIAL REGRESSION DEGREE 1
COEFFICIENTS

B(0)= 2169.404762
B(1)=-33.96428571

R SQUARE = 0.144412767

POLYNOMIAL REGRESSION DEGREE 2
COEFFICIENTS

B(0)=-12943.45973
B(1)= 745.4107094
B(2)=-9.742187439

R SQUARE = 0.549970123

POLYNOMIAL REGRESSION DEGREE 3
COEFFICIENTS

B(0)=-116376.8909
B(1)= 8777.978078
B(2)=-213.9946231
B(3)= 1.702103648

R SQUARE = 0.693774686

POLYNOMIAL REGRESSION DEGREE 4
COEFFICIENTS

B(0)=-500497.2979
B(1)= 48566.6612
B(2)=-1741.009184
B(3)= 27.44354102
B(4)=-0.160684422

R SQUARE = 0.956294780

POLYNOMIAL REGRESSION DEGREE 5
COEFFICIENTS

B(0)= 1515088.938
B(1)=-212135.3519
B(2)= 11631.53915
B(3)=-312.6351083
B(4)= 4.127682150
B(5)=-0.021457850

R SQUARE = 0.980800146

*Con A concentration expressed as mg

Table 13 Polynomial Regression of Degrees 1-5 and Statistics for Tetramer (Channel 24) Latex Particles as Affected by Con A Concentration

NO.	TETRAMER (24) CHANNEL Con A concentration* X	Latex count Y
1	30.0000	51.0000
2	34.0000	1091.0000
3	38.0000	842.0000
4	42.0000	1157.0000
5	46.0000	743.0000
6	50.0000	847.0000

NO. POINTS = 6

X: MEAN= 40 ST.DEV.= 7.483314774
Y: MEAN= 773.5 ST.DEV.= 382.5858074

CORR.COEFF.= 0.491929818

POLYNOMIAL REGRESSION DEGREE 1
COEFFICIENTS

B(0)=-232.5
B(1)= 25.15

R SQUARE = 0.241994946

POLYNOMIAL REGRESSION DEGREE 2
COEFFICIENTS

B(0)=-9334.062443
B(1)= 493.899997
B(2)=-5.659374964

R SQUARE = 0.690339195

POLYNOMIAL REGRESSION DEGREE 3
COEFFICIENTS

B(0)=-49124.93645
B(1)= 3584.031228
B(2)=-64.43535219
B(3)= 0.654799817

R SQUARE = 0.845637775

POLYNOMIAL REGRESSION DEGREE 4
COEFFICIENTS

B(0)=-114254.7067
B(1)= 10330.42570
B(2)=-343.3492387
B(3)= 5.019404952
B(4)=-0.027278656

R SQUARE = 0.851330827

POLYNOMIAL REGRESSION DEGREE 5
COEFFICIENTS

B(0)=-2107428.658
B(1)= 268133.5663
B(2)=-13567.20170
B(3)= 341.3165543
B(4)=-4.268158770
B(5)= 0.021219249

R SQUARE = 0.924565802

*Con A concentration expressed as mg

CHANNEL 11 LATEX COUNT (MONOMER CHANNEL) = 0, POLYNOMIAL DEGREE 1 = 1, POLYNOMIAL DEGREE 2 = 2, POLYNOMIAL DEGREE 3 = 3, POLYNOMIAL DEGREE 4 = 4, POLYNOMIAL DEGREE 5 = 5

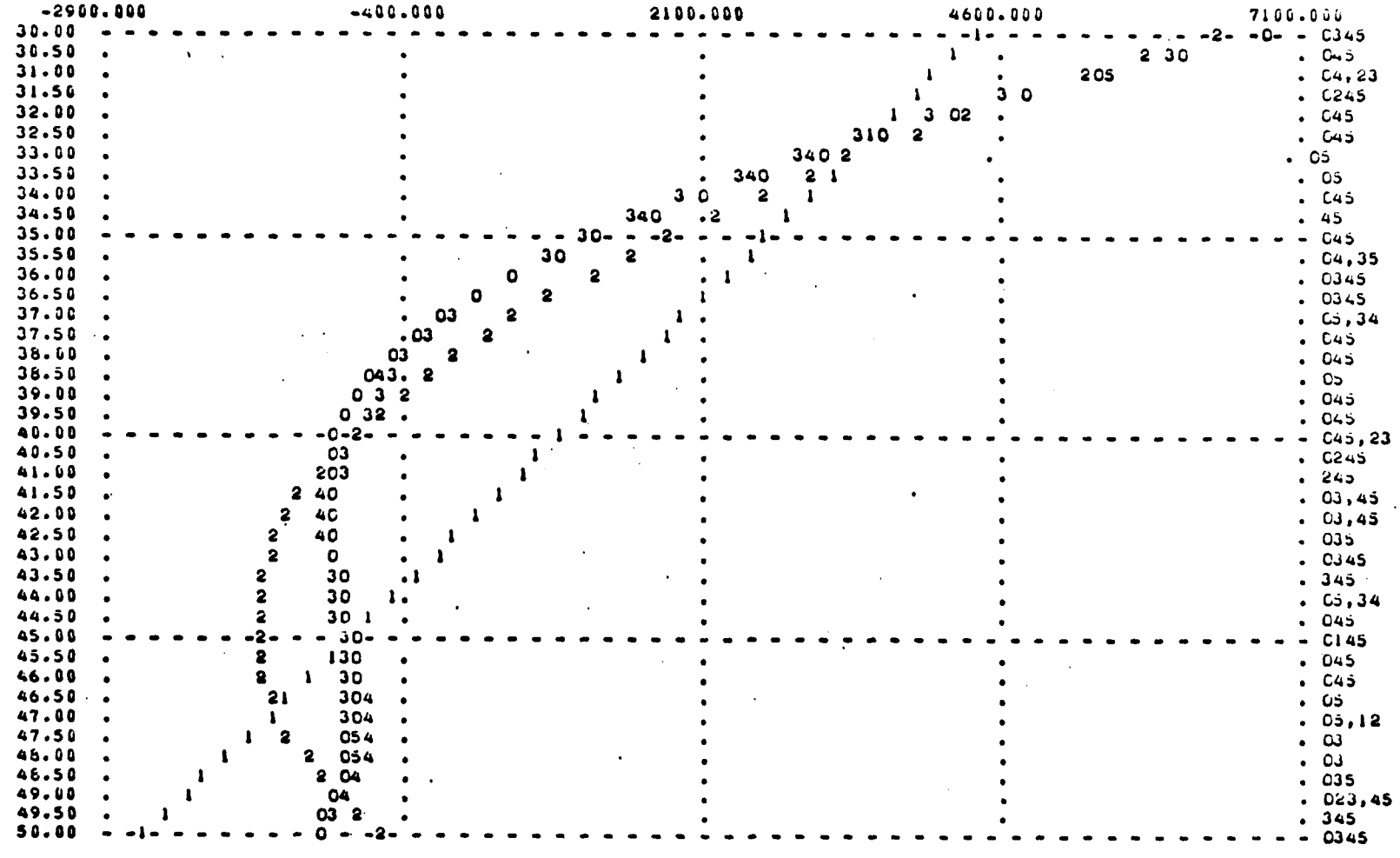

Figure 23 Polynomial regression of degrees 1-5 for monomer (channel 6) latex particle count as affected by Con A concentration

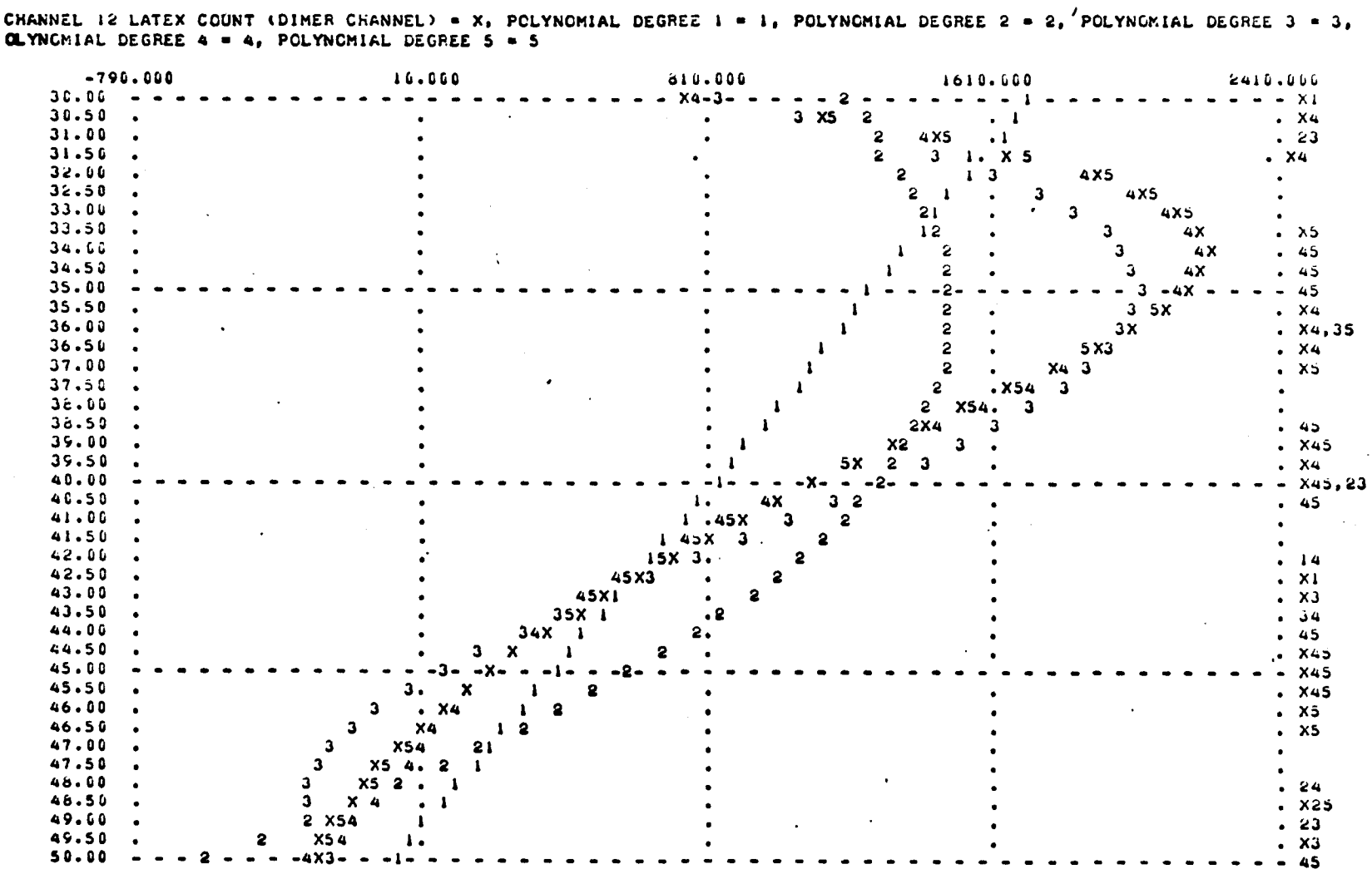

Figure 24 Polynomial regression of degrees 1-5 for dimer (channel 12) latex particle count as affected by Con A concentration

CHANNEL 13 LATEX COUNT (TRIMER CHANNEL) = +, POLYNOMIAL DEGREE 1 = 1, POLYNOMIAL DEGREE 2 = 2, POLYNOMIAL DEGREE 3 = 3, POLYNOMIAL DEGREE 4 = 4, POLYNOMIAL DEGREE 5 = 5

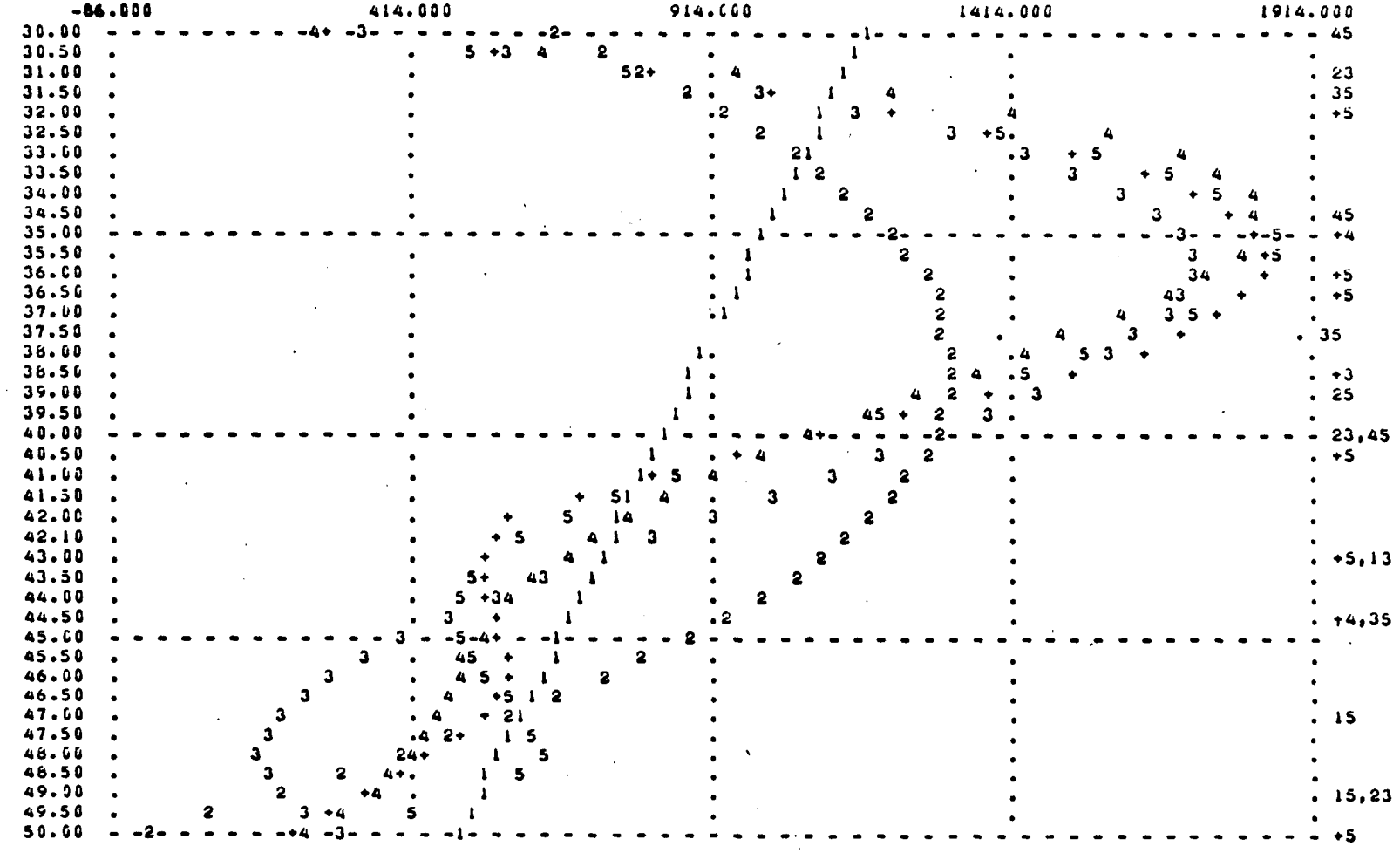

Figure 25 Polynomial regression of degrees 1-5 for trimer (channel 18) latex particle count as affected by Con A concentration

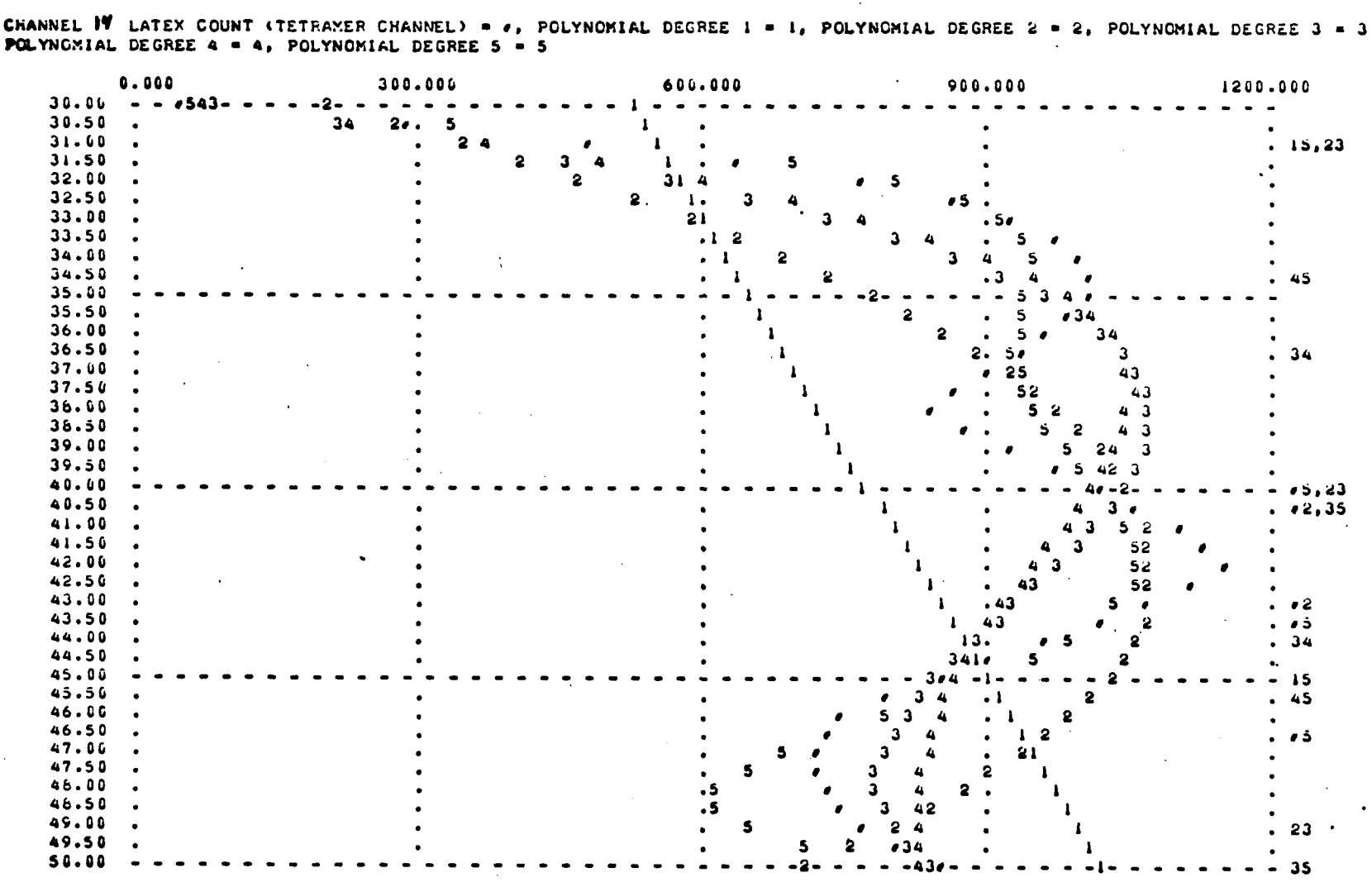

Figure 26 Polynomial regression of degrees 1-5 for tetramer (channel 24) latex particle count as affected by Con A concentration

Table 15 CENTROID ANALYSIS OF CON A INDUCED LATEX AGGLUTINATION (LATEX CONTROL)

CHANNEL	COUNT	MASS	MOMENT2	MOMENT3	MOMENT4	MOMENT5	MOMENT6
5	2026	1.01400E+04	5.07000E+04	2.53500E+05	1.26750E+06	6.33750E+06	3.16875E+07
6	5723	4.03380E+04	2.42028E+05	1.45216E+06	8.71300E+06	5.22780E+07	3.13668E+08
7	4217	2.95190E+04	2.06633E+05	1.44643E+06	1.01250E+07	7.08751E+07	4.96125E+08
8	2865	2.29200E+04	1.83360E+05	1.46688E+06	1.17350E+07	9.38803E+07	7.51042E+08
9	1998	1.79820E+04	1.61838E+05	1.45654E+06	1.31088E+07	1.17979E+08	1.06181E+09
10	868	8.68000E+03	8.68000E+04	8.68000E+05	8.68000E+06	8.68000E+07	8.68000E+08
11	599	6.58900E+03	7.24790E+04	7.97269E+05	8.76995E+06	9.64695E+07	1.06116E+09
12	729	6.74500E+03	1.04976E+05	1.25971E+06	1.51165E+07	1.81398E+08	2.17678E+09
13	521	6.90300E+03	8.97390E+04	1.16660E+06	1.51658E+07	1.97156E+08	2.56303E+09
14	685	9.59000E+03	1.34260E+05	1.87964E+06	2.63149E+07	3.68409E+08	5.15773E+09
15	395	5.92500E+03	8.88750E+04	1.33312E+06	1.99968E+07	2.99953E+08	4.49929E+09
16	273	4.36800E+03	6.98880E+04	1.11820E+06	1.78913E+07	2.86261E+08	4.58017E+09
17	206	3.50200E+03	5.95340E+04	1.01207E+06	1.72053E+07	2.92490E+08	4.97233E+09
18	188	3.38400E+03	6.09120E+04	1.09641E+06	1.97354E+07	3.55236E+08	6.39429E+09
19	78	1.48200E+03	2.81580E+04	5.35002E+05	1.01650E+07	1.93135E+08	3.66957E+09
----	------	----------	----------	----------	----------	----------	----------
180	22363	1.80070E+05	1.64018E+06	1.71415E+07	2.03990E+08	2.69866E+09	3.85967E+10
	CENTROIDS =		9.10856E+00	9.51937E+01	1.13283E+03	1.49867E+04	2.14342E+05

Table 16 CENTROID ANALYSIS OF CON A INDUCED LATEX AGGLUTINATION (+30 MG CON A)

CHANNEL	COUNT	MASS	MOMENT2	MOMENT3	MOMENT4	MOMENT5	MOMENT6
5	2500	1.25000E+04	6.25000E+04	3.12500E+05	1.56250E+06	7.81250E+06	3.90625E+07
6	6787	4.07220E+04	2.44332E+05	1.46599E+06	8.79595E+06	5.27757E+07	3.16654E+08
7	3965	2.77550E+04	1.94285E+05	1.35999E+06	9.51996E+06	6.66397E+07	4.66476E+08
8	2584	2.06720E+04	1.65376E+05	1.32300E+06	1.05840E+07	8.46725E+07	6.77380E+08
9	2041	1.83690E+04	1.65321E+05	1.48788E+06	1.33910E+07	1.20519E+08	1.08467E+09
10	921	9.21000E+03	9.21000E+04	9.21000E+05	9.21000E+06	9.21000E+07	9.21000E+08
11	608	6.68800E+03	7.35680E+04	8.09248E+05	8.90172E+06	9.79190E+07	1.07710E+09
12	756	9.07200E+03	1.08864E+05	1.30636E+06	1.56764E+07	1.88116E+08	2.25740E+09
13	553	7.18900E+03	9.34570E+04	1.21494E+06	1.57942E+07	2.05325E+08	2.66922E+09
14	666	9.32400E+03	1.30536E+05	1.82750E+06	2.55850E+07	3.58190E+08	5.01467E+09
15	361	5.41500E+03	8.12250E+04	1.21837E+06	1.82756E+07	2.74134E+08	4.11201E+09
16	423	6.76800E+03	1.08288E+05	1.73260E+06	2.77217E+07	4.43547E+08	7.09676E+09
17	181	3.07700E+03	5.23090E+04	8.89253E+05	1.51173E+07	2.56994E+08	4.36889E+09
18	273	4.91400E+03	8.84520E+04	1.59213E+06	2.86584E+07	5.15852E+08	9.28533E+09
19	65	1.23500E+03	2.34650E+04	4.45835E+05	8.47086E+06	1.60946E+08	3.05796E+09
----	------	----------	----------	----------	----------	----------	----------
180	22664	1.82910E+05	1.68408E+06	1.79066E+07	2.17265E+08	2.92554E+09	4.24446E+10
	CENTROIDS =		9.20714E+00	9.78983E+01	1.18782E+03	1.59944E+04	2.32051E+05

Table 17 CENTROID ANALYSIS OF CON A INDUCED LATEX AGGLUTINATION (+34 MG CON A)

CHANNEL	COUNT	MASS	MOMENT2	MOMENT3	MOMENT4	MOMENT5	MOMENT6
5	1075	5.37500E+03	2.68750E+04	1.34375E+05	6.71875E+05	3.35937E+06	1.67968E+07
6	2096	1.25760E+04	7.54560E+04	4.52736E+05	2.71641E+06	1.62984E+07	9.77909E+07
7	1529	1.07030E+04	7.49210E+04	5.24447E+05	3.67112E+06	2.56979E+07	1.79885E+08
8	997	7.97600E+03	6.38000E+04	5.10464E+05	4.08371E+06	3.26696E+07	2.61357E+08
9	3578	3.22020E+04	2.89818E+05	2.60836E+06	2.34752E+07	2.11277E+08	1.90149E+09
10	1332	1.33200E+04	1.33200E+05	1.33200E+06	1.33200E+07	1.33200E+08	1.33200E+09
11	2046	2.25060E+04	2.47566E+05	2.72322E+06	2.99554E+07	3.29510E+08	3.62461E+09
12	2213	2.65560E+04	3.18672E+05	3.82406E+06	4.58887E+07	5.50665E+08	6.60798E+09
13	2214	2.87820E+04	3.74166E+05	4.86415E+06	6.32340E+07	8.22042E+08	1.06865E+10
14	2076	2.90640E+04	4.06896E+05	5.69654E+06	7.97516E+07	1.11652E+09	1.56313E+10
15	1736	2.60700E+04	3.91050E+05	5.86575E+06	8.79862E+07	1.31979E+09	1.97969E+10
16	1800	2.88000E+04	4.60800E+05	7.37280E+06	1.17964E+08	1.88743E+09	3.01969E+10
17	1837	3.12290E+04	5.30693E+05	9.02518E+06	1.53428E+08	2.60827E+09	4.43407E+10
18	1710	3.07800E+04	5.54040E+05	9.97272E+06	1.79508E+08	3.23116E+09	5.81609E+10
19	1130	2.14700E+04	4.07930E+05	7.75067E+06	1.47262E+08	2.79799E+09	5.31618E+10
----	------	----------	----------	----------	----------	----------	----------
180	27371	3.27409E+05	4.35609E+06	6.26575E+07	9.52916E+08	1.50859E+10	2.45999E+11
	CENTROIDS =		1.33047E+01	1.91373E+02	2.91047E+03	4.60765E+04	7.51350E+05

Table 18 CENTROID ANALYSIS OF CON A INDUCED LATEX AGGLUTINATION (+38 MG CON A)

CHANNEL	COUNT	MASS	MOMENT2	MOMENT3	MOMENT4	MOMENT5	MOMENT6
5	0	0.00000E+00	0.00000E+00	0.00000E+00	0.00000E+00	0.00000E+00	0.00000E+00
6	0	0.00000E+00	0.00000E+00	0.00000E+00	0.00000E+00	0.00000E+00	0.00000E+00
7	0	0.00000E+00	0.00000E+00	0.00000E+00	0.00000E+00	0.00000E+00	0.00000E+00
8	168	1.34400E+03	1.07520E+04	8.60160E+04	6.88128E+05	5.50502E+06	4.40401E+07
9	36	3.24000E+02	2.91600E+03	2.62440E+04	2.36196E+05	2.12576E+06	1.91318E+07
10	501	5.01000E+03	5.01000E+04	5.01000E+05	5.01000E+06	5.01000E+07	5.01000E+08
11	0	0.00000E+00	0.00000E+00	0.00000E+00	0.00000E+00	0.00000E+00	0.00000E+00
12	1509	1.81080E+04	2.17296E+05	2.60755E+06	3.12906E+07	3.75487E+08	4.50584E+09
13	874	1.13620E+04	1.47706E+05	1.92017E+06	2.49623E+07	3.24510E+08	4.21863E+09
14	26	3.64000E+02	5.09601E+03	7.13440E+04	9.98816E+05	1.39834E+07	1.95767E+08
15	2065	3.09750E+04	4.64625E+05	6.96937E+06	1.04540E+08	1.56810E+09	2.35216E+10
16	1110	1.77600E+04	2.84160E+05	4.54656E+06	7.27449E+07	1.16391E+09	1.86227E+10
17	1167	1.98390E+04	3.37263E+05	5.73347E+06	9.74690E+07	1.65697E+09	2.81685E+10
18	1631	2.93580E+04	5.28444E+05	9.51199E+06	1.71215E+08	3.08186E+09	5.54739E+10
19	949	1.80310E+04	3.42589E+05	6.50919E+06	1.23674E+08	2.34981E+09	4.46465E+10
----	------	----------	----------	----------	----------	----------	----------
180	10036	1.52475E+05	2.39095E+06	3.84829E+07	6.32829E+08	1.05924E+10	1.79918E+11
	CENTROIDS =		1.56809E+01	2.52388E+02	4.15037E+03	6.94696E+04	1.17998E+06

Table 19 CENTROID ANALYSIS OF CON A INDUCED LATEX AGGLUTINATION (+42 MG CON A)

CHANNEL	COUNT	MASS	MOMENT2	MOMENT3	MOMENT4	MOMENT5	MOMENT6
5	0	0.00000E+00	0.00000E+00	0.00000E+00	0.00000E+00	0.00000E+00	0.00000E+00
6	0	0.00000E+00	0.00000E+00	0.00000E+00	0.00000E+00	0.00000E+00	0.00000E+00
7	0	0.00000E+00	0.00000E+00	0.00000E+00	0.00000E+00	0.00000E+00	0.00000E+00
8	0	0.00000E+00	0.00000E+00	0.00000E+00	0.00000E+00	0.00000E+00	0.00000E+00
9	0	0.00000E+00	0.00000E+00	0.00000E+00	0.00000E+00	0.00000E+00	0.00000E+00
10	0	0.00000E+00	0.00000E+00	0.00000E+00	0.00000E+00	0.00000E+00	0.00000E+00
11	0	0.00000E+00	0.00000E+00	0.00000E+00	0.00000E+00	0.00000E+00	0.00000E+00
12	717	8.60400E+03	1.03248E+05	1.23897E+06	1.48677E+07	1.78412E+08	2.14095E+09
13	193	2.50900E+03	3.26170E+04	4.24021E+05	5.51227E+06	7.16595E+07	9.31574E+08
14	454	6.35600E+03	8.89840E+04	1.24577E+06	1.74406E+07	2.44172E+08	3.41840E+09
15	627	9.40500E+03	1.41075E+05	2.11612E+06	3.17418E+07	4.76126E+08	7.14192E+09
16	388	6.20800E+03	9.93280E+04	1.58924E+06	2.54279E+07	4.06847E+08	6.50955E+09
17	972	1.65240E+04	2.80908E+05	4.77543E+06	8.11824E+07	1.38010E+09	2.34617E+10
18	579	1.04220E+04	1.87596E+05	3.37672E+06	6.07811E+07	1.09405E+09	1.96930E+10
19	936	0.77840E+04	3.37896E+05	6.42002E+06	1.21980E+08	2.31762E+09	4.40349E+10
----	------	----------	----------	----------	----------	----------	----------
180	4866	7.76120E+04	1.27165E+06	2.11863E+07	3.58934E+08	6.16899E+09	1.07332E+11
	CENTROIDS =		1.63426E+01	2.72275E+02	4.61284E+03	7.92807E+04	1.37938E+06

Table 20 CENTROID ANALYSIS OF CON A INDUCED LATEX AGGLUTINATION (+46 MG CON A)

CHANNEL	COUNT	MASS	MOMENT2	MOMENT3	MOMENT4	MOMENT5	MOMENT6
5	0	0.00000E+00	0.00000E+00	0.00000E+00	0.00000E+00	0.00000E+00	0.00000E+00
6	0	0.00000E+00	0.00000E+00	0.00000E+00	0.00000E+00	0.00000E+00	0.00000E+00
7	0	0.00000E+00	0.00000E+00	0.00000E+00	0.00000E+00	0.00000E+00	0.00000E+00
8	0	0.00000E+00	0.00000E+00	0.00000E+00	0.00000E+00	0.00000E+00	0.00000E+00
9	0	0.00000E+00	0.00000E+00	0.00000E+00	0.00000E+00	0.00000E+00	0.00000E+00
10	0	0.00000E+00	0.00000E+00	0.00000E+00	0.00000E+00	0.00000E+00	0.00000E+00
11	0	0.00000E+00	0.00000E+00	0.00000E+00	0.00000E+00	0.00000E+00	0.00000E+00
12	61	7.32000E+02	8.78400E+03	1.05408E+05	1.26489E+06	1.51787E+07	1.82145E+08
13	0	0.00000E+00	0.00000E+00	0.00000E+00	0.00000E+00	0.00000E+00	0.00000E+00
14	252	3.52800E+03	4.93920E+04	6.91488E+05	9.68083E+06	1.35531E+08	1.89744E+09
15	241	3.61500E+03	5.42250E+04	8.13375E+05	1.22006E+07	1.83009E+08	2.74514E+09
16	117	1.87200E+03	2.99520E+04	4.79232E+05	7.66771E+06	1.22683E+08	1.96293E+09
17	142	2.41400E+03	4.10380E+04	6.97646E+05	1.18599E+07	2.01619E+08	3.42753E+09
18	584	1.05120E+04	1.89216E+05	3.40586E+06	6.13059E+07	1.10350E+09	1.98631E+10
19	419	7.96100E+03	1.51259E+05	2.87392E+06	5.46044E+07	1.03748E+09	1.97122E+10
----	------	----------	----------	----------	----------	----------	----------
180	1816	3.06340E+04	5.23866E+05	9.06695E+06	1.58584E+08	2.79900E+09	4.97905E+10
	CENTROIDS =		1.71008E+01	2.95977E+02	5.17674E+03	9.13691E+04	1.62533E+06

Table 21 CENTROID ANALYSIS OF CON A INDUCED LATEX AGGLUTINATION (+50 MG CON A)

CHANNEL	COUNT	MASS	MOMENT2	MOMENT3	MOMENT4	MOMENT5	MOMENT6
5	0	0.00000E+00	0.00000E+00	0.00000E+00	0.00000E+00	0.00000E+00	0.00000E+00
6	0	0.00000E+00	0.00000E+00	0.00000E+00	0.00000E+00	0.00000E+00	0.00000E+00
7	0	0.00000E+00	0.00000E+00	0.00000E+00	0.00000E+00	0.00000E+00	0.00000E+00
8	0	0.00000E+00	0.00000E+00	0.00000E+00	0.00000E+00	0.00000E+00	0.00000E+00
9	0	0.00000E+00	0.00000E+00	0.00000E+00	0.00000E+00	0.00000E+00	0.00000E+00
10	0	0.00000E+00	0.00000E+00	0.00000E+00	0.00000E+00	0.00000E+00	0.00000E+00
11	0	0.00000E+00	0.00000E+00	0.00000E+00	0.00000E+00	0.00000E+00	0.00000E+00
12	0	0.00000E+00	0.00000E+00	0.00000E+00	0.00000E+00	0.00000E+00	0.00000E+00
13	0	0.00000E+00	0.00000E+00	0.00000E+00	0.00000E+00	0.00000E+00	0.00000E+00
14	100	1.40000E+03	1.96000E+04	2.74400E+05	3.84160E+06	5.37824E+07	7.52953E+08
15	0	0.00000E+00	0.00000E+00	0.00000E+00	0.00000E+00	0.00000E+00	0.00000E+00
16	0	0.00000E+00	0.00000E+00	0.00000E+00	0.00000E+00	0.00000E+00	0.00000E+00
17	465	7.90500E+03	1.34385E+05	2.28454E+06	3.88372E+07	6.60233E+08	1.12239E+10
18	208	3.74400E+03	6.73920E+04	1.21305E+06	2.18350E+07	3.93030E+08	7.07454E+09
19	0	0.00000E+00	0.00000E+00	0.00000E+00	0.00000E+00	0.00000E+00	0.00000E+00
180	673	1.30490E+04	2.21377E+05	3.77199E+06	6.45138E+07	1.10705E+09	1.90514E+10
	CENTROIDS =		1.69651E+01	2.89064E+02	4.94397E+03	8.48376E+04	1.45599E+06

Table 22 CENTROID ANALYSIS OF LATEX AGGLUTINATION AT VARIOUS CONCENTRATIONS OF CON A

LATEX CONTROL				+30 MG CON A			
*** INTERPOLATED ***		****** GIVEN ******		*** INTERPOLATED ***		****** GIVEN ******	
X	Y	X	Y	X	Y	X	Y
5.00	2028.0000	5.00	2028.0000	5.00	2500.0000	5.00	2500.0000
5.20	3944.1200			5.20	4336.5200		
5.40	5304.8300			5.40	5615.0800		
5.60	6177.0000			5.60	6404.0800		
5.80	6627.4400			5.80	6771.9200		
6.00	6722.9900	6.00	6723.0000	6.00	6787.0000	6.00	6787.0000
6.20	6530.5100			6.20	6517.7200		
6.40	6116.5300			6.40	6032.4800		
6.60	5548.7900			6.60	5399.6800		
6.80	4893.2300			6.80	4687.7200		
7.00	4216.9900	7.00	4217.0000	7.00	3965.0000	7.00	3965.0000
7.20	3875.6800			7.20	3592.6100		
7.40	3575.1800			7.40	3273.4400		
7.60	3310.1300			7.60	3002.0700		
7.80	3075.1900			7.80	2773.8600		
8.00	2864.9900	8.00	2865.0000	8.00	2584.0000	8.00	2584.0000
8.20	2676.7300			8.20	2453.6400		
8.40	2501.6800			8.40	2345.4800		
8.60	2334.4700			8.60	2248.2000		
8.80	2168.5000			8.80	2150.4800		
9.00	1998.0000	9.00	1998.0000	9.00	2041.0000	9.00	2041.0000
9.20	1757.0700			9.20	1818.8700		
9.40	1514.6100			9.40	1584.7300		
9.60	1279.6200			9.60	1349.6600		
9.80	1061.0800			9.80	1124.7200		
10.00	868.0000	10.00	868.0000	10.00	920.9990	10.00	921.0000
10.20	760.1030			10.20	804.9110		
10.40	682.9510			10.40	718.3350		
10.60	632.6470			10.60	658.5030		
10.80	606.0950			10.80	622.6470		
11.00	598.9990	11.00	599.0000	11.00	607.9990	11.00	608.0000
11.20	616.3430			11.20	626.7040		
11.40	643.8310			11.40	657.3520		
11.60	675.6470			11.60	693.4480		
11.80	705.9750			11.80	728.4960		
12.00	728.9990	12.00	729.0000	12.00	756.0000	12.00	756.0000
12.20	693.6800			12.20	722.1350		
12.40	651.0800			12.40	679.5670		
12.60	606.0400			12.60	633.6310		
12.80	564.2000			12.80	589.6630		
13.00	531.0000	13.00	531.0000	13.00	552.9990	13.00	553.0000
13.20	559.1110			13.20	573.6080		
13.40	594.9350			13.40	601.3840		
13.60	632.1030			13.60	629.6560		
13.80	664.2470			13.80	653.3520		
14.00	684.9990	14.00	685.0000	14.00	666.0000	14.00	666.0000
14.20	642.9360			14.20	613.3200		
14.40	588.0080			14.40	550.2000		
14.60	525.1120			14.60	482.9200		
14.80	459.1440			14.80	417.7600		

Table 22 (cont) CENTROID ANALYSIS OF LATEX AGGLUTINATION AT VARIOUS CONCENTRATIONS OF CON A

LATEX CONTROL				+30 MG CON A			
*** INTERPOLATED ***		****** GIVEN ******		*** INTERPOLATED ***		****** GIVEN ******	
X	Y	X	Y	X	Y	X	Y
15.00	395.0000	15.00	395.0000	15.00	361.0000	15.00	361.0000
15.20	360.7750			15.20	365.5110		
15.40	332.3670			15.40	379.3350		
15.60	308.8710			15.60	397.1030		
15.80	289.3830			15.80	413.4470		
16.00	272.9990	16.00	273.0000	16.00	422.9990	16.00	423.0000
16.20	255.3920			15.20	378.5030		
16.40	239.9360			16.40	326.9510		
16.60	226.5840			16.60	273.4470		
16.80	215.2880			16.80	223.0950		
17.00	206.0000	17.00	206.0000	17.00	180.9990	17.00	181.0000
17.20	202.9920			17.20	192.9670		
17.40	200.8160			17.40	213.2240		
17.60	198.3440			17.60	236.6960		
17.80	194.4480			17.80	258.3120		
18.00	188.0000	18.00	188.0000	18.00	273.0000	18.00	273.0000
18.20	173.3500			18.20	255.3700		
18.40	155.0240			18.40	225.7480		
18.60	133.0210			18.60	184.1410		
18.80	007.3460			18.80	130.5550		
19.00	78.0000	19.00	78.0000	19.00	65.0000	19.00	65.0000

Table 23 CENTROID ANALYSIS OF LATEX AGGLUTINATION AT VARIOUS CONCENTRATIONS OF CON A

+34 MG CON A				+38 MG CON A			
*** INTERPOLATED ***		****** GIVEN ******		*** INTERPOLATED ***		****** GIVEN ******	
X	Y	X	Y	X	Y	X	Y
5.00	1075.0000	5.00	1075.0000	5.00	0.0000	5.00	0.0000
5.20	1484.1400			5.20	8.0640		
5.40	1777.5300			5.40	10.7520		
5.60	1969.0400			5.60	9.4080		
5.80	2070.7700			5.80	5.3760		
6.00	2096.0000	6.00	2096.0000	6.00	0.0000	6.00	0.0000
6.20	2057.7000			6.20	-5.3760		
6.40	1968.8700			6.40	-9.4080		
6.60	1842.4800			6.60	-10.7519		
6.80	1691.5300			6.80	-8.0640		
7.00	1529.0000	7.00	1529.0000	7.00	0.0000	7.00	0.0000
7.20	1321.3000			7.20	35.1360		
7.40	1139.6300			7.40	73.2480		
7.60	1008.6000			7.60	110.5920		
7.80	952.8550			7.80	143.4240		
8.00	996.9990	8.00	997.0000	8.00	168.0000	8.00	168.0000
8.20	1518.2300			8.20	136.8960		
8.40	2100.4700			8.40	100.9680		
8.60	2660.2000			8.60	67.3920		
8.80	3193.8700			8.80	43.3440		
9.00	3577.9900	9.00	3578.0000	9.00	36.0000	9.00	36.0000
9.20	3265.7700			9.20	031.2560		
9.40	2822.7600			9.40	237.8880		
9.60	2311.2700			9.60	343.3920		
9.80	1793.5800			9.80	435.2640		
10.00	1331.9900	10.00	1332.0000	10.00	501.0000	10.00	501.0000
10.20	1350.2200			10.20	382.8470		
10.40	1456.7900			10.40	249.6630		
10.60	1629.6400			10.60	125.8550		
10.80	1834.7300			10.80	34.6319		
11.00	2046.0000	11.00	2046.0000	11.00	-0.0000	11.00	0.0000
11.20	2110.9600			11.20	273.9280		
11.40	2157.1000			11.40	595.0240		
11.60	2187.4500			11.60	930.0560		
11.80	2205.0700			11.80	1245.7900		
12.00	2212.9900	12.00	2213.0000	12.00	1509.0000	12.00	1509.0000
12.20	2225.6100			12.20	1491.7200		
02.40	2231.8000			12.40	1404.1400		
12.60	2231.7900			12.60	1261.6900		
12.80	2225.7600			12.80	1079.8300		
13.00	2213.9900	13.00	2214.0000	13.00	874.0000	13.00	874.0000
13.20	2199.4700			13.20	622.2400		
13.40	2178.8900			13.40	366.7600		
13.60	2151.7800			13.60	192.3600		
13.80	2117.6400			13.80	63.8400		
14.00	2075.9900	14.00	2076.0000	14.00	26.0000	14.00	26.0000
14.20	2005.2000			14.20	391.0310		
14.40	1931.2000			14.40	824.4950		
14.60	1858.8000			14.60	1279.3400		
14.80	1792.8000			14.80	1708.5200		

Table 23 (cont) CENTROID ANALYSIS OF LATEX AGGLUTINATION AT VARIOUS CONCENTRATIONS OF CON A

+34 MG CON A				+38 MG CON A			
*** INTERPOLATED ***		****** GIVEN ******		*** INTERPOLATED ***		****** GIVEN ******	
X	Y	X	Y	X	Y	X	Y
15.00	1738.0000	15.00	1738.0000	15.00	2064.9900	15.00	2065.0000
15.20	1731.9900			15.20	1995.3200		
15.40	1736.5900			15.40	1817.9400		
15.60	1754.3900			15.60	1594.8900		
15.80	1775.9900			15.80	1348.2300		
16.00	1799.9900	16.00	1800.0000	16.00	1109.9900	16.00	1110.0000
16.20	1813.8400			16.20	1059.8000		
16.40	1825.5800			16.40	1045.2400		
16.60	1834.0900			16.60	1061.4800		
16.80	1838.2700			16.80	1103.6600		
17.00	1837.0000	17.00	1837.0000	17.00	1167.0000	17.00	1167.0000
17.20	1833.9600			17.20	1276.9300		
17.40	1822.0600			17.40	1390.7200		
17.60	1798.9700			17.60	1495.9500		
17.80	1762.3900			17.80	1580.1800		
18.00	1710.0000	18.00	1710.0000	18.00	1631.0000	18.00	1631.0000
18.20	1630.1900			18.20	1586.1600		
18.40	1532.2800			18.40	1495.5200		
18.60	1416.2700			18.60	1359.0900		
18.80	1282.1700			18.80	1176.9100		
19.00	1130.0000	19.00	1130.0000	19.00	949.0000	19.00	949.0000

Table 24 CENTROID ANALYSIS OF LATEX AGGLUTINATION AT VARIOUS CONCENTRATIONS OF CON A

+42 MG CON A				+46 MG CON A			
*** INTERPOLATED ***		****** GIVEN ******		*** INTERPOLATED ***		****** GIVEN ******	
X	Y	X	Y	X	Y	X	Y
5.00	0.0000	5.00	0.0000	5.00	0.0000	5.00	0.0000
5.20	0.0000			5.20	0.0000		
5.40	0.0000			5.40	0.0000		
5.60	0.0000			5.60	0.0000		
5.80	0.0000			5.80	0.0000		
6.00	0.0000	6.00	0.0000	6.00	0.0000	6.00	0.0000
6.20	0.0000			6.20	0.0000		
6.40	0.0000			6.40	0.0000		
6.60	0.0000			6.60	0.0000		
6.80	0.0000			6.80	0.0000		
7.00	0.0000	7.00	0.0000	7.00	0.0000	7.00	0.0000
7.20	0.0000			7.20	0.0000		
7.40	0.0000			7.40	0.0000		
7.60	0.0000			6.60	0.0000		
7.80	0.0000			7.80	0.0000		
8.00	0.0000	8.00	0.0000	8.00	0.0000	8.00	0.0000
8.20	0.0000			8.20	0.0000		
8.40	0.0000			8.40	0.0000		
8.60	0.0000			8.60	0.0000		
8.80	0.0000			8.80	0.0000		
9.00	0.0000	9.00	0.0000	9.00	0.0000	9.00	0.0000
9.20	0.0000			9.20	0.0000		
9.40	0.0000			9.40	0.0000		
9.60	0.0000			9.60	0.0000		
9.80	0.0000			9.80	0.0000		
10.00	0.0000	10.00	0.0000	10.00	0.0000	10.00	0.0000
10.20	-22.9440			10.20	-1.9520		
10.40	-40.1520			10.40	-3.4160		
10.60	-45.8880			10.60	-3.9040		
10.80	-34.4160			10.80	-2.9280		
11.00	-0.0000	11.00	0.0000	11.00	-0.0000	11.00	0.0000
11.20	148.6950			11.20	13.1760		
11.40	310.4060			11.40	27.3280		
11.60	469.4710			11.60	40.9920		
11.80	610.2230			11.80	52.7040		
12.00	717.0000	12.00	717.0000	12.00	61.0000	12.00	61.0000
12.20	646.6470			02.20	44.6400		
12.40	542.8630			12.40	26.8800		
12.60	421.8550			12.60	11.2000		
12.80	299.8310			12.80	1.0800		
13.00	192.9990	13.00	193.0000	13.00	0.0000	13.00	0.0000
03.20	210.3350			13.20	43.7919		
13.40	252.0870			13.40	95.4959		
13.60	311.2710			13.60	150.5030		
13.80	380.9030			13.80	204.2070		
14.00	453.9990	14.00	454.0000	14.00	251.9990	14.00	252.0000
14.20	506.0070			14.20	266.0400		
14.40	551.9030			14.40	270.7600		
14.60	589.0950			14.60	267.3600		
14.80	614.9910			14.80	257.0400		

Table 24 (cont) CENTROID ANALYSIS OF LATEX AGGLUTINATION AT VARIOUS CONCENTRATIONS OF CON A

+42 MG CON A				+46 MG CON A			
*** INTERPOLATED ***		****** GIVEN ******		*** INTERPOLATED ***		****** GIVEN ******	
X	Y	X	Y	X	Y	X	Y
15.00	626.9990	15.00	627.0000	15.00	241.0000	15.00	241.0000
15.20	572.6390			15.20	215.8050		
15.40	511.6790			15.40	190.2670		
15.60	453.9990			15.60	163.3910		
15.80	409.4790			15.80	138.2630		
16.00	387.9990	16.00	388.0000	16.00	116.9990	16.00	117.0000
16.20	496.5600			16.20	101.5030		
16.40	621.6400			16.40	94.1119		
16.60	754.8400			16.60	96.9679		
16.80	875.7600			16.80	112.2150		
17.00	972.0000	17.00	972.0000	17.00	141.9990	17.00	142.0000
17.20	916.2960			17.20	229.8080		
17.40	835.3280			17.40	326.1040		
17.60	742.9120			17.60	422.6960		
17.80	652.8640			17.80	511.3920		
18.00	579.0000	18.00	579.0000	18.00	584.0000	18.00	584.0000
18.20	590.4730			18.20	599.5000		
18.40	63 .9280			18.40	590.7360		
18.60	703.3460			18.60	557.7210		
18.80	804.7100			18.80	500.4700		
19.00	935.9990	19.00	936.0000	19.00	419.0000	19.00	419.0000

Table 25 CENTROID ANALYSIS OF LATEX AGGLUTINATION AT VARIOUS CONCENTRATIONS OF CON A

+50 MG CON A

*** INTERPOLATED ***		****** GIVEN ******	
X	Y	X	Y
4.00	0.0000	5.00	0.0000
5.20	0.0000		
5.40	0.0000		
5.60	0.0000		
5.80	0.0000		
6.00	0.0000	6.00	0.0000
6.20	0.0000		
6.40	0.0000		
6.60	0.0000		
6.80	0.0000		
7.00	0.0000	7.00	0.0000
7.20	0.0000		
7.40	0.0000		
7.60	0.0000		
7.80	0.0000		
8.00	0.0000	8.00	0.0000
8.20	0.0000		
8.40	0.0000		
8.60	0.0000		
8.80	0.0000		
9.00	0.0000	9.00	0.0000
9.20	0.0000		
9.40	0.0000		
9.60	0.0000		
9.80	0.0000		
10.00	0.0000	10.00	0.0000
10.20	0.0000		
10.40	0.0000		
10.60	0.0000		
10.80	0.0000		
11.00	0.0000	11.00	0.0000
11.20	0.0000		
11.40	0.0000		
11.60	0.0000		
11.80	0.0000		
12.00	0.0000	12.00	0.0000
02.20	-3.2000		
12.40	-5.6000		
12.60	-6.4000		
12.80	-4.8000		
13.00	0.0000	13.00	0.0000
13.20	21.5999		
13.40	44.7999		
13.60	67.1999		
13.80	86.3999		
14.00	99.9999	14.00	100.0000
14.20	86.4000		
14.40	67.2000		
14.60	44.8000		
14.80	21.6000		

Table 25 (cont) CENTROID ANALYSIS OF LATEX AGGLUTINATION AT VARIOUS CONCENTRATIONS OF CON A

+50 MG CON A

=== INTERPOLATED ===		====== GIVEN ======	
X	Y	X	Y
15.00	0.0000	15.00	0.0000
15.20	-19.6799		
15.40	-32.4099		
15.60	-35.3599		
15.80	-25.5199		
16.00	0.0000	16.00	0.0000
16.20	93.7839		
16.40	196.6710		
16.60	299.1670		
16.80	391.7750		
17.00	464.9990	17.00	465.0000
17.20	446.6980		
17.40	405.6640		
17.60	348.0960		
17.80	280.1510		
18.00	207.9990	18.00	208.0000
18.20	162.4840		
18.40	118.9280		
18.60	77.3294		
18.80	37.6671		
19.00	-0.0000	19.00	0.0000

gure 15 CENTROID ANALYSIS OF LATEX AGGLUTINATION AT VARIOUS CONCENTRATIONS OF CON A

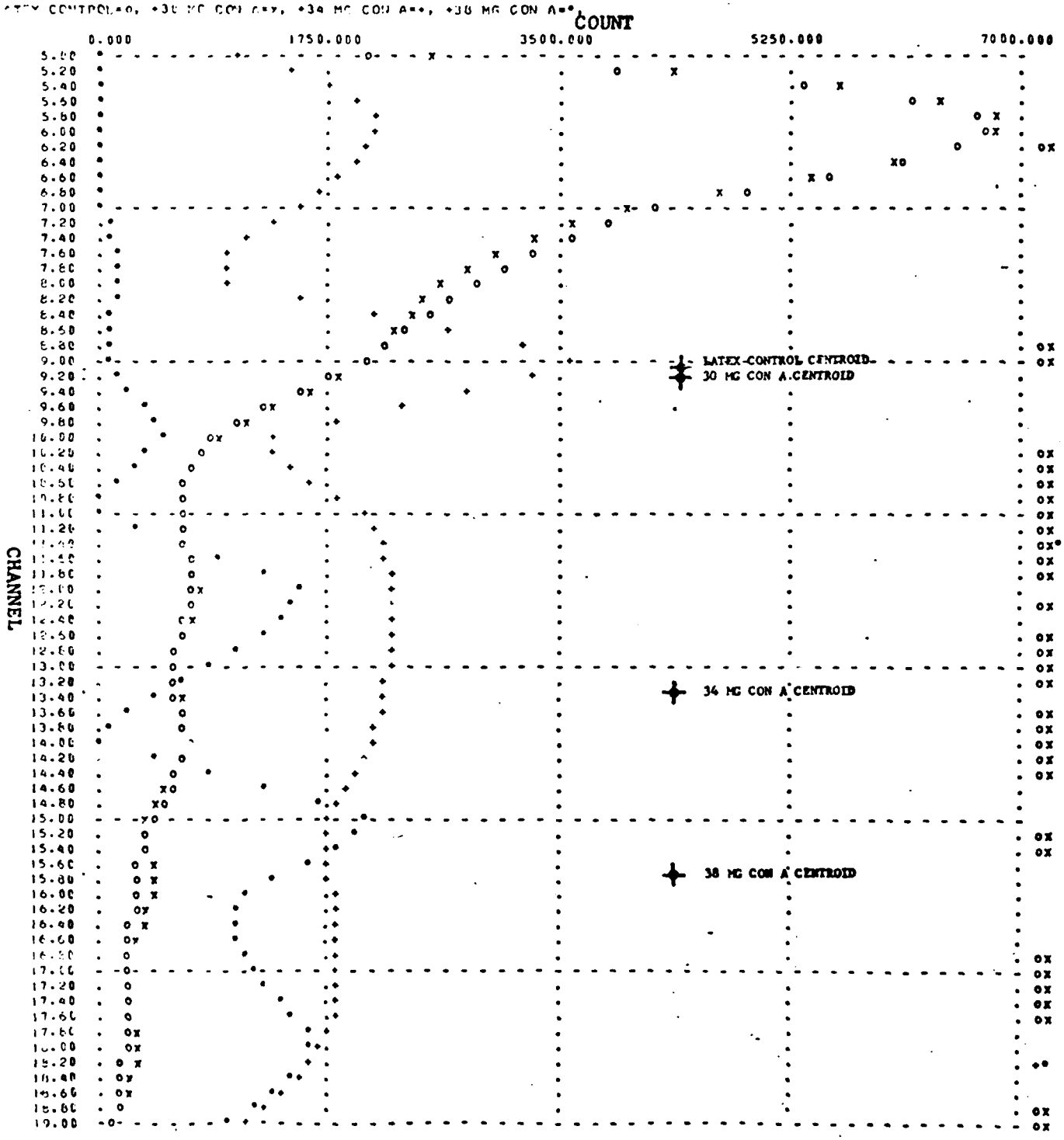

re 16 CENTROID ANALYSIS OF LATEX AGGLUTINATION AT VARIOUS CONCENTRATIONS OF CON A

MG CON A**, 46 MG CON A**, 50 MG CON A**,

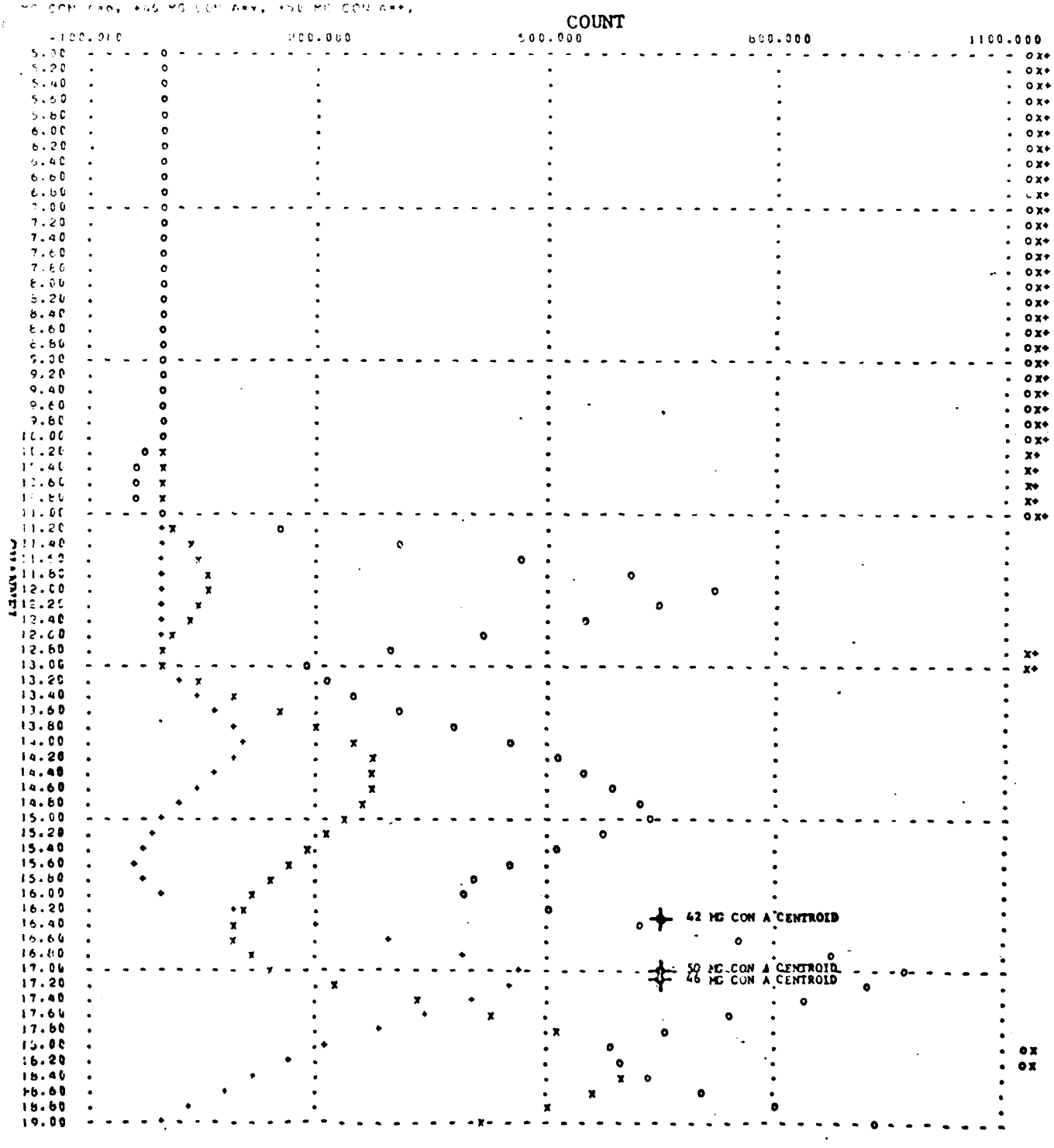

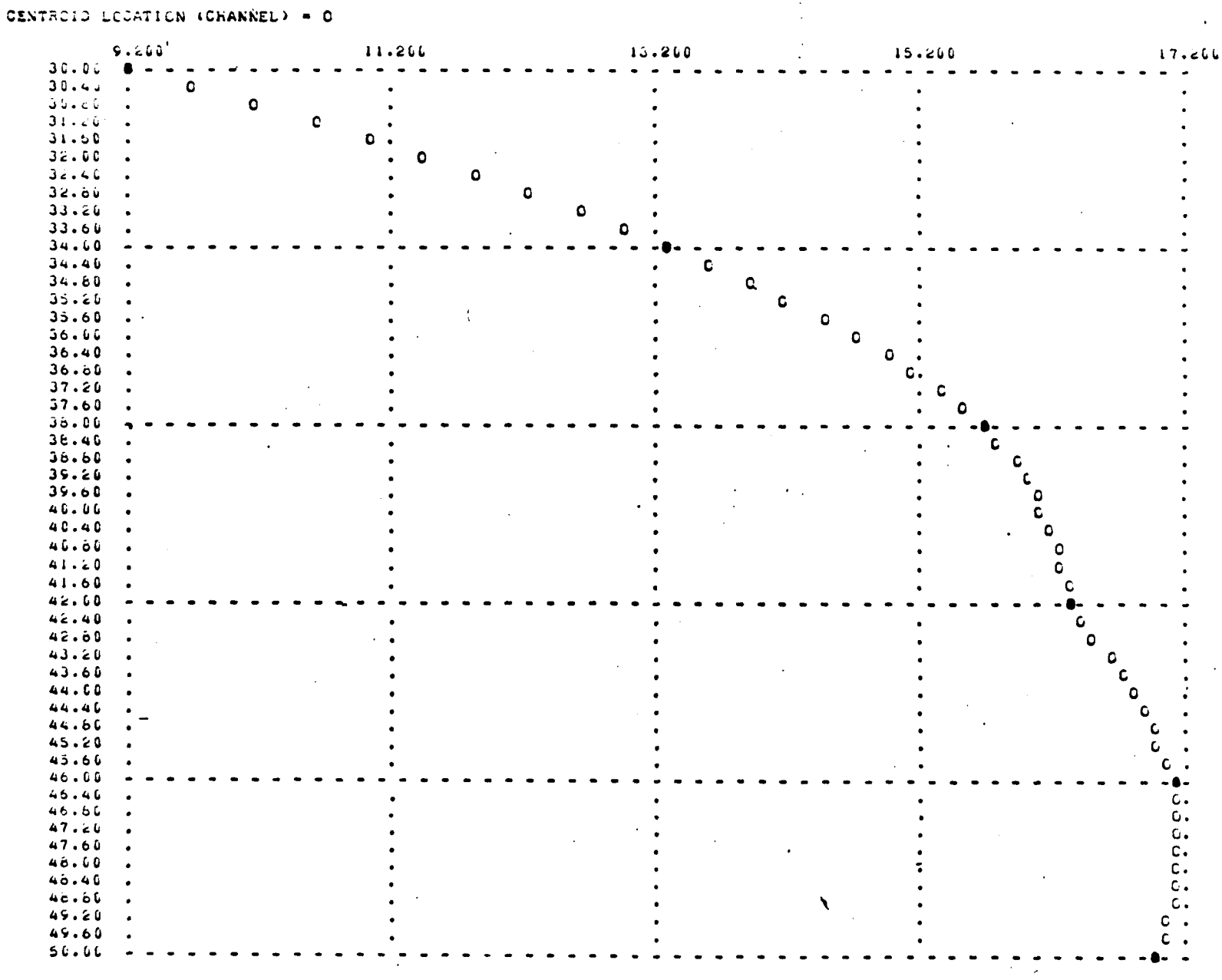

Fig 17 Centroid location shift as a function of Con A concentration (x-axis = mg Con A)

Table 26 Linear Regression and Statistics for Con A Induced Centroid Location Shift

Con A concentration*	Centroid
31.00	9.21
30.80	10.16
31.60	11.05
32.40	11.87
33.20	12.62
34.00	13.30
34.80	13.92
35.60	14.46
36.40	14.94
37.20	15.34
38.00	15.68
38.80	15.89
39.60	16.05
40.40	16.17
41.20	16.26
42.00	16.34
42.80	16.52
43.60	16.69
44.40	16.85
45.20	16.99
46.00	17.10
46.80	17.14
48.40	17.13
49.20	17.06
50.00	16.97

DATA SET #	1
# OF DATA POINTS	25.00
MEAN OF X	39.70
ST. DEV. OF X	6.04
MEAN OF Y	15.03
ST. DEV. OF Y	2.36
REGRESSION COEF.	0.35
STANDARD ERROR	1.06
CORRELATION COEF.	0.90
X-INTERCEPT	-3.12
Y-INTERCEPT	1.10

EQUATION : Y = (1.095) + (0.351) * X

*Con A concentration expressed as mg

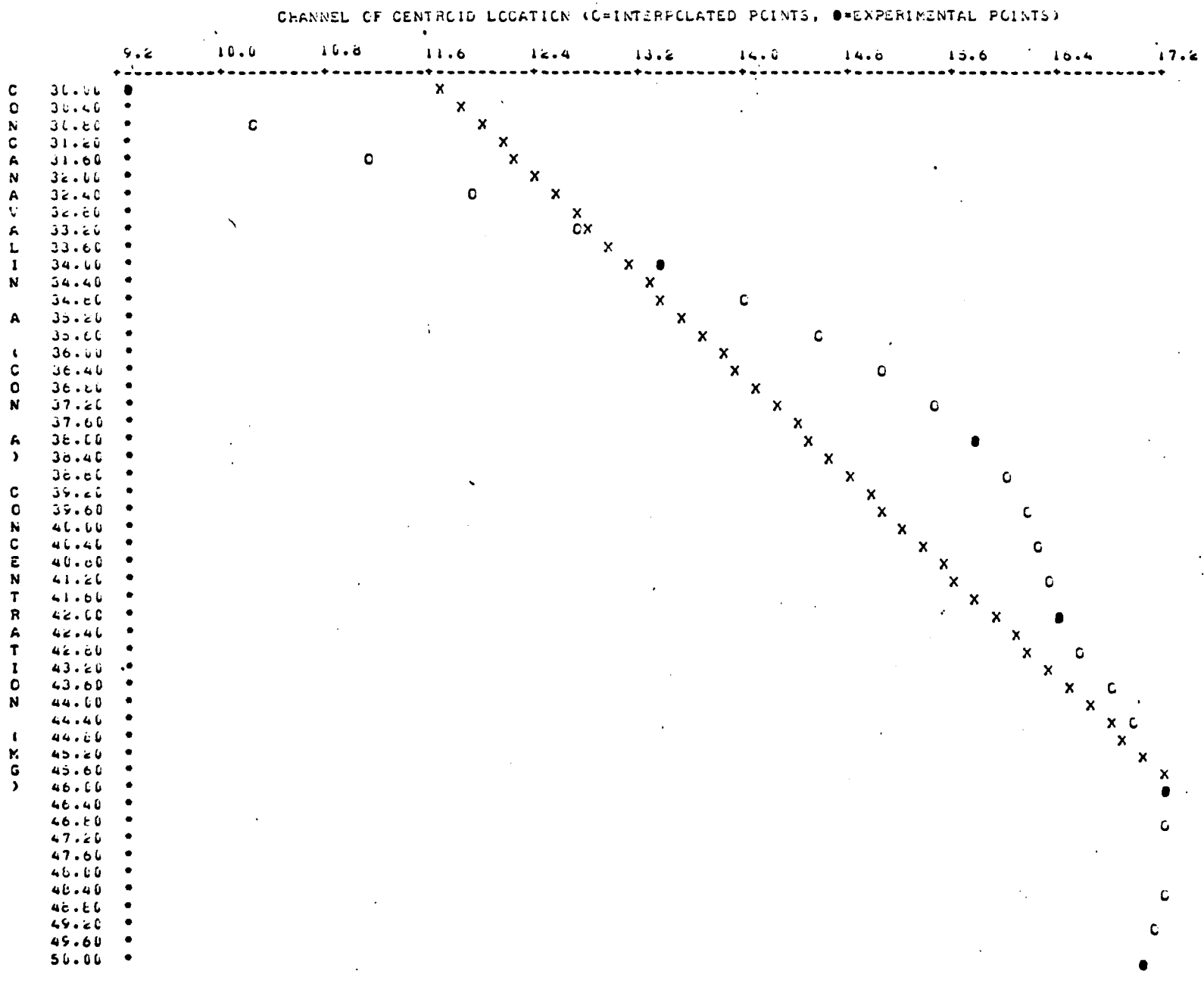

gure 18 Linear regression of Con A induced centroid location shift

Table 27 Polynomial Regression of Degrees 1-4 and Statistics for Con A Induced Centroid Location Shift

NO.	Con A concentration* X	Centroid Y
1	30.0000	9.2071
2	34.0000	13.3047
3	38.0000	15.6809
4	42.0000	16.3426
5	46.0000	17.1008
6	50.0000	16.9651

NO. POINTS = 6

X: MEAN= 40 ST.DEV.= 7.483314774
Y: MEAN= 14.76666667 ST.DEV.= 3.054400230

CORR.COEFF.= 0.889704067

POLYNOMIAL REGRESSION DEGREE 1
COEFFICIENTS

B(0)= 0.241152381
B(1)= 0.363142857

R SQUARE = 0.791573327

POLYNOMIAL REGRESSION DEGREE 2
COEFFICIENTS

B(0)=-47.67380631
B(1)= 2.630866052
B(2)=-0.030646540

R SQUARE = 0.986525355

POLYNOMIAL REGRESSION DEGREE 3
COEFFICIENTS

B(0)=-131.813944
B(1)= 9.365129645
B(2)=-0.197000054
B(3)= 1.38461E-03

R SQUARE = 0.997434023

POLYNOMIAL REGRESSION DEGREE 4
COEFFICIENTS

B(0)=-325.1472246
B(1)= 29.39134168
B(2)=-0.965568266
B(3)= 0.014340645
B(4)=-8.09754E-05

R SQUARE = 0.998193428

*Con A concentration expressed as mg

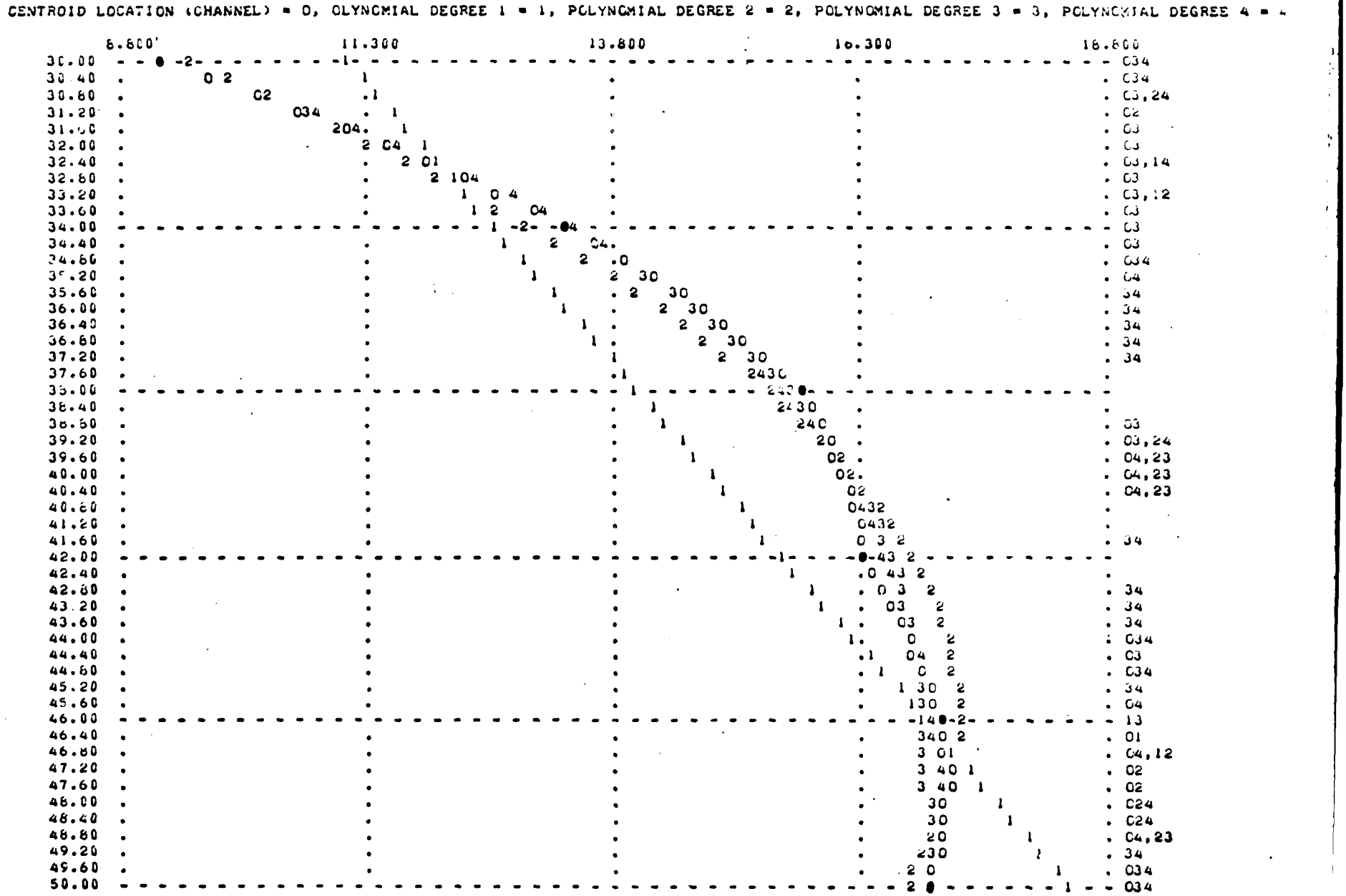

99

Figure 19 Polynomial regression of degrees 1-4 for Con A induced centroid location shift

CLAM PARTICLE DETECTION OF WEE VIRUS AND ANTIBODY BY CENTROID ANALYSIS AND SINGLE-CHANNEL SHIFT

To establish a normal or baseline curve for the latex, 10 sample vials, each containing 20 ml of a 1:20,000 dilution of 2.02 um diameter polyvinyltoluene latex (Dow Chemical Company, Indianapolis, Indiana), were diluted further with 2 ml of Isoton pH 7.4 (Coulter Electronics, Hialeah, Florida) and mixed for 10 cycles in a flip-flop manner. Each vial was counted three times at each threshold setting at the following instrument settings: Attenuation 1, Aperture 16 Sample size 100 , using a Coulter Counter model F equipped with a 70 μl aperture tube. Each group of three sample vials containing an identical 20 ml dilution of latex was prepared by adding 1 ml of Isoton and either 1 ml of WEE virus titered at $1.6x10^6$,10^7,10^8,10^9 LD_{50}/ml or 1 ml of WEE antibody titered at $4.096x10^0$,10^1, 10^2,10^3,10^4/ml hemagglutination inhibition (HI). To two sample vials, one which contained $4.096x10^4$/ml HI and the other which contained $4.096x10^3$/ml HI, was added $1.6x10^9$ LD_{50}/ml and $1.6x10^8$ LD_{50}/ml WEE virus respectively. After each latex-virus, latex-antiserum, or latex-antiserum-virus sampling vial was prepared, it was mixed as before, allowed to set at room temperature for 5 minutes, placed in a 37 C air incubator for 5 minutes, again agitated for 10 cycles, and immediately counted like the normal latex suspension. The threshold counts for normal latex and for each group of three sampling vials were averaged and the channel count was calculated as the difference between threshold counts. For example, if threshold 3 count = 10024 and threshold 4 count = 7531, the channel 3 count = 2493. The values for each concentration of WEE virus, WEE antibody, and WEE virus-WEE antibody combination, in addition to latex control, were then further processed by a computer program to determine interpolated counts (Tables 28-30) and to graph the resulting curve (Fig. 20-21).

Comparisons of channel counts between the suspension of normal latex and suspension to which virus or antibody had been added were accomplished by the process of centroid analysis. The process requires that only the channel and count within that channel be known. As the latex particles adsorb and subsequently aggregate, a shift in total particle mass occurs. According to the following relationships:

$$\text{Mass} = (\text{Channel}_n)\ (\text{Channel}_n\ \text{Count})$$
$$\text{Moment 2} = (\text{Channel}_n^2)\ (\text{Channel}_n\ \text{Count})$$
$$\text{Moment 3} = (\text{Channel}_n^3)\ (\text{Channel}_n\ \text{Count})$$
$$\text{Centroid} = \frac{\Sigma\ \text{Moments}}{\Sigma\ \text{Masses}}$$

the Σ mass of latex particles in any range of channels may be calculated. Also, the moment at various degrees of bias may be determined, depending on the bias desired by the investigator. Tables 37-47 represent centroid analysis of WEE virus and WEE antibody-induced latex adsorption and agglutination. Figures 22 and 23 are expanded graphs of the channels within which the centroid location shifts occur. For example, when 1.6×10^6 LD50/ml of WEE virus was added to the latex suspension, the count in channel 3 was 2540 (Table 28). The count in channel 4 was 2061, and the count in channel 5 was 1490. Therefore to calculate the mass and moment 2:

Channel	
3	Mass = (3)(2540) - 7620
	Moment 2 - (3^2)(2540) - 22860
4	Mass = (4)(2061) - 8244
	Moment 2 - (4^2)(2061) - 32976
5	Mass - (5)(1490) - 7450
	Moment 2 - (5^2)(1490) = 37250

The masses and moments from channel 1 to channel 14 were calculated, summed and the centroid determined:

$$\text{Centroid} = \frac{360760}{73520} = 4.90696$$

In cases where the channel count was negative, a zero value in that channel was assigned for centroid analysis. This was performed because of the operating characteristics of the Coulter Counter which dictate that negative counts in a channel are experimentally impossible. However, because a negative particle is paradoxical, a zero count is the nearest acceptable value for tracing particle movement.

The additional bias of calculating the centroids of moment 3-6 may play a significant role in developing, if required, a "weighing factor" of relative importance of latex aggregates when incorporated into a computer simulation model.

As the concentration of virus and antibody increased, the centroid location shifted from left to right (Figs. 22 and 23). This then indicated a true shift in the mass of the total measured phenomenon. In other words, the bulk of the centroidal cluster of particle counts moved from channels of lower volume displacement as additional adsorption on the latex occurred, or as the latex began to agglutinate and thus was counted in channels of higher volume displacement.

When a plot of the virus or antibody concentration vs. centroid location was derived (Tables 24 and 25, Figs. 48 and 49), the adsorbant induced shift was more dramatically represented. Because of limits in the computer analysis, the latex control sample (no WEE virus) was excluded and only concentrations of WEE virus from 1.6×10^6 to 1.6×10^9 LD_{50}/ml and their interpolated mid-points were plotted (Fig. 24). As the graph represents, the centroid location shifted rather smoothly from 1.6×10^6 LD_{50}/ml to 1.6×10^8 LD_{50}/ml. However a greater concentration of WEE virus (1.6×10^9 LD_{50}/ml) produced a reverse shift or what appeared to be a dissociation of the larger aggregates into those of a smaller size.

Graphic representation of centroid location shift of WEE antibody (Fig. 25) was also affected by computer limits. However, WEE antibody titers from>4.096 to>4.096 x 10^4/ml HI units were found to have almost a linear effect on the centroid location. An apparent stabilization of the centroid occurred between>4.096 x 10^2 and>4.096 x 10^3/ml HI with the maximum shift occurring between>4.096 x 10^3 and>4.096 x 10^4/ml HI.

The WEE antibody-induced centroid location shift curve was defined by linear regression and statistics performed on the data (Table 50, Fig. 26). The curve was fit to a straight line and thus the phenomenon was defined in terms of a linear equation which, within the titered range of antibody, served as a "fingerprint" of the adsorbant-induced effect (Table 50). Thus any new value of centroid location could serve to determine the antibody titer within the bounds of the statistical reliability of such data and statistical reliability of such linear regression.

Because the data did not precisely fit a linear regression, polynomials were then determined for both WEE virus and antibody (Tables 51 and 52) and then plotted (Figs. 27 and 28).

Based upon four data points (darkened in the graph), the polynomial of degree 3 fit the WEE virus curve the best with a R^2 of 1.0000. Although polynomials of degree 1 and 2 did fit exactly at some points on the curve, it was obvious that within the limits of the statistical reliability of the data, and within the interval of measured WEE virus concentration, the 3rd degree polynomial fit the best. Thus, the WEE virus concentration between 1.6 x 10^6 LD_{50}/ml and 1.6 x 10^9 LD_{50}/ml had the effect on centroid location which was expressed by the equation:

$$Y = 22.386616858 - X(-7.598373454) + X^2(1.085550915) + X^3(-0.050783374)$$

By reiteration or establishing a computer memory bank matrix of known centroid location and virus concentration values, the concentration of WEE virus may be determined in an unknown sample. For example, the sample need only be reacted with the latex suspension and counted in the identical channels (channels 1-14) as the known sample. From the data, the centroid location may be calculated, which may then be compared to the centroid location produced from known concentrations of WEE virus. With the relationship of centroid location to the concentration of WEE virus known, the process then becomes one of simply matching the values and determining the virus concentration in the unknown.

Although degree 1-3 polynomials provided certain fitting points on the data curve, WEE antibody was best fit with a polynomial of degree 4 which gave a R^2 of 1.0000. Again, then, the effect of the WEE antibody was described in an equation in which the value of the centroid location could be expressed as a function of WEE antibody. (Y = 4.7488 + X(-0.268233389) + X (0.469325072) + X (-0.194216695) + X (0.025225)). Subsequently, in a sample within which the antibody concentration was not known, computer matrix memory banking of the predetermined antibody concentrations and centroid location values permitted the determination of the antibody concentration in the unknown. Likewise, reiteration from the polynomial equation resulted in the determination of the concentration of antibody in the unknown.

Assuming that latex particles which adsorbed WEE virus at the proper concentration would increase their volume displacement, a shift in particle counts might occur from a channel of lower volume displacement to one of higher volume displacement. This shift would most likely be gradual as "layering" of virus would slowly occur. Because it had been previously determined that latex particles of 2.02 um diameter would be detected in Coulter counts within channel 3, a comparison of counts within channel 3 and within channel 4 was made (Table 53, Fig. 29). As the data and graph indicated, a drop in the count of channel 3 occurred simultaneously with an increase in the count of channel 4 as the WEE virus concentration increased from 1.6×10^6 to 1.6×10^9 LD50/ml. When the data was analyzed by linear regression, the linearity of drop in channel 3 count and linearity of increase in channel 4 count was determined (Fig 30). Likewise, the basic statistics of the regression as well as equations for both channel 3 and channel 4 were calculated (Table 54).

To permit a closer fit to the actual experimental values, polynomials of degree 1-3 were determined for the data of channels 3 and 4. In both cases a polynomial of degree 3 gave the best fit with an R^2 of 1.0000 (Tables 55 and 56, Fig. 31). Therefore, using the same process as described previously, the effect of WEE virus upon the count in channel 3 was defined as:

$Y = -25747.02658 + X(12238.51088) + X^2(-1731.001467) + X^3(79.50006508)$ and the effect in channel 4 was defined as:

$Y = 6358.002266 + X(-1193.167595) + X^2(63.50012503) + X^3(2.666661119)$ where Y = channel count and X = exponent of virus concentration.

By reiteration then, the concentration of WEE virus could be determined by knowing the latex counts within channels 3 and 4. Another method would utilize a table of the known values. Simple matching of data from an unknown sample to data of known samples would indicate the concentration of virus in the unknown.

Thus, it is apparent that the small adsorption of WEE virus on the surface of latex particles can be detected, and trends of adsorption may be projected if the concentration ratio of virus to latex is within the interval of the adsorption phenomenon. The process is, however, not limited to WEE virus and latex, but may also be applicable to other adsorbants such as bacterial toxins, hormones, antibodies, cellular constituents, enzymes, etc. Also particles other than latex may be employed in the method providing they are uniform in diameter to ensure reproducible results and an adsorbant can adsorb to their surfaces. Also, the process could be used to detect small changes in tissue culture or other cells when infected with viruses which induce cellular volume changes.

To determine if the adsorption phenomenon for WEE antibody coated latex (Table 53) was specific, channel 3 and channel 4 of the latex-WEE antibody-WEE virus complex were further analyzed by single channel shift in a like manner as described earlier for only WEE virus or WEE antibody. For example, when latex coated with $>4.096 \times 10^3$/ml HI WEE antibody were reacted with 1.6×10^8 LD_{50}/ml WEE virus, the count in channels 3 and 4 dropped (Fig. 32). In fact, the count dropped in all channels. However, the drop in channel 3 was at a greater slope than the drop in channel 4. Apparently the WEE virus concentration and WEE antibody concentration were not "matched" optimally to permit the demonstration of single channel shift. The most likely explanation was that the WEE antibody concentration was not sufficiently large to enable adequate adsorption of WEE virus in the mean volume population group (channel 3) with the subsequent shifting of count into channel 4.

When latex coated with 4.096×10^4/ml HI WEE antibody were reacted with 1.6×10^9 LD_{50}/ml WEE virus, single channel shift was demonstrated because the latex were (1) sufficiently coated with antibody, and (2) the virus concentration was great enough to permit adequate adsorption with subsequent increase in latex particle volume displacement. Thus the decrease in count in channel 3 (Fig. 33) was followed by an increase in count in channel 4.

Both cases were defined by linear regression and the basic statistics were performed on the experimental data (Tables 57-58). In this manner then, the phenomenon was expressed in a fashion which permitted the reconstruction of the two curves and, in effect, a reference to which the curves produced by an unknown concentration of antibody and virus could be compared and thus identified.

Table 24 Experimental and Interpolated Latex Counts in Channels 1-14 for Latex Control and 1.6×10^6 LD_{50}/ml WEE
CENTROID ANALYSIS OF LATEX AGGLUTINATION AT VARIOUS CONCENTRATIONS OF WEE VI

LATEX CONTROL				1.6X10E6 LD50/ML			
*** INTERPOLATED ***		****** GIVEN ******		*** INTERPOLATED ***		****** GIVEN ******	
X	Y	X	Y	X	Y	X	Y
1.00	10176.9000	1.00	10177.0000	1.00	9917.0000	1.00	9917.0000
1.20	10210.2000			1.20	9780.1500		
1.40	9906.6300			1.40	9384.5700		
1.60	9325.7200			1.60	8777.2200		
1.80	8527.0100			1.80	8005.0400		
2.00	7569.9900	2.00	7570.0000	2.00	7115.0000	2.00	7115.0000
2.20	6514.1800			2.20	6154.0300		
2.40	5419.0700			2.40	5169.0900		
2.60	4344.1600			2.60	4207.1400		
2.80	3346.9700			2.80	3315.1200		
3.00	2492.9900	3.00	2493.0000	3.00	2540.0000	3.00	2540.0000
3.20	2258.0400			3.20	2250.5300		
3.40	2175.7400			3.40	2091.4000		
3.60	2200.0100			3.60	2029.1100		
3.80	2284.7900			3.80	2030.1400		
4.00	2383.9900	4.00	2384.0000	4.00	2061.0000	4.00	2061.0000
4.20	2227.4700			4.20	1953.7700		
4.40	2049.2500			4.40	1842.9600		
4.60	1859.3000			4.60	1728.6700		
4.80	1667.5600			4.80	1610.9800		
5.00	1483.9900	5.00	1484.0000	5.00	1490.0000	5.00	1490.0000
5.20	1362.9600			5.20	1343.5100		
5.40	1258.9000			5.40	1199.4900		
5.60	1170.6500			5.60	1063.6200		
5.80	1097.0700			5.80	941.5670		
6.00	1036.9900	6.00	1037.0000	6.00	838.9990	6.00	839.0000
6.20	1010.7200			6.20	817.5270		
6.40	990.3030			6.40	812.9030		
6.60	969.2150			6.60	816.8150		
6.80	940.9520			6.80	820.9520		
7.00	893.9990	7.00	899.0000	7.00	816.9990	7.00	817.0000
7.20	769.2320			7.20	734.9520		
7.40	629.6560			7.40	643.6150		
7.60	490.6640			7.60	550.1040		
7.80	362.6480			7.80	461.5280		
8.00	256.0000	8.00	256.0000	8.00	384.9990	8.00	385.0000
8.20	258.6160			8.20	382.3520		
8.40	284.0080			8.40	392.2960		
8.60	323.1920			8.60	408.2640		
8.80	367.1840			8.80	423.6680		
9.00	407.0000	9.00	407.0000	9.00	432.0000	9.00	432.0000
9.20	382.8720			9.20	378.0870		
9.40	349.2950			9.40	316.0630		
9.60	309.9630			9.60	251.4950		
9.80	268.6480			9.80	189.9510		
10.00	229.0000	10.00	229.0000	10.00	136.9990	10.00	137.0000
10.20	214.1760			10.20	134.5600		
10.40	203.6080			10.40	142.7600		
10.60	196.1520			10.60	158.0800		
10.80	190.6640			10.80	177.0000		
11.00	186.0000	11.00	186.0000	11.00	196.0000	11.00	196.0000
11.20	177.7830			11.20	196.0710		
11.40	168.9110			11.40	193.0550		
11.60	159.0470			11.60	187.3030		
11.80	147.8550			11.80	179.1670		

Table 28(cont)

CENTROID ANALYSIS OF LATEX AGGLUTINATION AT VARIOUS CONCENTRATIONS OF VEE VIRUS

LATEX CONTROL				1.6X10E6 LD50/ML			
*** INTERPOLATED ***		****** GIVEN ******		*** INTERPOLATED ***		****** GIVEN ******	
X	Y	X	Y	X	Y	X	Y
12.00	134.9990	12.00	135.0000	12.00	168.9990	12.00	169.0000
12.20	112.5600			12.20	154.8160		
12.40	69.6800			12.40	139.8880		
12.60	67.9200			12.60	125.1520		
12.80	48.8400			12.80	111.5440		
13.00	34.0000	13.00	34.0000	13.00	100.0000	13.00	100.0000
13.20	31.2141			13.20	95.2072		
13.40	34.2246			13.40	93.4127		
13.60	43.0282			13.60	94.6145		
13.80	57.6211			13.80	98.8109		
14.00	78.0000	14.00	78.0000	14.00	106.0000	14.00	106.0000

Table 29 Experimental and Interpolated Latex Counts in Channels 1-14 for 1.6×10^7 LD_{50}/ml and 1.6×10^8 LD_{50}/ml WEE Virus
CENTROID ANALYSIS OF LATEX AGGLUTINATION AT VARIOUS CONCENTRATIONS OF EEE VIRUS

1.6X10E7 LD50/ML				1.6X10E8 LD50/ML			
*** INTERPOLATED ***		****** GIVEN ******		*** INTERPOLATED ***		****** GIVEN ******	
X	Y	X	Y	X	Y	X	Y
1.00	9470.0000	1.00	9470.0000	1.00	8287.9900	1.00	8288.0000
1.20	9468.6300			1.20	8516.7400		
1.40	9170.9700			1.40	8399.1100		
1.60	8629.1000			1.60	7994.2000		
1.80	7895.0800			1.80	7361.1300		
2.00	7021.0000	2.00	7021.0000	2.00	6556.9900	2.00	6559.0000
2.20	6058.9100			2.20	5646.9000		
2.40	5060.8900			2.40	4683.9500		
2.60	4079.0200			2.60	3729.2400		
2.80	3165.3660			2.80	2841.8900		
3.00	2372.0000	3.00	2372.0000	3.00	2080.9900	3.00	2081.0000
3.20	2104.0100			3.20	1928.0600		
3.40	1972.2000			3.40	1914.1900		
3.60	1940.3900			3.60	1992.8800		
3.80	1972.3800			3.80	2117.6500		
4.00	2031.9900	4.00	2032.0000	4.00	2241.9900	4.00	2242.0000
4.20	1933.9300			4.20	2076.1900		
4.40	1628.4000			4.40	1877.7700		
4.60	1716.5100			4.60	1661.0600		
4.80	1599.3400			4.80	1440.3600		
5.00	1476.0000	5.00	1478.0000	5.00	1229.9900	5.00	1230.0000
5.20	1336.5500			5.20	1103.3400		
5.40	1197.3700			5.40	1000.8700		
5.60	1065.8200			5.60	922.1270		
5.80	947.2470			5.80	866.6550		
6.00	846.9990	6.00	847.0000	6.00	833.9990	6.00	834.0000
6.20	826.1110			6.20	870.1990		
6.40	820.3350			6.40	916.6790		
6.60	821.1030			6.60	961.3590		
6.80	819.8460			6.80	992.1590		
7.00	806.0000	7.00	808.0000	7.00	996.9990	7.00	997.0000
7.20	706.7190			7.20	853.6560		
7.40	595.2790			7.40	687.7280		
7.60	482.6790			7.60	514.6720		
7.80	377.9190			7.80	349.9440		
8.00	289.9990	8.00	290.0000	8.00	209.0000	8.00	209.0000
8.20	295.1200			8.20	212.0640		
8.40	318.2800			8.40	243.6320		
8.60	351.6800			8.60	292.9660		
8.80	387.5200			8.80	349.3360		
9.00	416.0000	9.00	418.0000	9.00	402.0000	9.00	402.0000
9.20	388.8230			9.20	382.7190		
9.40	350.3110			9.40	352.6390		
9.60	306.2880			9.60	315.3990		
9.80	260.5750			9.80	274.6390		
10.00	216.9990	10.00	217.0000	10.00	233.9990	10.00	234.0000
10.20	196.7260			10.20	211.2950		
10.40	181.9040			10.40	192.4470		
10.60	172.0150			10.60	177.5510		
10.80	166.5510			10.80	166.7030		
11.00	165.0000	11.00	165.0000	11.00	159.9990	11.00	160.0000
11.20	172.2860			11.20	165.7920		
11.40	181.1040			11.40	173.8560		
11.60	189.5760			11.60	182.2240		
11.80	195.8320			11.80	188.9280		

21(cont)

CENTROID ANALYSIS OF LATEX AGGLUTINATION AT VARIOUS CONCENTRATIONS OF VEE VIRUS

1.6X10E7 LD50/ML				1.6X10E8 LD50/ML			
*** INTERPOLATED ***		****** GIVEN ******		*** INTERPOLATED ***		****** GIVEN ******	
X	Y	X	Y	X	Y	X	Y
12.00	196.0000	12.00	196.0000	12.00	192.0000	12.00	192.0000
12.20	177.0560			12.20	172.9270		
12.40	152.5680			12.40	150.4230		
12.60	126.9520			12.60	126.6550		
12.80	102.6240			12.80	103.7910		
13.00	82.0000	13.00	82.0000	13.00	83.9999	13.00	84.0000
13.20	77.1746			13.20	78.1327		
13.40	78.4660			13.40	77.5023		
13.60	85.8697			13.60	82.1054		
13.80	99.3823			13.80	91.9391		
14.00	119.0000	14.00	119.0000	14.00	107.0000	14.00	107.0000

Table 30 Experimental and Interpolated Latex Counts in Channels 1-12 for 1.6×10^9 LD_{50}/ml WEE Virus

CENTROID ANALYSIS OF LATEX AGGLUTINATION AT VARIOUS CONCENTRATIONS OF WEE VIRUS

1.6X10E9 LD50/ML

INTERPOLATED		GIVEN	
X	Y	X	Y
1.00	10461.9000	1.00	10462.0000
1.20	10355.8000		
1.40	9924.2800		
1.60	9228.9500		
1.80	8331.3400		
2.00	7292.9900	2.00	7293.0000
2.20	6175.4500		
2.40	5040.2400		
2.60	3946.9100		
2.80	2962.9800		
3.00	2143.9900	3.00	2144.0000
3.20	2039.7000		
3.40	2103.8700		
3.60	2276.4800		
3.80	2497.5300		
4.00	2706.9900	4.00	2707.0000
4.20	2524.4400		
4.40	2290.3800		
4.60	2024.8900		
4.80	1746.0700		
5.00	1479.9900	5.00	1480.0000
5.20	1333.3700		
5.40	1212.5200		
5.60	1114.3900		
5.80	1035.9000		
6.00	973.9990	6.00	974.0000
6.20	929.3590		
6.40	894.2390		
6.60	864.6390		
6.80	836.5590		
7.00	805.9990	7.00	806.0000
7.20	738.2070		
7.40	667.6230		
7.60	597.9350		
7.80	532.8320		
8.00	475.9990	8.00	476.0000
8.20	461.8800		
8.40	455.7200		
8.60	453.5200		
8.80	451.2800		
9.00	445.0000	9.00	445.0000
9.20	403.2240		
9.40	356.2720		
9.60	307.0080		
9.80	258.2960		
10.00	213.0000	10.00	213.0000
10.20	186.2390		
10.40	165.5590		
10.60	150.7590		
10.80	141.6390		
11.00	137.9990	11.00	138.0000
11.20	149.3680		
11.40	163.3840		
11.60	177.4160		
11.80	186.8320		

Table 20 (cont)

CENTROID ANALYSIS OF LATEX AGGLUTINATION AT VARIOUS CONCENTRATIONS OF WEE VIRUS

1.6X10E9 LD50/ML

*** INTERPOLATED ***		****** GIVEN ******	
X	Y	X	Y
12.00	195.0000	12.00	195.0000
12.20	169.7030		
12.40	139.7910		
12.60	108.5270		
12.80	79.1759		
13.00	54.9999	13.00	55.0000
13.20	52.3405		
13.40	58.1159		
13.60	72.3210		
13.80	94.9508		
14.00	125.9990	14.00	126.0000

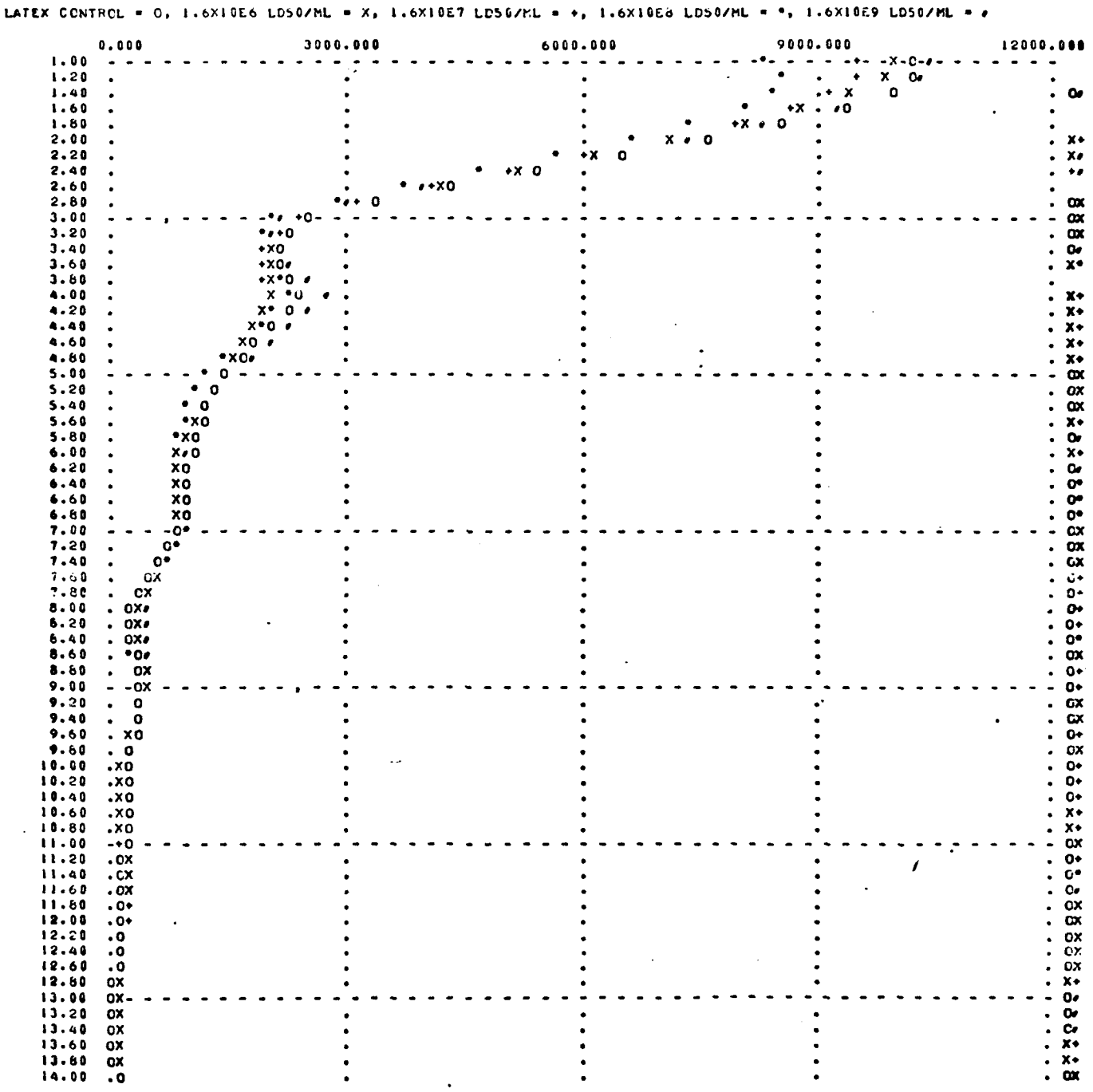

Figure 20 Experimental and interpolated latex counts in channels 1-14 for latex control and various concentrations of WEE virus

Table 31 Experimental and Interpolated Latex Counts in Channels 1-14 for Latex Control and >4.096/ml HI VEE Antibody
CENTROID ANALYSIS OF LATEX AGGLUTINATION AT VARIOUS CONCENTRATIONS OF VEE AB

LATEX CONTROL				>4.096/ML HI			
*** INTERPOLATED ***		****** GIVEN ******		*** INTERPOLATED ***		****** GIVEN ******	
X	Y	X	Y	X	Y	X	Y
1.00	10176.9000	1.00	10177.0000	1.00	6941.0000	1.00	6941.0000
1.20	10210.2000			1.20	6866.4100		
1.40	9906.6300			1.40	6868.4600		
1.60	9326.7200			1.60	6402.1500		
1.80	8527.0100			1.80	7726.3400		
2.00	7569.9900	2.00	7570.0000	2.00	6884.0000	2.00	6884.0000
2.20	6514.1800			2.20	5942.0500		
2.40	5419.0700			2.40	4951.4400		
2.60	4344.1600			2.60	3967.1100		
2.80	3348.9700			2.80	3043.9800		
3.00	2492.9900	3.00	2493.0000	3.00	2237.0000	3.00	2237.0000
3.20	2258.0400			3.20	1962.3700		
3.40	2175.7400			3.40	1823.4400		
3.60	2200.0100			3.60	1784.8300		
3.80	2284.7900			3.80	1811.1400		
4.00	2383.9900	4.00	2384.0000	4.00	1866.9900	4.00	1867.0000
4.20	2227.4700			4.20	1771.6700		
4.40	2049.2500			4.40	1671.4500		
4.60	1859.3000			4.60	1567.3000		
4.80	1667.5600			4.80	1.60.1600		
5.00	1483.9900	5.00	1484.0000	5.00	1351.0000	5.00	1351.0000
5.20	1362.9600			5.20	1227.8800		
5.40	1256.9000			5.40	1107.6600		
5.60	1170.6500			5.60	995.0960		
5.80	1097.0700			5.80	893.7520		
6.00	1036.9900	6.00	1037.0000	6.00	808.0000	6.00	808.0000
6.20	1010.7200			6.20	789.7830		
6.40	990.3030			6.40	783.5510		
6.60	969.2150			6.60	781.5270		
6.80	940.9520			6.80	775.9350		
7.00	898.4990	7.00	899.0000	7.00	756.9990	7.00	759.0000
7.20	769.2320			7.20	656.2560		
7.40	629.6560			7.40	543.2870		
7.60	490.6640			7.60	426.9910		
7.80	362.6480			7.80	322.2630		
8.00	256.0000	8.00	256.0000	8.00	232.0000	8.00	232.0000
8.20	258.6160			8.20	231.4800		
8.40	284.0080			8.40	249.1200		
8.60	323.1920			8.60	277.7200		
8.80	367.1840			8.80	310.0800		
9.00	407.0000	9.00	407.0000	9.00	339.0000	9.00	339.0000
9.20	382.8720			9.20	316.2550		
9.40	349.2950			9.40	285.9270		
9.60	309.9830			9.60	251.0710		
9.80	268.6480			9.80	214.7430		
10.00	229.0000	10.00	229.0000	10.00	179.9990	10.00	180.0000
10.20	214.1760			10.20	165.0320		
10.40	203.6080			10.40	153.9760		
10.60	196.1520			10.60	146.1040		
10.80	190.6640			10.80	140.6680		
11.00	186.0000	11.00	186.0000	11.00	137.0000	11.00	137.0000
11.20	177.7838			11.20	132.6390		
11.40	168.9118			11.40	129.3190		
11.60	159.8478			11.60	126.8790		
11.80	147.8558			11.80	122.7598		
12.00	134.9998	12.00	135.0000	12.00	118.9998	12.00	119.0000
12.20	118.5600			12.20	110.7600		
12.40	89.6800			12.40	102.2800		
12.60	67.9200			12.60	94.1200		
12.80	48.8400			12.80	86.8400		
13.00	34.0000	13.00	34.0000	13.00	81.0000	13.00	81.0000
13.20	31.2141			13.20	79.4048		
13.40	34.2246			13.40	79.6085		
13.60	43.0282			13.60	82.2097		
13.80	57.6211			13.80	86.6072		
14.00	76.0000	14.00	76.0000	14.00	92.9999	14.00	93.0000

Table 32 Experimental and Interpolated Latex Counts in Channels 1-14 for >40.96/ml HI and >409.6/ml HI VEE Antibody
CENTROID ANALYSIS OF LATEX AGGLUTINATION AT VARIOUS CONCENTRATIONS OF VEE AB

>40.96/ML HI				>409.6/ML HI			
*** INTERPOLATED ***		****** GIVEN ******		*** INTERPOLATED ***		****** GIVEN ******	
X	Y	X	Y	X	Y	X	Y
1.00	10016.0000	1.00	10016.0000	1.00	8148.9900	1.00	8149.0000
1.20	10149.2000			1.20	8136.3100		
1.40	9695.6600			1.40	7974.9300		
1.60	9322.4500			1.60	7562.9000		
1.80	8496.8300			1.80	6986.2400		
2.00	7486.0000	2.00	7486.0000	2.00	6288.6900	2.00	6289.0000
2.20	6357.1600			2.20	5513.1900		
2.40	5177.5400			2.40	4700.6500		
2.60	4014.3300			2.60	3694.0200		
2.80	2934.7500			2.80	3134.7200		
3.00	2006.0000	3.00	2006.0000	3.00	2464.9900	3.00	2465.0000
3.20	1753.3300			3.20	2213.3600		
3.40	1671.4000			3.40	2063.7400		
3.60	1712.9100			3.60	1986.5300		
3.80	1830.5400			3.80	1952.1500		
4.00	1976.9900	4.00	1977.0000	4.00	1931.0000	4.00	1931.0000
4.20	1907.1800			4.20	1730.7900		
4.40	1621.0300			4.40	1525.3100		
4.60	1720.6800			4.60	1325.6300		
4.80	1608.2900			4.80	1142.8300		
5.00	1485.9900	5.00	1486.0000	5.00	987.9990	5.00	988.0000
5.20	1339.6500			5.20	962.1190		
5.40	1191.7600			5.40	963.8790		
5.60	1048.5500			5.60	981.8790		
5.80	916.2230			5.80	1004.7100		
6.00	800.9990	6.00	801.0000	6.00	1020.9500	6.00	1021.0000
6.20	759.4310			6.20	955.4160		
6.40	734.8150			6.40	876.4480		
6.60	720.7630			6.60	788.6720		
6.80	710.9670			6.80	696.6640		
7.00	698.9990	7.00	699.0000	7.00	605.0000	7.00	605.0000
7.20	637.2950			7.20	528.9750		
7.40	571.0070			7.40	459.7670		
7.60	504.0710			7.60	399.2710		
7.80	440.4230			7.80	349.3638		
8.00	383.9990	8.00	384.0000	8.00	311.9990	8.00	312.0000
8.20	367.4390			8.20	315.9270		
8.40	358.7992			8.40	329.4240		
8.60	354.8390			8.60	347.6550		
8.80	352.3200			8.80	365.7920		
9.00	347.9990	9.00	348.0000	9.00	379.0000	9.00	379.0000
9.20	317.8390			9.20	352.0470		
9.40	284.5990			9.40	318.1030		
9.60	250.2390			9.60	279.9350		
9.80	216.7190			9.80	240.3110		
10.00	185.9990	10.00	186.0000	10.00	201.9990	10.00	202.0000
10.20	170.1200			10.20	178.4660		
10.40	158.4400			10.40	159.1440		
10.60	150.4000			10.60	144.0560		
10.80	145.4400			10.80	133.3120		
11.00	143.0000	11.00	143.0000	11.00	127.0000	11.00	127.0000
11.20	144.3430			11.20	133.5600		
11.40	146.6318			11.40	142.6480		
11.60	148.8478			11.60	152.2480		
11.80	149.9750			11.80	160.3680		
12.00	148.9990	12.00	149.0000	12.00	165.0000	12.00	165.0000
12.20	134.9520			12.20	47.1670		
12.40	119.2560			12.40	126.1030		
12.60	103.3840			12.60	104.2560		
12.80	88.6060			12.80	83.2719		
13.00	77.0000	13.00	77.0000	13.00	65.9999	13.00	66.0000
13.20	75.3303			13.20	63.4940		
13.40	77.8980			13.40	66.7445		
13.60	84.7006			13.60	75.7480		
13.80	95.7354			13.80	90.5018		
14.00	111.0000	14.00	111.0000	14.00	111.0000	14.00	111.0000

Table 33 Experimental and Interpolated Latex Counts in Channels 1-14 for >4,096/ml HI and >40,960/ml HI WEE Antibody
CENTROID ANALYSIS OF LATEX AGGLUTINATION AT VARIOUS CONCENTRATIONS OF WEE AB

>4,096/ML HI				>40,960/ML HI			
=== INTERPOLATED ===		====== GIVEN ======		=== INTERPOLATED ===		====== GIVEN ======	
X	Y	X	Y	X	Y	X	Y
1.00	9249.9900	1.00	9250.0000	1.00	9409.0000	1.00	9409.0000
1.20	8752.6700			1.20	9348.4200		
1.40	8142.2900			1.40	9037.6300		
1.60	7446.3800			1.60	8520.5200		
1.80	6692.4400			1.80	7841.0100		
2.00	5908.0000	2.00	5908.0000	2.00	7043.0000	2.00	7043.0000
2.20	5120.5500			2.20	6170.3800		
2.40	4357.6100			2.40	5267.0700		
2.60	3646.7000			2.60	4376.9600		
2.80	3015.3200			2.80	3543.9700		
3.00	2491.0000	3.00	2491.0000	3.00	2812.0000	3.00	2812.0000
3.20	2353.4200			3.20	2514.1500		
3.40	2314.8700			3.40	2332.8300		
3.60	2339.8000			3.60	2239.6300		
3.80	2392.6900			3.80	2206.1500		
4.00	2437.9900	4.00	2438.0000	4.00	2203.9900	4.00	2204.0000
4.20	2242.8300			4.20	2098.4200		
4.40	2018.3500			4.40	1993.9500		
4.60	1778.3500			4.60	1888.7600		
4.80	1536.6300			4.80	1781.0500		
5.00	1306.9900	5.00	1307.0000	5.00	1669.0000	5.00	1669.0000
5.20	1165.9900			5.20	1519.9300		
5.40	1048.9700			5.40	1370.6000		
5.60	954.0640			5.60	1226.9100		
5.80	879.3680			5.80	1094.7400		
6.00	823.0000	6.00	823.0000	6.00	979.9990	6.00	980.0000
6.20	802.9750			6.20	942.0790		
6.40	792.5280			6.40	919.9990		
6.60	784.7910			6.60	906.2790		
6.80	772.9030			6.80	893.4390		
7.00	749.9990	7.00	750.0000	7.00	873.9990	7.00	874.0000
7.20	644.0310			7.20	781.1200		
7.40	529.6150			7.40	681.5200		
7.60	416.1630			7.60	582.5600		
7.80	313.1670			7.80	491.6000		
8.00	229.9990	8.00	230.0000	8.00	416.0000	8.00	416.0000
8.20	251.4060			8.20	423.2800		
8.40	292.7040			8.40	445.6000		
8.60	344.4960			8.60	475.2800		
8.80	397.3920			8.80	504.6400		
9.00	442.0000	9.00	442.0000	9.00	526.0000	9.00	526.0000
9.20	411.9990			9.20	480.7990		
9.40	369.1590			9.40	424.9590		
9.60	318.3190			9.60	363.5190		
9.80	264.3190			9.80	301.5190		
10.00	211.9990	10.00	212.0000	10.00	243.9990	10.00	244.0000
10.20	187.1910			10.20	221.1200		
10.40	168.4950			10.40	206.5200		
10.60	155.5030			10.60	196.9600		
10.80	147.6070			10.80	197.2060		
11.00	144.9990	11.00	145.0000	11.00	200.0600	11.00	200.0000
11.20	153.5200			11.20	209.2550		
11.40	164.4000			11.40	219.8670		
11.60	175.5200			11.60	229.6320		
11.80	184.7600			11.80	236.7830		
12.00	190.0000	12.00	190.0000	12.00	238.9990	12.00	239.0000
12.20	171.5200			12.20	215.4240		
12.40	149.2000			12.40	187.7920		
12.60	125.3200			12.60	158.8480		
12.80	102.1600			12.80	131.3360		
13.00	82.0000	13.00	82.0000	13.00	106.0000	13.00	106.0000
13.20	76.2528			13.20	102.5760		
13.40	75.7824			13.40	104.0690		
13.60	80.5856			13.60	112.4730		
13.80	90.6592			13.80	127.7850		
14.00	106.0000	14.00	106.0000	14.00	150.0000	14.00	150.0000

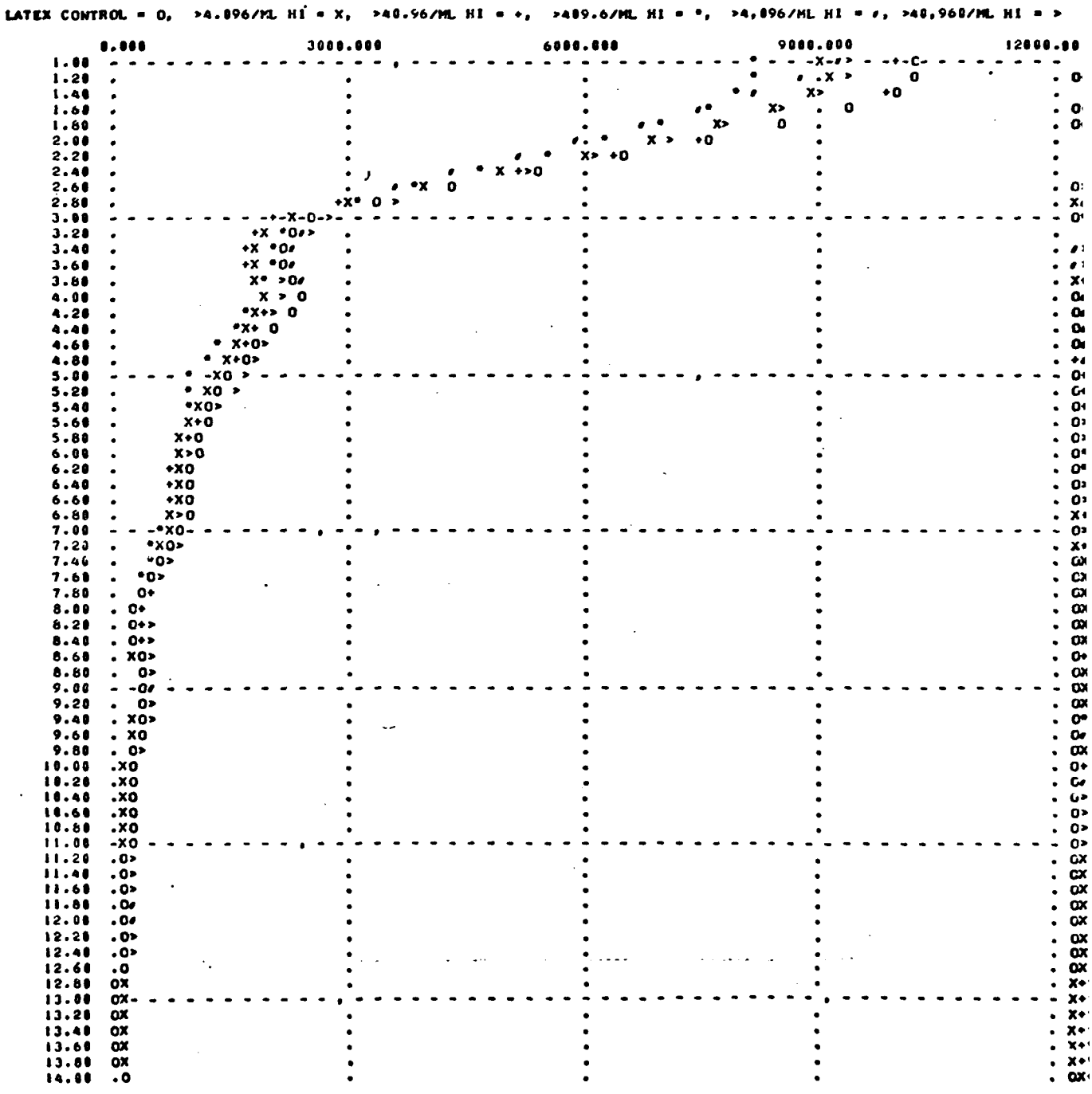

Figure 21 Experimental and interpolated latex counts in channels 1-14 for latex control and various concentrations of WEE antibody

Table 34 Experimental and Interpolated Latex Counts in Channels 1-14 for Latex Control and Latex Coated with >40,960/ml HI WEE Antibo
EFFECT OF WEE VIRUS ON WEE ANTIBODY-COATED 2.02 MICRON LATEX (APER=10,ATTN=1)

LATEX CONTROL COUNT/CHANNEL				>40,960/ML HI WEE ANTIBODY COUNT/CHANNEL			
*** INTERPOLATED ***		****** GIVEN ******		*** INTERPOLATED ***		****** GIVEN ******	
X	Y	X	Y	X	Y	X	Y
1.00	10176.9000	1.00	10177.0000	1.00	9409.0000	1.00	9409.0000
1.25	10163.5000			1.25	9292.4600		
1.50	9647.1200			1.50	8862.1200		
1.75	8743.8500			1.75	8023.7100		
2.00	7569.9900	2.00	7570.0000	2.00	7043.0000	2.00	7043.0000
2.25	6241.7600			2.25	5945.7100		
2.50	4875.3700			2.50	4817.6200		
2.75	3587.0400			2.75	3744.4600		
3.00	2492.9900	3.00	2493.0000	3.00	2812.0000	3.00	2812.0000
3.25	2224.9600			3.25	2459.0100		
3.50	2177.4300			3.50	2276.9900		
3.75	2260.4400			3.75	2210.4800		
4.00	2383.9900	4.00	2384.0000	4.00	2203.9900	4.00	2204.0000
4.25	2164.5600			4.25	2072.2700		
4.50	1955.1200			4.50	1941.5600		
4.75	1715.1200			4.75	1808.3200		
5.00	1483.9900	5.00	1484.0000	5.00	1669.0000	5.00	1669.0000
5.25	1335.4000			5.25	1482.3900		
5.50	1212.6700			5.50	1297.6600		
5.75	1114.1500			5.75	1126.3800		
6.00	1036.9900	6.00	1037.0000	6.00	979.9990	6.00	980.0000
6.25	1005.3200			6.25	935.3670		
6.50	960.2490			6.50	912.5620		
6.75	949.0460			6.75	896.9760		
7.00	898.9990	7.00	899.0000	7.00	873.9990	7.00	874.0000
7.25	784.6510			7.25	756.5620		
7.50	559.4370			7.50	631.5000		
7.75	393.0540			7.75	513.1870		
8.00	256.0000	8.00	256.0000	8.00	416.0000	8.00	416.0000
8.25	263.1790			8.25	427.7500		
8.50	302.4370			8.50	460.0000		
8.75	356.2260			8.75	497.7500		
9.00	407.0000	9.00	407.0000	9.00	526.0000	9.00	526.0000
9.25	375.2160			9.25	467.6400		
9.50	330.1250			9.50	394.6240		
9.75	278.9660			9.75	316.7960		
10.00	229.0000	10.00	229.0000	10.00	243.9990	10.00	244.0000
10.25	211.1790			10.25	216.7420		
10.50	199.5620			10.50	201.9370		
10.75	191.9140			10.75	197.1640		
11.00	186.0000	11.00	186.0000	11.00	200.0000	11.00	200.0000
11.25	175.6400			11.25	211.6510		
11.50	164.1240			11.50	224.9370		
11.75	150.7960			11.75	235.3040		
12.00	134.9990	12.00	135.0000	12.00	238.9990	12.00	239.0000
12.25	106.6200			12.25	208.7890		
12.50	78.5625			12.50	173.3120		
12.75	53.2734			12.75	137.9290		
13.00	34.0000	13.00	34.0000	13.00	106.0000	13.00	106.0000
13.25	31.4234			13.25	102.3010		
13.50	37.9025			13.50	107.4070		
13.75	53.4303			13.75	123.3100		
14.00	78.0000	14.00	78.0000	14.00	150.0000	14.00	150.0000

Table 35 Experimental and Interpolated Latex Counts in Channels 1-14 for Latex Coated with >40,960/ml HI WEE Antibody Plus 1.6×10^9 LD_{50}/ml WEE Virus and Latex Coated with >4,096/ml HI WEE Antibody
EFFECT OF WEE VIRUS ON WEE ANTIBODY-COATED .02 MICRON LATEX (APER=16, ATTN=1)

>40,960/ML HI AB + 1.6X10E9 LD50/ML WEE				>4,096/ML HI WEE ANTIBODY COUNT/CHANNEL			
*** INTERPOLATED ***		****** GIVEN ******		*** INTERPOLATED ***		****** GIVEN ******	
X	Y	X	Y	X	Y	X	Y
1.00	8691.9900	1.00	8692.0000	1.00	9249.9900	1.00	9250.0000
1.25	9408.1000			1.25	8669.6000		
1.50	9386.5600			1.50	7803.3100		
1.75	8780.9900			1.75	6884.8600		
2.00	7744.9900	2.00	7745.0000	2.00	5906.0000	2.00	5906.0000
2.25	6432.1900			2.25	4926.4400		
2.50	4996.1800			2.50	3993.9300		
2.75	3590.5800			2.75	3164.2100		
3.00	2368.9900	3.00	2369.0000	3.00	2491.0000	3.00	2491.0000
3.25	2113.0400			3.25	2335.8900		
3.50	2097.1200			3.50	2321.6200		
3.75	2223.6400			3.75	2378.7900		
4.00	2395.0000	4.00	2395.0000	4.00	2437.9900	4.00	2438.0000
4.25	2229.5000			4.25	2188.9200		
4.50	2027.3100			4.50	1899.4300		
4.75	1804.4600			4.75	1596.4700		
5.00	1577.0000	5.00	1577.0000	5.00	1306.9900	5.00	1307.0000
5.25	1386.5600			5.25	1134.5600		
5.50	1213.3700			5.50	998.8750		
5.75	1063.2500			5.75	896.2500		
6.00	942.0000	6.00	942.0000	6.00	823.0000	6.00	823.0000
6.25	900.9060			6.25	799.7340		
6.50	882.1240			6.50	788.7500		
6.75	873.2810			6.75	776.6400		
7.00	861.9990	7.00	862.0000	7.00	749.9990	7.00	750.0000
7.25	787.2730			7.25	615.8510		
7.50	704.8120			7.50	472.1870		
7.75	621.6950			7.75	337.4290		
8.00	545.0000	8.00	545.0000	8.00	229.9990	8.00	230.0000
8.25	506.9210			8.25	260.2340		
8.50	479.3750			8.50	317.8750		
8.75	459.3900			8.75	364.5760		
9.00	444.0000	9.00	444.0000	9.00	442.0000	9.00	442.0000
9.25	431.0540			9.25	402.3040		
9.50	416.4370			9.50	344.4370		
9.75	396.8510			9.75	277.8510		
10.00	369.0000	10.00	369.0000	10.00	211.9990	10.00	212.0000
10.25	298.8040			10.25	161.9660		
10.50	226.0620			10.50	161.3120		
10.75	159.7690			10.75	149.2570		
11.00	106.9990	11.00	109.0000	11.00	144.9990	11.00	145.0000
11.25	131.4210			11.25	156.1010		
11.50	167.6750			11.50	170.0620		
11.75	207.6900			11.75	182.7420		
12.00	241.0000	12.00	241.0000	12.00	190.0000	12.00	190.0000
12.25	210.4060			12.25	166.2180		
12.50	170.5000			12.50	137.3120		
12.75	129.3430			12.75	107.7570		
13.00	95.0000	13.00	95.0000	13.00	82.0000	13.00	82.0000
13.25	95.7157			13.25	75.6406		
13.50	111.2950			13.50	77.5250		
13.75	141.7270			13.75	87.6469		
14.00	187.0000	14.00	187.0000	14.00	106.0000	14.00	106.0000

Table 36 Experimental and Interpolated Latex Counts in Channels 1-14 for Latex Coated with >4,096/ml HI WEE Antibody Plus 1.6 x 10^8 LD_{50}/ml WEE Virus
EFFECT OF WEE VIRUS ON WEE ANTIBODY-COATED 2.02 MICRON LATEX (APER=16,ATTN=1)

>4,096/ML HI AB + 1.6X10E8 LD50/ML WEE

*** INTERPOLATED ***		****** GIVEN ******	
X	Y	X	Y
1.00	6586.9900	1.00	6587.0000
1.25	9131.3600		
1.50	8766.1800		
1.75	8299.4100		
2.00	7218.9900	2.00	7219.0000
2.25	5892.6900		
2.50	4469.0600		
2.75	3095.4400		
3.00	1920.0000	3.00	1920.0000
3.25	1724.6200		
3.50	1769.7400		
3.75	1949.7400		
4.00	2158.9900	4.00	2159.0000
4.25	1957.3400		
4.50	1707.5000		
4.75	1437.6500		
5.00	1175.9900	5.00	1176.0000
5.25	1027.9400		
5.50	913.5620		
5.75	830.1460		
6.00	774.9990	6.00	775.0000
6.25	781.0780		
6.50	795.7490		
6.75	802.0460		
7.00	782.9990	7.00	783.0000
7.25	616.4060		
7.50	432.6240		
7.75	256.7810		
8.00	113.9990	8.00	114.0000
8.25	146.9840		
8.50	216.2500		
8.75	299.8900		
9.00	376.0000	9.00	376.0000
9.25	342.2810		
9.50	289.3740		
9.75	227.5310		
10.00	166.9990	10.00	167.0000
10.25	149.0850		
10.50	140.5620		
10.75	139.2570		
11.00	143.0000	11.00	143.0000
11.25	150.2030		
11.50	157.8750		
11.75	163.6090		
12.00	165.0000	12.00	165.0000
12.25	145.4210		
12.50	122.3750		
12.75	99.1406		
13.00	78.9999	13.00	79.0000
13.25	73.4496		
13.50	74.2693		
13.75	81.4544		
14.00	94.9999	14.00	95.0000

Table 37 CENTROID ANALYSIS OF WEE VIPUS INDUCED LATEX AGGLUTINATION (LATEX CONTROL)

CHANNEL	COUNT	MASS	MOMENT2	MOMENT3	MOMENT4	MOMENT5	MOMENT6
1	10177	1.01770E+04	1.01770E+04	1.01770E+04	1.01770E+04	1.01770E+04	1.01770E+04
2	7570	1.51400E+04	3.02800E+04	6.05600E+04	1.21120E+05	2.42240E+05	4.844[illegible]E+05
3	2493	7.47900E+03	2.2437[illegible]E+04	6.73110E+04	2.01933E+05	6.05799E+05	1.81740E+06
4	2384	9.53600E+03	3.81440E+04	1.52576E+05	6.10304E+05	2.44122E+06	9.76488E+06
5	1484	7.42000E+03	3.71000E+04	1.85500E+05	9.27500E+05	4.63750E+06	2.31[illegible]E+07
6	1037	6.22200E+03	3.73320E+04	2.23992E+05	1.34395E+06	8.06371E+06	4.83822E+07
7	699	6.29300E+03	4.40510E+04	3.08357E+05	2.15650E+06	1.51095E+07	1.05766E+08
8	256	2.64800E+03	1.63840E+04	1.31072E+05	1.04858E+06	8.38861E+06	6.71089E+07
9	407	3.66300E+03	3.29670E+04	2.96703E+05	2.67033E+06	2.40329E+07	2.16296E+08
10	229	2.29000E+03	2.29000E+04	2.29000E+05	2.29000E+06	2.29000E+07	2.29000E+08
11	186	2.04600E+03	2.25060E+04	2.47566E+05	2.72323E+06	2.99555E+07	3.29510E+08
12	135	1.62000E+03	1.94400E+04	2.33280E+05	2.79936E+06	3.35923E+07	4.03108E+08
13	34	4.42000E+02	5.74600E+03	7.46980E+04	9.71074E+05	1.26240E+07	1.64112E+08
14	78	1.09200E+03	1.52880E+04	2.14032E+05	2.99645E+06	4.19503E+07	5.87304E+08
----	------	----------	----------	----------	----------	----------	----------
105	27369	7.54680E+04	3.54752E+05	2.43482E+06	2.08725E+07	2.04554E+08	2.18585E+09
	CENTROIDS =		4.70069E+00	3.22630E+01	2.76574E+02	2.71047E+03	2.89640E+04

Table 38 CENTROID ANALYSIS OF WEE VIRUS INDUCED LATEX AGGLUTINATION (1.6X10E6 LD50/ML)

CHANNEL	COUNT	MASS	MOMENT2	MOMENT3	MOMENT4	MOMENT5	MOMENT6
1	9917	9.91700E+03	9.91700E+03	9.91700E+03	9.91700E+03	9.91700E+03	9.91700E+03
2	7115	1.42300E+04	2.84600E+04	5.69200E+04	1.13840E+05	2.27680E+05	4.55360E+05
3	2540	7.62000E+03	2.28600E+04	6.85800E+04	2.05740E+05	6.17220E+05	1.85166E+06
4	2061	8.24400E+03	3.29760E+04	1.31904E+05	5.27616E+05	2.11046E+06	8.44186E+06
5	1490	7.45000E+03	3.72500E+04	1.86250E+05	9.31250E+05	4.65625E+06	2.32813E+07
6	839	5.03400E+03	3.02040E+04	1.81224E+05	1.08734E+06	6.52406E+06	3.91444E+07
7	617	5.71900E+03	4.40330E+04	2.60231E+05	1.96162E+06	1.37313E+07	9.61192E+07
8	365	3.06000E+03	2.46400E+04	1.97120E+05	1.57696E+06	1.26157E+07	1.00925E+08
9	432	3.88800E+03	3.49920E+04	3.14928E+05	2.83435E+06	2.55092E+07	2.29583E+08
10	137	1.37000E+03	1.37000E+04	1.37000E+05	1.37000E+06	1.37000E+07	1.37000E+08
11	196	2.15600E+03	2.37160E+04	2.60676E+05	2.86964E+06	3.15660E+07	3.47226E+08
12	169	2.02800E+03	2.43360E+04	2.92032E+05	3.50438E+06	4.20526E+07	5.04631E+08
13	100	1.30000E+03	1.69000E+04	2.19700E+05	2.85610E+06	3.71293E+07	4.82681E+08
14	106	1.48400E+03	2.07760E+04	2.90864E+05	4.07210E+06	5.70093E+07	7.98.31E+08
----	------	----------	----------	----------	----------	----------	----------
105	26304	7.35200E+04	3.60760E+05	2.62755E+06	2.39209E+07	2.47459E+08	2.76948E+09
	CENTROIDS =		4.90696E+00	3.57392E+01	3.25365E+02	3.36587E+03	3.76696E+04

Table 39 CENTROID ANALYSIS OF WEE VIRUS INDUCED LATEX AGGLUTINATION (1.6X10E7 LD50/ML)

CHANNEL	COUNT	MASS	MOMENT2	MOMENT3	MOMENT4	MOMENT5	MOMENT6
1	9478	9.47000E+03	9.47000E+03	9.47000E+03	9.47000E+03	9.47000E+03	9.47000E+03
2	7021	1.40420E+04	2.80840E+04	5.61680E+04	1.12336E+05	2.24672E+05	4.49344E+05
3	2372	7.11600E+03	2.13480E+04	6.40440E+04	1.92132E+05	5.76396E+05	1.72919E+06
4	2032	8.12800E+03	3.25120E+04	1.30048E+05	5.20192E+05	2.08077E+06	8.32307E+06
5	1478	7.39000E+03	3.69500E+04	1.84750E+05	9.23750E+05	4.61875E+06	2.3093cE+07
6	847	5.08200E+03	3.04920E+04	1.82952E+05	1.09771E+06	6.58627E+06	3.9517cE+07
7	866	5.65600E+03	3.95920E+04	2.77144E+05	1.94001E+06	1.35801E+07	9.5C604E+07
8	293	2.32000E+03	1.85600E+04	1.48480E+05	1.18784E+06	9.50272E+06	7.60218E+07
9	418	3.76200E+03	3.38580E+04	3.04722E+05	2.74250E+06	2.46825E+07	2.22142E+08
10	217	2.17000E+03	2.17000E+04	2.17000E+05	2.17000E+06	2.17000E+07	2.17000E+08
11	165	1.81500E+03	1.99650E+04	2.19615E+05	2.41577E+06	2.65734E+07	2.92308E+08
12	198	2.37600E+03	2.85120E+04	3.42144E+05	4.10573E+06	4.92687E+07	5.91225E+08
13	62	1.06600E+03	1.38580E+04	1.80154E+05	2.34200E+06	3.04460E+07	3.9579cE+08
14	119	1.66600E+03	2.33240E+04	3.26536E+05	4.57150E+06	6.40011E+07	8.96015E+08
----	------	----------	----------	----------	----------	----------	----------
105	25517	7.20590E+04	3.56225E+05	2.64323E+06	2.43309E+07	2.53651E+08	2.85869E+09
	CENTROIDS =		4.97127E+00	3.66814E+01	3.37653E+02	3.52282E+03	3.96716E+04

Table 40 CENTROID ANALYSIS OF WEE VIRUS INDUCED LATEX AGGLUTINATION (1.6X10E8 LD50/ML)

CHANNEL	COUNT	MASS	MOMENT2	MOMENT3	MOMENT4	MOMENT5	MOMENT6
1	6266	6.26600E+03	6.26600E+03	6.26600E+03	6.26600E+03	6.26600E+03	6.26600E+03
2	6559	1.31180E+04	2.62360E+04	5.24720E+04	1.04944E+05	2.09888E+05	4.19776E+05
3	2081	6.24300E+03	1.87290E+04	5.61870E+04	1.66561E+05	5.05683E+05	1.51705E+06
4	2242	8.96800E+03	3.58720E+04	1.43488E+05	5.73952E+05	2.29581E+06	9.183232+06
5	1230	6.15000E+03	3.07500E+04	1.53750E+05	7.68750E+05	3.84375E+06	1.92188E+07
6	834	5.00400E+03	3.00240E+04	1.80144E+05	1.08086E+06	6.48510E+06	3.69111E+07
7	997	6.97900E+03	4.88530E+04	3.41971E+05	2.39380E+06	1.67566E+07	1.17296E+08
8	209	1.67200E+03	1.33760E+04	1.07008E+05	8.56064E+05	6.84851E+06	5.47601E+07
9	402	3.61800E+03	3.25620E+04	2.93058E+05	2.63752E+06	2.37377E+07	2.13639E+08
10	234	2.34000E+03	2.34000E+04	2.34000E+05	2.34000E+06	2.34000E+07	2.34000E+08
11	160	1.76000E+03	1.93600E+04	2.12960E+05	2.34256E+06	2.57682E+07	2.83450E+08
12	192	2.30400E+03	2.76480E+04	3.31776E+05	3.98131E+06	4.77757E+07	5.73309E+08
13	84	1.09200E+03	1.41960E+04	1.84548E+05	2.39912E+06	3.11880E+07	4.05452E+08
14	107	1.49800E+03	2.09720E+04	2.93608E+05	4.11051E+06	5.75472E+07	8.05660E+08
----	------	----------	----------	----------	----------	----------	----------
105	23619	6.90340E+04	3.50266E+05	2.59326E+06	2.37663E+07	2.46371E+08	2.75685E+09
	CENTROIDS =		5.07382E+00	3.75649E+01	3.44269E+02	3.56884E+03	3.99347E+04

Table 41 CENTROID ANALYSIS OF WEE VIPUS INDUCED LATEX AGGLUTINATION (1.6X10E9 LD 50/ML)

CHANNEL	COUNT	MASS	MOMENT2	MOMENT3	MOMENT4	MOMENT5	MOMENT6
1	10462	1.04620E+04	1.04620E+04	1.04620E+04	1.04620E+04	1.04620E+04	1.04620E+04
2	7293	1.45860E+04	2.91720E+04	5.83440E+04	1.16688E+05	2.33376E+05	4.66752E+05
3	2144	6.43200E+03	1.92960E+04	5.78880E+04	1.73664E+05	5.20992E+05	1.56296E+06
4	2707	1.08280E+04	4.33120E+04	1.73248E+05	6.92992E+05	2.77197E+06	1.10879E+07
5	1480	7.40000E+03	3.70000E+04	1.85000E+05	9.25000E+05	4.62500E+06	2.31250E+07
6	974	5.84400E+03	3.50640E+04	2.10384E+05	1.26230E+06	7.57382E+06	4.54429E+07
7	806	5.64200E+03	3.94940E+04	2.76456E+05	1.93521E+06	1.35464E+07	9.48251E+07
8	476	3.80800E+03	3.04640E+04	2.43712E+05	1.94970E+06	1.55976E+07	1.24781E+08
9	445	4.00500E+03	3.60450E+04	3.24405E+05	2.91965E+06	2.62768E+07	2.36491E+08
10	213	2.13000E+03	2.13000E+04	2.13000E+05	2.13000E+06	2.13000E+07	2.13000E+08
11	138	1.51800E+03	1.66980E+04	1.83678E+05	2.02046E+06	2.22250E+07	2.44475E+08
12	195	2.34000E+03	2.80800E+04	3.36960E+05	4.04352E+06	4.85222E+07	5.82267E+08
13	55	7.15000E+02	9.29500E+03	1.20835E+05	1.57086E+06	2.04211E+07	2.65474E+08
14	126	1.76400E+03	2.46960E+04	3.45744E+05	4.84042E+06	6.77656E+07	9.48722E+08
185	27514	7.74740E+04	3.80378E+05	2.74012E+06	2.45909E+07	2.51391E+08	2.79173E+09
	CENTROIDS =		4.90975E+00	3.53682E+01	3.17408E+02	3.24484E+03	3.60344E+04

Table #2 CENTROID ANALYSIS OF WEE ANTIBODY INDUCED LATEX AGGLUTINATION (LATEX CONTROL)

CHANNEL	COUNT	MASS	MOMENT2	MOMENT3	MOMENT4	MOMENT5	MOMENT6
1	10177	1.01770E+04	1.01770E+04	1.01770E+04	1.01770E+04	1.01770E+04	1.01770E+04
2	7570	1.51400E+04	3.02800E+04	6.05600E+04	1.21120E+05	2.42240E+05	4.84480E+05
3	2493	7.47900E+03	2.24370E+04	6.73110E+04	2.01933E+05	6.05799E+05	1.81740E+06
4	2364	9.53600E+03	3.81440E+04	1.52576E+05	6.10304E+05	2.44122E+06	9.76486E+06
5	1464	7.42000E+03	3.71000E+04	1.85500E+05	9.27500E+05	4.63750E+06	2.31875E+07
6	1037	6.22200E+03	3.73320E+04	2.23992E+05	1.34395E+06	8.06371E+06	4.83823E+07
7	699	6.29300E+03	4.40510E+04	3.08357E+05	2.15850E+06	1.51095E+07	1.05766E+08
8	256	2.04800E+03	1.63840E+04	1.31072E+05	1.04858E+06	8.38861E+06	6.71089E+07
9	407	3.66300E+03	3.29670E+04	2.96703E+05	2.67033E+06	2.40329E+07	2.16296E+08
10	229	2.29000E+03	2.29000E+04	2.29000E+05	2.29000E+06	2.29000E+07	2.29000E+08
11	186	2.04600E+03	2.25060E+04	2.47566E+05	2.72323E+06	2.99555E+07	3.29510E+08
12	135	1.62000E+03	1.94400E+04	2.33280E+05	2.79936E+06	3.35923E+07	4.03108E+08
13	34	4.42000E+02	5.74600E+03	7.46980E+04	9.71074E+05	1.26240E+07	1.64112E+08
14	76	1.09200E+03	1.52880E+04	2.14032E+05	2.99645E+06	4.19503E+07	5.87304E+08
----	------	----------	----------	----------	----------	----------	----------
105	27369	7.54660E+04	3.54752E+05	2.43482E+06	2.08725E+07	2.04554E+08	2.16565E+09
	CENTROIDS =		4.70069E+00	3.22630E+01	2.76574E+02	2.71047E+03	2.89640E+04

Table #3 CENTROID ANALYSIS OF WEE ANTIBODY INDUCED LATEX AGGLUTINATION (>4.096/ML HI)

CHANNEL	COUNT	MASS	MOMENT2	MOMENT3	MOMENT4	MOMENT5	MOMENT6
1	6941	6.94100E+03	6.94100E+03	6.94100E+03	6.94100E+03	6.94100E+03	6.94100E+03
2	6884	1.37680E+04	2.75360E+04	5.50720E+04	1.10144E+05	2.20288E+05	4.40576E+05
3	2237	6.71100E+03	2.01330E+04	6.03990E+04	1.81197E+05	5.43591E+05	1.63077E+06
4	1667	7.46600E+03	2.98720E+04	1.19488E+05	4.77952E+05	1.91181E+06	7.64723E+06
5	1351	6.75500E+03	3.37750E+04	1.68875E+05	8.44375E+05	4.22188E+06	2.11094E+07
6	808	4.84800E+03	2.90880E+04	1.74528E+05	1.04717E+06	6.28301E+06	3.76980E+07
7	759	5.31300E+03	3.71910E+04	2.60337E+05	1.82236E+06	1.27565E+07	8.92956E+07
8	232	1.85600E+03	1.48480E+04	1.18784E+05	9.50272E+05	7.60218E+06	6.08174E+07
9	339	3.05100E+03	2.74590E+04	2.47131E+05	2.22418E+06	2.00176E+07	1.80158E+08
10	180	1.80000E+03	1.80000E+04	1.80000E+05	1.80000E+06	1.80000E+07	1.80000E+08
11	137	1.50700E+03	1.65770E+04	1.82347E+05	2.00582E+06	2.20640E+07	2.42704E+08
12	119	1.42800E+03	1.71360E+04	2.05632E+05	2.46758E+06	2.96110E+07	3.55332E+08
13	81	1.05300E+03	1.36890E+04	1.77957E+05	2.31344E+06	3.00747E+07	3.90972E+08
14	93	1.30200E+03	1.82280E+04	2.55192E+05	3.57269E+06	5.00176E+07	7.00247E+08
----	------	----------	----------	----------	----------	----------	----------
105	24026	6.58010E+04	3.12473E+05	2.21466E+06	1.98261E+07	2.03333E+08	2.26606E+09
	CENTROIDS =		4.74676E+00	3.36573E+01	3.01304E+02	3.09012E+03	3.44665E+04

Table 44 CENTROID ANALYSIS OF WEE ANTIBODY INDUCED LATEX AGGLUTINATION (>40.96/ML HI)

CHANNEL	COUNT	MASS	MOMENT2	MOMENT3	MOMENT4	MOMENT5	MOMENT6
1	10016	1.00160E+04	1.00160E+04	1.00160E+04	1.00160E+04	1.00160E+04	1.00160E+04
2	7486	1.49720E+04	2.99440E+04	5.98880E+04	1.19776E+05	2.39552E+05	4.79104E+05
3	2006	6.01800E+03	1.80540E+04	5.41620E+04	1.62486E+05	4.87458E+05	1.46237E+06
4	1977	7.90800E+03	3.16320E+04	1.26528E+05	5.06112E+05	2.02445E+06	8.09779E+06
5	1466	7.43000E+03	3.71500E+04	1.85750E+05	9.28750E+05	4.64375E+06	2.32188E+07
6	601	4.80600E+03	2.88360E+04	1.73016E+05	1.03810E+06	6.22860E+06	3.73716E+07
7	699	4.89300E+03	3.42510E+04	2.39757E+05	1.67830E+06	1.17481E+07	8.22307E+07
8	364	3.07200E+03	2.45760E+04	1.96608E+05	1.57286E+06	1.25829E+07	1.00663E+08
9	346	3.13200E+03	2.81880E+04	2.53692E+05	2.28323E+06	2.05491E+07	1.84941E+08
10	186	1.86000E+03	1.86000E+04	1.86000E+05	1.86000E+06	1.86000E+07	1.86000E+08
11	143	1.57300E+03	1.73030E+04	1.90333E+05	2.09366E+06	2.30303E+07	2.53333E+08
12	149	1.78800E+03	2.14560E+04	2.57472E+05	3.08966E+06	3.70760E+07	4.44912E+08
13	77	1.00100E+03	1.30130E+04	1.69169E+05	2.19920E+06	2.85896E+07	3.71664E+08
14	111	1.55400E+03	2.17560E+04	3.04584E+05	4.26418E+06	5.96985E+07	8.35776E+08
----	------	----------	----------	----------	----------	----------	----------
105	25869	7.00230E+04	3.34775E+05	2.40696E+06	2.18063E+07	2.25508E+08	2.53017E+09
	CENTROIDS =		4.78093E+00	3.43741E+01	3.11417E+02	3.22049E+03	3.61334E+04

Table 45 CENTROID ANALYSIS OF WEE ANTIBODY INDUCED LATEX AGGLUTINATION (>409.6/ML HI)

CHANNEL	COUNT	MASS	MOMENT2	MOMENT3	MOMENT4	MOMENT5	MOMENT6
1	6149	6.14900E+03	8.14900E+03	8.14900E+03	8.14900E+03	8.14900E+03	8.14900E+03
2	6269	1.25760E+04	2.51560E+04	5.03120E+04	1.00624E+05	2.01248E+05	4.02496E+05
3	2465	7.39500E+03	2.21850E+04	6.65550E+04	1.99665E+05	5.98995E+05	1.79699E+06
4	1931	7.72400E+03	3.08960E+04	1.23584E+05	4.94336E+05	1.97734E+06	7.90936E+06
5	968	4.94000E+03	2.47000E+04	1.23500E+05	6.17500E+05	3.08750E+06	1.54375E+07
6	1021	6.12600E+03	3.67560E+04	2.20536E+05	1.32322E+06	7.93930E+06	4.76358E+07
7	605	4.23500E+03	2.96450E+04	2.07515E+05	1.45261E+06	1.01682E+07	7.11776E+07
8	312	2.49600E+03	1.99680E+04	1.59744E+05	1.27795E+06	1.02236E+07	8.17889E+07
9	379	3.41100E+03	3.06990E+04	2.76291E+05	2.48662E+06	2.23796E+07	2.01416E+08
10	202	2.02000E+03	2.02000E+04	2.02000E+05	2.02000E+06	2.02000E+07	2.02000E+08
11	127	1.39700E+03	1.53670E+04	1.69037E+05	1.85941E+06	2.04535E+07	2.24986E+08
12	165	1.98000E+03	2.37600E+04	2.85120E+05	3.42144E+06	4.10573E+07	4.92687E+08
13	66	8.58000E+02	1.11540E+04	1.45002E+05	1.88503E+06	2.45053E+07	3.18569E+08
14	111	1.55400E+03	2.17560E+04	3.04584E+05	4.26418E+06	5.96985E+07	8.35776E+08
----	------	----------	----------	----------	----------	----------	----------
105	22810	6.48630E+04	3.20391E+05	2.34193E+06	2.14107E+07	2.22499E+08	2.50160E+09
	CENTROIDS =		4.93950E+00	3.61056E+01	3.30091E+02	3.43026E+03	3.85674E+04

Table 46 CENTROID ANALYSIS OF WEE ANTIBODY INDUCED LATEX AGGLUTINATION (>4,096/ML HI)

CHANNEL	COUNT	MASS	MOMENT2	MOMENT3	MOMENT4	MOMENT5	MOMENT6
1	9250	9.25000E+03	9.25000E+03	9.25000E+03	9.25000E+03	9.25000E+03	9.25000E+03
2	5908	1.18160E+04	2.36320E+04	4.72640E+04	9.45280E+04	1.89056E+05	3.78112E+05
3	2491	7.47300E+03	2.24190E+04	6.72570E+04	2.01771E+05	6.05313E+05	1.81594E+06
4	2438	9.75200E+03	3.90080E+04	1.56032E+05	6.24128E+05	2.49651E+06	9.98605E+06
5	1307	6.53500E+03	3.26750E+04	1.63375E+05	8.16875E+05	4.08438E+06	2.04219E+07
6	823	4.93800E+03	2.96280E+04	1.77768E+05	1.06661E+06	6.39965E+06	3.83979E+07
7	750	5.25000E+03	3.67500E+04	2.57250E+05	1.80075E+06	1.26053E+07	8.82368E+07
8	230	1.84000E+03	1.47200E+04	1.17760E+05	9.42080E+05	7.53664E+06	6.02931E+07
9	442	3.97800E+03	3.58020E+04	3.22218E+05	2.89996E+06	2.60997E+07	2.34897E+08
10	212	2.12000E+03	2.12000E+04	2.12000E+05	2.12000E+06	2.12000E+07	2.12000E+08
11	145	1.59500E+03	1.75450E+04	1.92995E+05	2.12295E+06	2.33524E+07	2.56876E+08
12	190	2.28000E+03	2.73600E+04	3.28320E+05	3.93984E+06	4.72781E+07	5.67337E+08
13	62	1.06600E+03	1.38580E+04	1.80154E+05	2.34200E+06	3.04460E+07	3.95798E+08
14	106	1.48400E+03	2.07760E+04	2.90864E+05	4.07210E+06	5.70093E+07	7.98131E+08
----	------	----------	----------	----------	----------	----------	----------
105	24374	6.93770E+04	3.44623E+05	2.52251E+06	2.30526E+07	2.39312E+08	2.68456E+09
	CENTROIDS =		4.96740E+00	3.63594E+01	3.32264E+02	3.44944E+03	3.66955E+04

Table 47 CENTROID ANALYSIS OF WEE ANTIBODY INDUCED LATEX AGGLUTINATION (>40,960/ML HI)

CHANNEL	COUNT	MASS	MOMENT2	MOMENT3	MOMENT4	MOMENT5	MOMENT6
1	9409	9.40900E+03	9.40900E+03	9.40900E+03	9.40900E+03	9.40900E+03	9.40900E+03
2	7043	1.40860E+04	2.81720E+04	5.63440E+04	1.12688E+05	2.25376E+05	4.50752E+05
3	2812	8.43600E+03	2.53080E+04	7.59240E+04	2.27772E+05	6.83316E+05	2.04995E+06
4	2204	8.81600E+03	3.52640E+04	1.41056E+05	5.64224E+05	2.25690E+06	9.02758E+06
5	1669	8.34500E+03	4.17250E+04	2.08625E+05	1.04313E+06	5.21563E+06	2.60781E+07
6	980	5.88000E+03	3.52800E+04	2.11680E+05	1.27008E+06	7.62048E+06	4.57229E+07
7	674	6.11600E+03	4.28620E+04	2.99034E+05	2.09847E+06	1.46893E+07	1.02825E+08
8	416	3.32800E+03	2.66240E+04	2.12994E+05	1.70394E+06	1.36315E+07	1.09052E+08
9	526	4.73400E+03	4.26060E+04	3.83454E+05	3.45109E+06	3.10598E+07	2.79538E+08
10	244	2.44000E+03	2.44000E+04	2.44000E+05	2.44000E+06	2.44000E+07	2.44000E+08
11	200	2.20000E+03	2.42000E+04	2.66200E+05	2.92820E+06	3.22102E+07	3.54312E+08
12	239	2.86800E+03	3.44160E+04	4.12992E+05	4.95590E+06	5.94708E+07	7.13650E+08
13	108	1.40400E+03	1.82520E+04	2.37276E+05	3.08459E+06	4.00996E+07	5.21295E+08
14	150	2.10000E+03	2.94000E+04	4.11600E+05	5.76240E+06	8.06736E+07	1.12943E+09
----	------	----------	----------	----------	----------	----------	----------
105	26674	8.01640E+04	4.17682E+05	3.17133E+06	2.96519E+07	3.12246E+08	3.53744E+09
	CENTROIDS =		5.21284E+00	3.95606E+01	3.69890E+02	3.89509E+03	4.41276E+04

Figure 22 CENTROID ANALYSIS OF LATEX AGGLUTINATION AT VARIOUS CONCENTRATONS OF WEE VIRUS

LATEX CONTROL = O, 1.6X10E6 LD50/ML = X, 1.6X10E7 LD50/ML = +, 1.6X10E8 LD50/ML = *, 1.6X10E9 LD50/ML = #

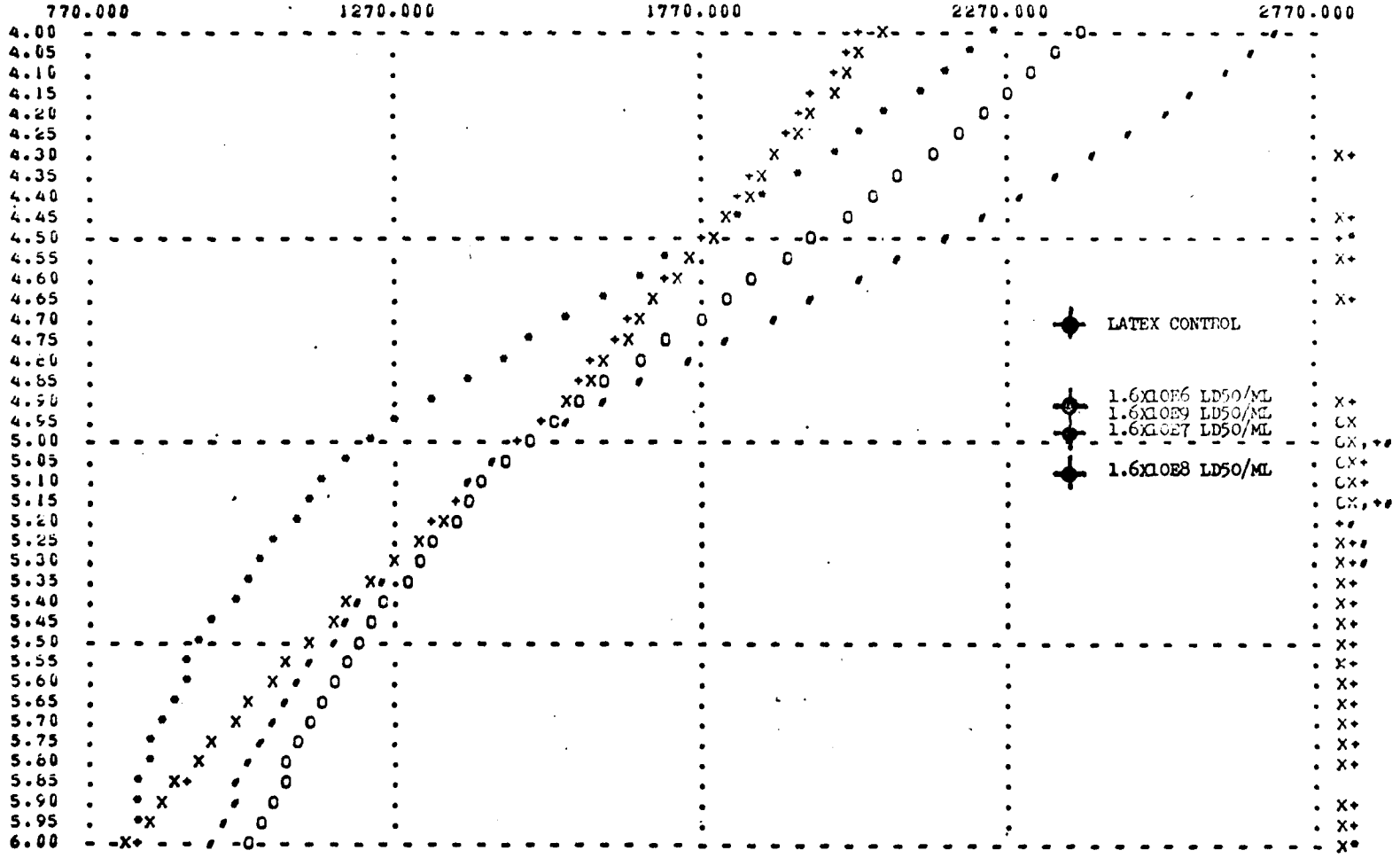

Figure 23 CENTROID ANALYSIS OF LATEX AGGLUTINATION AT VARIOUS CONCENTRATIONS OF WEE AB

LATEX CONTROL = O, >4.096/ML HI = X, >40.96/ML HI = +, >409.6/ML HI = *, >4,096/ML HI = #, >40,960/ML HI = >

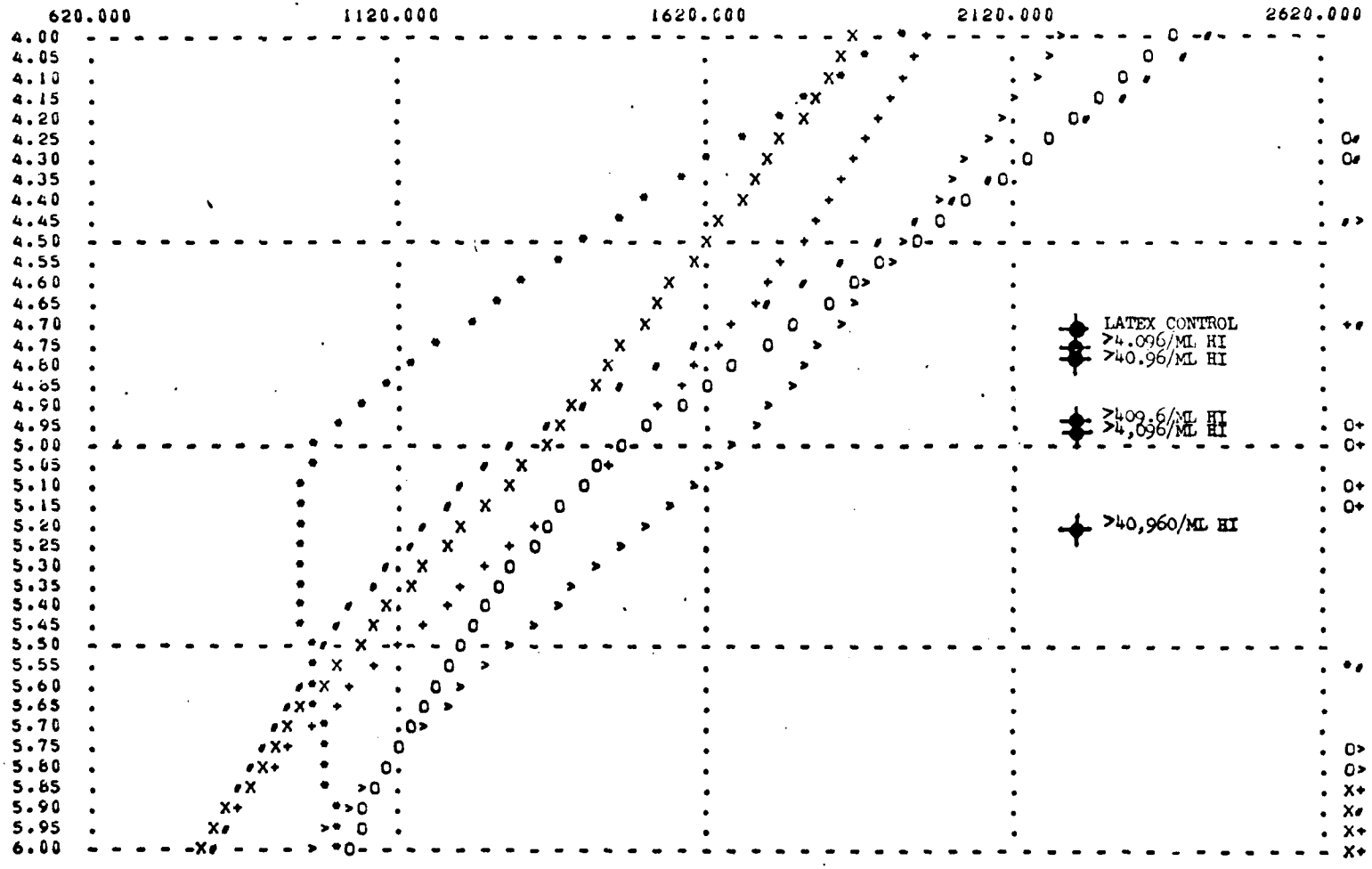

Table 48 WEE VIRUS INDUCED CENTROID LOCATION SHIFT (1.6X10E(X-AXIS)=WEE VIRUS LD5(

CENTROID LOCATION (CHANNEL)

*** INTERPOLATED ***		****** GIVEN ******	
X	Y	X	Y
6.00	4.9070	6.00	4.9070
6.10	4.9030		
6.20	4.9021		
6.30	4.9041		
6.40	4.9086		
6.50	4.9153		
6.60	4.9239		
6.70	4.9341		
6.80	4.9456		
6.90	4.9581		
7.00	4.9713	7.00	4.9713
7.10	4.9848		
7.20	4.9985		
7.30	5.0119		
7.40	5.0248		
7.50	5.0368		
7.60	5.0477		
7.70	5.0572		
7.80	5.0649		
7.90	5.0705		
8.00	5.0738	8.00	5.0738
8.10	5.0694		
8.20	5.0623		
8.30	5.0526		
8.40	5.0401		
8.50	5.0251		
8.60	5.0073		
8.70	4.9869		
8.80	4.9639		
8.90	4.9381		
9.00	4.9098	9.00	4.9098

Figure 24 WEE VIRUS INDUCED CENTROID LOCATION SHIFT (1.6X10E(X-AXIS)=WEE VIRUS LD50/ML)

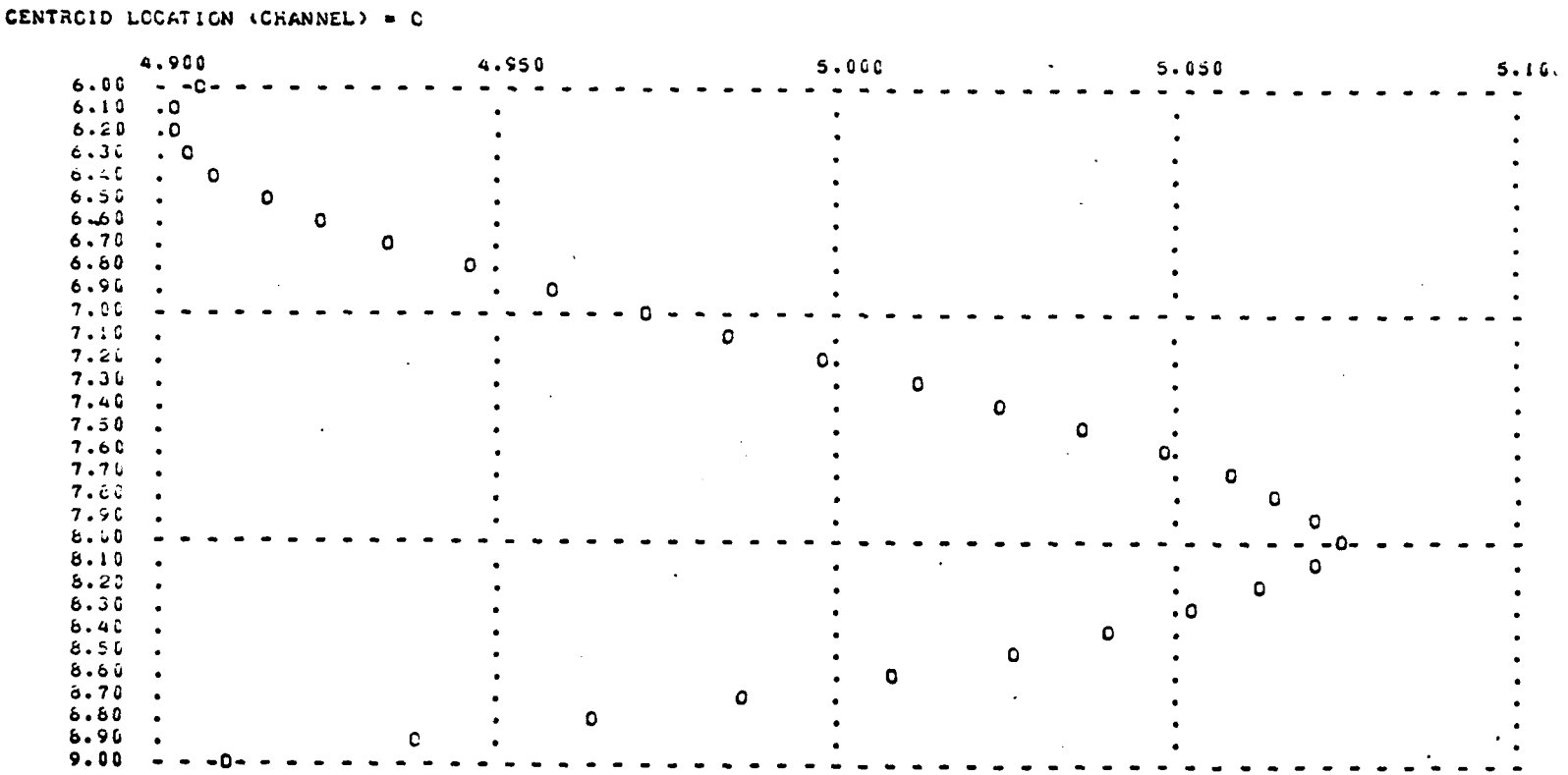

Table 49 VEE ANTIBODY INDUCED CENTROID LOCATION SHIFT (>4.096X10E(X-AXIS)=VEE AB/ML HI)

CENTROID LOCATION (CHANNEL)

*** INTERPOLATED ***		====== GIVEN ======	
X	Y	X	Y
0.00	4.7468	0.00	4.7468
0.10	4.7390		
0.20	4.7327		
0.30	4.7298		
0.40	4.7300		
0.50	4.7330		
0.60	4.7385		
0.70	4.7463		
0.80	4.7562		
0.90	4.7678		
1.00	4.7809	1.00	4.7809
1.10	4.7953		
1.20	4.8108		
1.30	4.8269		
1.40	4.8436		
1.50	4.8605		
1.60	4.8774		
1.70	4.8940		
1.80	4.9100		
1.90	4.9253		
2.00	4.9395	2.00	4.9395
2.10	4.9424		
2.20	4.9444		
2.30	4.9457		
2.40	4.9468		
2.50	4.9480		
2.60	4.9496		
2.70	4.9520		
2.80	4.9556		
2.90	4.9606		
3.00	4.9674	3.00	4.9674
3.10	4.9822		
3.20	4.9991		
3.30	5.0182		
3.40	5.0395		
3.50	5.0630		
3.60	5.0886		
3.70	5.1164		
3.80	5.1464		
3.90	5.1785		
4.00	5.2128	4.00	5.2128

Figure 25 WEE ANTIBODY INDUCED CENTROID LOCATION SHIFT (>4.096X10E(X-AXIS)=WEE AB/ML HI)

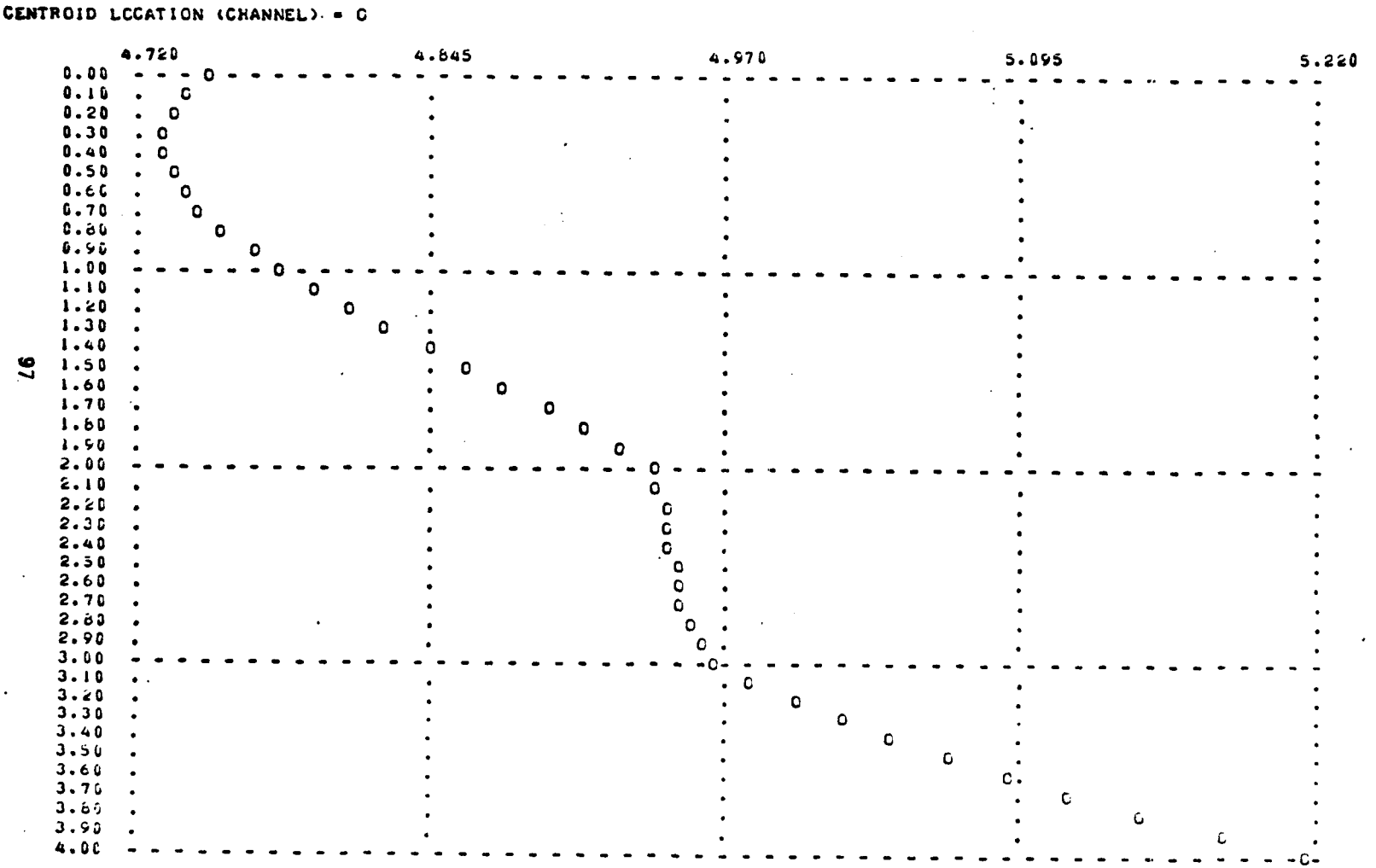

Table 50 Linear Regression and Statistics for WEE Antibody Induced Centroid Location Shift

WEE antibody*	Centroid
0.00	4.75
0.20	4.73
0.40	4.73
0.60	4.74
0.80	4.76
1.00	4.78
1.20	4.81
1.40	4.84
1.60	4.88
1.80	4.91
2.00	4.94
2.20	4.94
2.40	4.95
2.60	4.95
2.80	4.96
3.00	4.97
3.20	5.00
3.40	5.04
3.60	5.09
3.80	5.15
4.00	5.21

DATA SET #	1
# OF DATA POINTS	21.00
MEAN OF X	2.00
ST. DEV. OF X	1.24
MEAN OF Y	4.91
ST. DEV. OF Y	0.14
REGRESSION COEF.	0.11
STANDARD ERROR	0.03
CORRELATION COEF.	0.97
X-INTERCEPT	-43.01
Y-INTERCEPT	4.69

EQUATION : Y = (4.692) + (0.109) * X

*antibody concentration expressed as the exponent of $>4.096 \times 10^{e}$/ml HI WEE antibody

Figure 26 Linear regression of WEE antibody induced centroid location shift

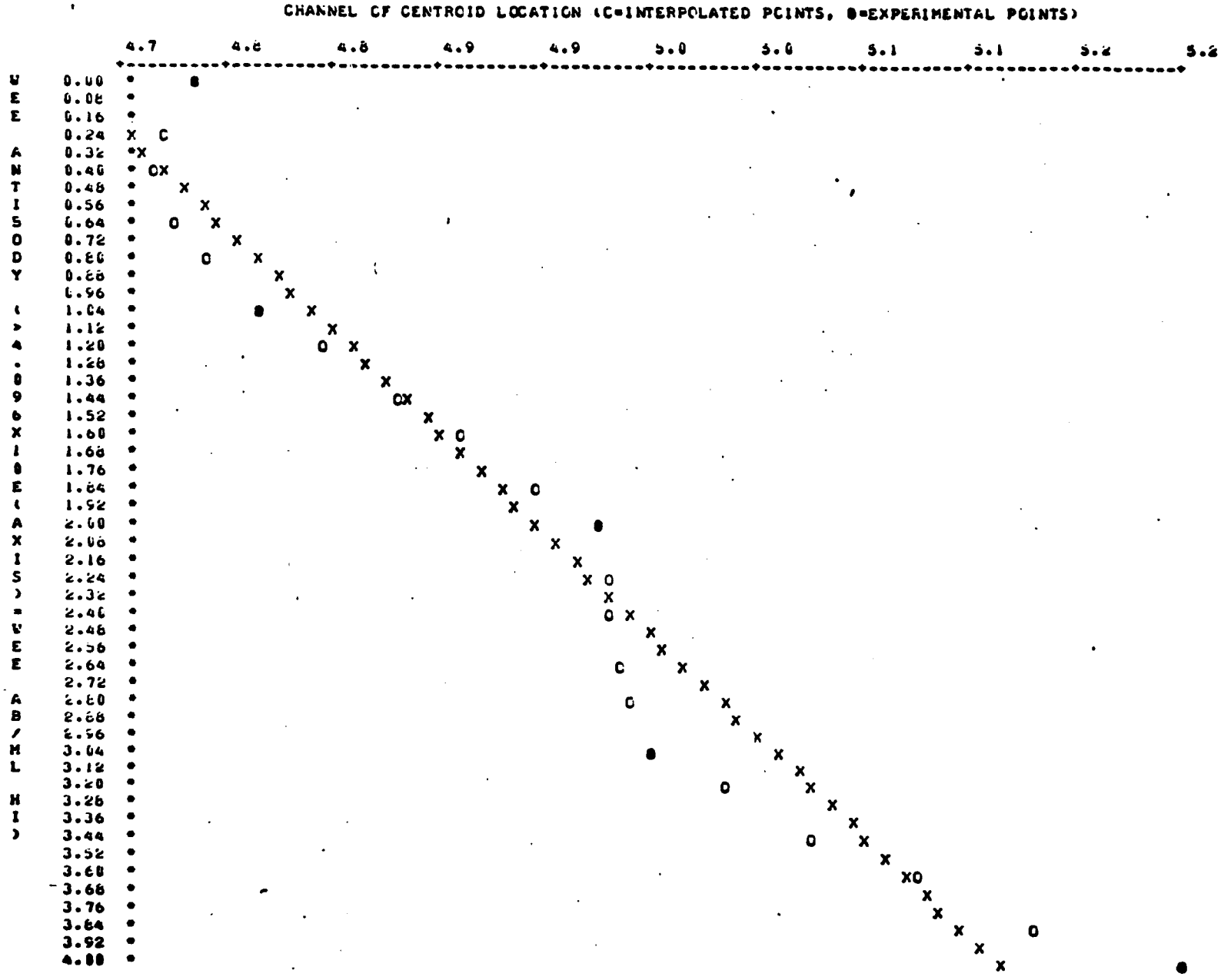

Table 51 Polynomial Regression of Degrees 1-3 and Statistics for WEE Virus Induced Centroid Location Shift

NO.	Virus concentration* X	Centroid Y
1	6.0000	4.9070
2	7.0000	4.9713
3	8.0000	5.0738
4	9.0000	4.9098

NO. POINTS = 4

X: MEAN= 7.5 ST.DEV.= 1.290994449
Y: MEAN= 4.965475 ST.DEV.= 0.078675323

CORR.COEFF.= 0.183375847

POLYNOMIAL REGRESSION DEGREE 1
COEFFICIENTS

B(0)= 4.8823
B(1)= 0.01109

R SQUARE = 0.033626702

POLYNOMIAL REGRESSION DEGREE 2
COEFFICIENTS

B(0)= 1.743174992
B(1)= 0.667215002
B(2)=-0.057075000

R SQUARE = 0.746156474

POLYNOMIAL REGRESSION DEGREE 3
COEFFICIENTS

B(0)= 22.38661656
B(1)=-7.598373454
B(2)= 1.065550915
B(3)=-0.050783374

R SQUARE = 1.000000185

*virus concentration expressed as the exponent of 1.6×10^6 LD_{50}/ml WEE virus

Figure 27 WEE VIRUS INDUCED CENTROID LOCATION SHIFT (1.6X10E(X-AXIS)=WEE VIRUS LD50/ML)

CENTROID LOCATION (CHANNEL) = C, POLYNOMIAL DEGREE 1 = 1, POLYNOMIAL DEGREE 2 = 2, POLYNOMIAL DEGREE 3 = 3

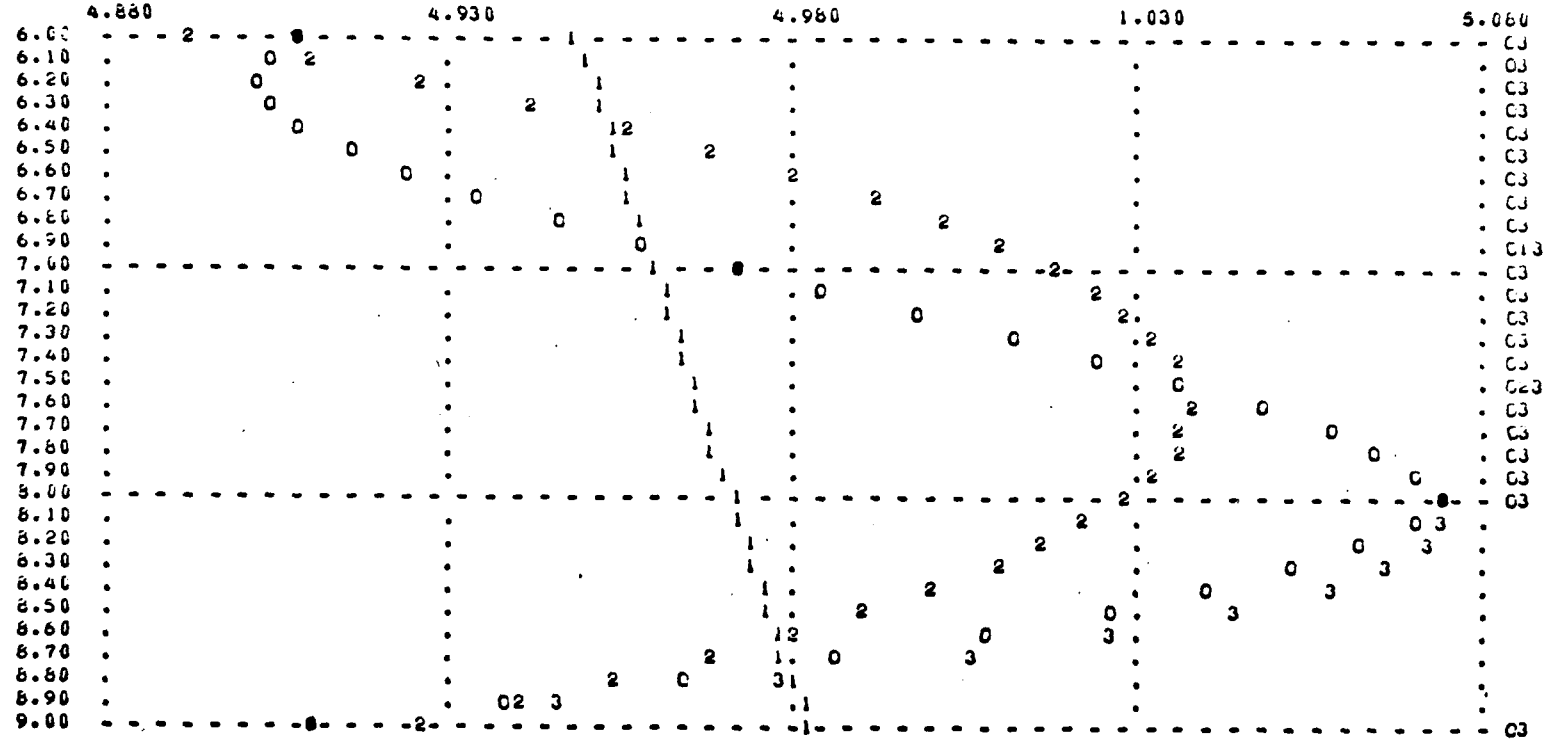

Table 52 Polynomial Regression of Degrees 1-4 and Statistics for WEE Antibody Induced Centroid Location Shift

NO.	Antibody concentration* X	Centroid Y
1	0.0000	4.7488
2	1.0000	4.7609
3	2.0000	4.9395
4	3.0000	4.9674
5	4.0000	5.2128

NO. POINTS = 5

X: MEAN= 2 ST.DEV.= 1.58113883
Y: MEAN= 4.92988 ST.DEV.= 0.184749173

CORR.COEFF.= 0.953622524

POLYNOMIAL REGRESSION DEGREE 1
COEFFICIENTS

B(0)= 4.70698
B(1)= 0.11145

R SQUARE = 0.909777400

POLYNOMIAL REGRESSION DEGREE 2
COEFFICIENTS

B(0)= 4.749251429
B(1)= 0.026907143
B(2)= 0.021135714

R SQUARE = 0.955584932

POLYNOMIAL REGRESSION DEGREE 3
COEFFICIENTS

B(0)= 4.740151429
B(1)= 0.092123806
B(2)=-0.024364283
B(3)= 7.58333E-03

R SQUARE = 0.961650308

POLYNOMIAL REGRESSION DEGREE 4
COEFFICIENTS

B(0)= 4.748800002
B(1)=-0.268233389
B(2)= 0.469325072
B(3)=-0.194216695
B(4)= 0.025225004

R SQUARE = 1.000000003

*antibody concentration expressed as the exponent of >4.096 x 10^6/ml HI WEE antibody

Figure 28 WEE ANTIBODY INDUCED CENTROID LOCATION SHIFT (>4.096X10E(X-AXIS)=WEE AB/ML HI)

CENTROID LOCATION (CHANNEL) = 0, POLYNOMIAL DEGREE 1 = 1, POLYNOMIAL DEGREE 2 = 2, POLYNOMIAL DEGREE 3 = 3, POLYNOMIAL DEGREE 4 = 4

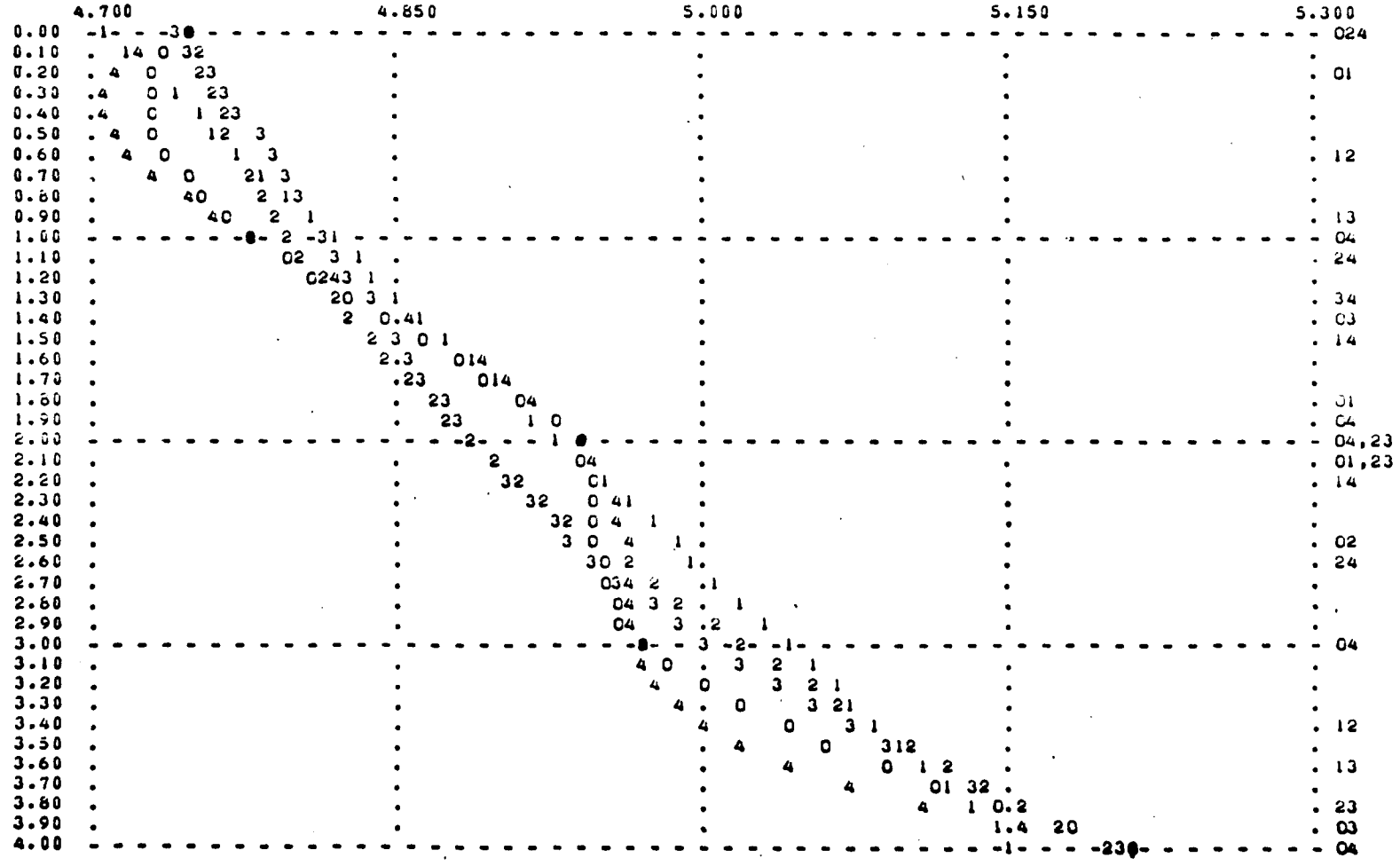

Table 53 CHANNEL 3 & 4 COUNT SINGLE CHANNEL SHIFT (1.6X10E(X-AXIS)=WEE VIRUS LE50/ML)

CHANNEL 3 LATEX COUNT				CHANNEL 4 LATEX COUNT			
*** INTERPOLATED ***		****** GIVEN ******		*** INTERPOLATED ***		****** GIVEN ******	
X	Y	X	Y	X	Y	X	Y
6.00	2540.0000	6.00	2540.0000	6.00	2061.0000	6.00	2061.0000
6.10	2542.3200			6.10	2047.8000		
6.20	2539.1300			6.20	2036.0400		
6.30	2530.5900			6.30	2028.1500		
6.40	2516.0600			6.40	2021.7400		
6.50	2501.1800			6.50	2017.6200		
6.60	2480.6700			6.60	2015.8100		
6.70	2457.0100			6.70	2016.3300		
6.80	2430.7000			6.80	2019.1900		
6.90	2402.2000			6.90	2024.4600		
7.00	2372.0000	7.00	2372.0000	7.00	2032.0000	7.00	2032.0000
7.10	2340.5600			7.10	2041.9500		
7.20	2308.3700			7.20	2054.3000		
7.30	2275.9100			7.30	2069.1700		
7.40	2243.6400			7.40	2086.4200		
7.50	2212.0600			7.50	2106.1200		
7.60	2181.6300			7.60	2126.2900		
7.70	2152.0300			7.70	2152.9500		
7.80	2126.1400			7.80	2180.1100		
7.90	2102.0400			7.90	2209.7800		
8.00	2081.0000	8.00	2081.0000	8.00	2242.0000	8.00	2242.0000
8.10	2071.3800			8.10	2277.0300		
8.20	2065.3100			8.20	2314.6200		
8.30	2062.7700			8.30	2354.7600		
8.40	2063.7700			8.40	2397.4400		
8.50	2066.3100			8.50	2442.6700		
8.60	2076.3800			8.60	2490.4400		
8.70	2087.9900			8.70	2540.7700		
8.80	2103.1300			8.80	2593.6300		
8.90	2121.8000			8.90	2649.0400		
9.00	2143.9900	9.00	2144.0000	9.00	2706.9900	9.00	2707.0000

Figure 29 CHANNEL 3 & 4 COUNT SINGLE CHANNEL SHIFT (1.6X10E(X-AXIS)=WEE VIRUS LD50/ML)

CHANNEL 3 LATEX COUNT = O, CHANNEL 4 LATEX COUNT = X

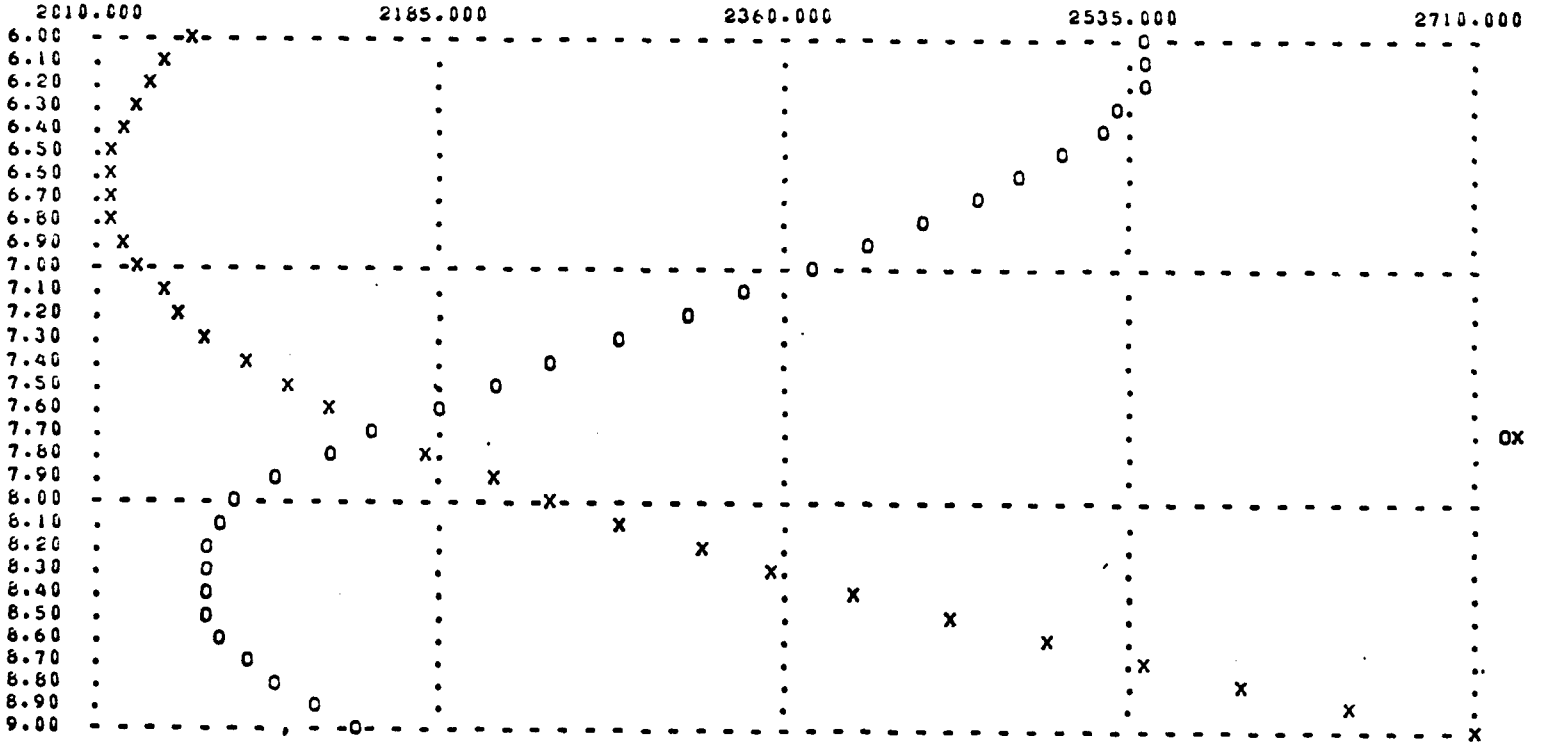

Figure 30 Linear regression of latex counts in channel 3 and channel 4 as affected by WEE virus concentration

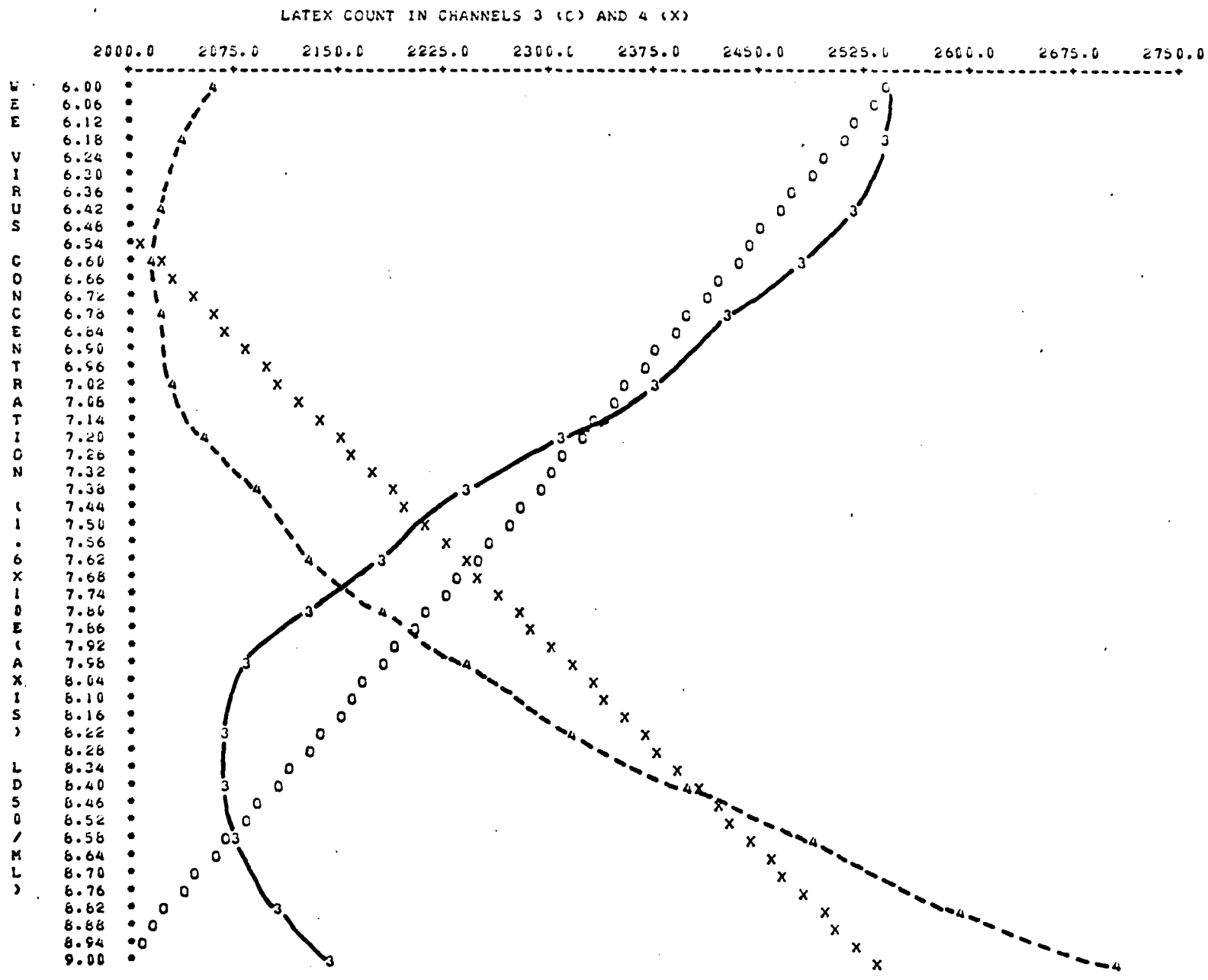

Table 54 Linear Regression and Statistics of Latex Counts in Channel 3 and Channel 4 as Affected by WEE Virus Concentration

CHANNEL 3		CHANNEL 4	
Virus concentration*	Latex count	Virus concentration*	Latex count
6.00	2540.00	6.00	2061.00
6.20	2539.13	6.20	2036.84
6.40	2518.08	6.40	2021.74
6.60	2460.67	6.60	2015.81
6.80	2430.70	6.80	2019.19
7.00	2372.00	7.00	2032.00
7.20	2308.37	7.20	2054.36
7.40	2243.64	7.40	2086.42
6.60	2181.63	7.60	2128.29
7.80	2126.14	7.80	2180.11
8.00	2081.00	8.00	2242.00
8.20	2065.31	8.20	2314.00
8.40	2063.77	8.40	2397.44
8.60	2076.38	8.60	2490.44
8.80	2103.13	8.80	2593.63
9.00	2144.00	9.00	2707.00

DATA SET #	1	2
# OF DATA POINTS	16.00	16.00
MEAN OF X	7.50	7.50
ST. DEV. OF X	0.95	0.95
MEAN OF Y	2267.12	2211.27
ST. DEV. OF Y	186.08	225.13
REGRESSION COEF.	-182.65	213.61
STANDARD ERROR	68.49	99.89
CORRELATION COEF.	-0.93	0.90
X-INTERCEPT	19.91	-2.85
Y-INTERCEPT	3636.99	609.17

CHANNEL 3
EQUATION $Y = (3636.988) + (-182.649) * X$

CHANNEL 4
EQUATION $Y = (609.166) + (213.613) * X$

*virus concentration expressed as the exponent of 1.6×10^{6} LD_{50}/ml WEE virus

Table 55 Polynomial Regression of Degrees 1-3 and Statistics for Channel 3 Latex Counts as Affected by WEE Virus Concentration

	CHANNEL 3	
	Virus concentration*	Latex count
NO.	X	Y
1	6.0000	2540.0000
2	7.0000	2372.0000
3	8.0000	2061.0000
4	9.0000	2144.0000

NO. POINTS = 4

X: MEAN= 7.5 ST.DEV.= 1.290994449
Y: MEAN= 2284.25 ST.DEV.= 211.4148765

CORR.COEFF.=-0.903144008

POLYNOMIAL REGRESSION DEGREE 1
COEFFICIENTS

B(0)= 3393.5000
B(1)= -147.9000

R SQUARE = 0.815669100

POLYNOMIAL REGRESSION DEGREE 2
COEFFICIENTS

B(0)= 6569.750009
B(1)=-1014.150003
B(2)= 57.75000017

R SQUARE = 0.915157312

POLYNOMIAL REGRESSION DEGREE 3
COEFFICIENTS

B(0)=-25747.02658
B(1)= 12236.51068
B(2)=-1731.001467
B(3)= 79.50006508

R SQUARE = 1.000000065

*virus concentration expressed as the exponent of 1.6×10^{6} LD_{50}/ml WEE virus

Table 56 Polynomial Regression of Degrees 1-3 and Statistics for Channel 4 Latex Counts as Affected by WEE Virus Concentration

CHANNEL 4

NO.	Virus concentration* X	Latex count Y
1	6.0000	2061.0000
2	7.0000	2032.0000
3	8.0000	2242.0000
4	9.0000	2707.0000

NO. POINTS = 4

X: MEAN= 7.5 ST.DEV.= 1.290994449
Y: MEAN= 2260.5 ST.DEV.= 311.8316854

CORR.COEFF.= 0.889279764

POLYNOMIAL REGRESSION DEGREE 1
COEFFICIENTS

B(0)= 649.5000000
B(1)= 214.8

R SQUARE = 0.790818499

POLYNOMIAL REGRESSION DEGREE 2
COEFFICIENTS

B(0)= 7442.000016
B(1)=-1637.700004
B(2)= 123.5000003

R SQUARE = 0.999956122

POLYNOMIAL REGRESSION DEGREE 3
COEFFICIENTS

B(0)= 6358.002266
B(1)=-1193.167595
B(2)= 63.50012503
B(3)= 2.666661119

R SQQARE = 1

*virus concentration expressed as the exponent of 1.6×10^{6} LD_{50}/ml WEE virus

Figure 31 CHANNEL 3 & 4 COUNT SINGLE CHANNEL SHIFT (1.6X10E(X-AXIS)=WEE VIRUS LD50/ML)

CHANNEL 3 LATEX COUNT = O, CHANNEL 4 LATEX COUNT = X, POLYNOMIAL DEGREE 1 = 1, POLYNOMIAL DEGREE 2 = 2, POLYNOMIAL DEGREE 3 = 3,
POLYNOMIAL DEGREE 1 = 1, POLYNOMIAL DEGREE 2 = 2, POLYNOMIAL DEGREE 3 = 3

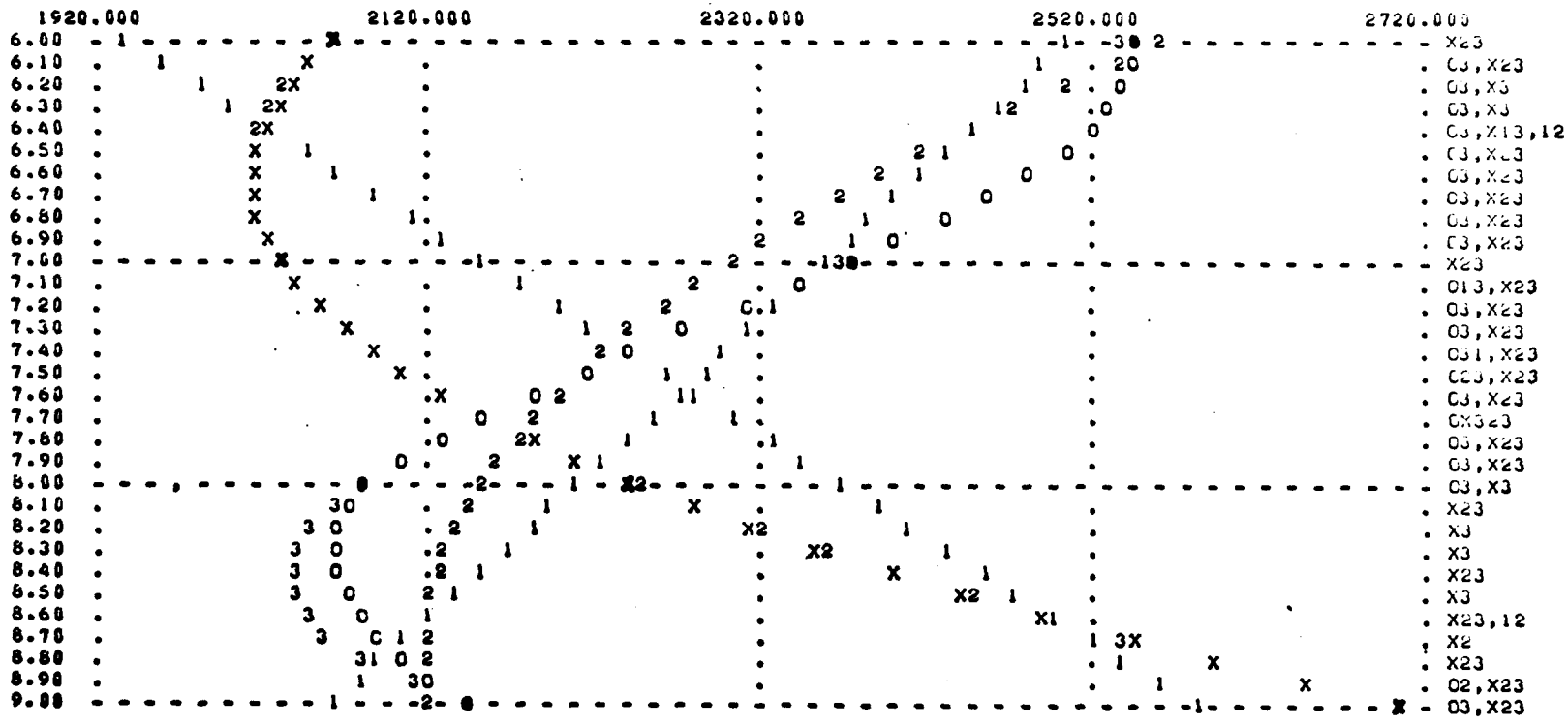

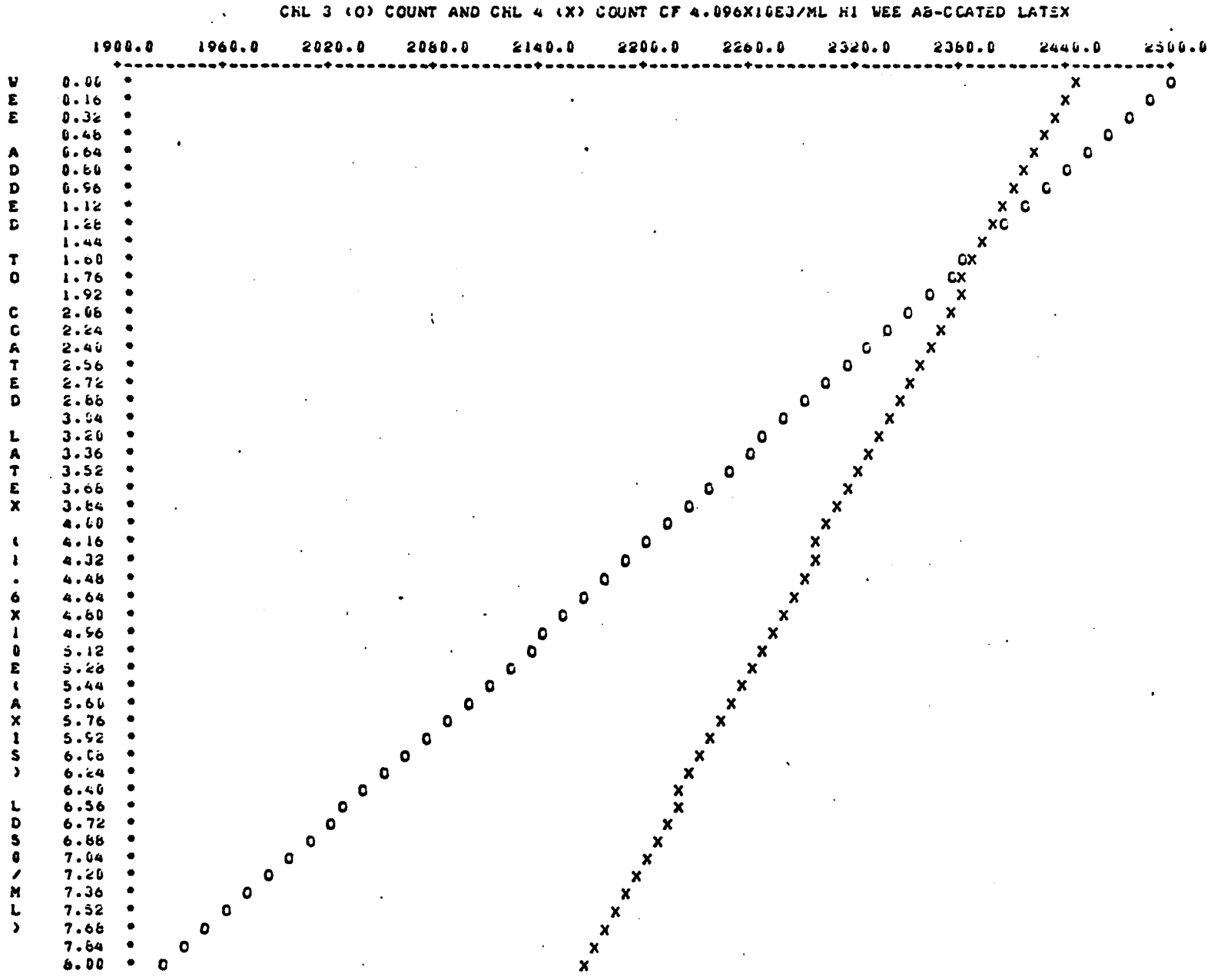

Figure 32 Linear regression of latex counts in channel 3 and channel 4 for latex particles coated with >4.096 x 10^3/ml HI WEE antibody and reacted with 1.6 x 10^6 LD_{50}/ml WEE virus

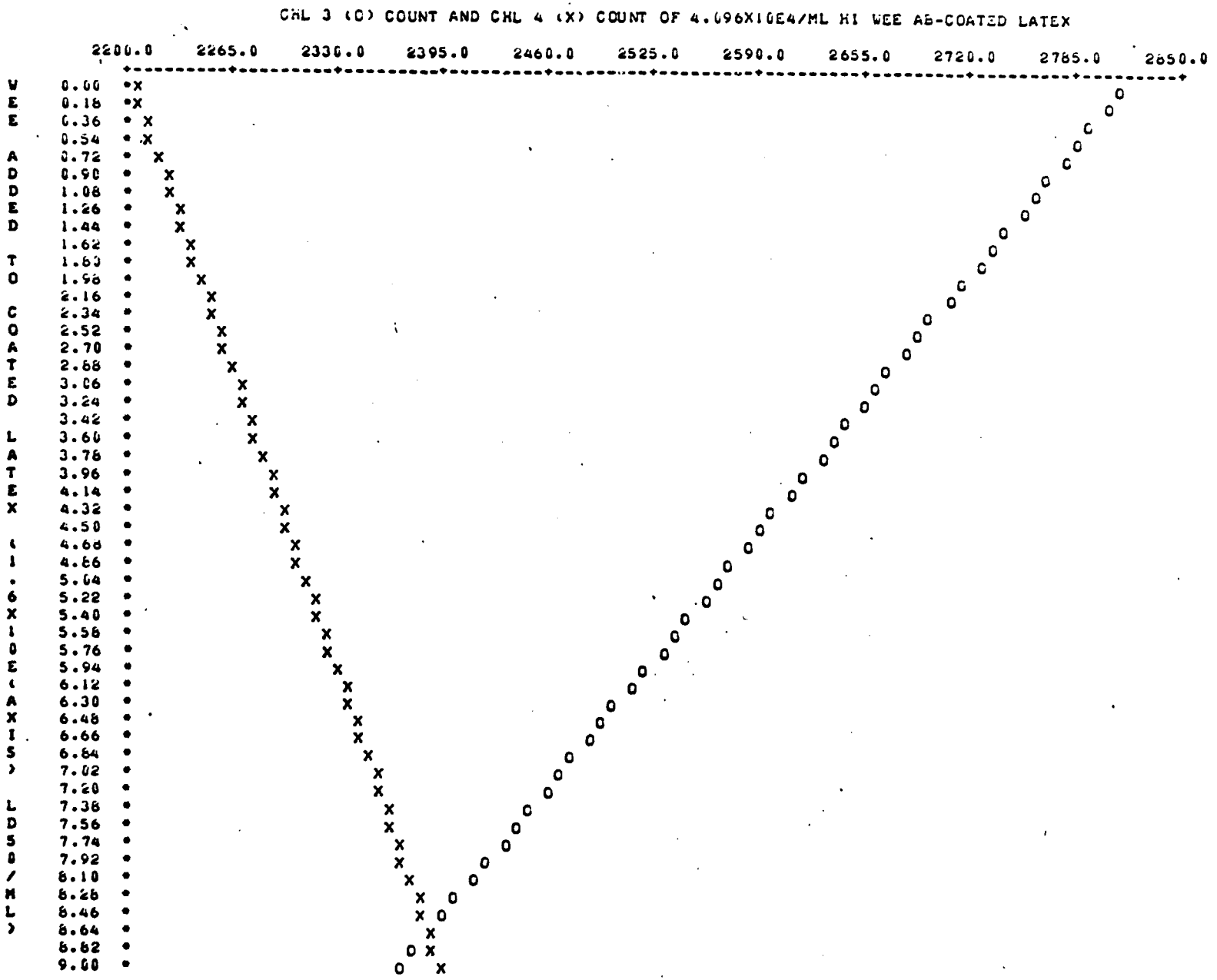

Figure 33 Linear regression of latex counts in channel 3 and channel 4 for latex particles coated with >4.096 x 10^4/ml HI WEE antibody and reacted with 1.6 x 10^9 LD_{50}/ml WEE virus

Table 57 Linear Regression and Statistics of Latex Counts in Channel 3 and Channel 4 for Latex Particles Coated with >4.096 x 10^3/ml HI WEE Antibody and Reacted with 1.6 x 10^8 LD_{50}/ml WEE Virus

CHANNEL 3		CHANNEL 4	
Virus concentration*	Latex count	Virus concentration*	Latex count
0.00	2491.00	0.00	2438.00
8.00	1920.00	8.00	2159.00

DATA SET #	1	2
# OF DATA POINTS	2.00	2.00
MEAN OF X	4.00	4.00
ST. DEV. OF X	5.66	5.66
MEAN OF Y	2205.50	2298.50
ST. DEV. OF Y	403.76	197.28
REGRESSION COEF.	-71.38	-34.88
STANDARD ERROR	1.00E+50	1.00E+50
CORRELATION COEF.	-1.00	-1.00
X-INTERCEPT	34.90	69.91
Y-INTERCEPT	2491.00	2438.00

CHANNEL 3
EQUATION : Y = (2491.000) + (-71.375) * X

FOR	X= 0.00	Y=	2491.00
FOR	X= 1.00	Y=	2419.63
FOR	X= 2.00	Y=	2348.25
FOR	X= 3.00	Y=	2276.88
FOR	X= 4.00	Y=	2205.50
FOR	X= 5.00	Y=	2134.13
FOR	X= 6.00	Y=	2062.75
FOR	X= 7.00	Y=	1991.38
FOR	X= 8.00	Y=	1920.00
FOR	X= 9.00	Y=	1848.63

CHANNEL 4
EQUATION : Y = (2438.000) + (-34.875) * X

FOR	X= 0.00	Y=	2438.00
FOR	X= 1.00	Y=	2403.13
FOR	X= 2.00	Y=	2368.25
FOR	X= 3.00	Y=	2333.38
FOR	X= 4.00	Y=	2298.50
FOR	X= 5.00	Y=	2263.63
FOR	X= 6.00	Y=	2228.75
FOR	X= 7.00	Y=	2193.88
FOR	X= 8.00	Y=	2159.00
FOR	X= 9.00	Y=	2124.13

*virus concentration expressed as the exponent of 1.6 x 10^8 LD_{50}/ml WEE virus

Table 56 Linear Regression and Statistics of Latex Counts in Channel 3 and Channel 4 for Latex Particles Coated with >4.096 x 10^4/ml HI WEE Antibody and Reacted with 1.6 x 10^9 LD_{50}/ml WEE Virus

CHANNEL 3		CHANNEL 4	
Virus concentration*	Latex count	Virus concentration*	Latex count
0.00	2812.00	0.00	2204.00
9.00	2369.00	9.00	2395.00

DATA SET #	1	2
# OF DATA POINTS	2.00	2.00
MEAN OF X	4.50	4.50
ST. DEV. OF X	6.36	6.36
MEAN OF Y	2590.50	2299.50
ST. DEV. OF Y	313.25	135.06
REGRESSION COEF.	-49.22	21.22
STANDARD ERROR	1.00E+50	1.00E+50
CORRELATION COEF.	-1.00	1.00
X-INTERCEPT	57.13	-103.85
Y-INTERCEPT	2812.00	2204.00

CHANNEL 3
EQUATION : Y = (2812.000) + (-49.222) * X

FOR	X= 0.00	Y=	2812.00
FOR	X= 1.00	Y=	2762.78
FOR	X= 2.00	Y=	2713.56
FOR	X= 3.00	Y=	2664.33
FOR	X= 4.00	Y=	2615.11
FOR	X= 5.00	Y=	2565.89
FOR	X= 6.00	Y=	2516.67
FOR	X= 7.00	Y=	2467.44
FOR	X= 8.00	Y=	2418.22
FOR	X= 9.00	Y=	2369.00

CHANNEL 4
EQUATION : Y = (2204.000) + (21.222) * X

FOR	X= 0.00	Y=	2204.00
FOR	X= 1.00	Y=	2225.22
FOR	X= 2.00	Y=	2246.44
FOR	X= 3.00	Y=	2267.67
FOR	X= 4.00	Y=	2288.89
FOR	X= 5.00	Y=	2310.11
FOR	X= 6.00	Y=	2331.33
FOR	X= 7.00	Y=	2352.56
FOR	X= 8.00	Y=	2373.78
FOR	X= 9.00	Y=	2395.00

*virus concentration expressed as the exponent of 1.6 x 10^9 LD_{50}/ml WEE virus

IMAGE ANALYSIS FOR CLAM SYSTEM AUTOMATION

Automated image analysis can provide a rapid means of identifying and quantifying large amounts of pictorial information. It can be used to extract essential information and features from data, thereby reducing human intervention and increasing the speed of analysis. Such a system would consist of a computer and a device to digitize and input the picture to the computer.

The input could be either a microdensitometer for scanning pictures or an image dissection tube (similar to a TV camera) for "live" images. The computer would be either general-purpose or specialized. A flow diagram of the steps involved in such an image analysis system might be as in Figure MM.

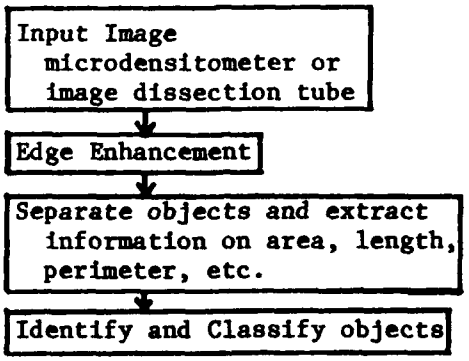

After the image is didgitized and input to the computer, the edges need to be enhanced since there is noise and lost resolution in digitizing. After the edges are enhanced, the objects can be separated and the desired information extracted from each. From this information the objects are identified.

The purpose of this particular work is to count the number of groups of latex particles and the number of particles in each group. Since no equipment for digitizing actual images was available and edge detection is not the goal, the data was simulated for the program such that no edge enhancement was needed. This is the first of three parts. The procedure in this part is to ask for the desired data for simulation. First the scale size of the picture is input. No units are input, the implied size may be miles, feet, meters, microns, etc. Then the radius is input. Since only 1024 (32 x 32) data points are used for the digitized picture, the ratio between the picture size and radius determines the size and resolution for particles. The data for the circles, in the form of where the centers are to be located, is then input. The data input is in terms of the number of implied units in the picture scale size, so the centers must lie within the picture boundaries. The co-ordinate system used has as its origin the upper left-hand corner of the picture. The first co-ordinate gives the distance down and the second the distance across. This system was chosen for compatability with a raster scan of the digitized picture. After the image is simulated, the digitized picture is printed out along with a list of the centers of the particles.

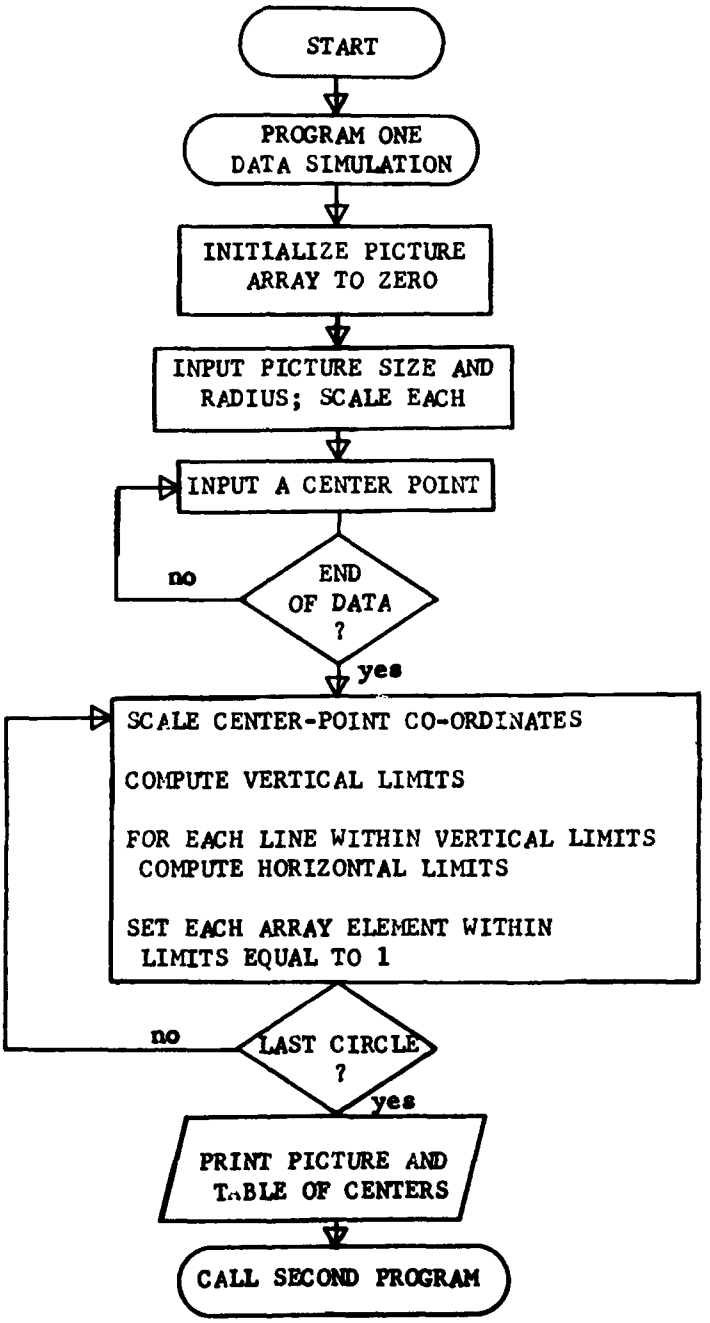
START
PROGRAM ONE DATA SIMULATION
INITIALIZE PICTURE ARRAY TO ZERO
INPUT PICTURE SIZE AND RADIUS; SCALE EACH
INPUT A CENTER POINT
END OF DATA ?
no
yes
SCALE CENTER-POINT CO-ORDINATES
COMPUTE VERTICAL LIMITS
FOR EACH LINE WITHIN VERTICAL LIMITS
COMPUTE HORIZONTAL LIMITS
SET EACH ARRAY ELEMENT WITHIN LIMITS EQUAL TO 1
LAST CIRCLE ?
no
yes
PRINT PICTURE AND TABLE OF CENTERS
CALL SECOND PROGRAM

The second segment does the separation of groups and finds the area of each. This is done by looking at the data in a raster-like scan, going from the top line to the bottom line and from left to right within each line. For each line, the segments of circles intersecting it are recorded and compared with like information from the previous line. For example, consider the following six lines:

```
.....................
.............0000...
.....00.......000000..
....0000......000000..
...000000...000000000.
...00000000000000000..
```

Whenever a segment lies directly under another segment from the previous line (as does the second segment in line three), the two segments are part of the same group. If not, a new group is tenatively formed (as would be for the first segment in line three). When a line segment lies below two or more segments from the previous line (as does the segment in line six), the two groups are merging into one. After the entire picture is scanned, a new picture is printed out showing the separate groups with different symbols along with the area of each group in terms of the equivalent number of particle areas it occupies.

The purpose of the third program is to refine the counting procedure. Since two particles may overlap, counting the number of particles in a group by area only may lead to inaccurate results. Knowing that there is a one-to-one relationship between the number of round particles and their centers, finding the centers of the particles may lead to more accurate counts. An algorithm that traces around the edge of each group and records the location of successive edge-points has been developed. The printout examples give the number of edge-points (N) and the data points in clockwise order around the group. For a given edge-point in a group, the next point is found by checking all eight neighbors in clockwise order. This process continues until the circle is completely traced. For each set of three edge-points in a group, a radius of curvature and center of curvature can be found. The many combinations of centers for each group should cluster together and be recognizable as distinct centers. Further work to be done includes finding suitable criteria for using the clusters to find the best-fitting centers.

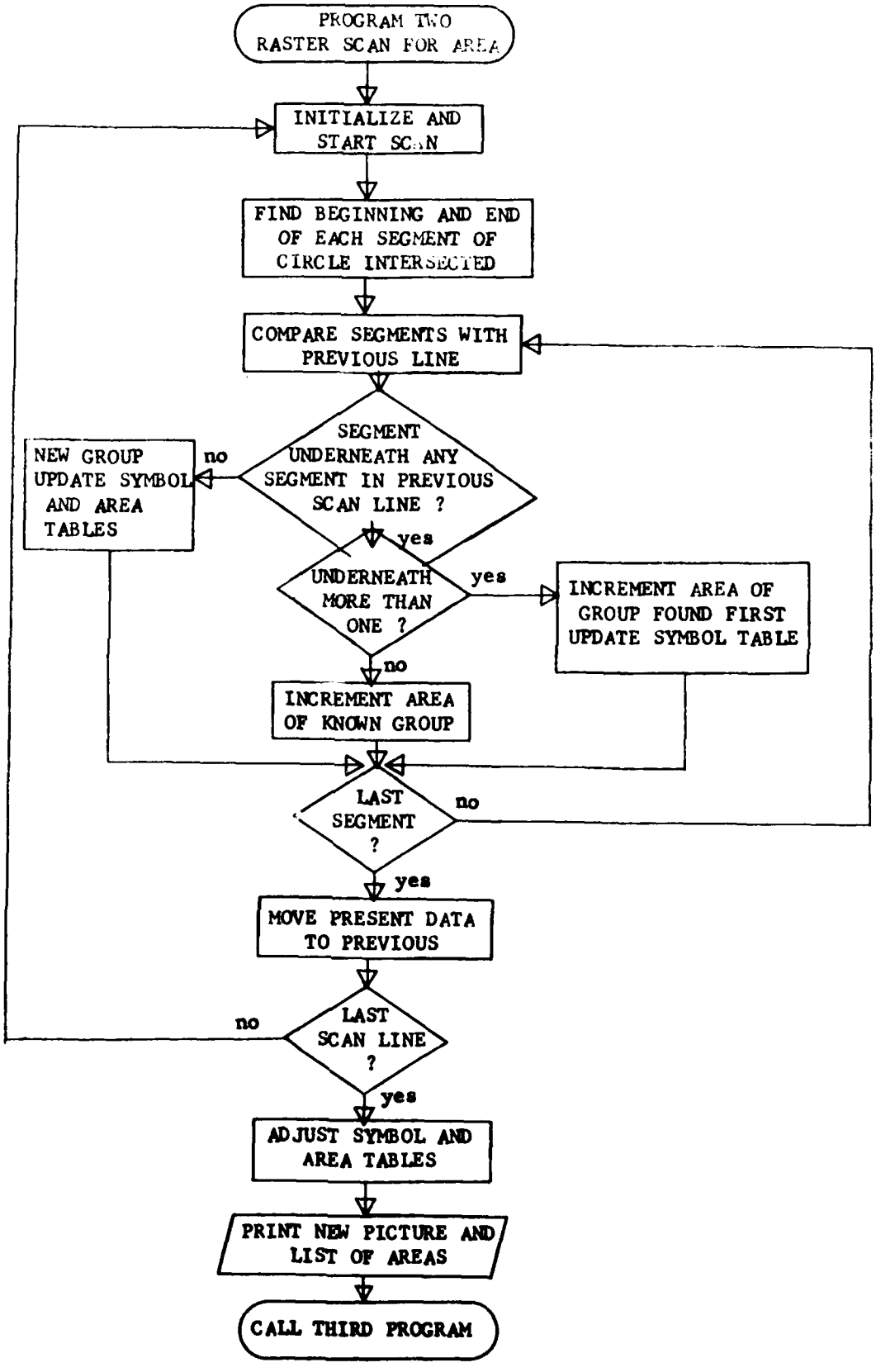
PROGRAM TWO
RASTER SCAN FOR AREA
INITIALIZE AND START SCAN
FIND BEGINNING AND END OF EACH SEGMENT OF CIRCLE INTERSECTED
COMPARE SEGMENTS WITH PREVIOUS LINE
SEGMENT UNDERNEATH ANY SEGMENT IN PREVIOUS SCAN LINE ?
no
NEW GROUP UPDATE SYMBOL AND AREA TABLES
yes
UNDERNEATH MORE THAN ONE ?
yes
INCREMENT AREA OF GROUP FOUND FIRST UPDATE SYMBOL TABLE
no
INCREMENT AREA OF KNOWN GROUP
LAST SEGMENT ?
no
yes
MOVE PRESENT DATA TO PREVIOUS
LAST SCAN LINE ?
no
yes
ADJUST SYMBOL AND AREA TABLES
PRINT NEW PICTURE AND LIST OF AREAS
CALL THIRD PROGRAM

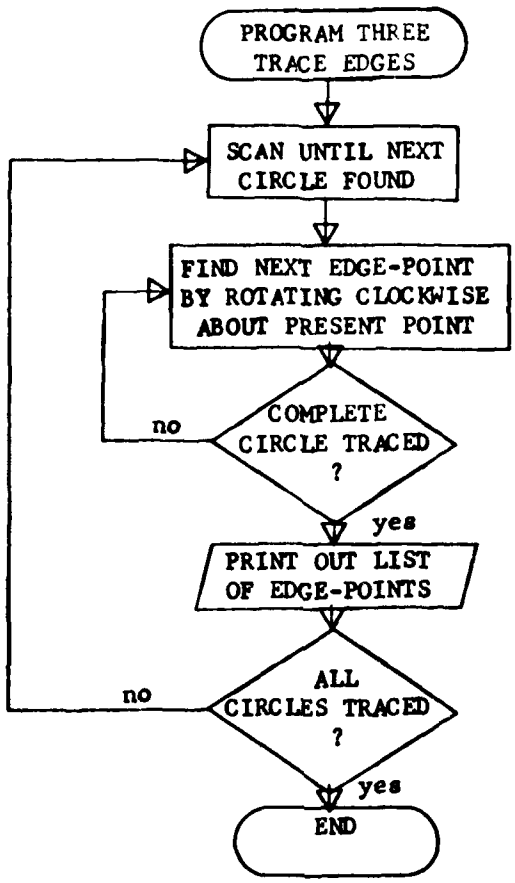
PROGRAM THREE
TRACE EDGES
SCAN UNTIL NEXT
CIRCLE FOUND
FIND NEXT EDGE-POINT
BY ROTATING CLOCKWISE
ABOUT PRESENT POINT
COMPLETE
CIRCLE TRACED
?
no
yes
PRINT OUT LIST
OF EDGE-POINTS
ALL
CIRCLES TRACED
?
no
yes
END

Image Analysis Example I.

```
ENTER PICTURE SIZE  ?          10
ENTER RADIUS OF SPHERES ?       1
ENTER A CENTER POINT ?          5.0,4.0
ENTER A CENTER POINT ?          3.5,6.0
ENTER A CENTER POINT ?          3.0,2.0
ENTER A CENTER POINT ?          2.0,7.0
ENTER A CENTER POINT ?          4.0,8.0
ENTER A CENTER POINT ?          7.5,7.0
ENTER A CENTER POINT ?          8.5,6.0
ENTER A CENTER POINT ?          8.0,3.0
ENTER A CENTER POINT ?          END
```

Image Analysis Example I. (cont)

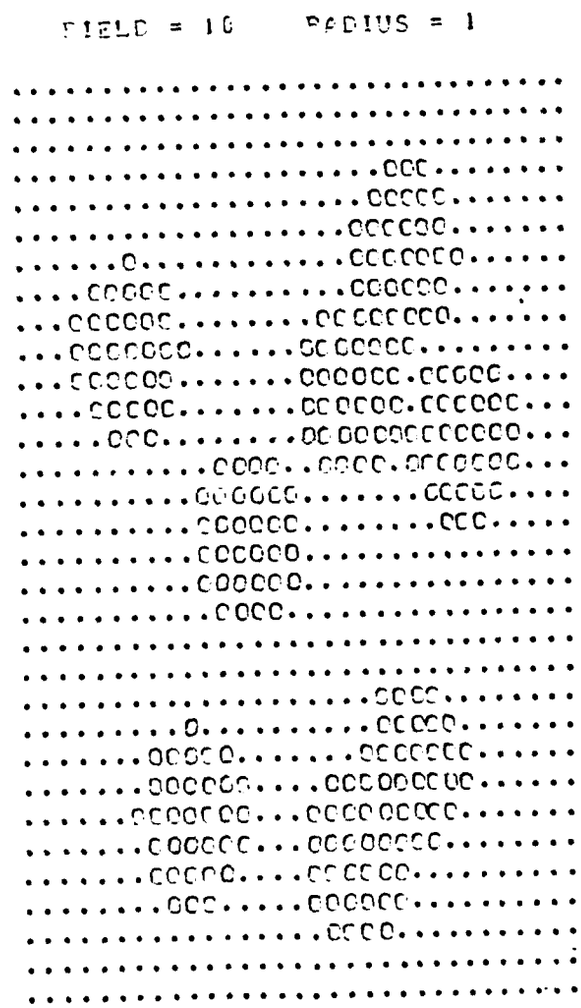

CENTERS

(5.0 , 4.0)
(3.5 , 6.0)
(3.0 , 2.0)
(2.0 , 7.0)
(4.0 , 8.0)
(7.5 , 7.0)
(8.5 , 6.0)
(8.0 , 3.0)

Image Analysis Example I. (cont)

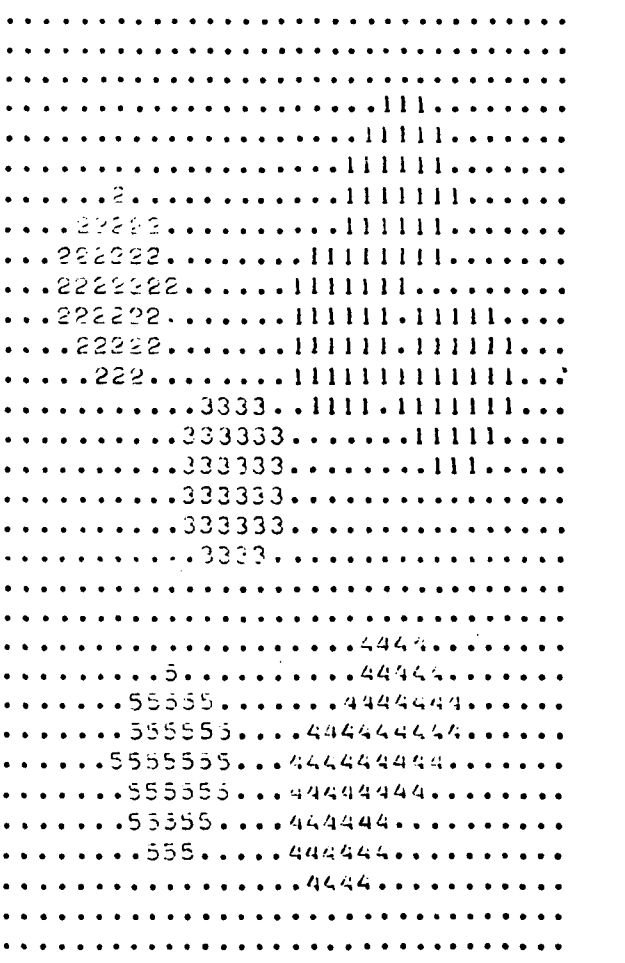

GROUP #	EQUIVALENT AREA
1	3.0152
2	1.0256
3	0.9947
4	1.8629
5	1.0256

Image Analysis Example I. (cont)

```
GROUP # 1     N = 43
(  4, 22)(  4, 23)(  4, 24)(  5, 25)(  6, 25)(  7, 26)(  8, 25)
(  9, 25)(  9, 24)( 10, 23)( 11, 22)( 12, 22)( 13, 23)( 12, 24)
( 11, 24)( 11, 25)( 11, 26)( 11, 27)( 11, 28)( 12, 29)( 13, 29)
( 14, 29)( 15, 28)( 16, 27)( 16, 26)( 16, 25)( 15, 24)( 14, 23)
( 13, 22)( 14, 21)( 14, 20)( 14, 19)( 14, 18)( 13, 17)( 12, 17)
( 11, 17)( 10, 17)(  9, 18)(  9, 19)(  8, 20)(  7, 20)(  6, 20)
(  5, 21)

GROUP # 2     N = 16
(  7,  7)(  8,  8)(  8,  9)(  9,  9)( 10, 10)( 11,  9)( 12,  9)
( 13,  8)( 13,  7)( 13,  6)( 12,  5)( 11,  4)( 10,  4)(  9,  4)
(  8,  5)(  8,  6)

GROUP # 3     N = 16
( 14, 12)( 14, 13)( 14, 14)( 14, 15)( 15, 16)( 16, 16)( 17, 16)
( 18, 15)( 19, 15)( 19, 14)( 19, 13)( 19, 12)( 18, 11)( 17, 11)
( 16, 11)( 15, 11)

GROUP # 4     N = 24
( 22, 21)( 22, 22)( 22, 23)( 22, 24)( 23, 25)( 24, 26)( 25, 26)
( 26, 25)( 27, 24)( 27, 23)( 28, 22)( 29, 22)( 30, 21)( 30, 20)
( 30, 19)( 30, 18)( 29, 17)( 28, 17)( 27, 17)( 26, 17)( 25, 18)
( 25, 19)( 24, 20)( 23, 21)

GROUP # 5     N = 16
( 23, 10)( 24, 11)( 24, 12)( 25, 13)( 26, 13)( 27, 13)( 28, 12)
( 29, 11)( 29, 10)( 29,  9)( 28,  8)( 27,  8)( 26,  7)( 25,  8)
( 24,  8)( 24,  9)
```

Image Analysis Example II.

```
ENTER PICTURE SIZE  ?          10
ENTER RADIUS OF SPHERES ?       1
ENTER A CENTER POINT ?          1.3,3.0
ENTER A CENTER POINT ?          3.2,3.8
ENTER A CENTER POINT ?          3.8,1.8
ENTER A CENTER POINT ?          4.5,4.5
ENTER A CENTER POINT ?          2.0,7.0
ENTER A CENTER POINT ?          3.5,6.0
ENTER A CENTER POINT ?          4.0,8.0
ENTER A CENTER POINT ?          8.3,1.9
ENTER A CENTER POINT ?          7.1,2.5
ENTER A CENTER POINT ?          8.5,7.0
```

Image Analysis Example II. (cont)

FIELD = 10 RADIUS = 1

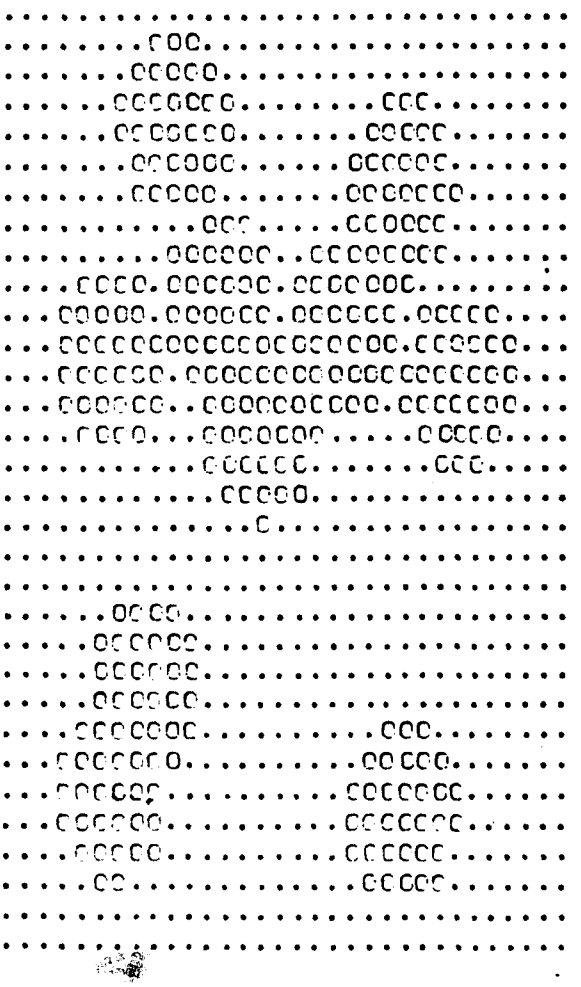

CENTERS

(1.3 , 3.0)
(3.2 , 3.8)
(3.6 , 1.6)
(4.5 , 4.5)
(2.0 , 7.0)
(3.5 , 6.0)
(4.0 , 8.0)
(6.3 , .9)
(7.1 , 2.5)
(8.5 , 7.0)

Image Analysis Example II. (cont)

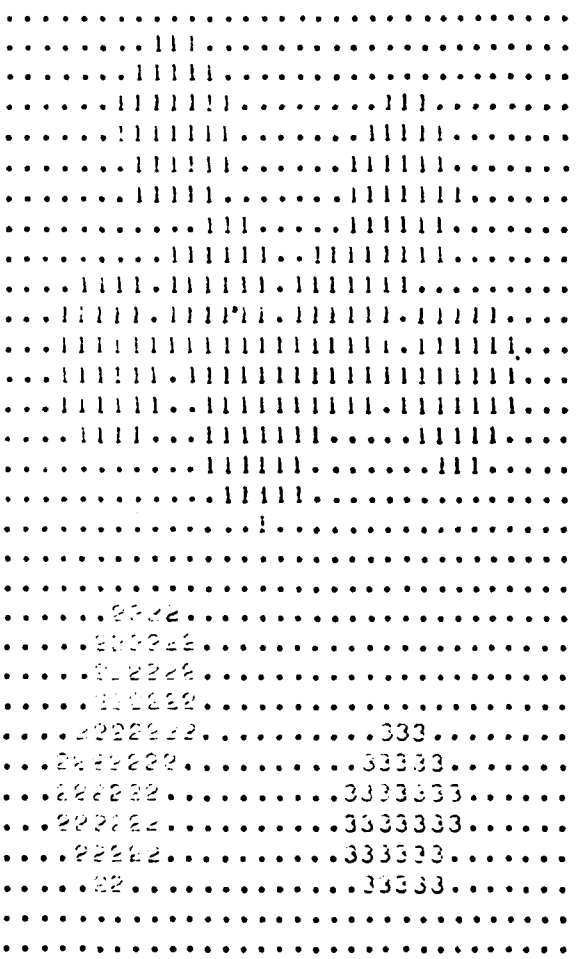

GROUP #	EQUIVALENT AREA
1	0.0367
2	1.7697
3	1.0258

Image Analysis Example II. (cont)

```
GROUP # 1     N = 95
(  2,  9)(  2, 10)(  2, 11)(  3, 12)(  4, 13)(  5, 13)(  6, 13)
(  7, 12)(  8, 13)(  8, 14)(  9, 15)( 10, 15)( 11, 15)( 12, 16)
( 11, 17)( 10, 17)(  9, 18)(  9, 19)(  8, 20)(  7, 20)(  6, 20)
(  5, 21)(  4, 22)(  4, 23)(  4, 24)(  5, 25)(  6, 25)(  7, 26)
(  8, 25)(  9, 25)(  9, 24)( 10, 23)( 11, 22)( 12, 22)( 13, 23)
( 12, 24)( 11, 24)( 11, 25)( 11, 26)( 11, 27)( 11, 28)( 12, 29)
( 13, 29)( 14, 29)( 15, 28)( 16, 27)( 16, 26)( 16, 25)( 15, 24)
( 14, 23)( 13, 22)( 14, 21)( 14, 20)( 14, 19)( 15, 18)( 16, 17)
( 17, 17)( 17, 16)( 18, 15)( 17, 14)( 17, 13)( 16, 12)( 15, 12)
( 14, 12)( 13, 11)( 12, 10)( 13,  9)( 14,  9)( 15,  8)( 15,  7)
( 15,  6)( 15,  5)( 14,  4)( 13,  4)( 12,  4)( 11,  4)( 10,  5)
( 10,  6)( 10,  7)( 10,  8)( 11,  8)( 12,  9)( 11, 10)( 10, 10)
(  9, 10)(  9, 11)(  8, 12)(  7, 11)(  7, 10)(  7,  9)(  7,  8)
(  6,  8)(  5,  7)(  4,  7)(  3,  8)

GROUP # 2     N = 23
( 21,  7)( 21,  8)( 21,  9)( 21, 10)( 22, 11)( 23, 11)( 24, 11)
( 25, 11)( 26, 10)( 27,  9)( 28,  9)( 29,  9)( 29,  8)( 30,  7)
( 30,  6)( 29,  5)( 28,  4)( 27,  4)( 26,  4)( 25,  5)( 24,  6)
( 23,  6)( 22,  6)

GROUP # 3     N = 16
( 25, 22)( 25, 23)( 25, 24)( 26, 25)( 27, 26)( 28, 26)( 29, 25)
( 30, 25)( 30, 24)( 30, 23)( 30, 22)( 30, 21)( 29, 20)( 28, 20)
( 27, 20)( 26, 21)
```

COMPUTER SIMULATION MODEL OF THE IMMUNE RESPONSE OF MICE TO WESTERN EQUINE ENCEPHALITIS (WEE) VIRUS

BY

GILBERT CHI KUAN HO

A thesis submitted
in partial fulfillment of the requirements for the
degree Master of Science, Major in
Microbiology, South Dakota
State University

1975

COMPUTER SIMULATION MODEL OF THE IMMUNE RESPONSE OF MICE TO WESTERN EQUINE ENCEPHALITIS (WEE) VIRUS

This thesis is approved as a creditable and independent investigation by a candidate for the degree, Master of Science, and is acceptable as meeting the thesis requirements for this degree, but without implying that the conclusions reached by the candidate are necessarily the conclusions of the major department.

Head, Microbiology Department	Date
Thesis Advisor	Date

TABLE OF CONTENTS

TABLE OF CONTENTS (Con't.)

TABLE OF CONTENTS (Con't.)

LIST OF FIGURES

LIST OF TABLES

LIST OF FIGURES (Con't.)

LIST OF TABLES (Con't.)

ACKNOWLEDGEMENTS

I wish to express my sincere gratitude to my major advisor, Dr. Gokaldas C. Parikh, for his counsel and advice during the course of this study and for his patience and understanding during the preparation of this thesis.

I wish to thank Mr. Tom Sorensen for proofreading my thesis and Mr. Steve Duvall for his past effort and advice in this research project.

I am also grateful to Mr. Wilbur Reitzel for his technical assistance and advice in the handling of animals and the computer expertise of Mr. Landon Nusz.

I am indebted to Dr. Paul R. Midlaugh for his proofreading of this thesis and to Mrs. Charlotte Dennis for typing and proofreading this thesis.

The financial support of the Naval Weapons Laboratory, Office of Naval Research in this research project is gratefully acknowledged.

I also wish to extend this gratitude to Dr. David Reed of the Veterinary Science Laboratory, Professor Eugene Whitehead and Dr. I. Palmer of Station Biochemistry, Dr. J. Grove of the Chemistry Department, and Dr. S. Friefeld for their valuable advice and their provision of facilities, equipment and chemicals, which are vital to their studies.

Lastly, I wish to thank my wife, Mei Yu, for her patience, understanding, encouragement, and help during the preparation of this thesis.

GCH

INTRODUCTION

The lymphatic system of an animal is optimally developed to protect the body from antigenic invasion. The epithelial and subepithelial compartments of the body are provided with a vast number of wandering cells and a network of centralized lymphorecticular tissues. All of these are capable of reacting to intruding foreign antigens. Upon antigenic challenge, immunocompetent cells (ICC) or antigen-specific lymphocytes are activated; this leads either to cell mediated and/or humoral antibody immune responses. The subsequent effect is an accumulation of the responding cells, both by local proliferation and recruitment from the circulation. Through the interaction of both cellular and humoral components of the immune system, the phagocytic cells and the complement system are activated, thereby leading to the localization, destruction, and elimination of the antigen. Collectively, this set of phenomena is called an immune response. In the course of this response, immunologically committed cells are released from initially activated lymphoid tissue via the efferent lymphatic ducts and the bloodstream to other lymphoid organs with resulting logarithmic amplification of the immune response and the development of the capacity to respond much more efficiently to a second encounter with the same antigen. The immune response to most pathogenic antigens (such as bacterial, fungal, and viral infections) cannot be initiated without the complex reaction of phagocytosis by the macrophages and, probably, by the monocytes.

Primary Immune Response

With most antigens, the initial exposure evokes a smaller antibody response than do subsequent identical exposures, and the antibodies thus formed differ in their avidity. The immune response to the first exposure of an immunogen is known as a primary response and thus a secondary exposure induces a secondary response. The manifestation of an immune response following antigenic stimulation may vary from one to thirty days. It is predictable for antibodies to be detected three to four days after stimulation of erythrocytes, five to seven days after soluble antigens, and ten to fourteen days after bacterial cells. In contrast to most antigens, bacteriophage ϕ X 174 evoked detectable antibody formation 24 hours after an intravenous injection. The antibody formed in a primary response is dominantly of the 19S immunoglobulin M (IgM) class of antibody, and their concentration usually increases exponentially for four to five days before leveling off. 7 S immunoglobulin G (IgG) antibody could be detected shortly afterwards. The synthesis of IgM antibody usually diminishes one or two weeks after immunization while the level of IgG is still increasing. Experimental evidence suggests that IgG, by some kind of direct feedback mechanism, inhibits the synthesis of IgM.

Secondary Response

Secondary or anamnestic immune responses have characteristic features which differ from the initial response. As a whole, secondary responses require a lower threshold dose of antigen, have a shorter time lag period, have a higher level of antibody production, and have

a longer persistence of antibody synthesis. In addition, the antibody formed has a much higher avidity and is usually predominantly of the IgG class. The higher level of IgG formed during a secondary response is due to the increased number of antibody-forming cells rather than due to an increase of the production rate per cell. Although some antigens such as pneumococcal polysaccharides and lipopolysaccharides do not elicit a secondary response, most antigens elicit a pronounced secondary response many weeks, or even years, after a primary stimulus. This capacity provides a long-lasting immunity against infection.

Under normal circumstances, an animal will not form antibodies to a substance that is antigenically related to its own. Thus, the basic characteristic of an immunogen is its foreignness to a host. The degree of foreignness is impossible to define but is strongly related to the phylogenic similarity between the antigen and the responding host. For example, serum protein of human is a much better immunogen to rabbits and guinea pigs than to monkeys since only a few of the protein potential antigenic determinants are foreign to monkeys. Different varieties of antibodies could be formed to almost any biological macromolecules, and antibody is always heterogeneous in nature even when produced against the same antigen. Protein is, by far, the most outstanding for its potential antigenicity. Large molecular weight, complexity of structure, and foreignness to a host are some basic characteristics of an immunogen although these properties are always provisional. Many substances that were thought to be non-immunogenic had been found later to induce antibody formation at least in certain

animal hosts or different individuals under particular experimental conditions such as the appropriate choice of dosage, route, adjuvant and carrier. Following the intravenous injection of a dose of antigen, the elimination curve of this antigen is usually triphasic. First, there is a rapid decline due to diffusion into the extravascular space; then, there is a period of metabolic decay followed by a sharp decline which signals the formation of the antibody. During the terminal phase, the antigen exists in the form of an antibody-antigen complex, and as the antibody level becomes detectable, the antigen level usually diminishes. This does not, however, mean that the antigen has been completely eliminated from the body. Antigen molecules or their fragments usually persist for a long period of time within the phagocytic cells of the reticuloendothelial system (Kupffer cells and the macrophages) and retain some of the antigenic determinants. Cellular and particulate antigens such as bacterial, erythrocytes, and bacteriophages do not exhibit the initial phase of decline because they do not diffuse into the extravascular space. These particles are much more rapidly removed from the bloodstream than are soluble antigens because they are phagocytized much more effectively by the macrophages.

The Immune Response Model

Despite the recent advances in immunology, there have been a lot of doubts and controversy concerning the control mechanisms involved in an immune response. The purpose of this study is to simulate a computer model of the immune response of mice (as hosts) to western equine encephalitis virus (WEE) - the antigen.

The choice of the Mouse-WEE system for this study has several reasons, as follows:

1. Much is known about the physiological and immunological capacity of mice.
2. Mice are inexpensive and easy to handle.
3. The antigenic property of WEE to mice or other rodents is not yet known in detail.
4. WEE virus is of great significance in epidemiology for both animals and humans.

In compliance with the future development and extension of the Coated Latex Adsorption Method (CLAM) to include the application of viral detection in vivo, this model could provide a clear insight of the limiting parameters through a cybernetic analysis. In other words, this model could provide information concerning important elements such as the earliest detectable humoral antibody response, the level of circulating antibody at the peak of a primary response, and the latent period required for the activation and maturation of the immunocompetent cells of an animal.

Under the guidelines of this in vivo model, the CLAM system can be expanded to detect viruses and their antibodies in vivo. The basic CLAM will be modified, if necessary, to make it suitable for in vivo detection. The immediate purpose of making this model is to find out the time of early antibody formation after an animal or a human was infected. This provides, theoretically speaking, an early warning signal for possible viral infection. A latent period or symptom-free

stage has commonly been associated with viral diseases. If patients at this stage could be screened out for early medical treatment, lives and costs might be saved.

This model is a stochastic model and is simulated by a computer program which has been formulated for a Hewlett-Packard (Model 9830) desk-top programmable calculator and was written in the Basoc Language. The aim of the in vivo model is to understand the mechanisms of immune response and the interactions among them. Each step in an evaluation process represents a small building block in which one major phenomenon was expected to be observed. The resultant expression of this phenomenon is interpreted in numerical terms.

The comparison of experimental and simulated data can well reflect the reliability of specific mechanisms involved in any type of immunological response. An understanding of these mechanisms could greatly assist in the study of preventive measures, both experimentally and theoretically against various ailments. Latent viral diseases such as viral hepatitis can be analyzed by the computer in a subroutine of the proposed CLAM in vivo model system which predicts how long a patient has been infected and whether a patient is a potential carrier. A study of this sort would be of immunological and clinical, as well as epidemiological, values.

In order to provide maximum insight of the immunological expression of mice to WEE virus, a careful selection of immunological parameters is vital. The major difficulty confronting modeling is the expression of a phenomenon in quantitative terms before mathematical

formulation could be derived, and in order to do so, certain assumptions and simplifications have to be made.

The theoretical background of this model is the clonal selection theory of immune response. According to this theory, the lymphocyte population of a host is heterologous in nature and is composed of different groups or clones of cells, each of which is capable of synthesizing one or a few antibodies of one antigenic specificity. Each clone is made up of immunocompetent cells capable of reacting with specific antigens which have binding affinity to the cell surface receptors. Immunocompetent cells are lymphocytes which could react with an antigen in a specific manner and, in so doing, could initiate an immune response. There are basically two systems of immunity - humoral and cell mediated.

Humoral antibody responses consist of reactions mediated by immunoglobulin proteins containing various types of specific antibodies. Examples of these reactions include atopic diseases such as allergic rhinitis and allergic asthma, antitoxic protection against certain bacterial diseases and some antiviral activity, some drug reactions, immune complex diseases such as systemic lupus erythematosus, and some autoimmune processes such as autoimmune hemolytic anemia or erythroblastosis fetalis.

Cell mediated immunity includes graft rejection, delayed hypersensitivity, cytotoxic activity against intracellular organisms, and possibly offering surveillance to endogenous tumor formations. Furthermore, most humoral antibody responses cannot be initiated

without the cooperation of cellular components. These two types of immunity are mediated respectively by the bursa (or its equivalent in mammals) dependent B cells and by the thymus dependent T cells.

The outline of this model is shown in the conceptual flow diagram (Fig. 1). The initial step in this model is to estimate the number of antigen specific B lymphocyte precursors that are capable of transforming into plasma cells. This is made possible by the fact that there are available data on the weight of the lymphoid tissues, the weight of a lymphocyte, and the percentage weight of lymphocytes in the lymphoid tissues. Lymphocytes present in the bloodstream are estimated from the total volume of blood which is based on the body weight of the animal. The total number of lymphocytes present in an animal is the sum of the lymphocytes present in these two compartments (lymphatic and circulatory). Studies with surface markers and rosette-forming method, the ratio of T and B lymphocytes in the various lymphatic tissues such as the bone marrow, spleen, lymph nodes, thymus, gut associated lymphoid tissues, and the peripheral blood are known. Since the prime interest in an immune response is the antibody forming cells, this model does not follow the activity of the T cells in detail; the magnitude of an immune response depends only on the number of B lymphocytes and the dose of the antigen.

It is known that only a small portion of these lymphocytes could respond specifically to any one antigen. This population of antigen-specific or, in this case, the WEE-specific antibody forming precursor lymphocytes is referred to as immunocompetent cells (ICC).

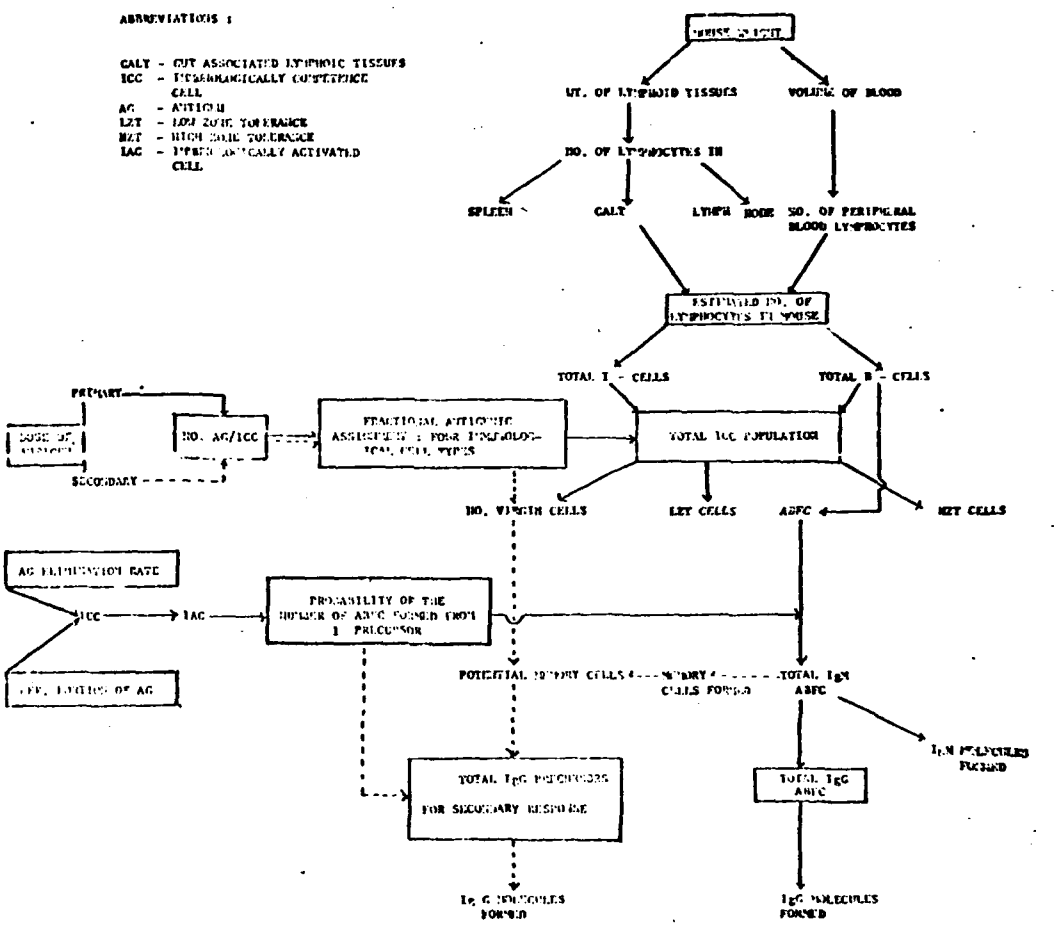

Figure 1. A conceptual flow diagram of the immune response model.

In a given dose of antigen, most will be eliminated through biological degradation and only a small portion is effective in stimulating the lymphocytes of the host. After the initial administration of the antigen, a latent period is required for the immunocompetent cells to be activated and another time lapse is needed for these activated cells to differentiate and proliferate before plasma cells appear. Furthermore, these lymphocytes may either be activated or paralyzed depending upon the number of surface receptors occupied by the antigens. The distribution of antigens among the host lymphocytes is predicted to follow a Poisson distribution which assumes that the occurrence of individual contacts of antigen with the cell surface receptors are entirely independent events and are dependent only on the mean value of the average number of antigens available per antigen-specific lymphocytes. Based on this assumption, four types of cells are assigned to the antigen-specific lymphocyte population by Poisson distribution equations. The first type is called the virgin cells or cells that have made no contact with antigens. The second type is the low zone tolerant cells which have come in contact with the antigen but the signal is not strong enough to elicit an effective activation. The third type is the antibody-forming cells which have the potential to divide and transform, and their progeny cells will either become memory cells or plasma cells. The last type is the high dose tolerant cells which have received over-stimulating signals and the consequence is either cell death or abortive proliferation of the tolerant cells. Whether an animal can respond to a given dose of antigen depends upon

the resultant fraction of cell type that dominates the immunocompetent cell population. The fraction of virgin cells is considered potential memory cells, and together with memory cells that are produced during the course of a primary response, they are the potential antibody-forming cell precursors in a secondary response. Since no data is available as to the ratio of the number of plasma cells to memory cells formed, it is assumed that during the entire course of a primary immune response, this ratio remains constant. In other words, the number of memory cells is presumed to increase proportionally with the number of antibody-forming cells.

The activated antibody-forming cell precursor usually undergoes nine to eleven successive divisions before division stops. The generation time of a plasmablast is about ten hours, and a mature plasma cell has a life span of about two to three days. Successive proliferation of the plasmablast is assumed to be dependent on a continuous stimulation of the antigen. The number of antibody-forming cells formed from one precursor depends mainly upon the effective dose of the antigen and the elimination rate of the antigen which defines the duration and extent of a continuous antigenic challenge.

A Poisson probability equation is used to simulate the number of plasma cells formed from a single precursor cell. This model accepts the hypothesis that during a primary response some IgM producing cells are switched to IgG forming precursor cells and that no IgG antibody would be formed before the sixth day after antigenic challenge. The rate of antibody formation of both IgM and IgG is assumed to be equal

and constant. The prolongation of the antibody level in blood is based on the amount of antibody produced and the half-lives of the two classes of antibody formed. This model takes into account a secondary response in which the basic format is the same as the primary response. Only the number of antigen-specific B cells are substituted by the number of memory cells, and the latent period of plasma cell formation is shortened.

LITERATURE REVIEW

Modeling

Since the era of Issac Newton, the science of Physics has progressed from verbal expressions to symbolic and mathematical languages. Biology, on the other hand, has remained largely in a descriptive state. Unlike many physical phenomena, biological systems are far more complex to be related from component interactions. Even a simple biological system such as the vital functions of a small microorganism is mathematically intractable even if all component interactions are known. Despite this handicap, mathematical descriptions of biological systems have become an increasingly important tool of theoretical biology. Mathematical models provide a clear insight of a biological system, whether in an approximative or confirmative sense, which cannot be obtained otherwise. Considerable successes have been achieved in making partial models of a large variety of biological systems, but they seldom provide reliable prediction of unknown quantitative data. Available invariants among all possible pertinent similarity criteria are few and not enough to assure real physical or operational similarity in the general sense. That is what makes them 'models' (72).

Modeling is a synthetic method and is capable of providing insight into situations far more complex than manageable. Computer modeling of both physical (determinative) and cybernetic (stochastic) systems has added broad new capabilities to the synthetic simulation approach

and promises to be of much value for biological simulation in all its varieties.

A model of two similar systems can be transformed or applied to each other; any two systems which are similar to each other, as in the case of an immune response of two responding animals to the same antigen, share at least one invariant of some sort which is maintained during certain stated transformation. In modern science, the mere verbal statement of a theory is no longer considered adequate and mathematical constructions of various kinds are expected. These may be in the form of conventional mathematical equations or presented in axiomatic statements, and all these representations may be encompassed by computer simulation. If it is granted that theoretical biology does now, or will shortly, fulfill these scientific requirements, modeling analysis may be construed as a means of comparing 'theories' or specific symbolic representation of systems with the goal of discovering their similarities. Alternatively, one may say the goal is to find isomorphism among various descriptions of biological systems. Although many scientists associate modeling theory mainly with the laboratory fabrication of small models, the important progress is largely along theoretical mathematical lines. It is very important to know what kind of model to make before commencing to build it and to be able to predict what conditions must be fulfilled before it can yield quantitative data that is acceptable in a practical sense (67, 72, 74).

It is of critical importance to investigate quite precisely the

set of phenomena which a model describes and to find out what type of model could adequately describe these phenomena. It is usually quite difficult to state with certainty whether or not a given mathematical model is adequate before some observational data are obtained.

There are basically two types of models - deterministic and probabilistic (or commonly known as stochastic) models. A deterministic model is one which stipulates that the conditions under which an experiment is performed determine the outcome of the experiment. For a large number of phenomena, the deterministic model is suitable, but for most biological systems that are usually time dependent, goal seeking, and the critical conditions are usually unknown, a stochastic model is more adequate. It is this type of model that this study is based on.

Stochastic models are numerical formulations in which the main emphasis is place on the probabilities of changes in certain parameters with time. There are many models of this type in medicine and biology (50).

Immune Response Models

Hege and Cole (32) developed a continuous model which equates the number of antibody-forming cells and the titer of circulating antibody. They used data of Jerne's antibody plaque forming cells in mouse spleen following sheep erythrocyte immunization to match the simulated data and found them in close agreement. The information describing average cellular rate of antibody synthesis was unavailable at that time and so was selected arbitrarily. Recently, Hiromoto

et al. (35) tested this model with a murine myloma system, fitting in experimental IgM immunoglobulin forming rate by plasmacytoma cells. They found that simulated values agreed with the experimentally determined antibody level. This model does not provide much insight to the interacting elements in an immune response.

Bell (5, 6) had simulated a series of mathematical models accounting for the various aspects of an immunological response. These models started at a cellular level. The immunological background is highly theoretical and is thus difficult to be tested experimentally. However, these were among the few models that emphasized on the quantitative aspect of an immune response.

Marchalonis and Gledhill (47) simulated an elementary stochastic model on the induction of immunity and tolerance based on the hypothesis of Mitchison (53) and of Nossal (57). The main concept of this model is that antibody production and tolerance can be induced simultaneously in a cellular level and that these phenomena are dose dependent and are related to the statistical distribution of antigen molecules among the potential reactive cells. The second sector of the present model follows closely to this concept. This hypothesis has yet to be substantiated experimentally.

Another model by Cohen et al. was formulated to describe immunological tolerance based on the frequency and configuration of the distribution of antigens on cell surface receptor sites (14, 15, 16, 17).

A series of interesting models were formulated by Jelek and Sterzl (41) and by Sterzl et al. (73) to describe the various aspects of an immune response based on their own experimental findings. These included the probability of the number of antibody-forming cells produced from one precursor cell and the memory cells formed during the course of an immune response. The former is adapted in the probabilistic progeny cell sector of this study.

Theory of Immunity - Interaction of Lymphocytes with Antigen

From the selection theory of antibody formation (10, 37, 38, 39) it was postulated that lymphocytes are precommitted to respond specifically to a single antigenic determinant leading to the production of a class of specific antibody. Mitchison (53, 54) proposed that the initial recognition of an antigen by responding lymphocytes was through receptors which are immunoglobulin in structure. The best experimental evidence supporting this theory was the demonstration by several techniques that only a small fraction could bind a given antigen in any normal lymphocyte population in any animal species. Although the value of this fraction varied with the techniques used and the kind of antigen involved, it was however a sound evidence.

Immunoglobulin receptors had been detected on the surface of lymphocytes from man, rabbit, guinea pigs, mice and chickens using various antiimmunoglobulin sera. Nota et al. (59) found that when mouse splenic lymphocytes were mixed with sheep red blood cells (SRBC), some of these lymphocytes were surrounded by SRBC in a rosette-like formation. This phenomenon had presented an improved method over the

traditional plaque forming cell (PFC) technique first used by Jerne (40) and had been used as an immune response index since the number of rosette-forming cells (RFC) increased substantially in hyperimmunized animals.

This method was extensified by the work of Biozzi et al. (7) and Paulovsky et al. (60). They found that the population of RFC in a normal mouse spleen is heterogeneous, consisting of lymphocytes, blast cell, plasmocytes and macrophages. Rosette formation depends upon the temperature of incubation as well as the interference of cytophilic antibody. Working with homogeneous mouse spleen lymphocytes that were free from macrophages and by incubating with SRBC at 4 C to eliminate the biologically active antibody-forming cells, Wilson (81, 82) was able to demonstrate that rosette formation was due to the action of cell surface receptors rather than the absorption of cytophilic antibody. The specificity of RFC was demonstrated by the fact that when lymphocytes were exposed to two distinguishable types of erythrocytes, no heterogeneous rosettes were found while macrophages mixed with cytophilic antibody formed mixed rosettes. The development of this method opens the way to the determination and quantitation of antigen-specific lymphocytes.

Interacting Components of an Immune Response

A simplified review of an immune response may be described as the interaction of three components: the antigen, the antibody, and the immunocompetent cells. There is a quantitative balance between the stimulation of an immune response and the induction of low or

high dose tolerance following the introduction of a foreign antigen to an animal host. This balance varies with each antigen as well as with each host. The molecular structure, molecular weight, and foreignness of an antigen are the crucial factors in determining the immunological activity of the antigen: the extent of which is dependent upon the dosage, route of administration and the biological catabolic rate of the antigen in vivo. Aggregates of this antigen could protect itself from enzymatic degradation and tend to provide a slow but effective release of stimulation over a longer period of time.

Immunoglobulins

One characteristic of an immunological response is the exquisite specificity of the reaction between an antigen and its corresponding antibody molecules which may either be free in circulation or act as receptors on the cell surface. The antibody molecule belongs to a class of proteins collectively known as immunoglobulins and is composed of two heavy and two light polypeptide chains that are joined to one another by several disulfide bridges. In the molecule the four chains are related in bilateral symmetry. Each chain is divided into two portions - the constant region and the variable region (25, 65).

The light chain of an antibody molecule may be either kappa or lambda and in any one molecule both light chains are always of the same type. Five types of heavy chains exist. They are as follows: the mu, gamma, alpha, delta, and epsilon and specify, respectively, five classes of immunoglobulin molecules: IgM, IgG, IgA, IgD, and IgE. Some immunoglobulins have additional polypeptides (IgM and IgA)

and some form oligomeric association of from two to five units, each unit consisting of paired light and heavy chains. In addition, within one class of immunoglobulins there might be subclasses and allelic variation or different idiotypes within each subclass. The general properties of the immunoglobulins are summarized in Table 1.

The constant region of an antibody molecule has the sequence of amino acids which is essentially the same in all antibodies of a given class. The variable region in which the amino acid sequence varies in different antibody molecules is the region which provides the specificity required for the binding of specific antigens. The constant portion is mainly involved in effector functions such as the binding and activation of the complement system. The various regions of an antibody molecule are shown in Figure 2.

The conceptual framework of the antibody can be summarized as follows:

1. Antibodies are specific and the specificity is based on the amino acid sequence and three dimensional structures of the molecule.
2. Antibodies may bind antigens that are closely related to the eliciting antigen and the avidity is usually lower.
3. Antibodies are heterogeneous in nature. Many classes and groups of immunoglobulins are produced in response even against the same antigenic determinant.

Recently it was found that the antigen receptor sites of an antibody molecule are polyfunctional or they contain subsites at which

Table 1. Different classes of immunoglobulins (20).

IMMUNO-GLOBULIN	LIGHT CHAIN	HEAVY CHAIN	OTHER CHAIN	STRUCTURE
Ig M	kappa or lambda	mu	J	
Ig G	"	gamma 1 gamma 2 gamma 3 gamma 4		
Ig A	"	alpha 1 alpha 2	J, Sc	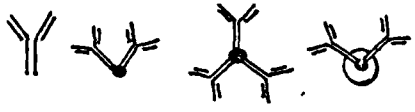
Ig D	"	delta		
Ig E	"	epsilon		

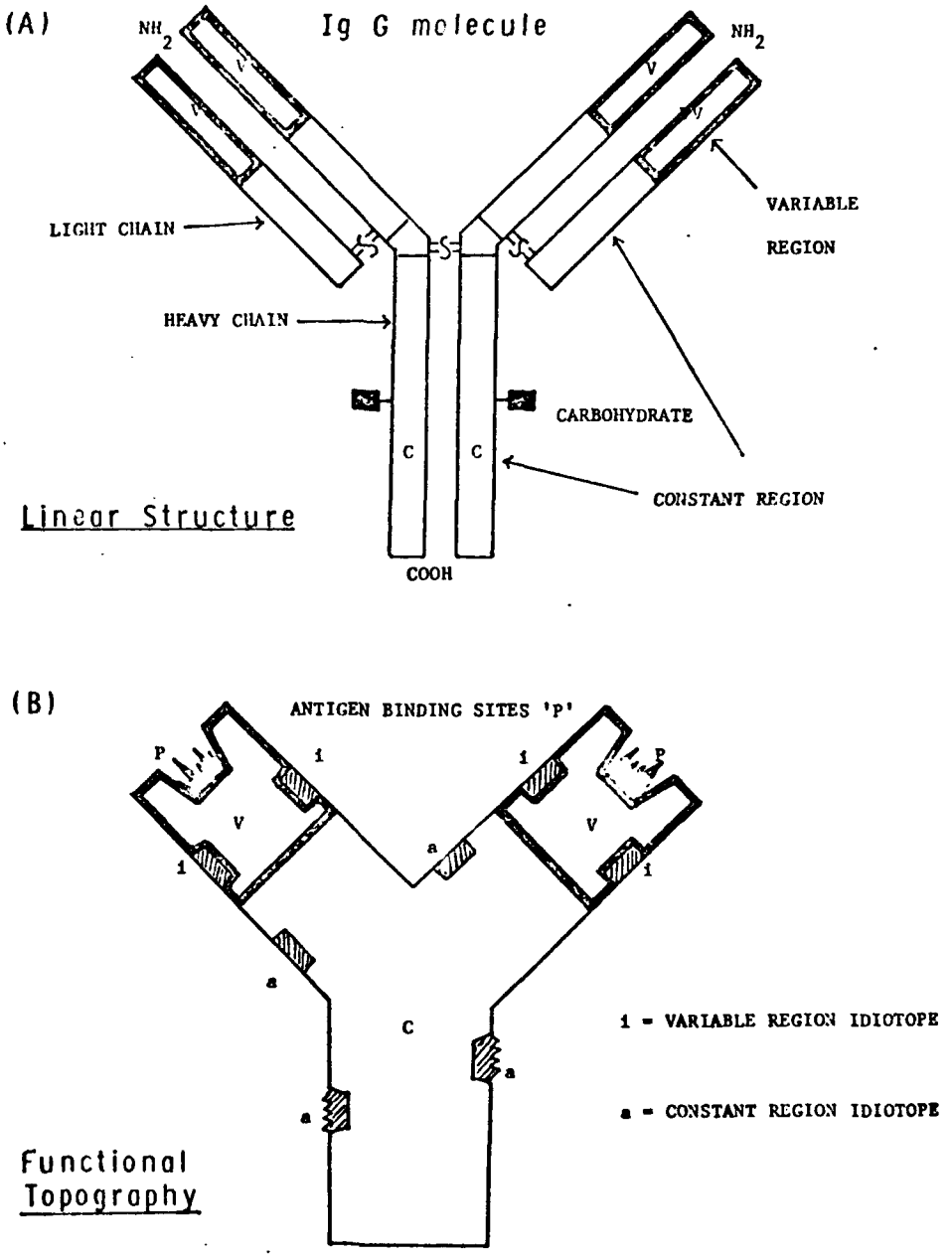

Figure 2. (A) represents the linear structure of an IgG molecule and (B) shows the functional topography of the same molecule (39).

structurally diverse antigenic determinants bind. This concept provides a simple, unifying explanation for a number of seemingly unrelated immunological phenomena (61).

The Immunocompetent Cells

A couple of decades ago it was generally believed that antibodies were produced by phagocytic cells or the macrophages. The first evidence was brought forth by Fagracus suggesting that the antibody forming cells are a family of specialized cells called the plasma cells which are derived from another family of cells called the lymphocytes. Since then, the role of the lymphocytes in an immune response was well defined.

The functional heterogeneity of the lymphocyte population had long been suspected but it was not until 1961 through the work of Miller (51, 52) that these cells had been classically divided into T and B cells.

T and B lymphocytes are morphologically alike but can be distinguished by an array of surface markers (58, 62, 63). Some of these markers are antigens analogous to blood group antigens and are collectively known as 'differentiation antigens' since their expressions are confined only to some cell types. The 'theta antigen' and the 'thymic leukemia antigen' in mice are present only in the T cells where B cells possess other surface antigens such as the 'mouse-specific B lymphocyte antigen'. The ultimate precursor of both the T and B cells is the hemapoietic stem cells of the bone marrow. In both mammals and birds, these precursor cells first appear in the

yolk sac which is a membranous structure connected to the intestinal cavity of the embryo (Fig. 3). During embryonic development, the pluripotential stem cells migrate through the bloodstream to the liver (in mammals) and spleen (in both birds and mammals) before settling permanently in the bone marrow. The pattern of differentiation of a stem cell is controlled genetically but could be influenced by the microenvironment of the site to which the stem cells migrate (20). The development and functioning of the T cells arises primarily in the thymus. The structural framework of the thymus is formed from the epithelial cells that initially line the third and fourth pharyngeal pouches, embryonic structures in the region which eventually becomes the throat. Early in embryonic development, these epithelial cells migrate down into the chest and develop into the thymus which controls the immunological differentiation of the stem cells into T lymphocytes either by direct contact or by the action of thymic hormones. The B cells are developed in practically the same way, but their immunological differentiation is dependent upon the influence of the bursa of Fabricius in avian species and the fetal liver and/or spleen in mammals. These phenomena are illustrated in Figure 3.

T cells are highly motile; they are present in practically all parts of the body and have a longer life span than the B cells. These properties make the T cells the logical candidate for initial antigenic recognition and memory retention for an anamnestic immune response. The majority of the B lymphocytes do not recirculate and upon antigenic stimulation the B lymphocytes start to transform and

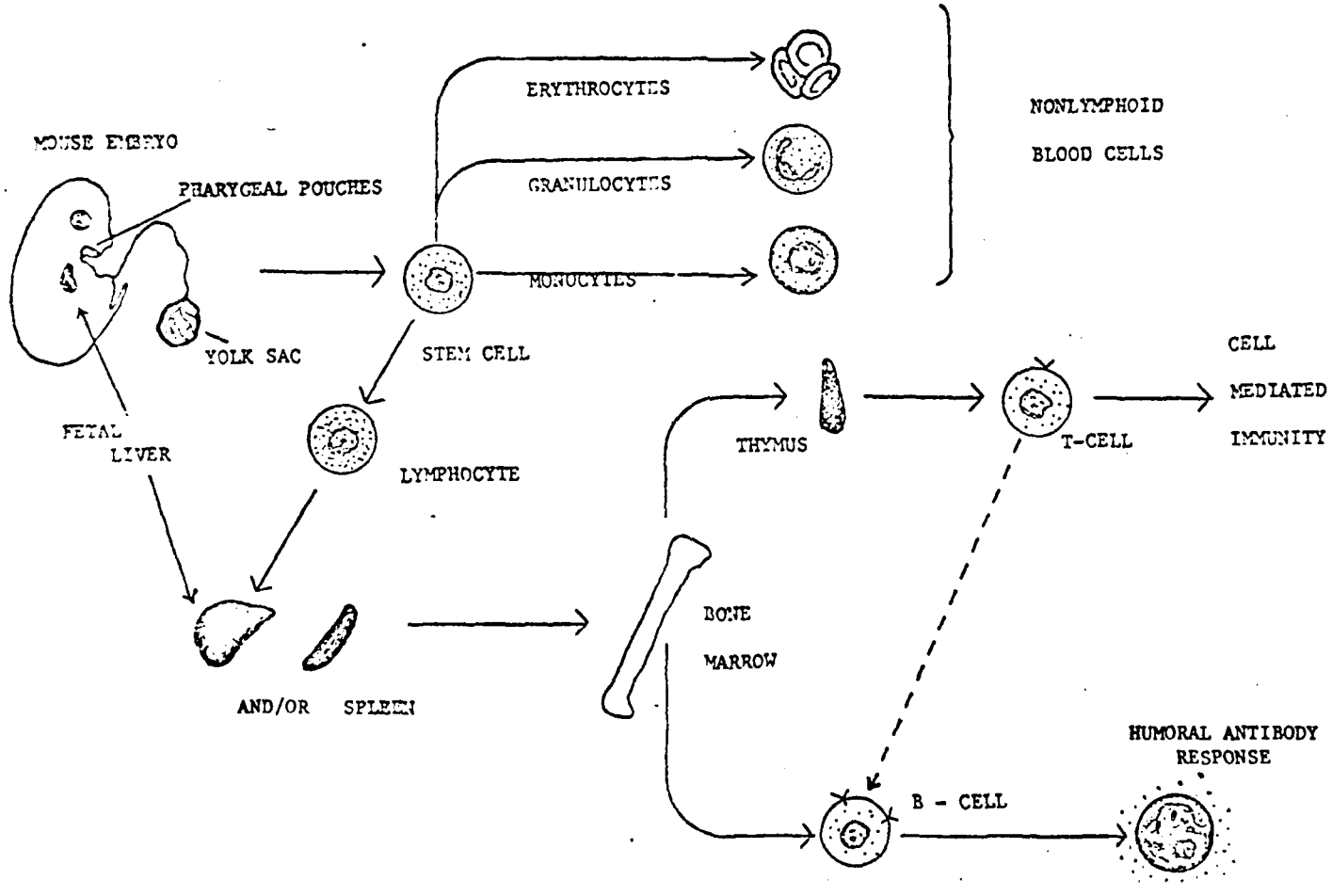

Figure 3. Illustration of the origin and stages of development of mouse lymphocytes (20).

proliferate. The progeny cells thus formed may either differentiate into plasma cells and die two or three days later or may transform back to long-lived small lymphocytes and remain in an intermitotic state as memory cells (21, 22, 43, 48). The undifferentiated small or virgin lymphocyte and the plasma cell represent, respectively, the beginning and the end of the process of lymphocyte differentiation. Lymphopoiesis, unlike normal erythropoiesis or myeloidpoiesis, occurs outside the bone marrow and largely in the peripheral lymphatic tissues such as the lymph nodes, the spleen, and the gut associated lymphoid tissues.

As lymphocytes proceed along the line of differentiation, the number of surface receptors decreases. Immunoglobulin molecules serving as receptors on the cell surface can be visualized by fluorescent microscopy or by autoradiography. Experimental evidence suggests that surface immunoglobulin molecules may differ from that of the circulating antibody molecules.

The Lymphocyte Network

There are three dualisms within the immune system (39). One is the functional diversity of the lymphocytes into T and B cells mediating, respectively, cell mediated and humoral antibody immune responses. The other is the duality of the potential response of a lymphocyte when its receptors recognize an epitope (or an antigenic determinant). It can either respond positively (being activated) or negatively (paralyzed). The immune system also displays a third dualism, and that is the same antibody molecule displays both epitopes

and receptors. This is true for both antibody molecules serving as surface receptors and the freely circulating antibody molecules. Epitopes occur on both the constant and the variable regions of an antibody molecule (See Fig. 2). Epitopes of the variable regions are numerous and the set of epitopes on a given antibody molecule is named the idiotype of that molecule. Due to these complex properties of the antibody molecules, there exists a network of lymphocytes and antibody molecules which recognize other lymphocytes and other antibody molecules which in turn recognize still others. This network, as a whole, functions in a way that is peculiar to and characteristic of the internal interaction of the elements of the immune system itself. All these result in a continuous interaction of lymphocytes and antibody molecules with idiotopes or combining sites that fit.

Under normal conditions, the immune system of an animal is in a dynamic steady state as its elements interact. Foreign antigens could modulate this network by activating some of the lymphocytes and disbalancing the steady state. They leave imprints to the lymphocyte population and induce the expansion of selected clones which is a mechanism of the retention of immunological memory. This is not, however, the only imprint made by the foreign epitope. The set of combining sites that recognizes the epitope also recognizes a set of idiotopes within the system, a set of idiotopes that constitute the 'internal image' of the foreign epitope. The lymphocytes representing the internal image will therefore be affected secondarily and so forth in successive recognition waves throughout the framework. The

modulation of the network by foreign signals represents the adaptation of the immune system to the outside environment and thereby builds up a memory that is sustained by transmission to progeny cells. An outline of this network is presented in Figure 4.

The first detectable step for the differentiation of B cells into plasma cells is the production of IgM antibodies, most of which are incorporated into the cell membrane where they serve as specific antigen receptors. Still under the influence of the microenvironment, the clonal precursors undergo a series of mitotic division, producing from one cell to a family of progeny cells. The majority of these progeny cells migrate to the peripheral tissues and some take a further step of differentiation by switching from IgM producing cells to IgG plasma cell precursors. The change is believed to involve only the expression of the two genes that specify the constant regions of the 'mu' and 'gamma' heavy chains. The exact mechanism in which antigens induce B cells to divide and differentiate is uncertain; two types of signals are probably involved. One is the direct interaction of antigens with surface receptors of the B cells presumably through some correspondence of shape. Antigens with closely spaced repeating antigenic determinants such as polysaccharides are most efficient in this mode of stimulation. Another signal is through the interaction of the T cells, either by direct contact or by some T cell factors. The requirement of the participation of the T cell varies with different classes of antibodies involved. The production of IgM antibody is least dependent and IgA antibody response is most dependent. The

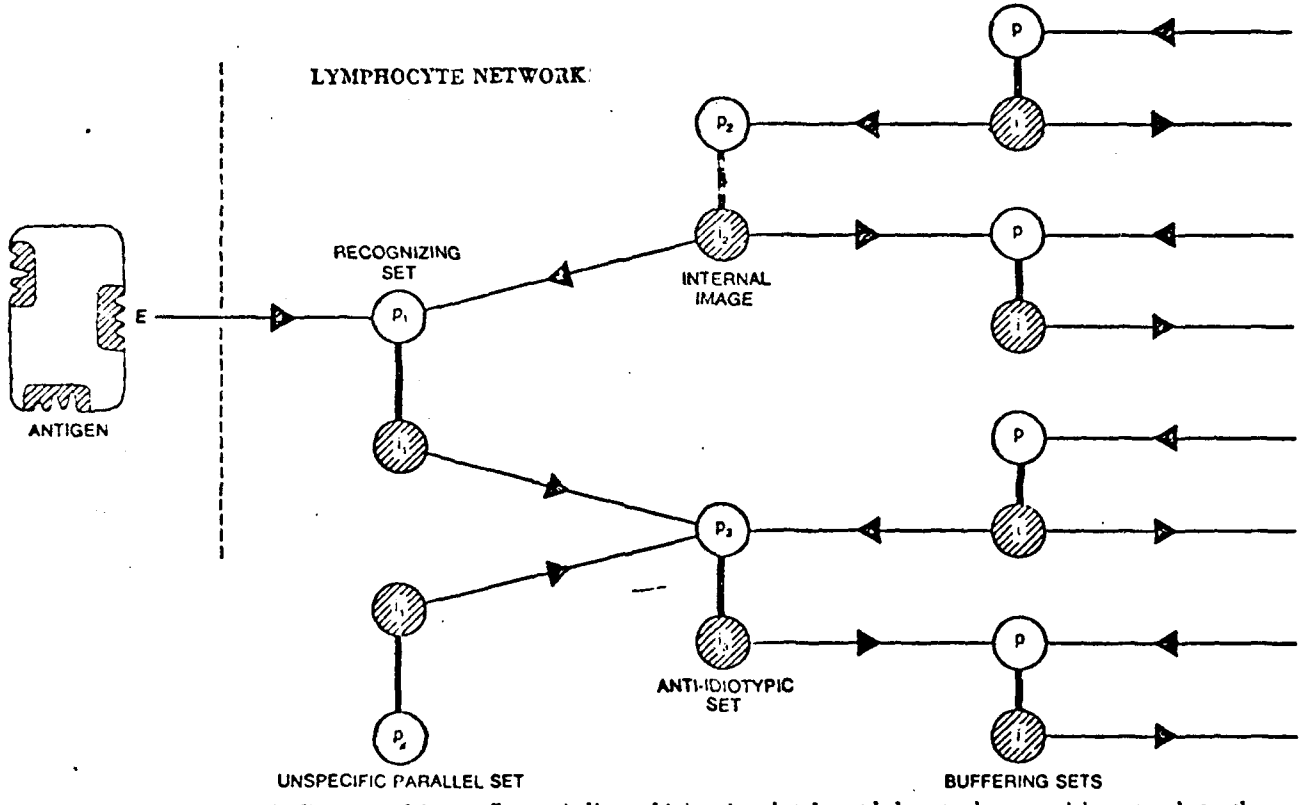

Figure 4. (39) is diagrammed in an effort to indicate how its steady-state ("eigen") behavior is established and how the network responds to an antigen. An epitope (*E*) on the antigen is recognized by a set (p_1) of combining sites on antibody molecules, both circulating antibody and cell-surface receptors. Cells with *receptors of the recognizing* set p_1 are potentially capable of responding to the antigenic stimulus (*arrowhead*) of epitope *E*, but *there are constraints. The same* molecules that carry combining sites p_1 carry a set of idiotopes (i_1). These are recognized within the system by a set of combining sites (p_3), called the anti-idiotypic set because they tend to suppress (*reverse arrowhead*) the cells of set i_1. (These idiotypes i_1 are also found on molecules with combining sites that do not belong to the *recognizing* set p_1 but rather are unspecific with regard to epitope *E*.) On the other hand, the set p_1 also recognizes internal epitopes i_2, which therefore constitute an internal image of the foreign epitope *E*. In the steady state, molecules of the internal image tend to stimulate cells of set p_1 and thus to balance the suppressive tendency of the anti-idiotypic set. When the foreign antigen enters the system, its stimulatory effect on recognizing set p_1 allows cells of that set to escape from suppression. (The same thing happens to unspecific cells of the parallel set p_4.) The resulting immune response to the antigen is modulated by the buffering *effects of many more* sets of combiniug sites and idiotopes (*right*), which have a controlling influence on the response.

development and differentiation of a lymphocyte are illustrated in Figure 5.

It is believed that the primary differentiation of stem cell into diversified lymphocyte populations is genetically determined. The synthesis of most protein molecules or single polypeptide chains is determined by a single gene. Through heredity studies and amino acid sequence analysis, it is found that the synthesis of immunoglobulins is quite peculiar. The constant and variable regions of each polypeptide chain are specified by different genes, and there are in fact three to four structural gene groups that code for the antibody molecules (20, 31). One group codes for the kappa light chains, the second codes for the lambda, the third codes for the various classes and subclasses of heavy chains, and finally a fourth group might be involved in coding the J chain (in IgM and IgA) or for the linkage of the light and heavy chains and the carbohydrate portion of the antibody molecule. Genes within the same group are linked, but the groups are not and are probably located in separate chromosomes. The lymphocytes, like most somatic cells, are diploidal, and the chromosomes are paired. For a heterozygote, a plasma cell expresses only one of the alleles. In other words, plasma cells display allelic exclusion.

The Genetic Control of Immune Response

The influence of inheritance on immune response had been observed more than half a century ago. It was documented by Cooke and Van der Veer (19) that human sicknesses such as hay fever, bronchial asthma, and gastro-enteris have been genetically related. Later, the genetic

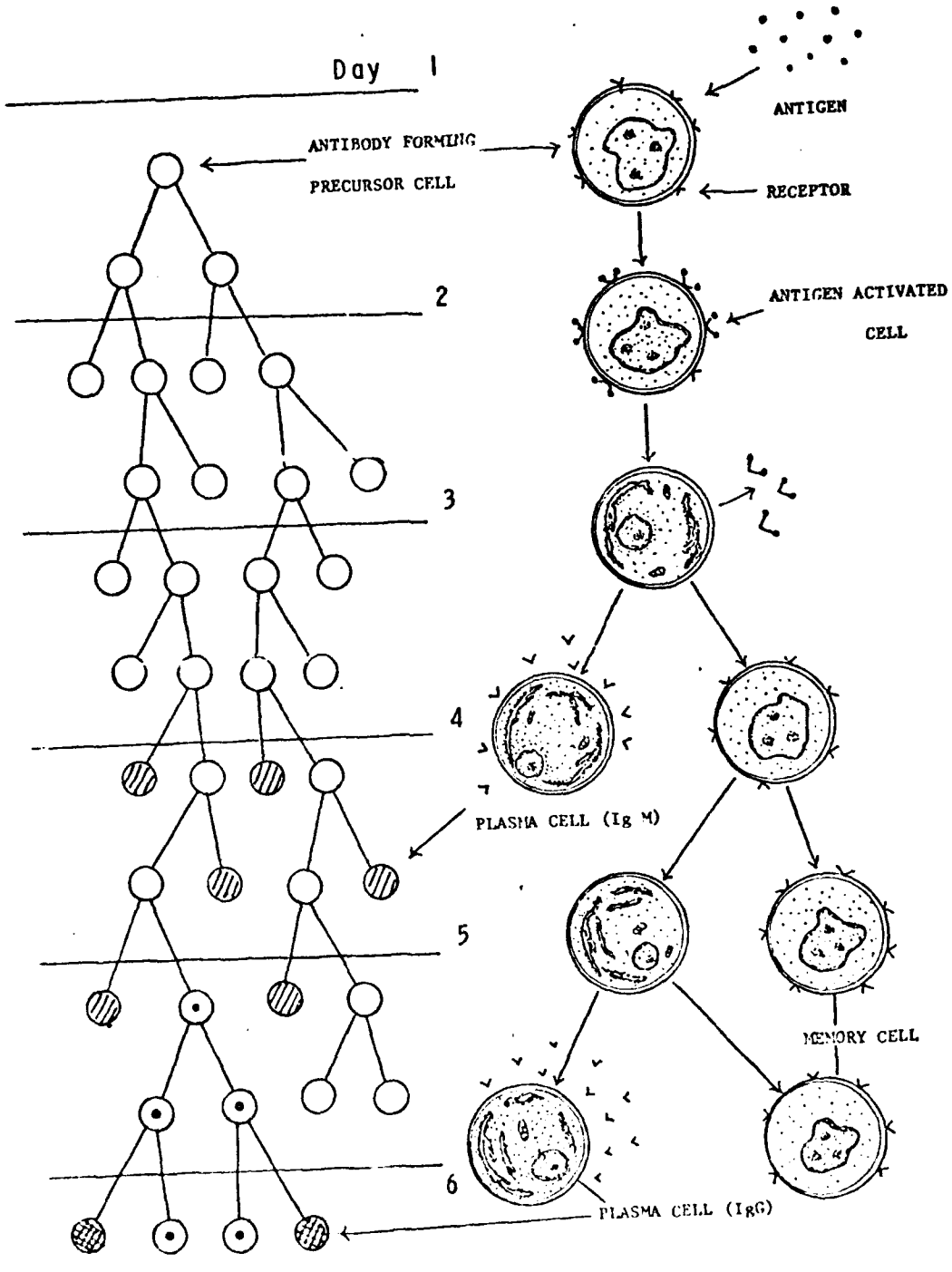

Figure 5. Illustration of the differentiation and development of an antigen-activated plasma cell precursor.

control of antibody responses to diptheria toxoid (68), to pneumococcal polysaccharide (28), and to insulin (4) were discovered. Since then, there have been significant progress in the elucidation of the complexity of genetic control of immune response. This progress has mainly been achieved in three areas (56) as follows:

1. The preparation and characterization of synthetic polypeptide antigens of determined size, structure, and amino acid sequences which possess limited number of antigenic determinants.
2. The development of inbred and congenic strains of rodents, some of which differ distinctly within a limited and defined region of the genome.
3. The partial dissection of the immune process into steps which require immunogen induced activation of distinct lymphoid cell populations.

Thus, it is not surprising that most contributions to the genetic study of the immune response is through the study of inbred strains of guinea pigs and mice to various synthetic haptens.

The antibody responses of inbred and congenic strains of mice to a series of related synthetic polypeptides have been shown to be determinant specific, and are linked to the major H-2 (histocompatibility locus) histocompatibility region of the ninth mouse linkage group (49). The genes associated with the responsiveness, either in high or low responder, to synthetic polymers are called the 'Ir' or immune response genes.

Different inbred strains of mice could produce equal amounts of antibody against the same antigen but are directed towards different determinants within the complex immunogen.

Genetic regulation of immunological responsiveness in mice to complex multideterminant protein antigens had been demonstrated by immunization with low doses of native albumin proteins and bovine pancretic ribonuclease (79). Responsiveness was dominant and was determined by a H-2 linked gene. All strains irrespective of their H-2 types were found to respond equally to a second immunization or to a primary immunization with a high dose of antigen.

A number of experiments had been designed to associate the expression of immune antibody response genes at the cellular level. This was done by transferring limited donor lymphoid cells of the thymic and/or bone marrow origins to syngeneic normal or X-irridiated recipients to characterize the immune responsiveness of these lymphoid cells. So far, information of the genetic control at a cellular level is very limited. It was found that both T and B cell types play a role in this control but the mechanism remains unclear. It is now obvious that immune responsiveness is genetically linked to the major histocompatibility loci and that two functionally distinct populations of antigen sensitive cells are involved (13, 75). One recognizes foreign antigens and expresses V-genes coding for antibodies against histocompatibility antigens of the same individual (self), and the other expresses V-genes coding for reactivity against histocompatibility antigens which the individual does not possess (non-self).

Genetic control of immune responses may be qualitative or quantitative and may determine the class of immunoglobulin produced.

MATERIALS AND METHODS

Animal

Male and female mice (8-12 weeks old) of an inbred C_3HSW strain, raised and bred in our laboratory, were used in all experiments. These mice weighed between 24 and 34 grams. Mice to be injected with radioisotope Iodine-125 were fed with water containing 1 mM of potassium iodide (KI) for 72 hours before use.

Virus

Western equine encephalitis (WEE) virus was used in all experiments and the virus was propagated routinely in our laboratory by successive passages through suckling mouse brains. The brain material was then harvested and suspended in borate saline pH 9.0 to a 10-20% concentration and was stored at -70 C.

Chick Embryo Fibroblast (CEF)

Primary culture chick embryo fibroblasts were prepared from embryonated Leghorn eggs incubated for 9-12 days before use. The egg embryo was minced and trypsinized to form single cell suspension and was maintained in Eagle's minimum essential medium supplemented with 10% fetal calf serum. Monolayers of CEF were used for virus propagation and titration.

The Counting Chamber

A counting chamber or hemacytometer was used to assess the number of cells. This is a rectangular glass slide with two deep transverse

ditches running across its entire width. Between the ditches, the glass is ground down and polished so that the level is 0.1 nm lower than that of the remaining slide surface. A plane glass cover-slip is placed over the center part of the slide, creating an enclosed space into which the cell suspension is introduced. An etched lattice pattern on the center section enables the cells to be counted. The center section is frequently subdivided by a transverse ditch, each section having a lattice engraved upon its surface.

Mouse Anti-WEE Virus Antiserum

A group of sixty mice were immunized with single i.v. injections of 0.3 ml WEE viral vaccine (8.8×10^7 pfu/ml) through the caudal veins. At various time intervals, six mice were exsanguinated and their serum was pooled. Ten serum samples were collected between day 1 and day 16 after the immunization to be tested for the formation of antiserum against WEE virus by the radioimmunoprecipitation test.

Mouse Blood Lymphocyte

Mouse lymphocytes were obtained from cardiac blood of mice; the heparinized blood was purified in ficoll-hypaque gradient and was maintained in RMPI 1640 medium supplemented with 5% fresh human serum. This lymphocyte culture was used to estimate activated lymphocyte generation time, the latent period required before activated lymphocytes start to proliferate, and how many cell generations an activated lymphocyte would go through before division stopped.

Rabbit Anti-Mouse Immunoglobulin (Ig) Antiserum

Anti-mouse Ig antiserum was obtained from two rabbits which had received four intravenous injections of normal mouse Ig at an interval of one injection per week. The antiserum was harvested two weeks after the last injection. The LD_{50} of this serum was found to be 0.2 ml when given to mice intravenously.

Reagents and Media

A. Antibiotics

Penicillin G (Sodium Salt)

Prepared as a stock solution containing 100,000 units/ml. Used at a final concentration of 100 units/ml.

1. Dissolve individual vials of antibiotic in sterile, deionized water.
2. Store frozen at approximately -20 C.

Add 1 ml of stock solution to each liter of medium to give a final concentration of 100 units/ml.

Streptomycin (Sulfate)

Prepared as a stock solution containing 100,000 µg/ml. Used at a final concentration of 100 µg/ml.

1. Dissolve individual vials of antibiotic in sterile, deionized water.
2. Store frozen at approximately -20 C.

Add 1 ml of stock solution to each liter of medium to give a final concentration of 100 µg/ml.

Mycostatin

This antibiotic is almost insoluble in water. It is prepared as a stock suspension containing 50,000 units/ml and used at a final concentration of 25 units/ml.

1. Suspend individual vials of antibiotic in sterile, deionized water.
2. Store frozen at approximately -20 C.

Add 0.5 ml of stock suspension to each liter of medium to give a final concentration of 25 units/ml.

Kanamycin

Prepared as a stock solution containing 50,000 µg/ml. Used at a final concentration of 50 µg/ml.

1. Dissolve individual vials of antibiotic in sterile, deionized water.
2. Store frozen at approximately -20 C.

Add 1 ml of stock solution to each liter of medium to give a final concentration of 50 µg/ml.

B. Eagle's Minimum Essential Medium (MEM)

Solution A

L-arginine HCl	1.05 g
L-histidine HCl	0.31 g
L-lysine HCl	0.58 g
L-tryptophane	0.10 g
L-phenylalanine	0.32 g
L-threonine	0.48 g
L-leucine	0.52 g
L-valine	0.46 g
L-methionine	0.15 g

The above amino acids are weighed out freshly as required.

Solution B

L-tyrosine	0.36 g
L-cystine	0.24 g

Dissolve in 200 ml of 0.075 N/1 HCl (prepared by adding 2 ml of commercial concentrated hydrochloric acid to 315.4 ml of deionized water) at 80 C. Solution B is prepared freshly as required.

Solution C

Nicotinamide	0.20 g
Pyridoxal	0.20 g
Thiamine	0.20 g
Pantothenic acid	0.20 g
Choline	0.20 g
L-inositol	0.40 g
Riboflavin	0.02 g

1. Dissolve in 200 ml of deionized water.
2. Dispense in 10 ml volumes.
3. Store at approximately -20 C.

Solution D (Folic acid, 0.20 g)

1. Dissolve in 200 ml of Hanks' saline, pH 7.8.
2. Dispense in 10 ml volumes.
3. Store at approximately -20 C in tightly stoppered bottles.

Glutamine Solution (L-glutamine, 12.0 g)

1. Dissolve in 400 ml of deionized water.
2. Sterilize by positive pressure filtration.

3. Dispense aseptically in 50 ml volumes.

4. Store at approximately -20 C.

Preparation of 10 X concentrated Eagle's MEM from the above solutions

1. Dissolve the following in solution B:

NaCl	68.0 g
KCl	4.0 g
$MgSO_4 \cdot 7H_2O$	2.0 g

2. Dissolve 1.25 g of NaH_2PO_4 in 55 ml of deionized water and add to the above pool.

3. Dissolve 10.0 g of glucose in 50 ml of deionized water and add 20 ml of 1% phenol red. Add the mixture to the pool.

4. Dilute the pool to 600 ml with deionized water and add the following:

Solution C	10 ml
Solution D	10 ml

5. Dissolve 2.0 g of $CaCl_2$ in 160 ml of deionized water and add to the pool slowly with continuous stirring.

6. Add the amino acids of Solution A to the pool.

7. Dilute the pool to exactly 1,000 ml with deionized water to give a 10 X concentrated stock solution. Sterilize by positive pressure filtration and store at 4 C.

C. Chick Embryo Fibroblast Culture Medium

10 X MEM	90 ml
Heat inactivated fetal calf serum (56 C for 30 min)	10.0 ml
Penicillin	0.1 ml
Streptomycin	0.1 ml
Kanamycin	0.1 ml

D. Amino Acids Supplement for Lymphocyte Culture

Stock Solution (100 X)

L-asparagine	18 mg
L-glutamine	108 mg
L-arginine HCl	58 mg
RMPI 1640 complete medium (stored at 4 C)	5 ml

Add 1 ml to each of 100 mls of medium to give a final concentration of:

L-asparigine	36 mg/l
L-glutamine	216 mg/l
L-arginine HCl	116 mg/l

E. Lymphocyte Culture Medium

Roswell Memorial Park Institute (RMPI) 1640 medium	93.0 ml
Heat inactivated (56 C for 30 min) human serum	5.0 ml
Phytohemagglutinin-P (50 µg/ml)	1.0 ml
Amino acid supplement	1.0 ml
Penicillin	0.1 ml
Streptomycin	0.1 ml
Kanamycin	0.05 ml
Mycostatin	0.1 ml

F. Tris (Tris Hydroxymethyl Amino Methane) Buffer

Gey's Solution A

NaCl	70.0	g
KCl	3.7	g
Na_2HPO_4	1.19	g
KH_2PO_4	0.237	g
Glucose	10.0	g
1% Phenol red	10.0	ml
Deionized water	990.0	ml

Dissolve the salts and glucose in water in the order listed, and add the phenol red. This is a 10 X concentrated stock solution and is stored at 4 C. For use, dilute the stock solution ten times with deionized water and sterilize by autoclaving. Store at room temperature or at 4 C.

Gey's Solution B

$NaCl_2 \cdot 6H_2O$	0.42	g
$MgSO_4 \cdot 7H_2O$	0.14	g
$CaCl_2$	0.34	g
Deionized water	100.0	ml

1. Dissolve the salts in water in the order listed.
2. Sterilize by autoclaving.
3. Store at room temperature or 4 C.

Preparation of 0.1 M/l Tris Buffer

1. Prepare modified Gey's saline by adding 20 ml of solution B to 360 ml of Solution A.
2. Dissolve 4.84 g of Tris in approximately 100 ml of modified Gey's saline.

3. Add 76.8 ml of 0.2 M/l HCl (prepared by diluting commercial concentrated hydrochloric acid 50 times with deionized water) to the Tris solution.
4. Add modified Gey's saline to give a total volume of 400 ml. This represents a 0.05 M/l stock solution of Tris at pH 7.6.
5. Sterilize by positive pressure filtration.
6. Dispense in 100 ml volumes taking aseptic precautions.
7. Store at 4 C.

G. Calcium and Magnesium Free Saline (GKN)

10 X stock solution

NaCl	80.0 g
KCl	4.0 g
Glucose	10.0 g

Prepare in 1,000 ml distilled water and sterilize by autoclaving. For use, dilute 1:10 in sterile distilled water.

H. Wright's Stain

Wright stain dye	0.3 g
Glycerol	3.0 g
Methyl alcohol (100%)	97.0 ml

Grind the stain in a mortar with glycerol thoroughly. Add absolute methyl alcohol, mix well, store overnight. Shake 15 min every day for 1 week and filter. Store at room temperature.

I. Trypan Blue

Prepared as 0.5% solution.

Trypan blue, vital	0.5 g
Phosphate-buffered saline	100.0 ml

1. Dissolve the trypan blue in phosphate-buffered saline.
2. Store at room temperature.
3. Filter a few ml through paper on the day of use.

J. May-Grunwald and Giemsa Stain

Solution A

May-Grunwald stain powder	1.25 g
Absolute methyl alcohol	500.0 ml

1. Grind the stain in a mortar with a small quantity of methyl alcohol until the powder is uniformly suspended.
2. Transfer to a flask with the remaining methyl alcohol and place on a magnetic stirrer at 37 C overnight.
3. Dispense in 100 ml volumes and incubate at 37 C for at least a month before use.
4. Store in tightly stoppered bottles at room temperature.

Solution B

Giemsa stain powder	0.6 g
Glycerol	50.0 ml
Absolute methyl alcohol	50.0 ml

1. Grind the Giemsa powder in a mortar with the glycerol.
2. Transfer completely to a flask containing a few glass beads and place on a shaking machine at 37 C overnight.
3. Add the methyl alcohol and continue shaking until mixed.
4. Store in tightly stoppered bottles at room temperature. Allow to ripen for two weeks before using.

Solution C

$NaHCO_3$	5.6 g
Deionized water	100.0 ml

1. Dissolve the bicarbonate in water.
2. Store at room temperature.

Procedure for Use

1. Rinse cultures twice with phosphate-buffered saline to remove protein.
2. Fix 3-5 minutes in absolute methyl alcohol.
3. Transfer to fresh absolute methyl alcohol for 3-5 minutes.
4. Dry in air.
5. Cover with May-Grunwald stain for ten minutes.
6. Without washing, transfer to freshly prepared dilute Giemsa stain for 20 minutes. (Prepare stain by diluting ten times with deionized water. Add four drops of 5.6% sodium bicarbonate per 100 ml of diluted stain.)
7. Wash in running tap water.
8. Two changes in acetone, three minutes each.
9. Two changes in xylene, three minutes each.
10. Mount.

Nuclei stains red-purple; cytoplasm stains blue.

Procedure for the Assessment of Viable Cell Numbers (36)

1. Prepare the counting chamber by drying its parts. Then press the cover-slip gently but firmly onto the slide so that it adheres.
2. Adjust the cell concentration to slightly in excess of an estimated total count of 1.0×10^6 cells/ml.
3. Prepare the cell suspension for counting by adding 1.0 ml of suspension to 0.5 ml of trypan blue solution. Phosphate-buffered saline is a suitable diluent.
4. Mix thoroughly and immediately introduce a drop of the stained cell suspension into the counting chamber. This is done by bringing a loaded Pasteur pipette to the edge of the space immediately beneath the cover-slip. The fluid is drawn in by capillary action.
5. Count immediately under the low power (100X) of the microscope.

NOTE 1: It is essential that the differential count be made immediately after trypan blue has been added to the cell suspension since prolonged exposure results in significant numbers of healthy cells taking up the dye, thereby leading to an erroneously low assessment of the proportion of viable cells.

NOTE 2: Only the large squares at each corner of the lattice are used in counting; each of these, 1.0 sq. mm. in area, is made up of 16 smaller squares. For convenience each 1.0 sq. mm. should contain about 100 cells, and for best results

a total of about 400 cells (four squares of 1.0 sq. mm. each) should be counted. Counting is most readily done by assessing the cells in each of the 16 small squares separately, proceeding along each row of squares in a left-to-right direction and then onto the line of squares next below. In order that cells lying upon the lines intersecting the small squares are not counted twice, only those lying on the upper and right hand lines of each square are included in the count. By covering all 16 small squares in this way, it is obvious that there will be no exclusions from the total count.

NOTE 3: Trypan blue is selectively absorbed by the non-viable cells, which are stained an intense blue color, while the viable cells remain unstained.

Procedure for the Purification of Mouse Lymphocytes (9)

1. Prepared layering solution by mixing 6.8 parts of 50% Hypaque or sodium diatrizoate (Winthrop Laboratories, New York) with 24 parts of 9% w/v ficoll (Pharmicia Fine Chemicals, Sweden) giving a density of 1.08.
2. Heparinized cardiac blood (10 µg/ml) was drawn in an aseptic condition from anaesthetized mice and was diluted 1:1 with sterile physiological saline containing 5% heat inactivated (56 C, 30 min) fetal calf serum.
3. Three volumes of diluted blood were layered carefully over 2 volumes of layering solution in sterile plastic tubes (Falcon, Becton, Dickinson and Co., California).
4. The tubes were centrifuged in a centrifuge (International Equipment Co., Boston, Mass.) with a swinging bucket rotor at 900 r.p.m. for 40 min at room temperature.
5. Following centrifugation, the lymphocytes should appear as a white band at the interface between the ficoll-hypaque gradient and the serum portion of the blood.
6. The lymphocytes were removed aseptically by a sterile Pasteur pipette and were washed three times by 2% GKN supplemented with heat inactivated fetal calf serum.
7. A sample of lymphocytes was stained with 0.5% trypan blue exclusion stain and the number of living cells were counted in a hemocytometer.

8. The homogeneity of the lymphocyte population was examined by Giemsa stain. Usually 80-90% of the cells were lymphocytes when collected by this method.

Procedure for the Culture of Primary Chick Embryo Fibroblast (36)

1. Rinsed the egg shell thoroughly with 70% alcohol.
2. Opened the egg on the side of the air sac by punching the shell with the back of a heavy sterile forcep.
3. Peeled off the shell and removed the whole embryo by quickly turning the egg upside down into a 100 mm sterile petri dish.
4. The embryo was then decapitated, eviscerated and placed into a beaker of 2% GKN to remove its fat content.
5. The embryo was then cut into small pieces and was removed with a sterile magnetic stirrer into a 50 ml beaker containing 5 ml of pre-warmed 0.25% trypsin.
6. The mince was gently stirred and the temperature was maintained at 37 C.
7. Removed a test sample after 5-10 min to assure that the trypsin was working.
8. Trypsinization should be completed after 45 min to one hour.
9. The cell suspension was collected in plastic centrifuge tubes containing cold MEM medium and was centrifuged at 1000 r.p.m. for 10 min.
10. The supernatant should be almost clear and should be discarded.
11. Resuspended the cell pellet in MEM (about 5 ml) and pipetted vigorously to promote single cell suspension.
12. Took a sample of the cell suspension and counted immediately in a hemocytometer.

13. About 50 x 10^6 cells were seeded in 35 ml of MEM medium in 250 ml bottles (Falcon, Becton, Dickinson and Co., California).
14. Cells were then incubated at 37 C in a 5% CO_2 incubator.
15. Confluent monolayers should be formed in 48 hours and should be ready for use.

Procedure for the Preparation of Rabbit Antiserum to Mouse Immunoglobulin (Ig)

1. A group of 40 normal mice was exsanguinated by cardiac puncture and the blood was collected in small serum tubes.
2. The blood was set at room temperature to clot, was then refrigerated overnight at 4 C to allow maximum contraction of the clot to occur.
3. The serum from each tube was pooled and centrifuged at 3000 r.p.m. for 15 min at 4 C to remove contaminating erythrocytes and the fat content.
4. The serum was constantly stirred while an equal volume of 70% cold ammonium sulfate solution was added dropwise (33).
5. The mixture was set at room temperature for 4 hr and then centrifuged at 3000 r.p.m. for 15 min.
6. Discarded the supernatant and resuspended the precipitate with a volume of distilled water approximately equal to the original serum volume.
7. Another equal volume of ammonium sulfate was added dropwise. The mixture was centrifuged immediately and the supernatant was discarded. The precipitate was dissolved and brought to volume as before. The mixture was treated in the same way as before for a third precipitation.
8. The precipitate from the last fractionation was dialyzed against physiological saline adjusted to pH 8.0. Frequent changes were made until sulfate was no longer detectable in the dialysate.

9. To test for the presence of sulfate, one ml of saturated barium chloride was added to an equal volume of well-mixed saline dialysate. The appearance of cloudiness was an indication of residual sulfate (34).
10. The immunoglobulin solution was diluted to 20 ml and was used as inoculum.
11. Two normal rabbits were collected and blood was taken from the ear to obtain normal blood samples.
12. The rabbits were immunized with an intravenous injection with 2 ml of mouse immunoglobulin solution through the ear veins. Three more injections were given at one-week intervals.
13. Ten days after the last injection, the hyperimmunized rabbits were exsanguinated by cardiac puncture and the antiserum was collected in the same manner as in steps 2 and 3.
14. The antiserum was tested against mouse immunoglobulin solution by the precipitation test.

Procedure for the Preparation of WEE Viral Vaccine (12)

1. Ten ampoules (2 ml) of WEE viral suspension (8.8×10^7 pfu) were thawed in a 37 C water bath.
2. The suspension was pipetted out by sterile Pasteur pipettes into a beaker immersed in an ice bath.
3. Added one-tenth volume of 1.0 Tris buffer (Tris hydroxymethyl amino methane, Fisher Scientific Co., California, No. T395) and allowed it to stand for 15 min.
4. Prepared a 10% solution of beta-propiolactone (BPL)[1] in cold physiological saline.
5. BPL was added to the viral suspension with Tris buffer to a final concentration of 0.3%. Placed the mixture on a magnetic stirrer at 4 C and agitated gently for 72 hours.
6. Removed an aliquot for test and stored the remainder at -20 C.
7. Sample of the virus vaccine was injected into suckling mice and observed for ten days to see whether live viruses were present.

[1]Betaprone, Fellows Testagar, Detroit, Michigan.

Procedure for the Estimation of the Average Radius of Mouse Lymphocytes

1. A mouse was sacrificed by decapitation and blood was collected immediately by a Pasteur pipette.
2. One freely flowing drop of blood was collected on the surface of a clear slide at one edge and was spread along the sharp edge of another slide at an angle of about 45 degrees.
3. Allowed the blood smear to air dry by blowing or waving in the air and stained immediately.
4. Added about 10 drops of Wright's stain to the smear and allowed to stand for 8 min.
5. Added an equal amount of distilled water and blowed constantly to mix. After diluting the stain, allowed the preparation to stand for five minutes.
6. After staining, rinsed quickly with water and dried immediately.
7. Observed the smear under an inverted microscope at a magnification of 200X. Lymphocytes could be distinguished by its blue mononucleus and slightly reddish cytoplasm.
8. The diameter of 40 lymphocytes was measured by an ocular micrometer which had been precalibrated with a stage micrometer.

Propagation and Titration of WEE Virus

A. Propagation procedure (36)

1. Added 2 ml of 20% WEE mouse brain suspension (10 LD_{50}/ml) to a confluent monolayer of CEF.
2. Incubated the cells at 37 C in a 5% CO_2 in air atmosphere and 80% humidity.
3. Checked the cells after 36 hours of incubation. Peeling off of the monolayer was an indication of viral multiplication.
4. Harvested the viral suspension when approximately one-half of the monolayer was peeled off.
5. The crude harvest was centrifuged at 5000 r.p.m. at 4 C in an International refrigerated centrifuge, model PR-2 (International Equipment Co., Boston, Mass.) for 10 min. The precipitate was discarded.
6. An equal volume of dimethyl sulfoxide (Fisher Science Co., New Jersey) was added to the viral suspension.
7. Dispensed the viral suspension into 2 ml ampoules.
8. The ampoules were flame sealed and were stored at -70 C for future use.

B. Procedure for the titration of the virus by plaque assay (36)

1. Prepared confluent CEF monolayers in 60 x 15 mm tissue culture dishes (Falion, Becton, Dickinson and Co., California).
2. Removed the growth medium as completely as possible.
3. Rinsed each dish twice with 2% GKN.
4. Prepared serial ten-fold dilution of the viral suspension in 2 X MEM.
5. Inoculated 0.2 ml of each dilution directly onto each monolayer; rotated gently to allow even distribution. Plates were inoculated in duplicate.
6. Incubated the cultures at 37 C for one hour to allow adsorption to take place. Rocked gently at 15 min intervals.
7. Mixed 1.8% Gum Tragcanth (National Biochem. Corp., California) with an equal volume of 2 X MEM and allowed to equilibrate in a 44 C waterbath.
8. Carefully overlaid 10 ml of the gum medium onto each monolayer.
9. Incubated in a humidified atmosphere of 0.5 g CO_2 in air.
10. After a 36 hr incubation period, the gum overlay was poured off and the plaques were stained with crystal violet and counted.

Procedure for Radioiodination of WEE Viral Particles and Mouse IgG (71)

1. Prepared fresh solutions of chloramine-T (Eastman Kodak, Rochester, New York, #1022) and sodium metabisulfite (Fisher Scientific Co., Fair Lawn, New Jersey, #S-244) at a concentration of 200 ug/ml (5 mg/25 ml) in distilled water and stored at 4 C.
2. Dispensed 4 ml of WEE viral suspension or 4 ml of mouse IgG[1] (2 mg/ml) to a vial containing a small magnetic bar. The vial was set on the top of a magnetic stirrer and was kept inside a refrigerator.
3. One-half millicurie (mci) of carrier-free ^{125}I was added to the vial through a microsyringe while the solution was constantly stirred.
4. Injected 0.5 ml of chloramine-T through a 1 cc disposable plastic syringe and allowed to set for 10 min.
5. At the end of ten minutes, added an equal amount of sodium metabisulfite to the vial.
6. Removed the content of the vial to a dialysis bag (Spectrapor membrane tubing, molecular weight cutoff - 12,000 to 14,000)[2] through a Pasteur pipette and allowed to dialyze against 3 liters of physiological saline in a multiple dialyser (Scientific Inc., Los Angeles, California) at 4 C with constant stirring.
7. Changed the dialysate (saline) every 12 hr and collected a sample after 48 hours to be counted for radioactive content.

8. Recovered the viral suspension as the radioactivity of the dialysate was down to background level. Stored the radioactive WEE virus solution at 4 C for future use.

[1]Miles Laboratories Inc., Kankakee, Ill.

[2]Spectrum Medical Industries Inc., Los Angeles, California.

Procedure for the Estimation of the Biological Half-Life of Mouse Immunoglobulin (IgG)

1. Two groups of mice were prepared for this experiment. One group was normal mice fed with water containing potassium iodide (mM/ml) for 72 hours. Another group had received a single intravenous injection of 0.2 ml of BPL inactivated WEE viral vaccine (8.8×10^7 pfu). Five days after the injection these mice were treated in the same way as the other group and both groups were used on the same day.
2. 0.2 ml of radioactive ^{125}I labeled mouse Ig with a concentration of 1 mg/ml was injected intravenously into both groups of mice.
3. At various time intervals after the injection, groups of two mice were anaesthesized by an intravenous injection of 0.03 ml of sodium pentobarbital, and cardiac blood was taken and placed in plastic tubes. The volumes of the blood samples were recorded.
4. After the animals were sacrificed, their body weights were recorded and their tails were cut off and kept in plastic tubes.
5. After all blood samples were collected, the tubes containing the blood samples and mouse tails were counted by a Packard Tri-Carb scintillation spectrophotometer.

Procedure for the Study of the Elimination Rate of WEE Virus in the Circulatory System of Mice

1. A group of normal mice was fed with water containing potassium iodide (KI) with a concentration of 1mM/ml for 72 hr to avoid non-specific uptake of ^{125}I by the thyroid.
2. Following this treatment 0.2 ml of radioactive (^{125}I) labeled WEE viral antigen (1.28×10^7 pfu/ml) was injected into all mice intravenously through the caudal vein.
3. At various time intervals after the injection, groups of two mice were anaesthesized by an intravenous injection of 0.03 ml of sodium pentobarbital (Anesthesal, Norclon Laboratories, Inc., Lincoln, Nebraska) and blood samples were collected by cardiac puncture and were placed in plastic tubes. Volumes of the blood samples were recorded.
4. After the animals were sacrificed, their body weights were recorded.
5. After all blood samples were taken, the plastic tubes were counted by a Packard Tri-Carb scintillation spectrophotometer.

Procedure for the Calibration of Ocular Micrometer

for Cell Measurement

1. Mounted an ocular micrometer with adjustable screw on an inverted microscope.
2. Set up the stage micrometer on the microscope stage just like any slide.
3. Adjusted the screw gauge of the ocular micrometer so that one end of the grid lined up with any line of a division in the stage micrometer.
4. Turned the screw gauge until the scale on the eyepiece went across one division (5 small units) and recorded the reading from the screw gauge.
5. Took ten or more readings, from which the average number of microns per unit was calculated.

Procedure for Radioimmunoprecipitation Test

for Antibody Detection (23, 30)

1. A volume of 0.05 ml of radioactive WEE viral solution was added to the same volume of Tris buffer containing 1 mg of bovine serum albumin per ml in a polyethylene micro-test tube.
2. To the above mixture was added 0.05 ml of hyperimmune mouse serum. The preparation was mixed gently with a Vortex mixer and was incubated for 60 min at 37 C.
3. A 0.05 ml amount of rabbit antiserum was then added. After thorough mixing, the mixture was again incubated for 60 min at 37 C.
4. After the final incubation the preparation was set at 4 C for 24 hr and was then centrifuged in a Beckman 152 microfuge at 12,000 X g for 5 min.
5. The top half 0.1 ml of the supernatant was carefully removed with a capillary pipette and was placed into a plastic tube. To the remaining pellet was added 0.2 ml of distilled water and was removed by a Pasteur pipette into a plastic tube after mixing.
6. All serum samples were tested in duplicate in the same manner. Three controls were prepared containing the following: a. WEE virus and Tris buffer. b. WEE virus and rabbit anti-mouse Ig. c. WEE virus and rabbit anti-mouse Ig and normal mouse serum.

Procedure for the Estimation of the Generation Time

of WEE Virus Activated Lymphocytes *in vitro*

1. Six hyperimmunized mice each had received an i.v. injection of 0.3 ml of WEE viral vaccine (8.8×10^7 pfu/ml) and were exsanguinated aseptically by cardiac puncture 8 days after receiving the injection.
2. Blood lymphocytes were collected after purification in a ficoll-hypaque gradient (density 1.08).
3. The cells were suspended in 5 ml of 2% GKN and were centrifuged at 2000 rpm at room temperature for 10 min. The supernatant was discarded. The cells were resuspended in a same volume of GKN and were centrifuged again.
4. After two washings, the cells were suspended in 2 ml of RMPI 1640 lymphocyte culture medium and the viable cell number was assessed by trypan blue exclusion stain.
5. The lymphocyte suspension was then transferred to two 12 x 75 mm sterile plastic tubes (Falcon, Becton, Dickinson and Co., Calif.) each containing 2 ml of lymphocyte culture medium and 0.1 ml of WEE viral vaccine (8.8×15^7 pfu/ml) so that the final concentration is about 1.0×10^6 cells/ml.
6. The tubes were loosely capped and were incubated in 5% CO_2 at 37 C inclined at an angle of 30 degrees.
7. Samples were taken at various time intervals and were counted by a Coulter Counter, Model F (Coulter Electronics, Inc., Hialeah, Florida) to estimate the increase in cell number.

RESULTS AND DISCUSSION

Immune Response Model

The first step towards making an immune response model is to gather as much information as possible and arrange them in an orderly manner. The best way to achieve this is to lay down all parameters in the form of individual blocks. Among all the information gathered, only those which can be expressed in quantitative terms are usable. These quantitative expressions may be obtained from one of the following sources: experimental data, literature data, or theoretical values. Theoretical values should be used with care. Only those which are logically supported by at least some experimental evidence should be used. Literature values usually have a defined range which may be wide or narrow depending upon the test systems, experimental conditions, and the methods used. For this reason, these values should be supplemented by experimental values to find out more precisely what value should be chosen.

The next task is to assemble all the chosen blocks and values into one piece of information, which not only conveys all the usable information, but are also linked in a sequential manner. The sequence in this model should closely resemble the actual phenomena which are occurring in nature. Due to the enormous complexity of a living system, certain assumptions and simplifications have to be made in order to visualize the general outlook of the whole system.

A block diagram of this immune response model is shown in Figure 6 and Table 2. Table 3 is a symbol key to the block diagram.

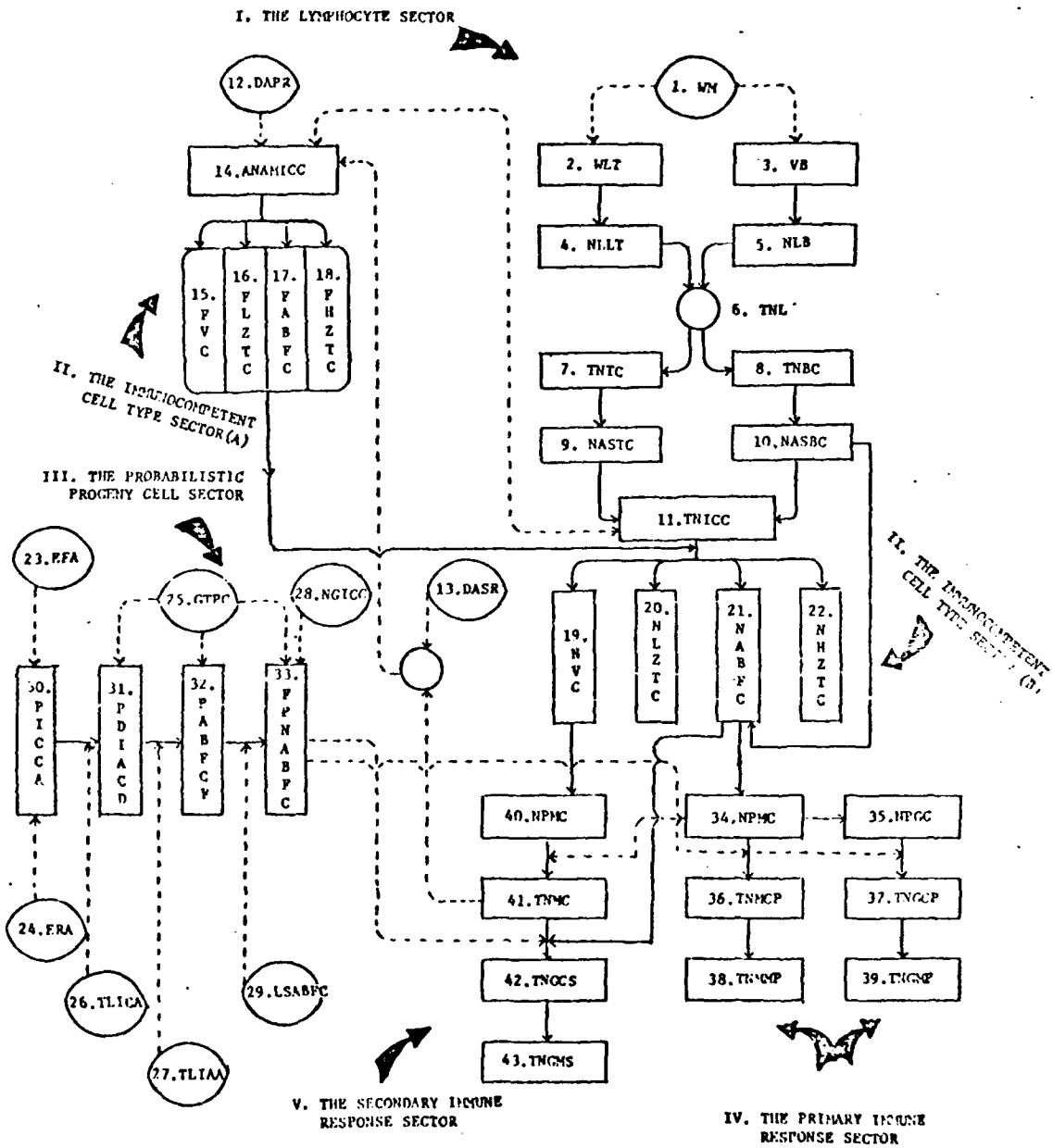

Figure 6. Block diagram of the 'immune response model'.

Table 2. Description of abbreviations of the immune response model.

I. THE LYMPHOCYTE SECTOR

Abbreviation	Description
1. WM	Weight of mouse (gm)
2. WLT	Weight of lymphoid tissues (gm)
3. VB	Volume of blood (ml)
4. NLLT	Number of lymphocytes in lymphoid tissues
5. NLB	Number of lymphocytes in blood
6. TNL	Total number of lymphocytes in the two compartments (blood and lymphoid tissues)
7. TNTC	Total number of T cells
8. TNBC	Total number of B cells
9. NASTC	Number of antigen specific T cells
10. NASBC	Number of antigen specific B cells
11. TNICC	Total number of immunocompetent cells

II. THE IMMUNOCOMPETENT CELL TYPE SECTORS (A)

12. DAPR	Dose of antigen in primary response (pfu/ml)
13. DASR	Dose of antigen in secondary response (pfu/ml)
14. ANAMICC	Average number of antigen molecules per immunocompetent cell (ICC)
15. FVC	Fraction virgin cells
16. FLZTC	Fraction low zone tolerant cells
17. FABFC	Fraction antibody forming cells (precursors)
18. FHZTC	Fraction high zone tolerant cells

(Sector B)

19. NVC	Number of virgin cells
20. NLZTC	Number of low zone tolerant cells
21. NABFC	Number of antibody forming cells (precursors)
22. NHZTC	Number of high zone tolerant cells

III. PROBABILISTIC PROGENY CELL SECTOR

23. EFA	Effective fraction of antigen that can activate the ICC

Table 2 (Con't.).

Abbreviation	Description
24. ERA	Elimination rate of antigen (%/hr)
25. GTPC	Generation time (hr) of the proliferating (antigenically activated) cells
26. TLICA	Time (hr) lapse between Icc developing into immunologically activated cells (IAC)
27. TLIAA	Time (hr) lapse IAC developing into antibody forming cells (ABFC)
28. NGICC	Number of generations an ICC undergoes before division stops and before antibody appears
29. LSABFC	Life span of antibody forming cells
30. PICCA	Delay period of ICC activation (a single cell)
31. PDIACD	Delay period of IAC deferentiation
32. PABFCF	Delay period of antibody forming cell formation
33. FPNABFC	The function of the probable number of ABFC formed from one precursor cell within the immune response period.

IV. PRIMARY IMMUNE RESPONSE SECTOR

34. NPMC	Number of precursors of IgM producing cells
35. NPGC	Number of precursors of IgG producing cells
36. TNMC	Total number of IgM producing cells formed versus time
37. TNGCP	Total number of IgG producing cells formed versus time (primary response)
38. TNMM	Total number of IgM molecules formed versus time
39. TNGMP	Total number of IgG molecules formed versus time (primary response)

Table 2 (Con't.).

V. SECONDARY IMMUNE RESPONSE SECTOR

Abbreviation	Description
40. NPMC	Number of potential antibody forming memory cells
41. TNMC	Total number of antibody forming memory cells formed that would participate in the secondary immune response
42. TNGCS	Total number of IgG producing cells formed versus time (secondary response)
43. TNGMS	Total number of IgG molecules formed versus time (secondary response)

Table 3. Symbol key of the block diagrams of the immune response model.

SYMBOL	DESCRIPTION
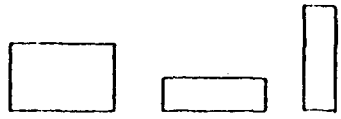	PROCESS BLOCK
	INPUT/OUTPUT BLOCK
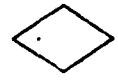	DECISION BLOCK
	INPUT
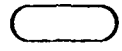	TERMINAL, START, INTERRUPTION
	OFFPAGE CONNECTOR
	CONNECTOR
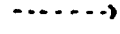	INFORMATIONAL FLOW
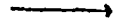	MATERIAL FLOW
	COMMUNICATION LINK

The model consists of five sectors. The first sector is called the 'lymphocyte sector'. In this sector, the immune system of a mouse is divided into two compartments: blood and the lymphatic tissues. The weight of the lymphoid tissues of an animal is about 1-2% of the body weight (33), and the volume of blood has the average value of 7.78 ml per kg of mouse body weight (3). It was found that even at the peak of an immune response, the weight of lymphocytes in any lymphoid tissue is less than 1% of the tissue weight (47). With this data, it is possible to estimate the weight and the number of lymphocytes present in the lymphatic compartment of a mouse. Mice have exceptionally high numbers of lymphocytes in the blood (3) which comprise about 80-90% of all mouse white blood cells. It is assumed in this model that the spleen, lymph nodes and gut-associated lymphoid tissues account for all activities of the immune system of mice and that the number of T and B cells in the lymphatic compartment are assigned according to the ratio of T and B cells in these tissues as reviewed by immunofluorescence (72, 73). It was known that most of the blood lymphocytes (80%) are the T cells and that only a small fraction are the B cells (21). Not all lymphocytes are responsive to any single antigen. As a matter of fact, only a small fraction of all lymphocytes could respond specifically to one antigen or one antigenic determinant (66). For most antigens, the number of specific precursor cells is on the order of a few hundred per million in normal mice and a few thousand per million in hyperimmunized ones. These specific lymphocytes are referred to as immunocompetent cells (ICC) in this

model and represent the precursor population which could be activated by WEE virus. These factors are explained schematically in Figure 7 and are explained in Table 4.

The second sector is the 'immunocompetent cell type sector' which is divided into two parts. In this sector, the calculated ICC population was assigned into four immunological cell types (47): the virgin cells, low zone tolerant cells, antibody forming cells and high zone tolerant cells. Part A evaluates the fractions of the different cell types based on the average number of probable contacts between a given dose of WEE virus and the ICC while part B gives the number of cells present in each cell type. This sector is based on the hypothesis that immunological responsiveness and tolerance could occur simultaneously at a cellular level. A schematic representation of the various parameters in this sector is shown in Figure 8 and explained in Table 5.

There has been no direct evidence supporting this hypothesis. But through the studies of dose-dependent immunological tolerance, it was found that between a wide range of antigenic dosage, two zones of tolerance occurred (low and high) and within which normal immunological reactions were found (24, 69, 70). This phenomenon revealed that different levels of immunological expressions occurred at different thresholds of antigenic stimulation. All these suggest that activation is a continuous process and occurs at a cellular level rather than in the animal as a whole. It is logical to assume that in a given population of ICC different immunological cell types exist, resulting

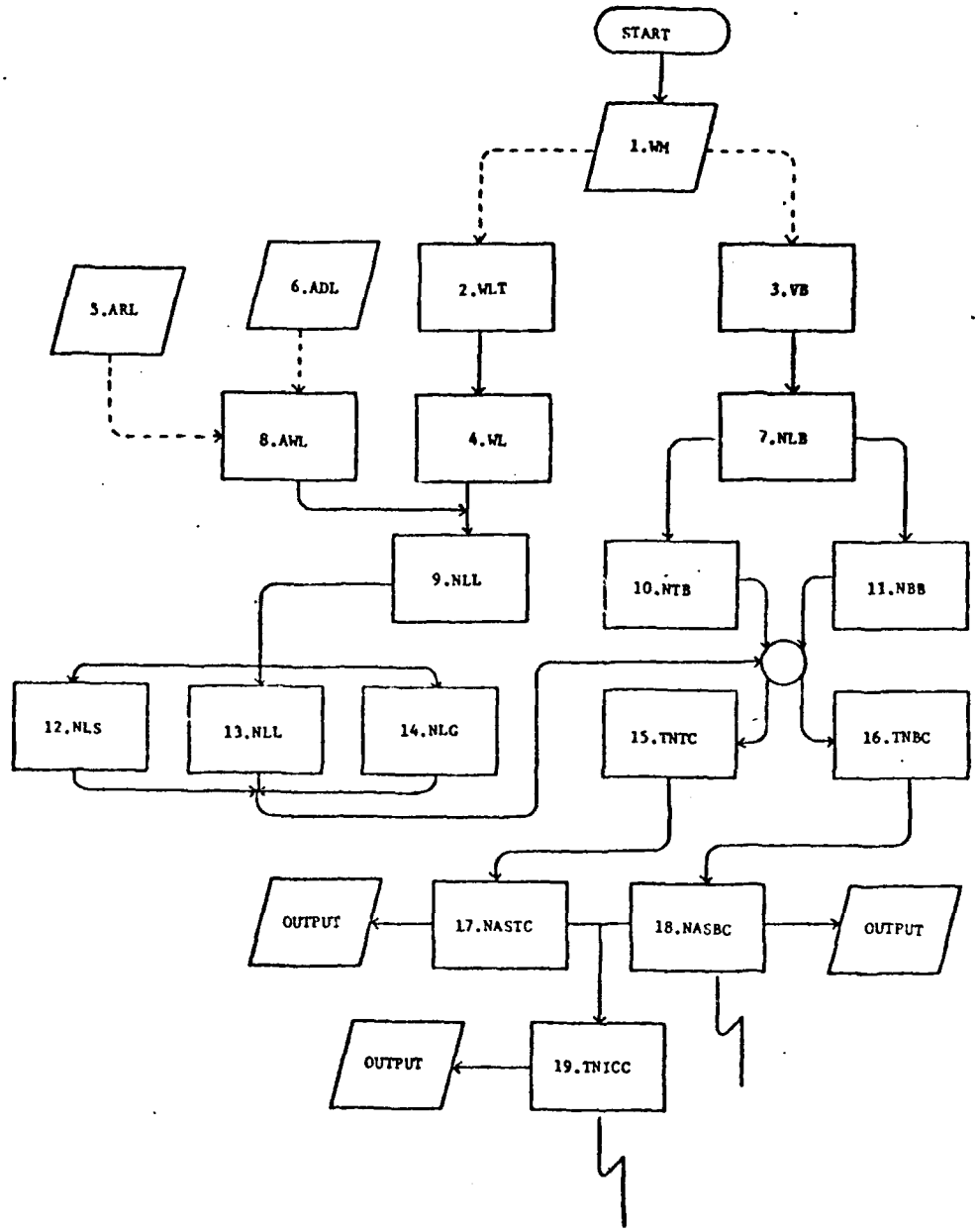

Figure 7. Block diagram of the 'lymphocyte sector'.

Table 4. The lymphocyte sector.

	Abbreviation	Decription	Equation	Var.(1)	Ref.(2)
1.	WM	Weight of mouse (gm)		W, E	
2.	WLT	Weight of lymphoid tissues (gm)	W X 2%	L1	83
3.	VB	Volume of blood (ml)	W X 0.0778	L4	3
4.	WL	Weight of lymphocytes in entire lymphoid system (gm)	LI X 2%	L2	47
5.	ARL	Average radius of one lymphocyte (μ)		R1	
6.	ADL	Average density of lymphocyte (gm/ml)		D6	
7.	NLB	Number of lymphocytes in blood	L4 X 5.5 X 10^7	L5	83
8.	AWL	Average weight of one lymphocyte (gm)	4/3X Xr1^3*D6	L8	
9.	NLL	Number of lymphocytes in the entire lymphatic system	L2/L8	L3	
10.	NTB	Number of T cell in blood	L5 X 80%	V4	63
11.	NBB	Number of B cells in blood	L5 X 20%	B4	63
12.	NLS	Number of lymphocytes in spleen	L3 X 70%	C1	63
13.	NLL	Number of lymphocytes in lymp nodes	L3 X 15%	C2	63
14.	NLG	Number of lymphocytes in gut associated lymphoid tissues	L3 X 15%	C3	63
15.	TNTC	Total number of T cells (in both blood and lymphoid tissues)	0.5XC1+0.7C2X0.7XC3	V5	73
16.	TNBC	Total number of B cells (in both blood and lymphoid tissues)	0.5XC1+0.3XC2+0.3XC3	B5	73
17.	NASTC	Number of antigen specific T cells	V5X10^{-4}	S1+S2	66
18.	NASBC	Number of antigen specific B cells	B5X10^{-4}	S3+S4	66
19.	TNICC	Total number of immunocompetent cells	S1+S2+S3+S4	S	

(1) Variable

(2) Reference

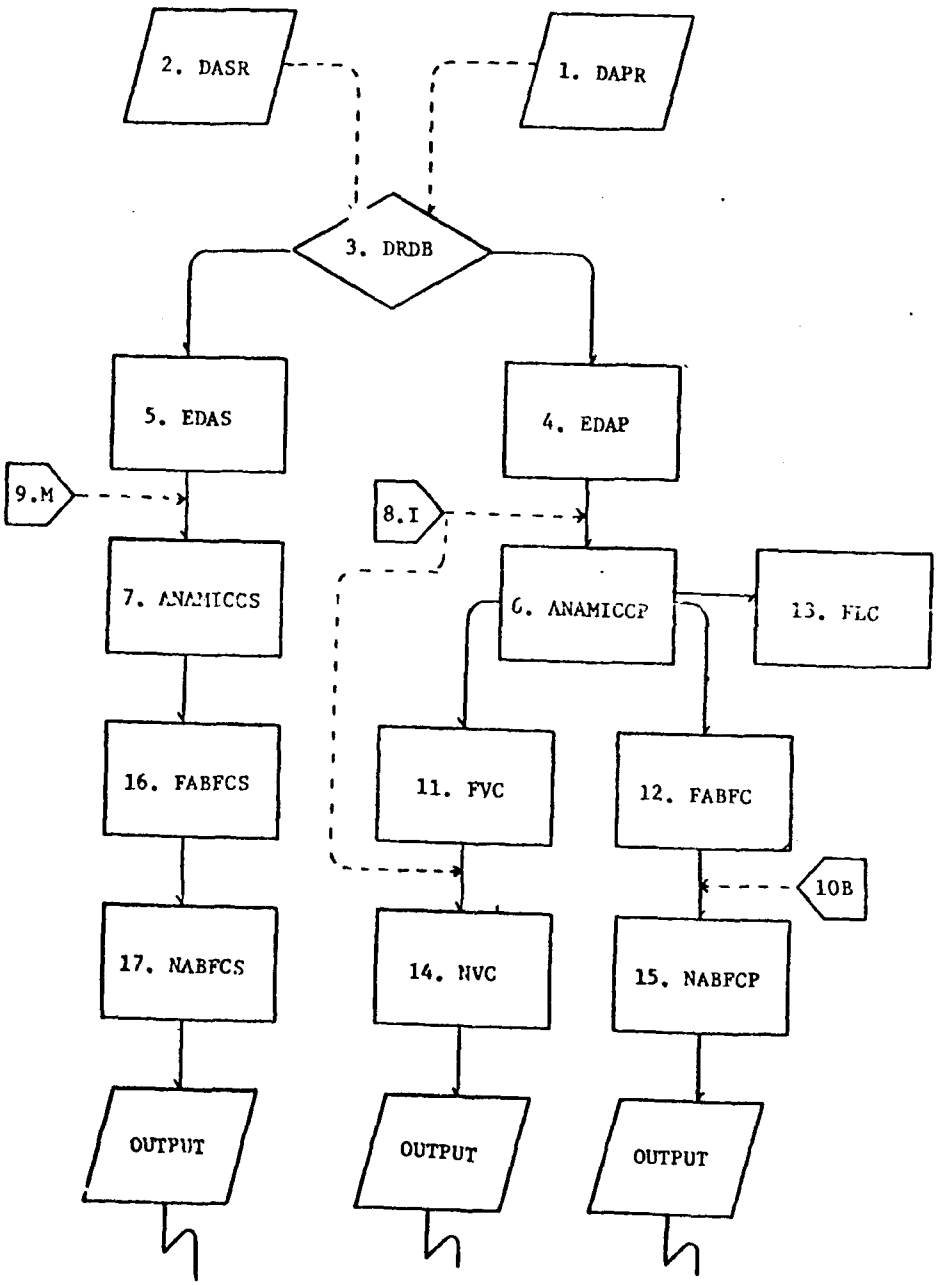

Figure 8. Block diagram of the 'immunocompetent cell type sector'.

Table 5. The immunocompetent cell type sector.

	ABBREVIATION	DESCRIPTION	EQUATION	VAR.	REF.
1.	DAPR	Dose of antigen in primary response (pfu/ml)	--	DD	
2.	DASR	Dose of antigen in secondary response (pfu/ml)	--	D9	
3.	DRDB	Dose range decision block	--	--	
4.	EDAP	Effective dose of antigen in primary response	F7 = 0.002*D0	F7	
5.	EDAS	Effective dose of antigen in secondary response	F8 = 0.01*D9	F8	
6.	ANAMICCP	Average number of antigen molecules per ICC in primary response	R = F7/5	R	47
7.	ANAMICCS	Average number of antigen molecules per ICC in secondary response	R = F8/M8	R	47
8.	I	Total number of ICC (from lymphocyte sector No. 19)	--	S	
9.	M	Number of memory cells (from primary response sector No. 10) and number of virgin cells (in this sector No. 14)	--		
10.	B	Number of antigen specific B cells (from lymphocyte sector No. 18)	--	S3+S4	
11.	FVC	Fraction virgin cell	*	F0	47
12.	FABFC	Fraction ABFC	*	F2	47
13.	FLC	Fraction (low and high zone) tolerant cell	*	F2,F3	47

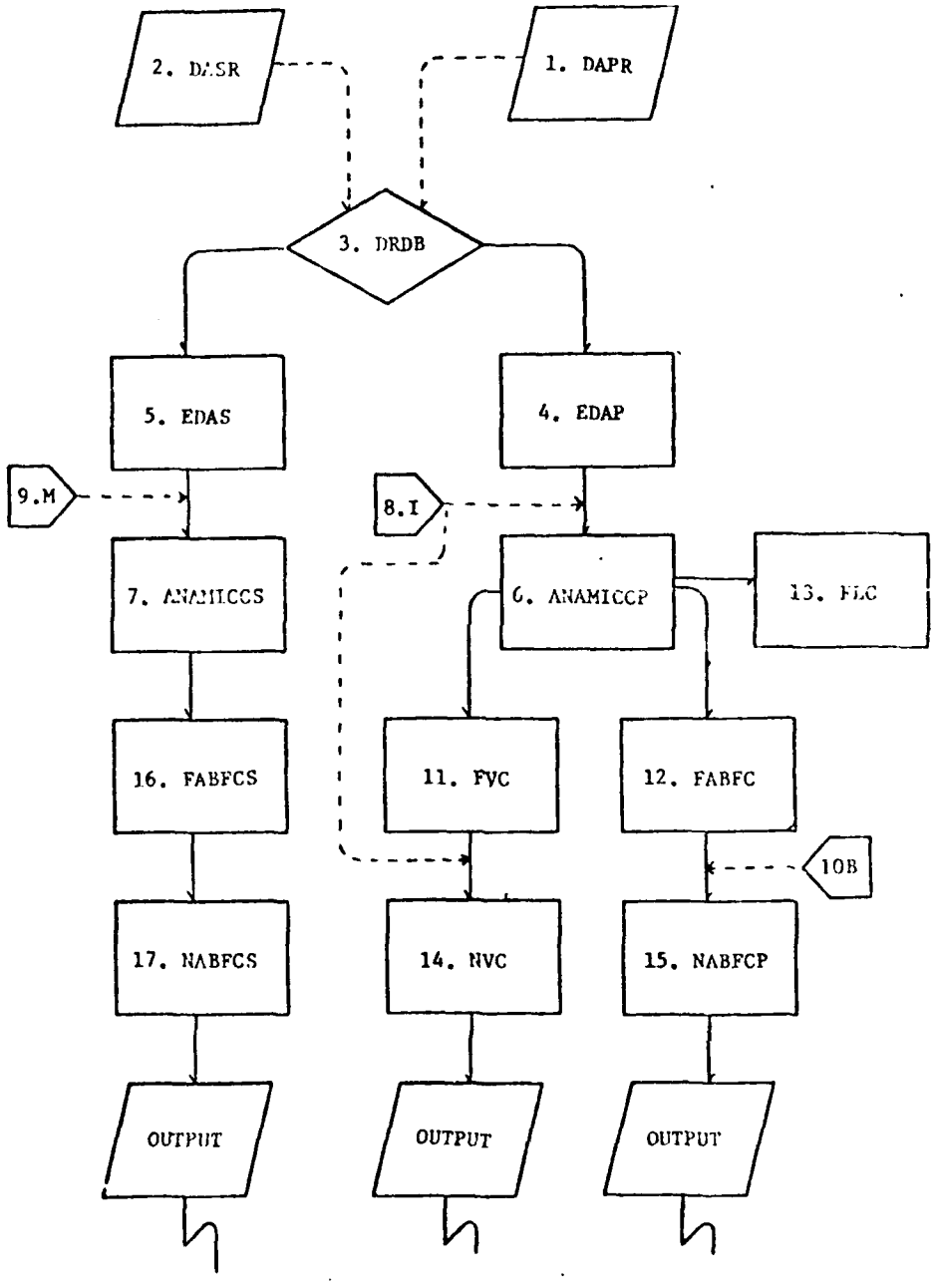

Figure 8. Block diagram of the 'immunocompetent cell type sector'.

Table 5. The immunocompetent cell type sector.

	ABBREVIATION	DESCRIPTION	EQUATION		VAR.	REF.
1.	DAPR	Dose of antigen in primary response (pfu/ml)	--		DD	
2.	DASR	Dose of antigen in secondary response (pfu/ml)	--		D9	
3.	DRDB	Dose range decision block	--		--	
4.	EDAP	Effective dose of antigen in primary response	F7 = 0.002*DO		F7	
5.	EDAS	Effective dose of antigen in secondary response	F8 = 0.01*D9		F8	
6.	ANAMICCP	Average number of antigen molecules per ICC in primary response	R = F7/5		R	47
7.	ANAMICCS	Average number of antigen molecules per ICC in secondary response	R = F8/M8		R	47
8.	I	Total number of ICC (from lymphocyte sector No. 19)	--		S	
9.	M	Number of memory cells (from primary response sector No. 10) and number of virgin cells (in this sector No. 14)	--			
10.	B	Number of antigen specific B cells (from lymphocyte sector No. 13)	--		S3+S4	
11.	FVC	Fraction virgin cell	*		FO	47
12.	FABFC	Fraction ABFC	*		F2	47
13.	FTC	Fraction (low and high zone) tolerant cell	*		F2,F3	47

Table 5 (Con't).

Description	Equation
Fraction virgin cell	$F(V) = e^{-r}$
Fraction LZT cell	$F(LZT) = \sum_{m=1}^{i=0} \frac{e^{-r} x\ r^m}{m!}$
Fraction ABFC	$F(ABFC) = \sum_{m=6}^{i=1} \frac{e^{-r} x\ r^m}{m!}$
Fraction HZT cell	$F(HZT) = \sum_{m=7}^{i=6} \frac{e^{-r} x\ r^m}{m!}$

e = exponential
r = average number of antigen per ICC
i,m = range of antigen that determines the immunological state of an ICC
! = factorial

in different levels of activation. The resultant immune expression depends upon the majority of ICC that is in a particular immunological state.

The third sector is the 'probabilistic progeny cell sector'. In this sector the development and differentiation of any antibody-forming precursor cell was followed. Under a given threshold of antigenic stimulation, a single precursor cell could be activated and proliferated into a colony of progeny cells which could be matured into plasma cells. The probable number of progeny cells formed and the possibility of their subsequent development into plasma cells depended upon the availability of a continuous antigenic challenge and the time period in which this stimulation is available. In other words, this sector defines the number of antibody-forming cells formed from one precursor as a function of time (41, 42). Figure 9 explains this phenomenon diagrammatically; an explanation of abbreviations is given in Table 6.

The immune response of mice to WEE virus was known to be dependent upon the cooperation of the macrophages (21). The nonspecific action of the macrophages plays an essential role in resistance to most bacterial and viral infections by degrading these antigens into nonviable components while presenting small fragments of these antigens in persisting immunogenic form. Other humoral factors and hormoses such as immunogenic RNA (29), cyclic AMP, and the thymus hormones (80) are also needed for optimal immune response. Information concerning these parameters are too limited to allow adequate

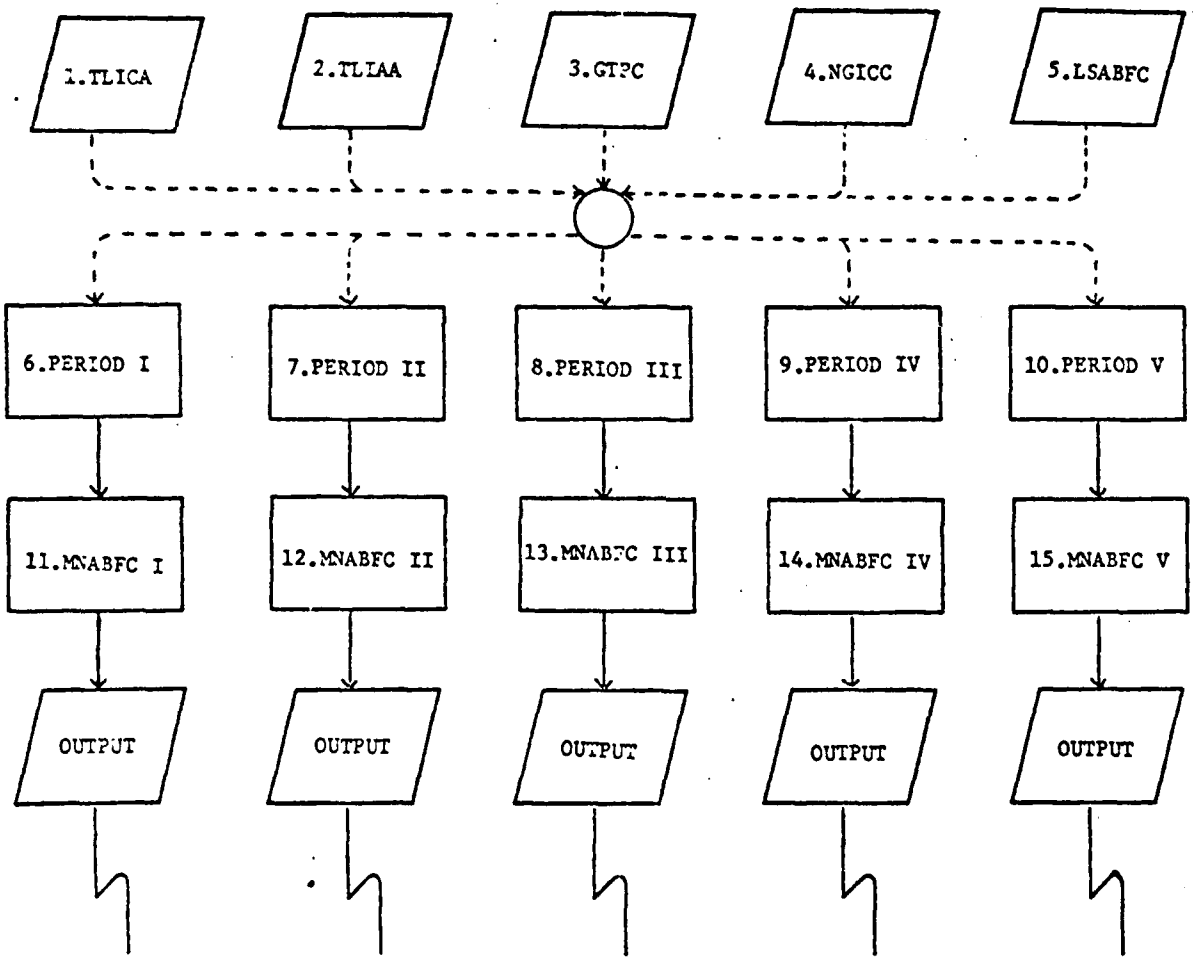

Figure 9. Block diagram of the 'probabilistic progeny cell sector'.

Table 6. The probabilistic progeny cell sector.

	ABBREVIATION	DESCRIPTION	EQUATION	VAR.	REF.
1.	TLICA	Time (hr) lapse between ICC developing into immunologically activated cells (IAC)	--	T5	
2.	TLIAA	Time (hr) lapse IAC developing into antibody forming cells (ABFC)	--	T2	
3.	GTPC	Generation time (hr) of the proliferating (antigenically activated cells	--	T8	
4.	NGICC	Number of generations an ICC undergoes before division stops and before antibody appears	--	G5	
5.	LSABFC	Life span (hr) of antibody forming cells	--	T9	
6.	Period I	Time before IAC proliferation	$T < T1+T2+G3$	D	
7.	Period II	Period at which IAC start to proliferate	$T3+G3 \leqslant T < T3+T9+G3$	D	
8.	Period III	Time during which IAC divides	$T3+G3 \leqslant T < T3+G4$	D	
9.	Period IV	Time at which IAC completes its last division and ABFC are formed	$T3+G3 \leqslant T < T3+T9+G3$	D	
10.	Period V	Period in which AFBC starts to die off	$T \leqslant T3+T9+G3$	D	
11.	MNABFC I	Mean number of antibody producing cells formed at period I	*	Y	
12.	MNABFC II	Mean number of antibody producing cells formed at period II	*	Y	
13.	MNABFC III	Mean number of antibody producing cells formed at period III	*	Y	

Table 6 (Con't.).

ABBREVIATION	DESCRIPTION	EQUATION	VAR.	REF.
14. MNABFC IV	Mean number of antibody producing cells formed at period IV	*	Y	41, 42
15. MNABFC V	Mean number of antibody producing cells formed at period V	*	Y	41, 42

* Equations are shown on the next page.

Table 6 (Con't)

Description	Equation

PERIOD I

$$2^{g-1}\, e^{-a/l} \left\{ \frac{e^{a/l\left[1-e^{-at_1}\,(1-e^{-a(g-1)t_8})\right]}}{1-e^{-at_1}\,(1-e^{-a(g-1)t_8})} \right.$$

$$+ \frac{1}{1-e^{-at_1}} \left[\frac{e^{a/l\left[1+e^{a(g-1)t_8}(e^{at_1}-1)\right]} e^{-a(t-t_2)}}{1+e^{a(g-1)t_8}\,(e^{at_1}-1)} \right.$$

$$\left. \left. - e^{a/l\left[1-e^{-at_1}+e^{-a(t-t_2)}\right]} \right] \right\}$$

PERIOD II

$$2^{g-1}\, e^{-a/l} \left\{ \frac{e^{a/l\left[1-e^{-at_1}\,(1-e^{-a(g-1)t_8})\right]}}{1-e^{-at_1}\,(1-e^{-a(g-1)t_8})} \right.$$

$$\left. - \frac{e^{a/l\left[1-e^{-at_1}\,(1-e^{-agt_8})\right]}}{1-e^{-at_1}\,(1-e^{-agt_8})} \right\}$$

$$+ \left\{ \frac{1}{1-e^{-at_1}} \left[\frac{e^{a/l\left[1+e^{a(g-1)t_8}\,(e^{at_1}-1)\right]} e^{-a(t-t_2)}}{1+e^{a(g-1)t_8}\,(e^{at_1}-1)} \right. \right.$$

$$\left. \left. - \frac{e^{a/l\left[1+e^{agt_8}\,(e^{at_1}-1)\right]} e^{-a(t-t_2)}}{1+e^{agt_8}\,(e^{at_1}-1)} \right] \right\}$$

Table 6 (Con't)

Description	Equation

PERIOD III

$$2^{g-1}\, e^{-a/l}\left\{\frac{1}{1-e^{-at_1}}\left[\frac{1}{1+e^{a(g-1)t_8}\,(e^{at_1}-1)}\right.\right.$$
$$\times\, e^{a/l}\left[1+e^{a(g-1)t_8}\,(e^{at_1}-1)\right]\, e^{-a(t-t_2)}$$
$$-\, e^{a/l}\left[1+e^{a(g-1)t_8}(e^{at_1}-1)\right]e^{-a(t-t_2-t_9)}$$
$$+\, e^{a/l}\left[1-e^{-at_1}+e^{-a(t-t_2-t_9)}\right]$$
$$\left.\left.-\,\frac{e^{a/l}\left[1+e^{agt_8}\,(e^{at_a}-1)\right]e^{-a(t-t_2)}}{1+e^{-at_1}\,(1-e^{-agt_8})}\right]\right\}$$

PERIOD IV

$$\frac{2^{g-1}\, e^{-a/l}}{1-e^{-at_1}}\left\{\frac{1}{1+e^{a(g-1)t_8}\,(e^{at_1}-1)}\right.$$
$$\times\, e^{a/l}\left[1+e^{a(g-1)t_8}(e^{at_1}-1)\right]\, e^{-a(t-t_2)}$$
$$-\, e^{a/l}\left[1+e^{a(g-1)t_8}\,(e^{at_1}-1)\right]\, e^{-a(t-t_2-t_9)}$$
$$-\,\frac{1}{(1+e^{agt_8}\,(e^{at_1}-1)}$$
$$\times\, e^{a/l}\left[1+e^{agt_8}\,(e^{at_1}-1)\right]\, e^{-a(t-t_2)}$$
$$\left.-\, e^{a/l}\left[1+e^{agt_8}\,(e^{at_1}-1)\right]e^{-a(t-t_2-t_9)}\right\}$$

Table 6 (Con't)

Description	Equation
PERIOD V	$$2^{g-1}\, e^{-a/l}\left\{\frac{e^{a/l\left[1-e^{-at_1}\,(1-e^{-a(g-1)t_8})\right]}}{1-e^{-at_1}\,(1-e^{-a(g-1)t_8})}\right.$$ $$+\frac{1}{1-e^{-at_1}}\left\{\frac{e^{a/l\left[1+e^{a(g-1)t_8}(e^{at_1}-1)\right]}e^{-a(t-t_2)}}{1+e^{a(g-1)t_8}\,(e^{at_1}-1)}\right.$$ $$\left.\left.-\; e^{a/l\left[1-e^{-at_1}+e^{-a(t-t_2)}\right]}\right\}\right\}$$ $$2^{g-1}\, e^{-a/l}\left\{\frac{e^{a/l\left[(1-e^{-at_1})\right]}}{1-e^{-at_1}}\times\left(e^{a/l}\,e^{-a(t-t_2-t_9)}-e^{a/l}\,e^{-a(t-t_2)}\right)\right.$$ $$+\frac{1}{(1-e^{-at_1})\left[1+e^{a(G-1)t_8}(e^{at_1}-1)\right]}$$ $$\times\, e^{a/l\left[1+e^{a(G-1)t_8}\,(e^{at_1}-1)\right]}e^{-a(t-t_2)}$$ $$\left.-\, e^{a/l\left[1+e^{a(g-1)t_8}\,(e^{at_1}-1)\right]}e^{-a(t-t_2-t_9)}\right\}$$

g = number of cell generation ; e = exponential ; a = antigen elimination rate

l = proportionality constant (effective portion of antigen) ; t = period of time

t_1 = latent period for ICC to become IAC ; t_2 = latent period for IAC to become ABFC

t_8 = generation time of activated lymphocytes ; t_9 = maximum number of cell generations an IAC will undergo

quantitative studies so they are not incorporated into this model. In a simplified version, actions of the macrophages and the humoral factors involved in an immune response may be incorporated into the effective portion of a given dose of antigen and the elimination rate or the period of availability of this antigen, since the function of these two factors is to define the level of activation of the ICC.

The fourth sector is the 'primary immune response sector' which gathers information obtained from the previous sectors to simulate the number of antibody-forming cells and the level of antibodies (both IgM and IgG) at different time periods in the course of a primary immune response. As shown in Figure 10 and Table 7 the duration of the primary immune response is defined by the period and step of run in the computer program. This determines the probable number of generations an antibody-forming precursor cell will undergo and the number of antibody-forming cells that will be formed. The persistence of the antibody level depends upon the amount of antibodies formed and their catabolic rate in vivo. The production rates of both IgM and IgG are assumed to be equal but their catabolic rates are different.

The last sector is the 'secondary immune response sector' which describes a secondary immune response and has the same format as that of the primary response. In this sector, only the IgG producing cells are taken into account, and the number of precursor cells is the sum of the virgin cells and the memory cells formed during the course of the primary response. All factors involved in this sector are shown in Figure 11 and Table 8. The number of antibody forming progeny cells

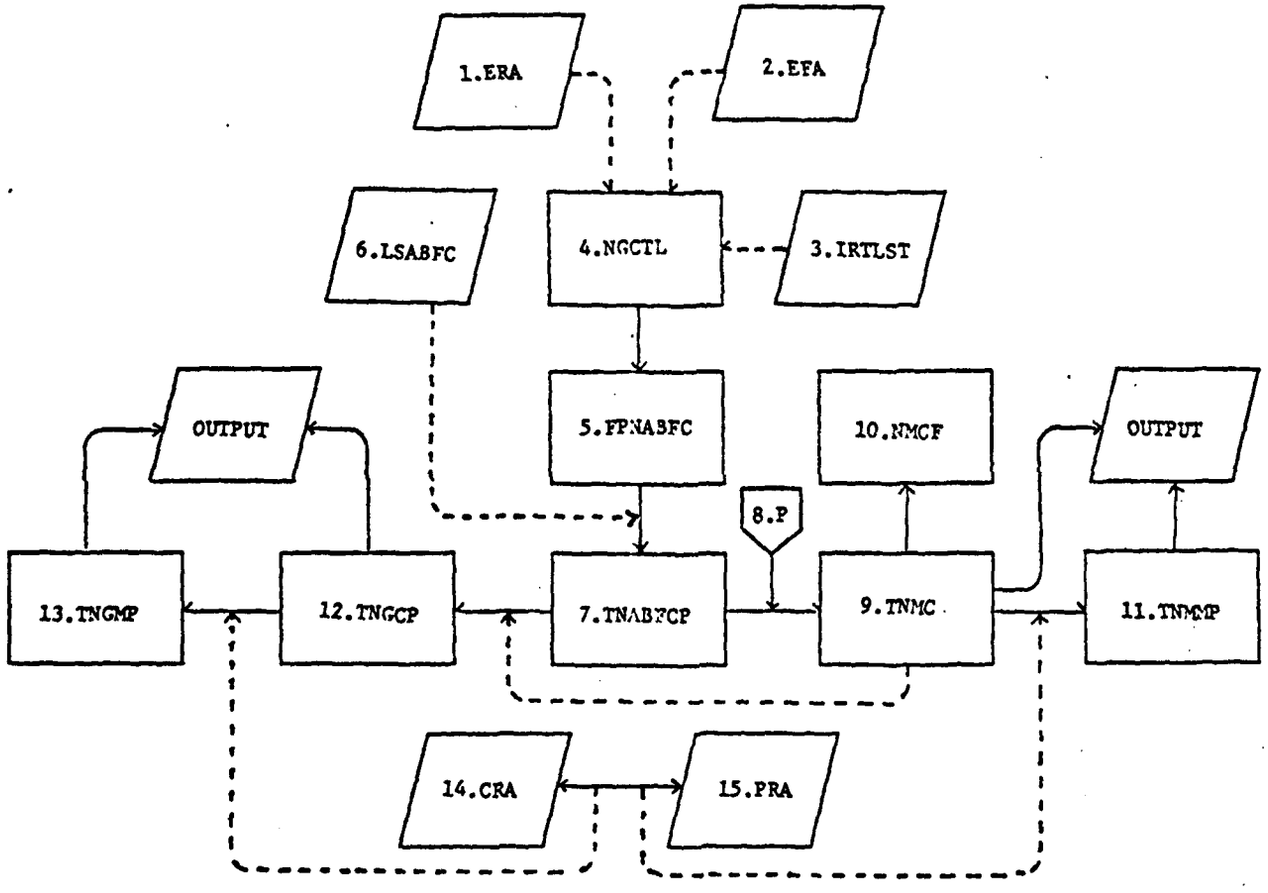

Figure 10. Block diagram of the 'primary immune response sector'.

Table 7. The primary immune response sector.

	ABBREVIATION	DESCRIPTION	EQUATION	VAR.	REF.
1.	ERA	Elimination rate of antigen	--	A	
2.	EFA	Effective fraction of antigen that can activate the ICC	--	L	
3.	IRTLST	Immune response time limit with specified interval	--	T7,HO	
4.	NGCTL	Number of generations completed in this time limit	--	69	
5.	FPNABFC	The function of the probable number of ABFC formed from one precursor cell within the immune response period	*	FNZ(Y)	4
6.	LSABFC	Life span of ABFC	--	T9	
7.	TNABFCP	Total number of ABFC formed from 1 precusor (primary)	*	D[N,2]	41
8.	P	Number of IgM cell precursor from the immunocompetent cell sector	--	AO	
9.	TNMC	Total number of IgM producing cells formed versus time	D[N,2]XAO	AOXD[N,2]	
10.	NMCF	Number of memory cells formed	--	D[168/HO]	
11.	TNMP	Total number of IgM molecules formed versus time	D[N;2]X2.52X10^6	D[N,4]	

Table 7. (Con't.).

ABBREVIATION	DESCRIPTION	EQUATION	VAR.	REF.
12. TNGCP	Total number of IgG producing cells formed versus time	$D[N,2]X2.52X10^6$	D[N,4]	
13. TNGMP	Total number of IgG molecules formed versus time (primary response)	$D[N,6]X2.52X10^6$	D[N,6]	
14. CRA	Catabolic rate of antibody (molecules/hr)	$N_o = e^{-ht}N_t$	--	78
15. PRA	Production rate of antibody (molecules/hr)	$2.52X10^6$	--	18

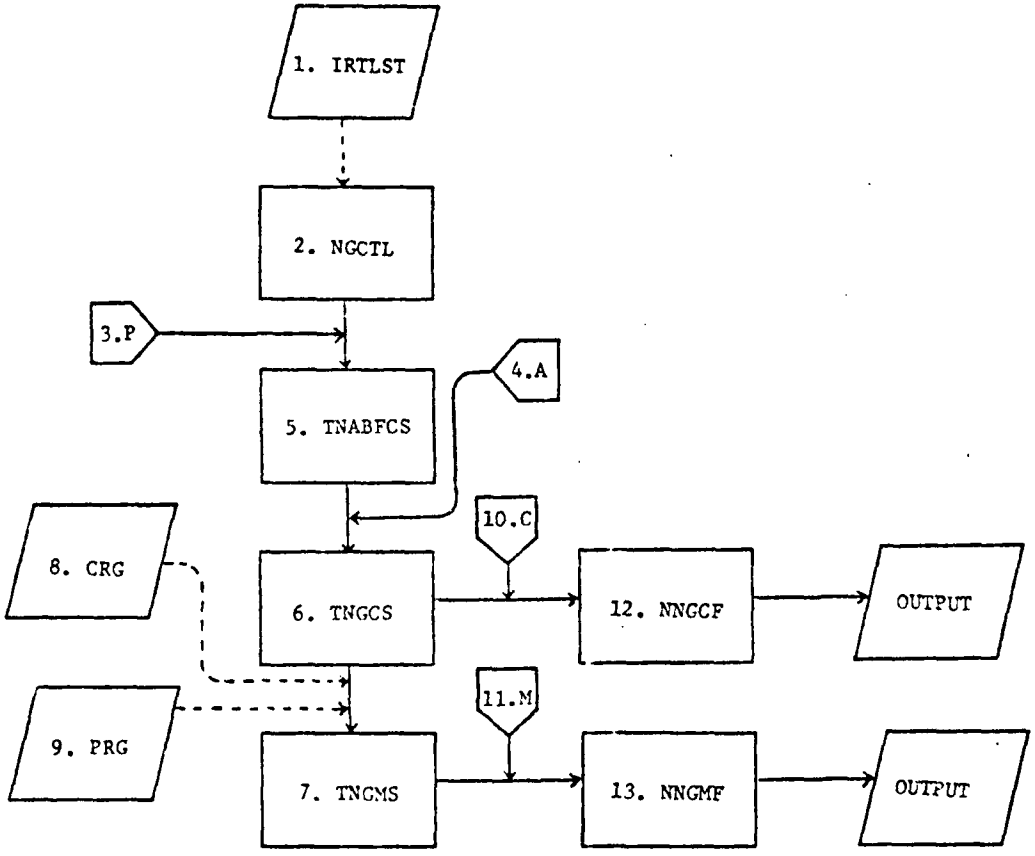

Figure 11. Block diagram of the 'secondary immune response sector'.

Table 8. The secondary immune response sector.

	ABBREVIATION	DESCRIPTION	EQUATION	VAR.	REF.
1.	IRTLST	Immune response time limit with specified intervals (hr)	--	T7,HO	
2.	NGCTL	Number of generations completed in this time limit	--	G9	
3.	P	Number of IgG precursors	W8=M7+AO	WS	41
4.	A	Number of activated IgG ABFC precursors	K XW8	A3	
5.	TNABFCS	Total number of ABFC formed from 1 precursor (secondary response)	A3*D[X,6]	A3*D[X,6]	42
6.	TNGCS	Total number of IgG producing cells formed versus time (secondary response)	D N,20 =A2*D[N,2]	D[N,10]	
7.	TNGMS	Total number of IgG molecules formed versus time (secondary response)		D[N,8]	
8.	CRG	Catabolic rate of IgG (molecule/hr)	$N = C^{-ht} N_t$	--	78
9	PRG	Production rate of IgG (molecule/hr)	2.52×10^6	--	18
10.	C	Residual number of IgG cells in the primary response sector	--	--	
11.	M	Residual number of IgG molecules from the primary response sector	--	--	
12.	NNGCF	Net number of IgG ABFC formed	D[N,10]+D[X,6]	--	
13.	NNGMF	Net number of IgG molecules formed	D[N,8]=2.52×10^6 X(D N,10 +D X,6)	--	

Table 8 (Con't.).

ABBREVIATION	DESCRIPTION	EQUATION	VAR.	REF.
14. NVC	Number of virgin cells	FO*S	--	47
15. NABFCP	Number of ABFC in primary response	F2*B5	AO	47
16. FABFCS	Fraction of ABFC (precursors) in secondary response	K2	--	47
17. NABFCS	Number of ABFC (precursors) in secondary response	K2*M7	A3	47

from one precursor is derived from the same function used in the primary response. The level of IgG and the residual number of IgG forming cells that remained at the time of a second injection were taken into account so that the net antibody level is equal to the sum of the residual IgG and the newly formed IgG.

The basic assumptions made in this model are:

1. The contact between antigen and ICC is an entirely random and independent event.
2. The rate of antibody formation remains constant throughout the entire course of the immune response.
3. Generation time of proliferating ICC is assumed to be constant.
4. The effective dose of antigen and the elimination rate of the antigen is assumed to vary directly with the size of the dose.
5. At about day 5 after initial challenge, IgG precursors are formed which is part of the proliferating IgM precursors.
6. The ratio between the memory cell and the ABFC remains constant in the primary response.
7. From a given number of ICC progeny cells, the number going to the memory pool is proportional to the number of ABFC formed.

Experimental Values Used in the Immune Response Model

A histogram was plotted from the body weights of a hundred mice and the average was found to be around 30 grams. This result is shown in Tables 9 and 10 and in Figure 12. The weight of a mouse lymphocyte is important in determining the number of lymphocytes in the lymphatic compartment. This was estimated from the volume and density of an average small lymphocyte. Volume was evaluated from the average radius of the lymphocyte using the equation which calculates the volume of a perfect sphere. Results of the measured radii and the calculated volumes of mouse lymphocytes are shown in Tables 11 and 12 and Figures 13 and 14.

Density was estimated by isopycnic centrifugation of mouse peripheral blood over Ficoll-hypaque gradient of different densities. Different elements of the blood are characterized by differences in size and density; both of these parameters can be utilized for selective purification purposes. Rate zonal centrifugation is applied on the basis of size while isopycnic zonal sedimentation is based on density. The first step in determining the density of lymphocytes is to remove the erythrocytes and other leucocytes. Various gradient systems such as Isopaque-Dextran, Isopaque-Ficoll, EDTA-Ficoll, EDTA-Dextran and Ficoll-Hypaque could be used (9). Ficoll is a large molecular weight erythrocyte-aggregating agent while hypaque serves as a layering material. Ficoll is a sucrose polymer with a molecular weight of about 400,000. It is highly soluble in water or aqueous solutions and has a relatively low viscosity and a spherical shape. Ten and eleven

Table 9. Estimation of average mouse weight.

DATA :

MOUSE WEIGHT (gm)	MOUSE WEIGHT (gm)	MOUSE WEIGHT (gm)
32.3000	32.1000	27.3000
32.0000	34.5000	28.8000
34.0000	32.3000	33.5000
27.0000	28.2000	34.4000
30.000	24.2000	32.4000
25.8000	30.1000	33.1000
33.6000	34.2000	33.6000
34.3000	32.5000	26.0000
30.7000	32.6000	34.2000
29.3000	32.4000	30.6000
30.6000	29.4000	29.5000
25.1000	28.4000	30.4000
27.4000	28.3000	28.6000
27.2000	33.4000	25.8000
31.6000	28.1000	26.2000
28.4000	28.0000	24.2000
31.6000	27.2000	25.5000
28.2000	29.8000	32.3000
29.4000	29.1000	34.2000
29.8000	28.7000	34.3000
30.9000	33.5000	33.9000
31.3000	32.5000	31.0000
32.2000	25.4000	32.5000
32.6000	26.0000	26.6000
32.7000	28.8000	30.8000
33.2000	27.5000	30.0000
33.5000	27.0000	25.5000
33.7000	27.6000	32.3000
32.5000	26.8000	33.9000
26.6000	30.0000	31.0000
30.0000	29.8000	32.5000
30.8000	31.1000	30.2000
	26.3000	31.0000
	27.2000	29.8000

Table 10. Mouse weight histogram.

CELL STATISTICS

CELL#	LOWER LIMIT	NO. OF OBS	%RELATIVE FREQ
1	0.0000	0	0.00000
2	1.0000	0	0.00000
3	2.0000	0	0.00000
4	3.0000	0	0.00000
5	4.0000	0	0.00000
6	5.0000	0	0.00000
7	6.0000	0	0.00000
8	7.0000	0	0.00000
9	8.0000	0	0.00000
10	9.0000	0	0.00000
11	10.0000	0	0.00000
12	11.0000	0	0.00000
13	12.0000	0	0.00000
14	13.0000	0	0.00000
15	14.0000	0	0.00000
16	15.0000	0	0.00000
17	16.0000	0	0.00000
18	17.0000	0	0.00000
19	18.0000	0	0.00000
20	19.0000	0	0.00000
21	20.0000	0	0.00000
22	21.0000	0	0.00000
23	22.0000	0	0.00000
24	23.0000	0	0.00000
25	24.0000	2	2.00000
26	25.0000	6	6.00000
27	26.0000	7	7.00000
28	27.0000	9	9.00000
29	28.0000	11	11.00000
30	29.0000	9	9.00000
31	30.0000	13	13.00000
32	31.0000	7	7.00000
33	32.0000	17	17.00000
34	33.0000	11	11.00000
35	34.0000	8	8.00000

HISTOGRAM WITH PLOT OVERLAY

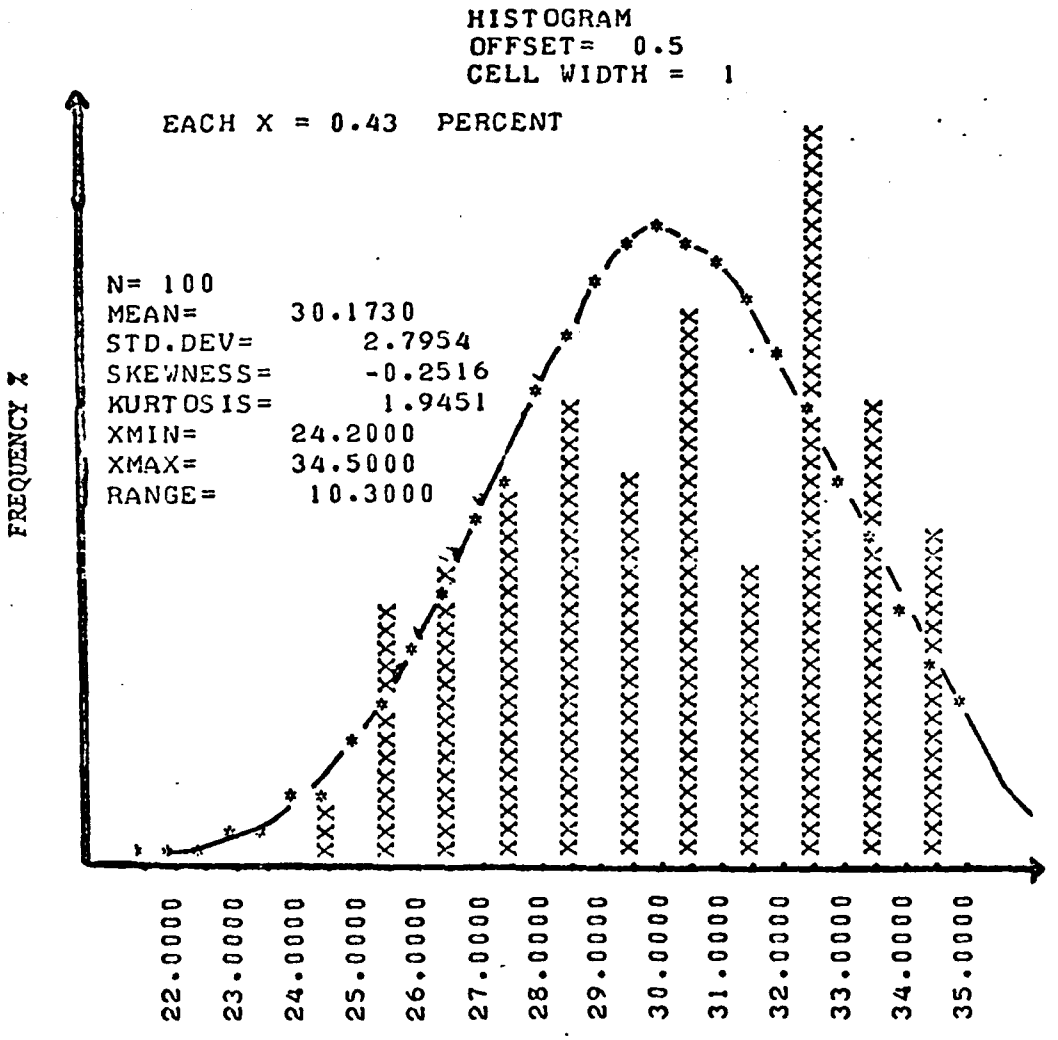

Figure 12. Histogram of the body weight range of mice.

Table 11. Estimation of the average radius of mouse lymphocytes.

Radius (Micron)	Radius (Micron)	Radius (Micron)	Radius (Micron)
3.2736	3.4596	3.1248	3.1620
3.3666	3.4131	3.4689	3.3015
3.2271	3.5433	4.087	3.1806
3.2736	3.2736	4.4826	3.572
3.4689	3.2922	3.2644	3.3945
3.3945	4.0176	3.5898	3.3494
3.5211	3.9525	3.6177	3.4782
3.5433	3.4503	3.3852	3.3945
3.3852	3.1620	3.0703	3.2271
4.3686	3.5433	3.2271	3.3945

CELL STATISTICS

CELL #	LOWER LIMIT	NO. OF OBS	%RELATIVE FREQ
1	0.1000	0	0.00000
2	0.3000	0	0.00000
3	0.5000	0	0.00000
4	0.7000	0	0.00000
5	0.9000	0	0.00000
6	1.1000	0	0.00000
7	1.3000	0	0.00000
8	1.5000	0	0.00000
9	1.7000	0	0.00000
10	1.9000	0	0.00000
11	2.000	0	0.00000
12	2.3000	0	0.00000
13	2.5000	0	0.00000
14	2.7000	0	0.00000
15	2.9000	1	2.50000
16	3.1000	12	30.00000
17	3.3000	15	7.50000
18	3.5000	7	7.50000
19	3.7000	0	0.00000
20	3.9000	3	7.50000
21	4.1000	0	0.00000
22	4.3000	2	5.00000

Table 12. Calculated average volume of mouse lympocytes.

Volume* (cubic micron)	Volume* (cubic micron)
173.4500	127.8100
166.5500	174.8500
186.3400	349.2300
146.9500	377.2900
149.4500	145.700
271.6400	193.7800
258.6500	198.3300
172.0500	162.5000
132.4300	121.2400
118.3400	140.7800
146.9500	132.4300
159.8300	1[illegible].7400
140.7800	134.7800
146.9500	190.7800
174.8500	163.8400
163.8400	154.6000
182.8600	163.8400
186.3400	140.7800
162.5000	163.8400
285.9800	176.2600

CELL STATISTICS

CELL #	LOWER LIMIT	NO.OF OBS.	% RELATIVE FREQ.
1	-9.0000	0	0.00000
2	11.0000	0	0.00000
3	31.0000	0	0.00000
4	51.0000	0	0.00000
5	71.0000	0	0.00000
6	91.0000	0	0.00000
7	111.0000	3	7.50000
8	131.0000	12	22.50000
9	151.0000	9	22.50000
10	171.0000	9	5.00000
11	191.0000	2	0.00000
12	211.0000	0	0.00000
13	231.0000	0	0.00000
14	251.0000	1	2.50000
15	271.0000	2	5.00000
16	291.0000	0	0.00000
17	311.0000	0	0.00000

* By formulae : $4/3 \times \pi \times (r)^3$

HISTOGRAM WITH PLOT OVERLAY

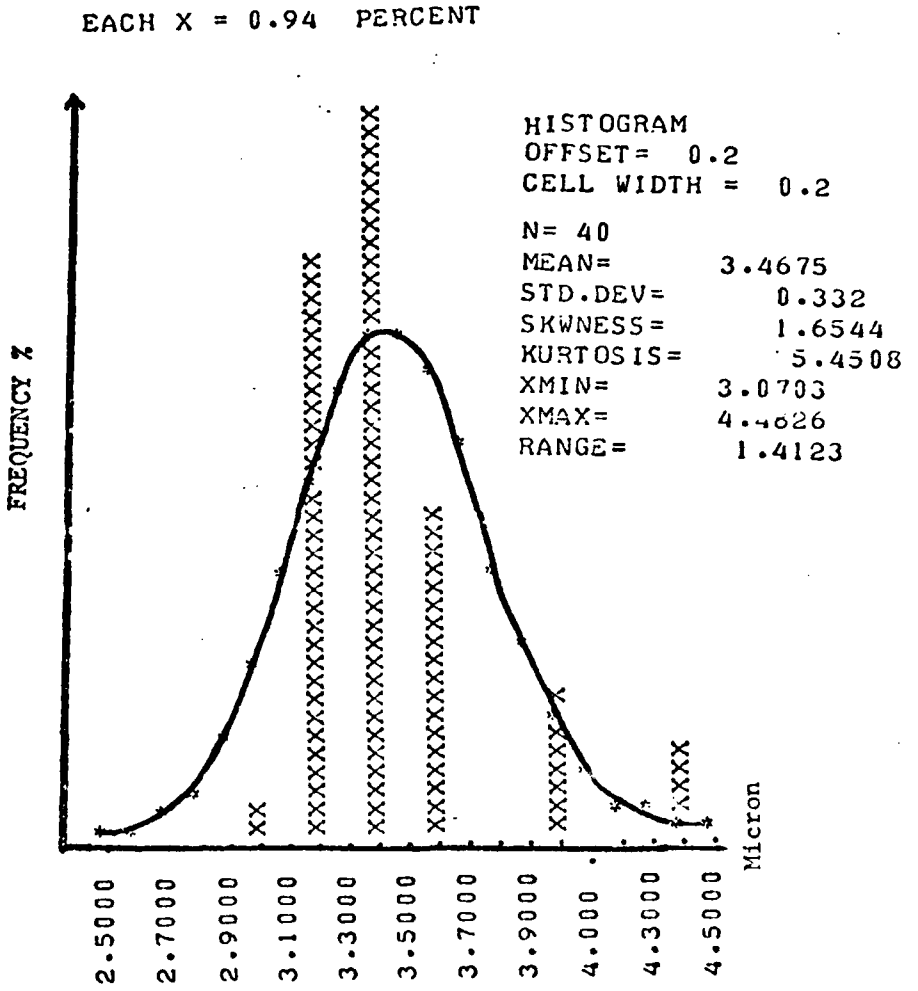

Figure 13. Histogram of measured radii of mouse lymphocytes.

HISTOGRAM WITH PLOT OVERLAY

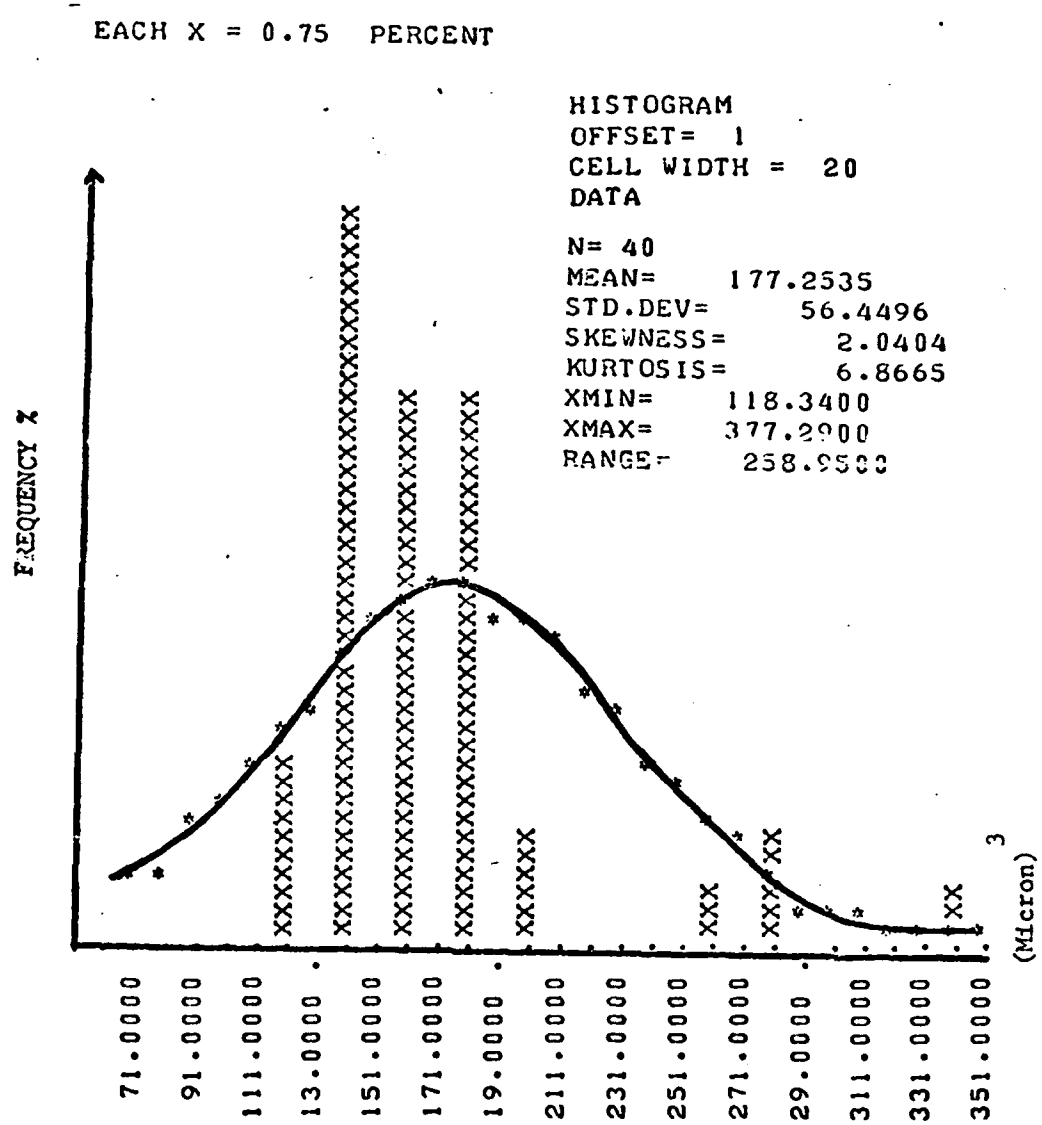

Figure 14. Histogram of calculated volume range of mouse lymphocytes.

percent solutions have relative viscosity of 5.4 and 6.4, respectively. Hypaque or sodium diatrizoate is a water soluble radiopaque medium with a molecular weight of 635.92. It is sensitive to light and should be prepared freshly before use. Oral preparations containing caramel should be avoided. Following centrifugation, the blood components would be distributed as follows: the top layer is a clear zone of plasma, followed by a small band of mononuclear cells and platelets. Below this is a cloudy zone containing mainly granulocytes, and the erythrocytes were in the bottom zone. Purity of white blood cells is a function of the efficiency of red blood removal which in turn is a function of the cell-clumping mixture, of its density and of the concentration of cell-clumping compound, viscosity, osmolarity and ionic composition. It is also a function of the top phase, of the height of the blood column, and of the degree of dilution. The whole procedure is greatly influenced by temperature changes.

An increase in white cell yield is obtained by the following:

1. diluting the blood
2. increasing the blood volume
3. increasing the osmolarity of the lower phase
4. raising the temperature to 37 C.

The catabolic rate of WEE virus in mice was determined by single i.v. injections of ^{125}I labeled WEE virus into mice. The rate of removal of the injected virus was reflected by the rate of disappearance of radioactivity in the blood of mice. The radioactivity of the blood sample was first converted by volume ratio into radioactivity

of the total volume of blood in each mouse. When the logarithm (log) of these data (in CPM) was plotted against time, the curve appeared to be biphasic. The first linear portion represents the catabolic decay of WEE virus and the second portion is the increased immunological removal phase. Data between the first linear portion of this curve were used to estimate the average catabolic rate of WEE virus by a first order exponential equation and the results are shown in Tables 13, 14, 15, 16 and in Figure 15. The half-life of mouse IgG *in vivo* was estimated in a similar fashion and, again, only the linear portion of the curve was used. It was found that in hyperimmunized mice where the IgG level was expected to be higher, the catabolic rate of the passively injected ^{125}I labeled mouse IgG was much faster. Results are summarized in Tables 17, 18, 19 and 20 and in Figure 16.

Generation time of mouse lymphocytes was estimated *in vitro* by tissue culture technique. Peripheral blood lymphocytes were first purified by an isopycnic centrifugation in a layering solution of Ficoll-Hypaque with a density of 1.08 and the lymphocytes harvested as inoculum were found to contain about 80% lymphocytes as revealed by Wright's stain and 90% of the cells were viable as determined by trypan blue exclusive stain.

Concentration of cells in the culture was found to be about one million cells per ml. The increase in cell numbers of this culture was determined by a Coulter Counter at various time intervals. Since the number of cells were compared in a relative basis, no attempt was made to estimate the absolute cell number or size. The cell counts

Table 13. Elimination rate of WEE virus in mice using the following data: mouse weight, blood volume and CPM of sample.

Time	Mouse Weight (grams)		Blood Volume (ml)		CPM of Sample	
	1	2	1	2	1	2
5 min	33.7	34.3	2.6180	2.6685	96175	89622
15 min	26.0	30.7	2.0228	2.3885	97738	84299
30 min	34.2	29.3	2.6608	2.2795	56422	70032
45 min	30.6	29.7	2.3807	2.3107	58909	53408
90 min	29.5	30.6	2.2951	2.3807	76008	62894
2 hr	30.4	25.1	2.3651	1.9528	43240	59928
5.5 hr	28.6	27.4	2.2251	2.1317	32155	32858
20 hr	25.8	27.2	1.9866	2.1162	10766	9639
24 hr	29.8	31.6	2.3184	2.4585	11776	11823
48 hr	26.2	31.6	2.0384	2.4585	1074	1200
53 hr	24.0	28.4	1.8674	2.2095	220	175
72 hr	30.6	28.9	2.3807	2.2484	38	30

Table 14. Elimination rate of WEE virus in mice using data of CPM in a whole mouse.

Time	Counts Per Minute (CPM)			
	1	2	Average	log
5 min	251782	239160	245471	5.39
15 min	197704	201348	199526	5.30
30 min	150126	159638	154882	5.19
45 min	140243	123409	131826	5.12
90 min	174630	149732	162181	5.21
2 hr	102268	117028	109648	5.04
5.5 hr	71547	70043	70795	4.85
20 hr	21387	20399	20893	4.32
24 hr	27301	29067	28184	4.45
48 hr	2189	2951	2570	3.41
53 hr	410	386	398	2.60
72 hr	91	67	79	1.90

Table 15. Calculation of the elimination rate of WEE virus in mice using the first order exponential decay equation: $C = 2.3 \times \log (D_o/D_t) \times 1/T$.

Time (hr)	D_o*	D_t+	T[a]	C[b]
0-20	245471	20893	20	2.3 x log (245471/20893) x 1/20 hr = 0.123/hr
0-24	245471	28184	24	2.3 x log (245471/28184) x 1/24 hr = 0.090/hr
0-48	245571	2570	48	2.3 x log (245571/2570) x 1/48 hr = 0.095/hr
20-48	20893	2570	28	2.3 x log (20893/2570) x 1/28 hr = 0.071/hr
24-48	28184	2570	24	2.3 x log (28184/2570) x 1/24 hr = 0.100/hr

* - D_o = CPM at time zero

\+ - D_t = CPM at time t

[a] - T = time between two counts (hr)

[b] - C = elimination rate constant/hr

Table 16. Summary of the elimination rate of WEE virus in mice.

Time Between	Time Lapse	C Value*	Elimination Rate (0/0/hr)
0-20	20	0.123	12.3
0-24	24	0.090	9.0
0-48	48	0.095	9.5
20-24	4	--	--
20-48	28	0.071	7.1
24-48	24	0.100	10.0
	Total	0.479	
	Average	0.096	9.6

*From equation $C = \ln (D_o/D_t) \times 1/T$.

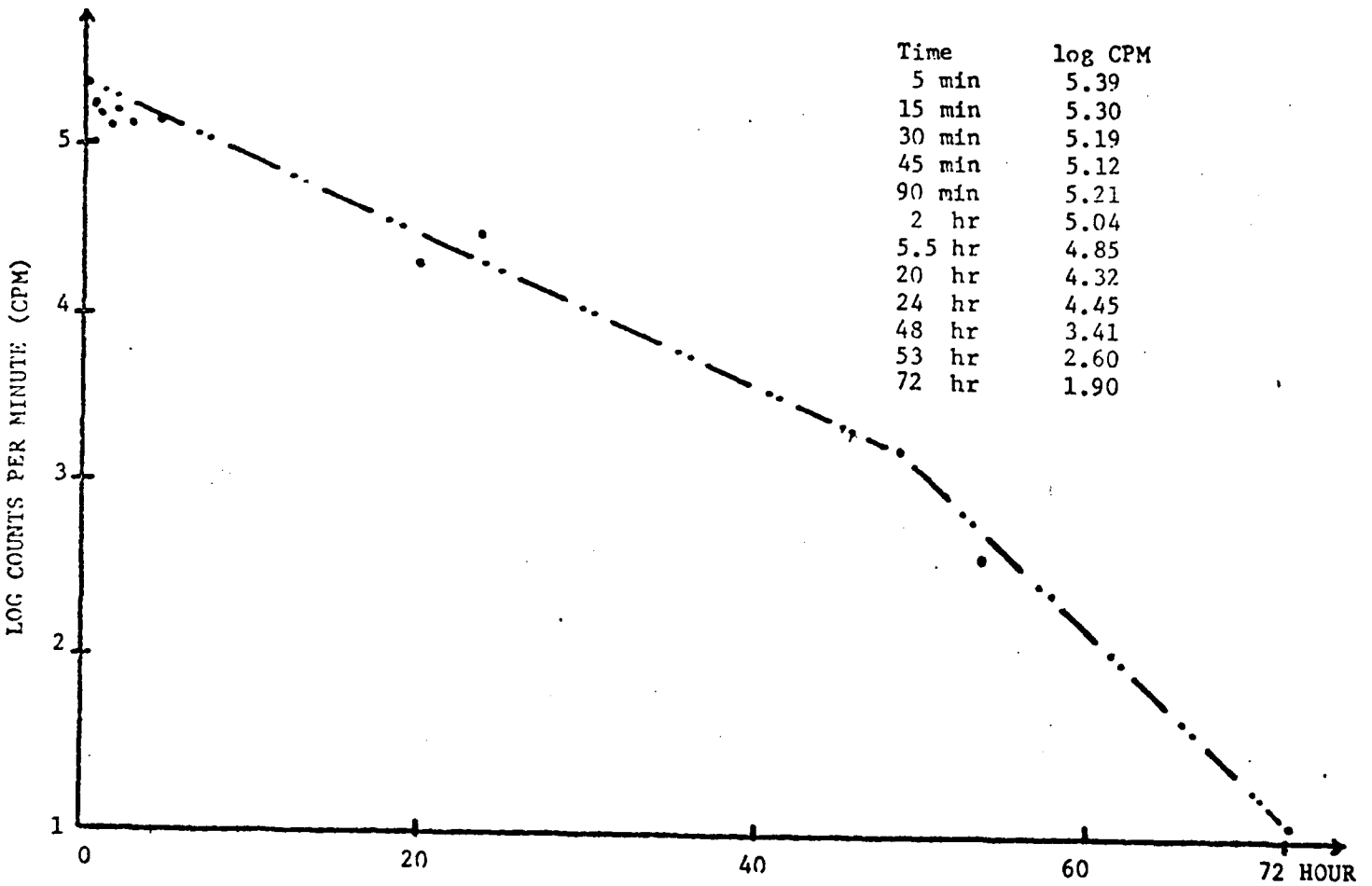

Time	log CPM
5 min	5.39
15 min	5.30
30 min	5.19
45 min	5.12
90 min	5.21
2 hr	5.04
5.5 hr	4.85
20 hr	4.32
24 hr	4.45
48 hr	3.41
53 hr	2.60
72 hr	1.90

Figure 15. The elimination curve of passively injected ^{125}I labeled WEE viral particle in the blood of mice.

Table 17. Catabolic rate of mouse Ig in normal mice.

Time (hr)	Mouse Weight (gm)		Blood Sample (ml)		Total Blood Volumes (ml)*	
	1	2	1	2	1	2
8	29.7	27.8	0.9	1.0	2.31	2.16
24	30.2	30.5	0.6	0.4	2.35	2.35
32	31.9	25.2	0.3	0.4	2.48	1.96
48	26.2	27.1	0.2	1.0	2.04	2.10
58	34.1	29.8	0.9	0.6	2.65	2.32
80	23.8	24.1	0.45	0.5	1.85	1.94

Time (hr)	Counts per Minute (CPM)						Average	Log
	Tail		Blood		Total			
	1	2	1	2	1	2		
8	2706	12194	19024	12441	21728	14636	21728	4.2794
24	674	676	11754	10862	12228	11530	12031	4.0612
32	1082	2930	10888	7134	11970	10094	11324	4.0540
48	3904	2656	6854	6825	10758	9481	10240	4.0100
58	2286	990	7032	8104	9318	9094	9377	3.9720
80	2350	2060	5032	5322	7382	7382	7622	3.8820

* Volume of blood = 7.78 ml/kg of body weight of mouse.

Table 18. Catabolic rate of mouse IgG in WEE hyperimmune mice.

Time (hr)	Mouse Weight (gm)		Blood Sample (ml)		Total Blood Volumes (ml)	
	1	2	1	2	1	2
8	26.7	28.5	1.0	0.7	2.20	2.22
24	27.6	--	0.5	--	2.15	--
48	29.8	28.7	0.6	0.6	2.32	2.23

Time (hr)	Counts per Minute (CPM)						Average	Log
	Tail		Blood		Total			
	1	2	1	2	1	2		
8	1080	1107	12304	11340	12283	11347	12798.8	4.1068
24	1296	--	9742	--	11038	--	11038	4.0429
48	2663	956	5474	7284	8137	8343	8339	3.9211

Table 19. Catabolic rate of mouse IgG.

Time Between (hours)	Time Lapse (hours)	k Value*	Half-life $T_{1/2}$ [a]	
			hours	days
24-32	8	0.007570	91.15	3.80
24-48	24	0.006716	102.74	4.28
24-58	34	0.007331	94.12	3.92
24-80	56	0.008150	84.66	3.53
32-48	16	0.006289	109.56	4.57
32-58	26	0.007258	94.72	3.95
32-80	48	0.008247	83.67	3.49
48-58	10	0.008087	85.32	3.55
48-80	32	0.009226	74.79	3.12
58-80	22	0.009415	73.29	3.05
		Average	89.40	3.73
8-24[b]	16	0.009250	74.59	3.11
8-48[b]	40	0.013390	51.53	2.15
24-48[b]	24	0.011680	59.07	2.46
		Average	61.73	2.57

* - $k = \ln D_o/D_t \times 1/T$

a - $T_{1/2} = 0.69/k$

b - WEE hyperimmunized mice, all others are normal mice.

Table 20. Calculation of the catabolic rate of mouse IgG.

$k = \ln (D_o/D_t) \times 1/T$ $\qquad T_{1/2} = 0.69/k$

Time (hr)	D_o*	D_t+	T[a]	k[b] or $T_{1/2}$[c]
24-32	12031	11324	8	$k = \ln (12031/11324) \times 1/8$ $= 0.007570\ (hr^{-1})$ $T_{1/2} = (0.69/0.007570)$ hr $= 91.1493$ hr
24-48	12031	10240	24	$k = \ln (12031/10240) \times 1/24$ $= 0.006716\ (hr^{-1})$ $T_{1/2} = (0.69/0.006716)$ hr $= 102.7397$ hr
24-58	12031	9376.6	34	$k = \ln (12031/9376.6) \times 1/34$ $= 0.007331\ (hr^{-1})$ $T_{1/2} = (0.69/0.007331)$ hr $= 94.1209$ hr
24-80	12031	7622.3	56	$k = \ln (12031/7622.3) \times 1/56$ $= 0.008150\ (hr^{-1})$ $T_{1/2} = (0.69/0.008150)$ hr $= 84.6625$ hr
32-48	11324	10240	16	$k = \ln (11324/10240) \times 1/16$ $= 0.006289\ (hr^{-1})$ $T_{1/2} = (0.69/0.006289)$ hr $= 109.7586$ hr
32-58	11324	9376.6	26	$k = \ln (11324/9376.6) \times 1/26$ $= 0.007258\ (hr^{-1})$ $T_{1/2} = (0.69/0.007258) = 94.7152$ hr
32-80	11324	7622.3	48	$k = \ln (11324/7622.3) \times 1/48$ $= 0.008247\ (hr^{-1})$ $T_{1/2} = (0.69/0.008247) = 83.6678$ hr
48-58	10240	9376.6	10	$k = \ln (10240/9376.6) \times 1/10$ $= 0.008087\ (hr^{-1})$ $T_{1/2} = (0.69/0.008087)$ hr $= 85.3221$ hr
48-80	10240	7622.3	32	$k = \ln (10240/7622.3) \times 1/32$ $= 0.009226\ (hr^{-1})$ $T_{1/2} = (0.69/0.009226)$ hr $= 74.7656$ hr
58-80	9376.6	7622.3	22	$k = \ln (9376.6/7622.3) \times 1/22$ $= 0.009415\ (hr^{-1})$ $T_{1/2} = (0.69/0.009415)$ hr $= 73.2873$ hr

* - D_o = CPM at time zero

\+ - D_t = CPM at time t

[a] - T = Time between two counts (hr)

[b] - k = decay constant (hr^{-1})

[c] - $T_{1/2}$ = half-life of Ig (hr)

CATABOLIC RATE OF MOUSE IMMUNOGLOBULIN G (IgG)

Time	log CPM Normal	HI
8	4.2794	4.1068
24	4.0612	4.0429
32	4.054	-
48	4.010	3.9211
58	3.972	-
80	3.882	-

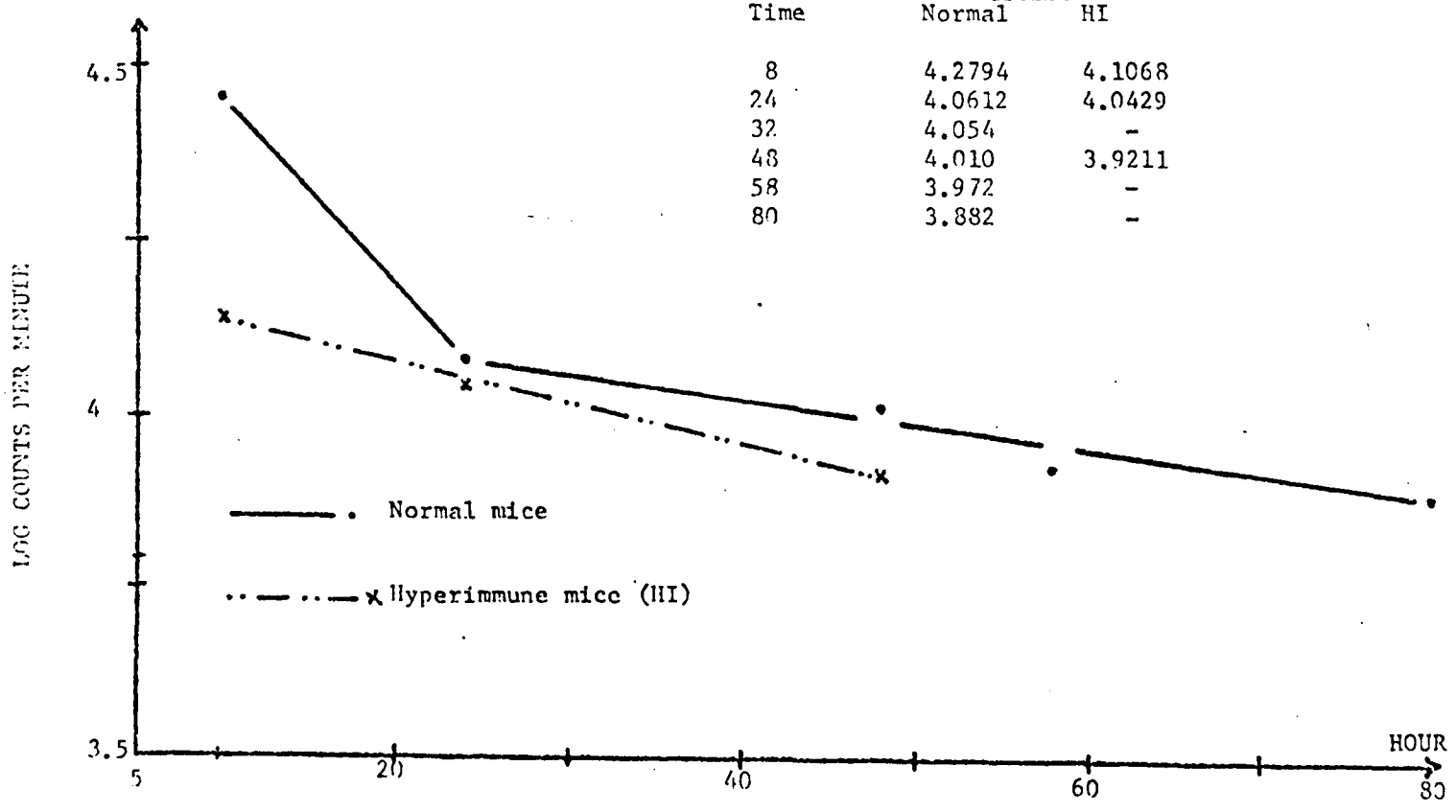

Figure 16. Catabolic rate of mouse immunoglobulin G (IgG).

throughout the experiment were low so no coincidence corrections were necessary. Since most of the peripheral blood lymphocytes were the small lymphocytes, only these cells were taken into consideration. The cell growth rate was calculated by a natural growth equation and assumed an exponential increase of cells by binary fission. Only data points lying between the linear portion of the curve in a log-plot were used. Results are summarized in Tables 21, 22, 23 and 24 and in Figures 17, 18 and 19. The Coulter Counter could rapidly determine both cell volume and cell concentration far more efficiently and accurately than by other techniques (1, 44, 45). A Coulter Counter provides an unique advantage for studying cell population as a function of cell size and for studying synchronized cell cultures where both cell counts and volume profiles are needed for optimal information. Although the lymphocyte culture in this study was not experimentally designed for synchronous growth, it is safe to assume that it is a synchronous culture. Basically, the small lymphocytes in the culture were mostly memory T cells since the source of these cells was from the blood of WEE hyperimmunized mice. Under normal conditions these cells should be in an intermitotic state until further antigenic challenge was met. This further stimulation was provided by the WEE virus in the medium, and activation and allogenic interaction of the small lymphocytes should be almost simultaneous.

The propagation and titration of WEE virus were done in primary tissue cultures of chick embryo fibroblast. The preparation of tissue cultures involves fairly precise control of a number of biophysical

Table 21. Coulter counter data for the estimation of the average generation time of mouse lymphocytes

Time of Sampling	Threshold Number	Counts 1	2	3	Average	Standard Deviation	% Standard Deviation
	3	58	53	48	53.00	5.00	9.43
	4	45	50	35	43.33	7.64	17.63
	5	19	17	21	19.00	2.00	10.52
0 hour	6	14	12	11	12.33	1.53	12.41
	7	12	10	10	10.67	1.15	10.78
	8	10	8	7	8.33	1.53	18.37
	9	11	12	10	11.00	1.00	9.10
	10	8	6	5	6.33	1.53	24.17
	3	30	32	39	33.67	4.73	14.05
	4	29	37	33	33.00	4.00	12.12
	5	7	11	9	9.00	2.00	22.22
24 hours	6	18	10	13	13.67	4.04	29.55
	7	8	13	11	10.67	2.52	23.62
	8	6	9	10	8.33	2.08	25.00
	9	63	67	65	65.00	2.00	3.08
	10	64	62	60	62.00	2.00	3.23
	3	187	202	186	191.67	8.96	4.67
	4	137	176	167	160.00	20.42	1.28
	5	102	103	119	108.00	9.54	8.83
48 hours	6	138	135	139	137.33	2.08	1.51
	7	110	114	125	116.33	7.77	6.67
	8	112	90	96	99.33	11.37	11.45
	9	315	280	322	205.67	22.50	7.36
	10	258	243	247	249.33	7.77	3.12
	3	536	524	550	536.67	13.01	2.42
	4	452	461	420	444.33	21.55	4.85
	5	262	266	290	272.67	15.14	5.55
70 hours	6	227	207	215	216.33	10.07	4.65
	7	199	194	205	199.33	5.51	2.76
	8	175	199	193	189.00	12.49	6.60
	9	136	133	138	135.67	2.52	1.86
	10	140	135	135	136.67	2.89	2.11
	3	960	959	898	939.00	35.51	3.78
	4	748	758	728	744.67	15.28	2.05
	5	575	610	583	589.33	18.33	3.11
76 hours	6	535	500	511	515.33	17.90	3.47
	7	423	438	428	429.67	7.64	1.77
	8	414	432	389	445.00	39.15	8.78
	9	403	377	371	383.67	17.01	4.43
	10	353	347	333	344.33	10.26	2.98

Aperture = 512
Attenuation = 0.707
Orifice = 50 ul

Sample size = 50 ul
Dilution of sample = 1/50

Table 22. Growth rate of mouse lymphocyte.

Channel Number	Channel Counts				
	0 hr	24 hr	48 hr	70 hr	76 hr
3*	10	1	32	92	194
4	24	24	52	172	155
5	7	0	0	56	74
6	2	3	21	17	86
7	2	2	17	10	18
8	0	0	0	53	28
Total	45	30	122	400	555
Log	1.6532	1.4771	2.0864	2.6026	2.7443

* Channel 3 are counts between threshold 3 and 4.

Table 23. Growth rate of mouse lymphocyte.

Resolution at Aperture = 512
Attenuation = 0.707

Threshold #	Volume Range (μ^3)
2	65.00 - 97.56
3	97.56 - 130.12
4	130.12 - 162.68
5	162.68 - 195.24
6	195.24 - 227.80
7	227.80 - 260.36
8	260.36 - 292.92
9	292.92 - 325.48
10	325.48 - 390.60
11	390.60 - 423.60
12	423.60 - 455.70
13	455.70 - 488.26

Table 24. Calculation of the growth rate of mouse lymphocytes using the following natural growth equation: $g = \log 2 \times T / \log N_t - \log N_o$ .....(1).

Time (hrs)	T*	N_t+	N_o[a]	g[b]
24-48	24	122	30	0.301 x 24 hr/(2.0864 - 1.4771) = 11.856 hr
24-70	46	400	30	0.301 x 46 hr/(2.6026 - 1.4971) = 12.302 hr
24-76	52	555	30	0.301 x 52 hr/(2.7443 - 1.4771) = 12.352 hr
48-70	22	400	122	0.301 x 22 hr/(2.6026 - 2.0864) = 12.786 hr
48-76	28	555	122	0.301 x 28 hr/(2.7443 - 2.0864) = 12.81 hr
70-76	6	555	400	0.301 x 6 hr/(2.7443 - 2.6026 = 12.75 hr

* - T = time (hr) between two cell counts

\+ - N_t = Number of cell at time t

[a] - N_o = Number of cell at time o

[b] - g = Generation time in hours

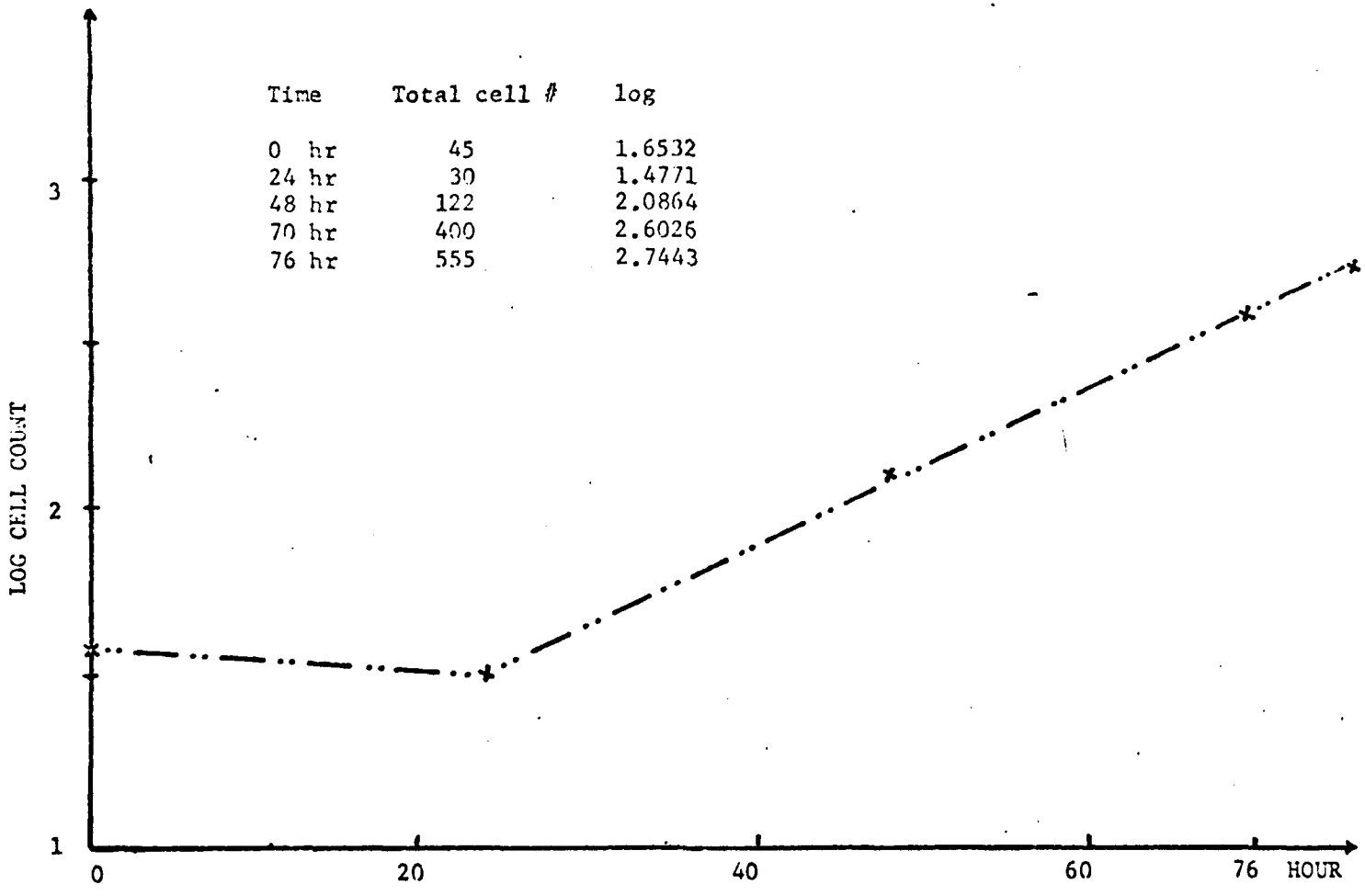

Figure 17. Growth rate of mouse lymphocytes in vitro.

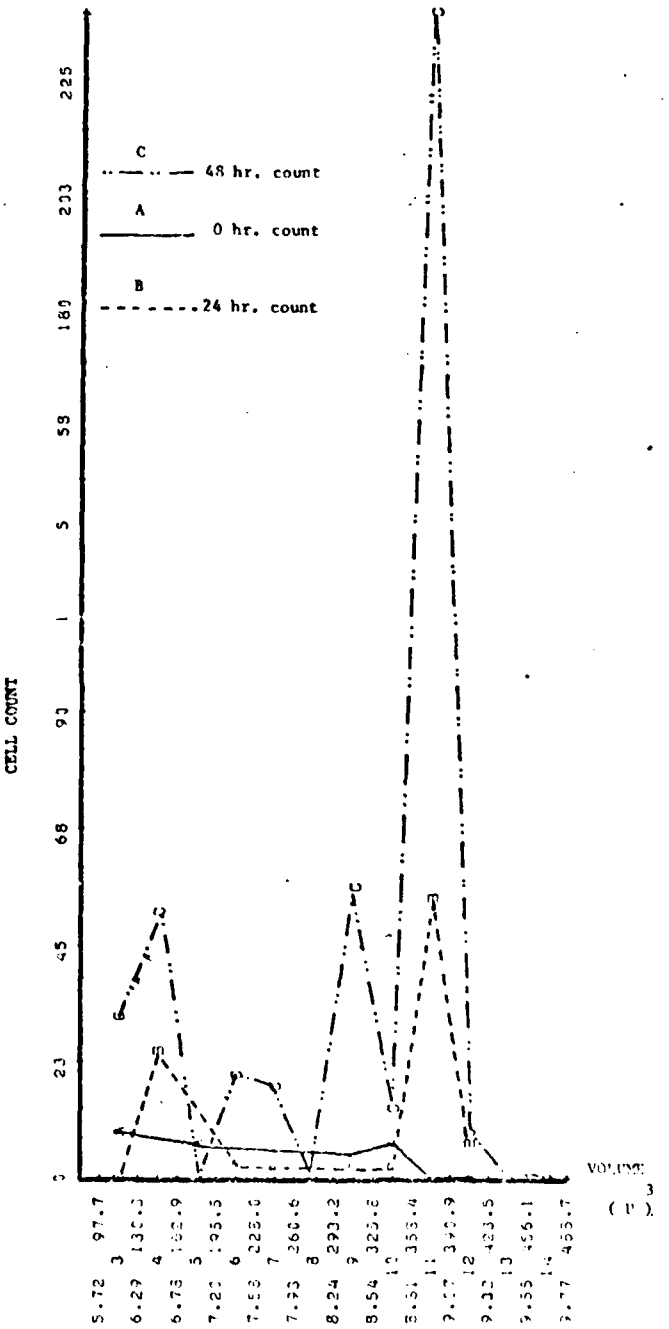

Figure 18. Cell volume distribution profile for the estimation of the generation time of mouse lymphocytes.

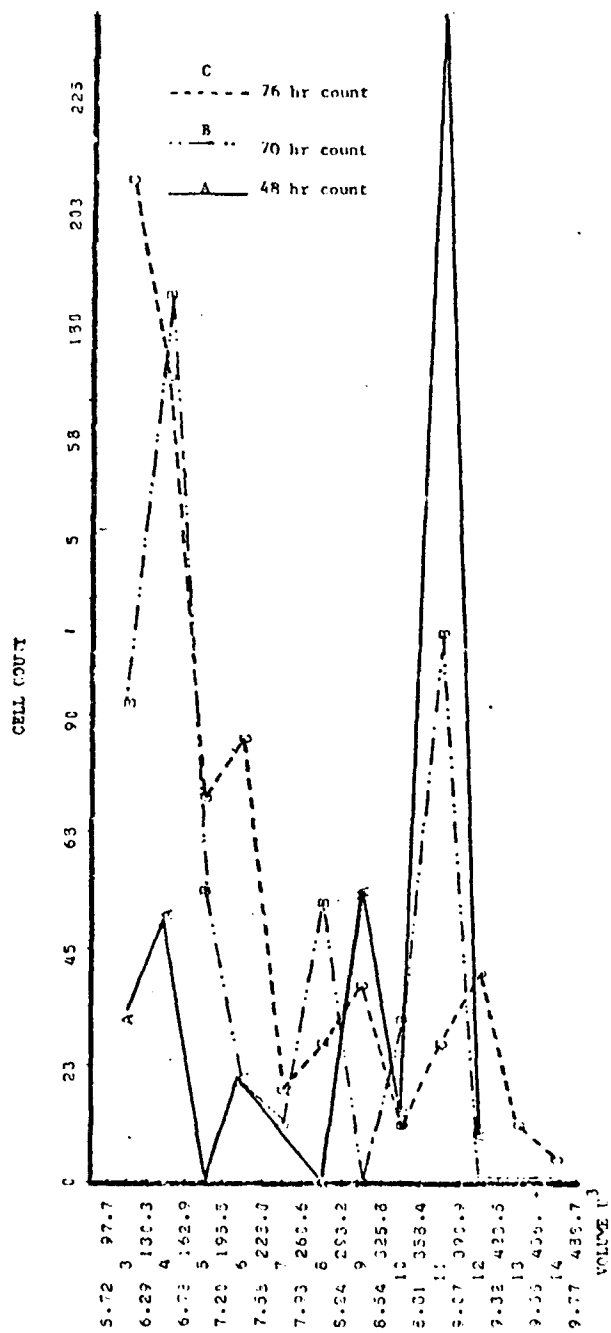

Figure 19. Cell volume distribution profile for the estimation of the generation time of mouse lymphocytes.

and biochemical parameters such as the composition of the growth medium, cell concentration and volume of culture medium. The medium is usually based on a balanced solution of physiological organic salts buffered with phosphate or bicarbonate. In addition, a protein source is provided as amino acids or as acid hydrolysate of a suitable protein, usually lactoalbumin. A further source of protein is serum, commonly used to supplement the other nutrients. The same component also supplies essential vitamins and additional buffering capacity. A controlled gas phase of approximately 5% CO_2 in air is employed to prevent excessive alkalinity developing in the culture medium. Phenol red is incorporated into most standard media as an inert pH indicator. To prevent contamination of highly nutritional medium, specific antibiotics are usually added. Penicillin and streptomycin are active against bacteria; mycostatin and amphistericin B are specifically active against yeasts and molds while aureomycin and kanamycin are used to prevent the contamination by mycoplasmas. A parameter closely related to buffering capacity in determining the readiness with which active cell growth is initiated is the concentration at the beginning. The size of inoculum directly influences the pH of the medium immediately following incubation. Too low a concentration would prolong the initial alkaline period while a high concentration would cause an abrupt rapid drop in pH; both can damage cells irrevocably. For setting most monolayer cultures a concentration of 1-10 x 10^5 cells/ml is usually satisfactory (36). The volume of culture medium affects the oxygen gradient across the medium, the total supply of nutrients, and the

adequate control of pH. For optimum growth of cell monolayer, the fluid phase should be about 1 cm in depth and represent 10-30% of the total volume of the culture vessel (36). Cells usually start to settle immediately after they are suspended in growth medium, and irreversible attachment to the culture vessel wall usually occurs within the first hour. To ensure uniform settling of cells, cultures should always be placed in a level position. In primary cultures the initial single cells tend to die while most active proliferation is initiated by the cell clumps. In fact, most primary cultures set with a high proportion of single-cells usually grow poorly.

Chick embryo fibroblasts (CEF) are a fast growing strain and monolayers should be formed 48-56 hours after incubation. For optimum growth it is advisable to add 5% chicken serum and 5% chick embryo extract. The serum should be heat inactivated to eliminate any infectious avian leukosis virus before use. CEF tends to degenerate in a short time so a fresh primary culture should be prepared for each experiment. CEF is very sensitive and is thus used most often for the propagation and titration of arboviruses. Results of the WEE titration are shown in Table 25.

WEE virus belongs to the group A arboviruses which by definition are those viruses which harbor in certain arthropods and are transmitted to man and other vertebrates. This definition specifically excludes those agents which are transmitted mechanically by anthropods and do not multiply in the tissue of the latter. WEE virus multiplies readily in both chick and duck embryo fibroblasts but cellular

Table 25. Titration of WEE virus by plaque assay.

Data:

Dilution	Plaque Count (pfu) 1	2	Average (pfu)
10^{-4}	N.C*	N.C.*	--
10^{-5}	149	169	158
10^{-6}	69	75	72
10^{-7}	9	3	6
10^{-8}	2	0	1

* Not countable.

Calculation:

0.2 ml of 10^{-5} viral solution contained 158 pfu

0.02 ml of 10^{-6} viral solution contained 72 pfu

0.002 ml of 10^{-7} viral solution contained 6 pfu

0.0002 ml of 10^{-8} viral solution contained 1 pfu

Therefore 0.2222 ml of viral solution contained 227 pfu.

Therefore the virus titer (pfu/ml) is:

$$227 \times 1/0.2222 = 1.02 \times 10^{8} \text{ pfu.}$$

destruction is frequently incomplete and cytopathic effects may be poorly if at all visible; thus, the plaque technique is more useful than the insulation of conventional tube cultures. Hemagglutinins are produced by most but not all arboviruses.

No single complement-fixing or other antigen is common to the entire arbovirus group. Primary grouping of the agents is based upon the hemagglutination-inhibition (HAI) test; four major groups are recognized: A, B, C, and Bunyamwera. Further subdivision of these main groups is possible by means of complement-fixation (CF) and neutralization tests. At least nine other minor groups are recognizable, each group consisting of 2 to 4 members. In addition, a large number of arboviruses exist whose relationships are uncertain at the present time.

In standard HAI and CF tests, cross reactions between groups limit the usefulness of standard test procedures. Cross reactions are also evident in neutralization tests but to a much lesser extent. The identification of a single agent is faciliated by using the plaque-inhibitation test. The determination of serum antibodies against the arboviruses is similarily tedious. Tests are often unreliable due to cross reactions between serotypes. Recently a method was developed to determine arboviruses or their antibodies. This is the radioimmunoprecipitation test (11, 23) which has the sensitivity of the plaque-inhibition test but offers much more rapid results. Like all immunoprecipitation systems, the sensitivity and specificity of this test depends upon the purity, specificity and concentration of labeled

antigens. The RIP test is based on the precipitation test; only the standard WEE virions are radioactively labeled with ^{125}I and anti-mouse Ig serum is added to enhance the precipitation of the antigen-antibody complex. Adequate controls are necessary to ensure the success of this test. Although this test does not allow the study of the formation rate of antibodies, it provides a rapid, specific and sensitive test to detect the overall antibody production from the serum of an animal. This test was used to study the kinetics of anti-WEE antibody formation in mice and the results are shown in Table 26 and Figure 20.

Table 26. Detection of WEE-antibody formation by RIP.

Time (days)	Counts Per Minute		Ratio of Precip./Super.
	Precipitate	Supernatant	
1	2457	2561	1
2	2536	2713	1
3	2497	2585	1
4	2564	1976	1.22
5	3764	1751	2.12
6	3785	1270	2.92
7	3274	994	3.31
8	3662	976	3.75
10	2642	803	3.52
16	3819	2400	1.59
Controls			
a. WEE* virus + Tris buffer	2371	2643	
b. WEE* virus + anti-mouse Ig serum	2530	2715	
c. WEE* virus + anti-mouse Ig serum + normal mouse serum	2458	2441	

* - ^{125}I labeled

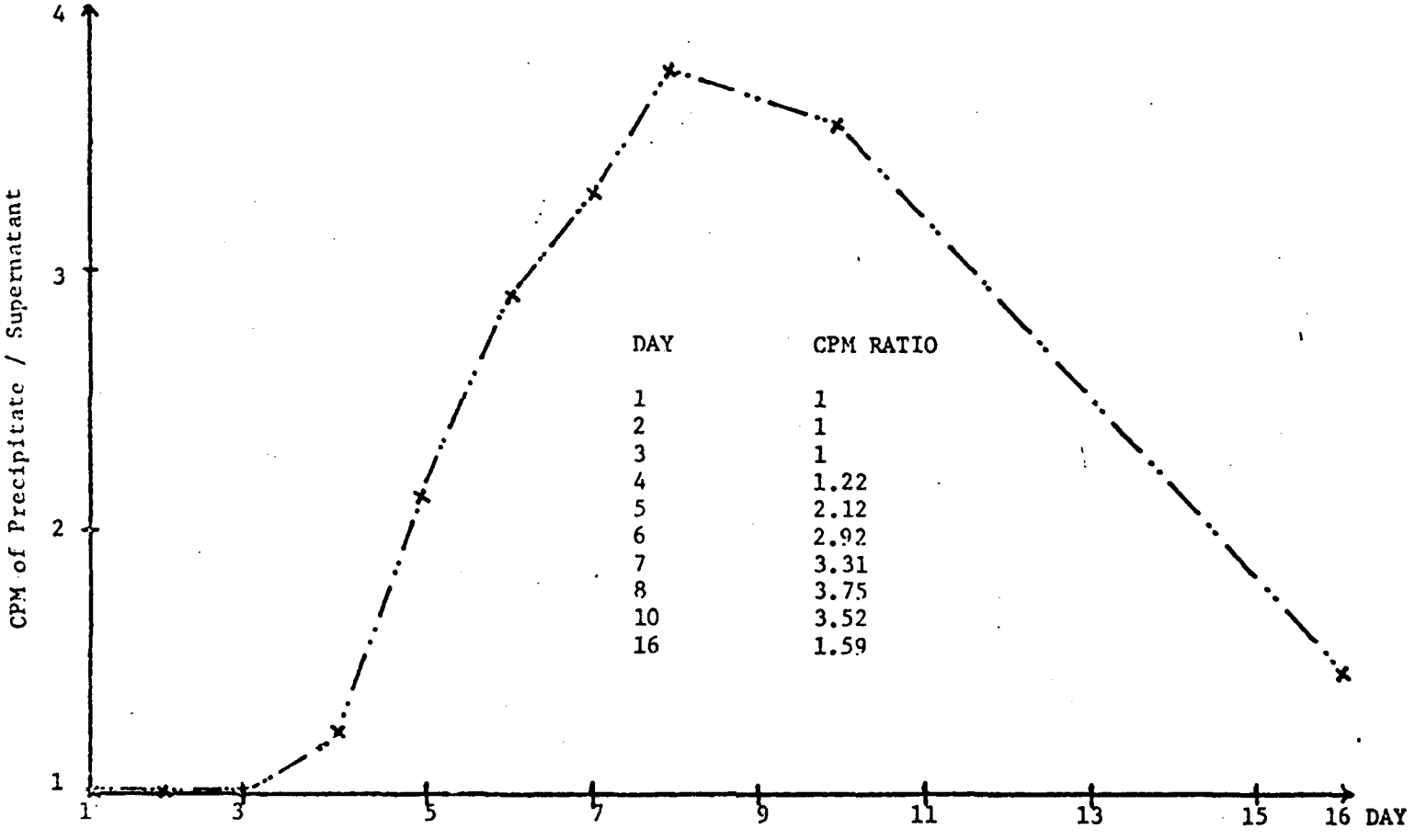

Figure 20. Detection of anti-WEE antibody formation by RIP test. Radioactivity (CPM) in supernatant represents I-125 labeled WEE viral particles and CPM in the precipitate represents the WEE antigen-antibody complex

Simulation Data

The above experimental values and some other theoretical and literary values are used as input data to test the model. The standard conditions set to simulate the immune response curve in Figure 20 are shown in Table 27. Results indicate that the number of IgM ABFC in the primary response is in good agreement with the findings of Hege and Cole (32), and the kinetics of IgG antibody formation in both primary and secondary responses are very similar to the finding of Adler (2) working with Venezuelan equine encephalitis (VEE) virus. The rate of production of an antibody molecule of either IgM or IgG is most controversial; it ranges from 0.5 to 20,000 molecules per cell per sec (18, 35). Since it may be true that the antibody production rate varies with factors such as time, species of animal hosts, and other microenvironmental conditions such as the physiological condition of the animal, the immunogenic characteristics of the antigen and the previous immunological experience of the host, a value of 2.52×10^6 molecules per cell per hour was chosen arbitrarily.

It is obvious that the kinetics of antibody formation are different with each host-antigen system (8, 76, 77, 78) but certain parameters and the steps of component interaction should not be too far off from each system. It should be emphasized that this model in its present condition is only valid for the mouse-WEE system. If other systems are used to test this model, the standard conditions have to be changed. The influences of mouse weight and the dose of antigen to other parameters of this model are shown in Table 28. The simulated

Table 27. Standard conditions of the immune response model

Description	Value
Mouse weight (gm)	30
Average radius of lymphocyte (u)	3.5
Average density of lymphocyte (gm/ml)	1.08
Primary dose of antigen (pfu/ml)	1.2×10^7
Secondary dose of antigen (pfu/ml)	1.0×10^7
Elimination rate of WEE virus (%/hr)	10
Elimination rate of the effective portion of WEE virus (%/hr)	1.2
Latent period for ICC to become IAC (hr)	20
Latent period for IAC to become ABFC	20
Cell generation time (hr)	12.5
Life span of ABFC (hr)	48
Maximum number of successive divisions an ABFC precursor could undergo (number of generations)	9

Simulated values of the number of lymphocytes present in the two compartments of a 30 gm mouse

Description	Lymphoid tissues	Blood	Total
Weight (gm)	0.6	-	-
Volume (ml)	-	2.4	-
Lymphocyte (no.)	6.19×10^7	1.28×10^8	1.9×10^8
T cell (no.)	3.74×10^7	1.03×10^8	1.4×10^8
B cell (no.)	2.44×10^7	2.57×10^7	5.0×10^7
WEE specific T cell	3.74×10^3	1.03×10^3	1.4×10^4
WEE specific B cell	2.44×10^3	2.57×10^3	5.0×10^3
WEE specific ICC	6.18×10^3	3.60×10^3	1.9×10^4

Table 28. The effect of mouse weights on the number of lymphocytes

Values are simulated under standard conditions

Mouse weight (gm)	Number			WEE specific		
	T cell $X10^8$	B cell $X\ 10^7$	Total $X10^8$	ICC $X10^4$	B cell	ABFC
24.5	1.14	4.10	1.55	1.55	4092	739
26.5	1.24	4.43	1.68	1.68	4426	759
28.5	1.33	4.76	1.80	1.80	4760	772
30.5	1.42	5.10	1.93	1.93	5094	785
32.5	1.52	5.43	2.06	2.06	5428	796
34.5	1.60	5.76	2.19	2.19	5762	807
36.5	1.70	6.10	2.31	2.31	6096	817

Effect of primary dose of antigen on the number of ABFC precursors

Values are simulated under standard conditions

Dose (pfu/ml)	Virgin cell	LZT cell	ABFC	HZT cell
		Fraction		
1.2×10^5	0.532	0.808	0.468	5×10^{-5}
1.2×10^6	0.388	0.755	0.612	4.4×10^{-4}
1.2×10^7	0.283	0.640	0.716	1.8×10^{-4}
1.2×10^8	0.207	0.532	0.792	5.4×10^{-3}
1.2×10^9	0.0014	0.024	0.466	0.98
		Number of cell		
1.2×10^5	511	775	449	-
1.2×10^6	396	770	612	-
1.2×10^7	309	699	782	-
1.2×10^8	244	621	924	6
1.2×10^9	2	30	574	1209

data of the standard immune response curve in the primary IgM response are shown in Table 29 and Figures 21 and 22; the IgG response in both primary and secondary responses is shown in Table 30 and Figures 23 and 24.

It is worthwhile mentioning that the kinetics of an immunological response to various viral antigens are somewhat peculiar. The immune response of guinea pigs to phage ϕ X 174 is detectable as early as one day after antigenic challenge (77). Another peculiar example is that the immune response of humans to yellow fever viral vaccine is predominately an IgM antibody response which persists for months with a high titer of circulating antibody. Only after repeated vaccinations over a long period of time will a dominant IgG response occur, and even then the titer of IgG antibody does not go beyond the previous IgM level (55).

Table 29. Computer output on the number of ABFC formed and the number and monograms of IgM antibody molecules formed in a primary response.

Time (hr)	ABFC (No.)	IgM (molecules)	IgM (nanogram)
0	0.	0	0
48	0.57	1.90×10^{7}	0.0284
96	11.	1.35×10^{9}	2.02
144	194.	1.08×10^{10}	3.63
192	31127.	3.76×10^{12}	569.0
240	17152.	4.20×10^{11}	627.8
288	9534.	9.68×10^{11}	333.45
336	5326.	2.81×10^{11}	133.26
384	2983.	2.65×10^{11}	113.96
432	1672.	8.59×10^{10}	128.4
480	940.	7.59×10^{10}	134.0
528	528.	3.05×10^{10}	45.5
576	297.	2.25×10^{10}	33.6
624	0.	0	0

COMPUTER SIMULATED DATA C .....No. of IgG ABFC

A ——————No. of IgM ABFC

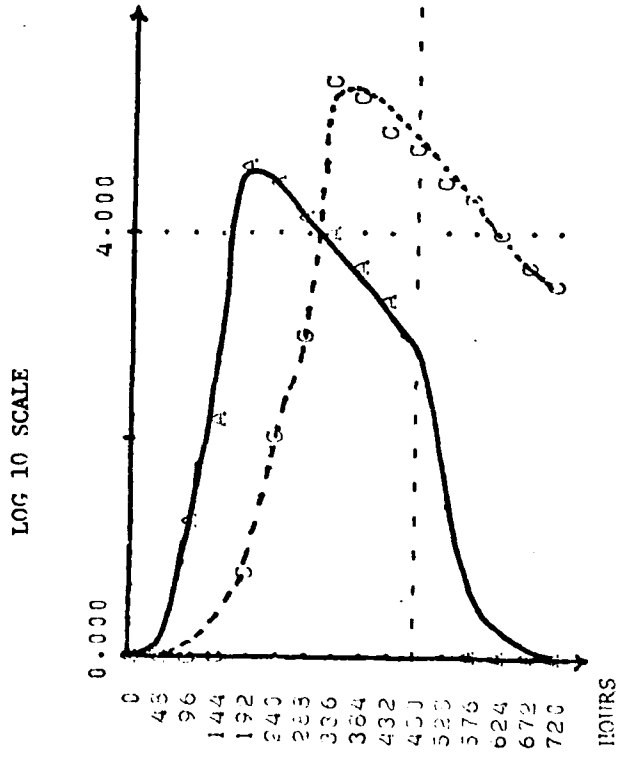

Figure 21. Standard curves of IgM and IgG antibody forming cells formed in MEE hyperimmunized in a primary immune response.

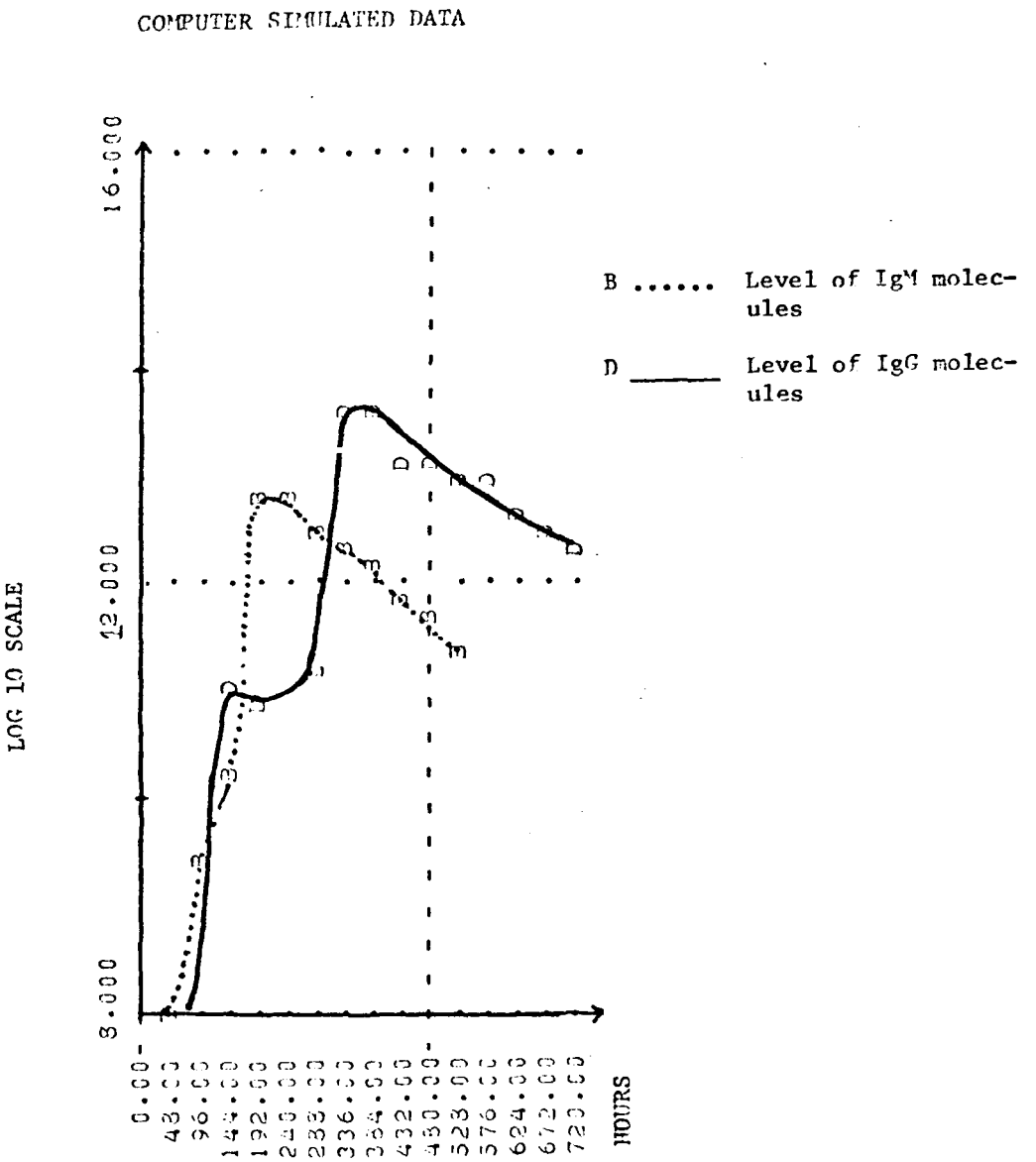

Figure 22. Standard curves of IgM and IgG antibody formation in hyperimmunized (against DNP) mice in a primary immune response.

Table 30. Computer output on the number of ABFC formed and the number and monograms of IgG antibody molecules formed in both primary and secondary immune response.

Time (hr)	ABFC (No.)	IgG (molecules)	IgG (nanogram)
0	0.	0	0.0
48	0.	0	0.0
96	0.	0	0.026
144	0.5	9.6×10^{7}	0.289
192	35.5	4.3×10^{9}	1.42
240	1298.	3.6×10^{10}	9.64
288	98666.	7.1×10^{12}	7311.
336	35468.	4.0×10^{12}	3874.
384	33023.	2.2×10^{12}	3104.
432	16882.	1.2×10^{12}	584.
480	9456.	6.9×10^{11}	327.
528	5306.	3.9×10^{11}	186.
576	2979.	2.2×10^{11}	101.
624	1168.	1.23×10^{11}	57.9
672	940.	1.2×10^{11}	32.5
720	70414.	1.28×10^{13}	260.
768	80415.	1.267×10^{13}	11365.
816	100592.	1.269×10^{13}	11700.
864	100592.	1.269×10^{13}	11700.
912	100592.	1.269×10^{13}	11700.
960	100592.	1.269×10^{13}	11700.

COMPUTER SIMULATION DATA

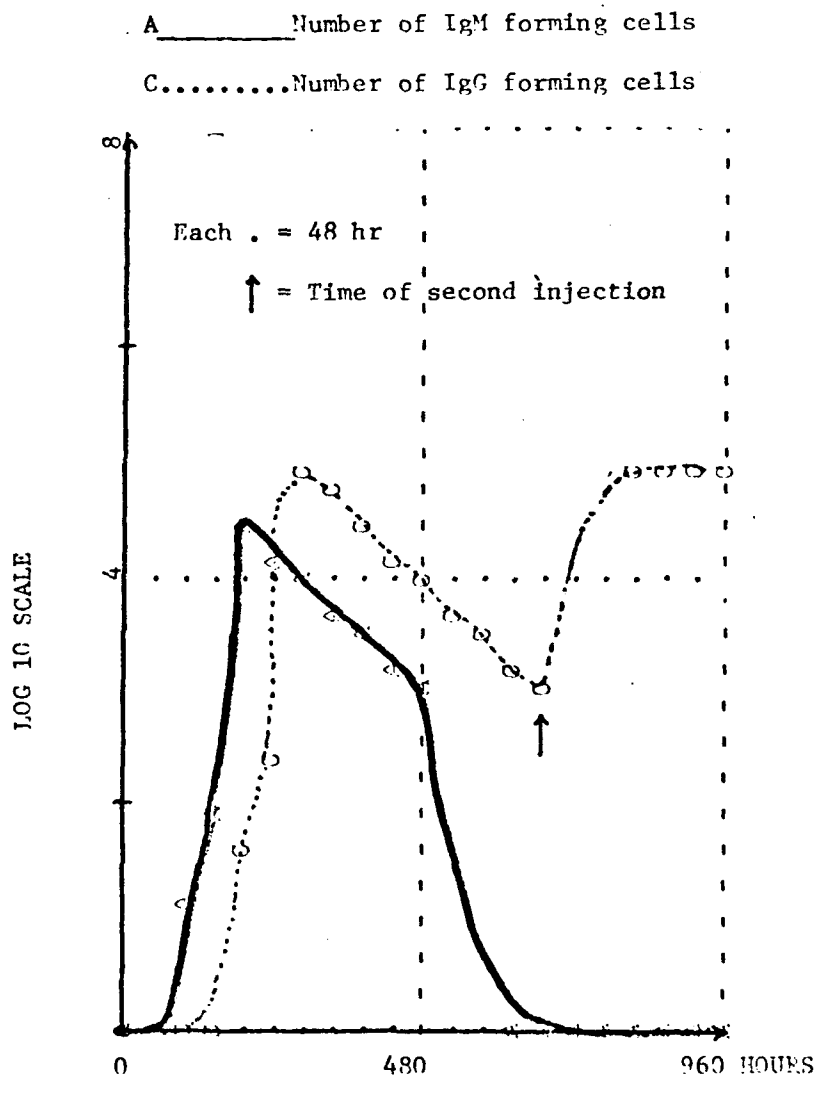

Figure 23. Standard curves of IgM and IgG antibody forming cells in both primary and secondary immune responses

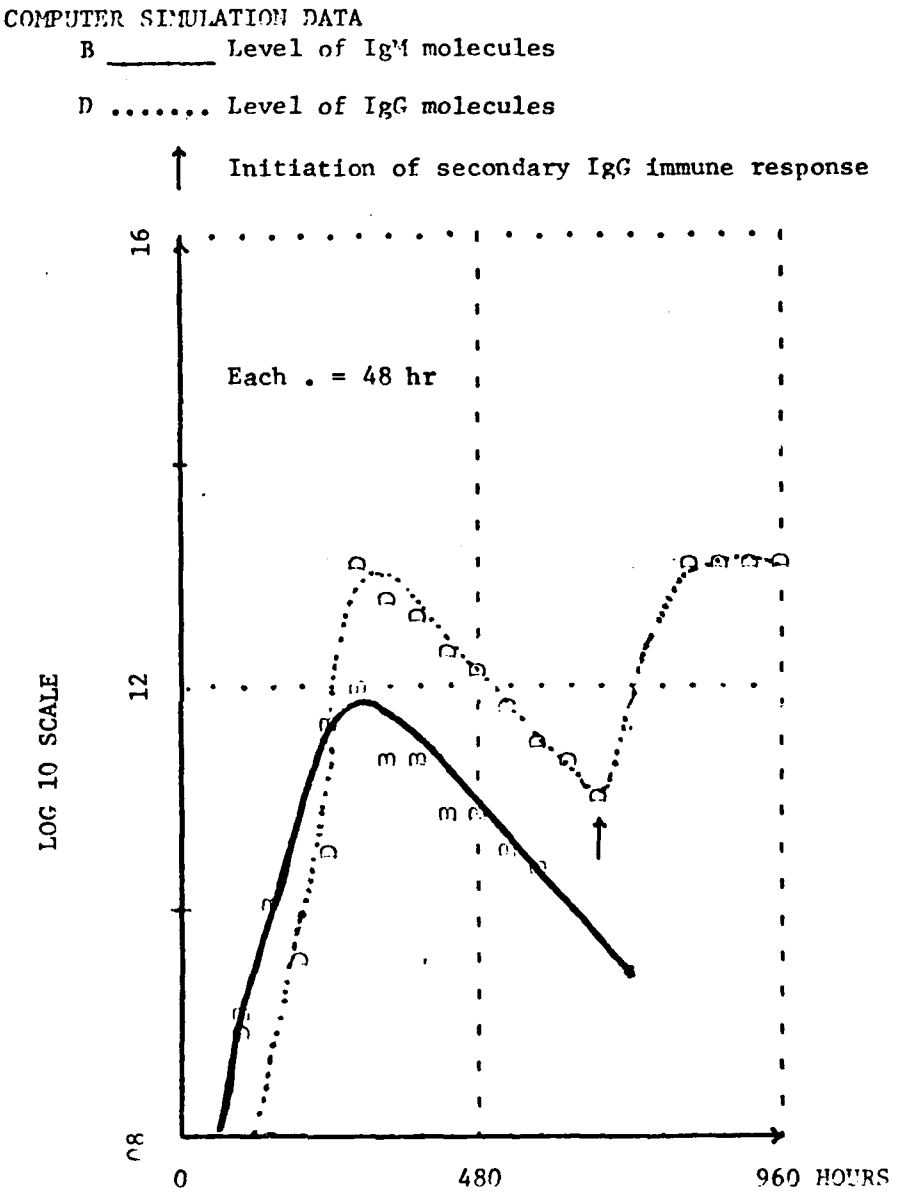

Figure 24. Standard curves of IgM and IgG antibody formation in both primary and secondary immune responses

CONCLUSIONS

Studies on 9-12 week old C_3HSW strain mice reveal that the average body weight is about 30 grams and the size of the small lymphocytes is in the area of 7 μ in diameter corresponding to an average volume of 177 μ^3. Volume profile studies of a lymphocyte culture in vitro reveal that a blood lymphocyte population is heterogeneous in nature. It consists of cells of diameters ranging from around 6.5 μ to 12 μ, and only cells belonging to the 6.5-8.5 μ size range could undergo successive divisions. Studies on the increase of cell concentration of this lymphocyte culture show that there is a linear exponential growth phase which initiates at about 24 hr after incubation and extends beyond 76 hr. The average generation time is about 12.5 hr. Studies on the elimination rate of passively injected ^{125}I labeled WEE virus and ^{125}I labeled mouse IgG indicate that the biological degradation rate of this virus is 10% per hour, and the catabolic rate of mouse IgG is directly proportional to the concentration of the Ig level in the circulatory system of mice. The biological half-life of mouse IgG is about 3.7 days in normal mice and about 2.5 days in WEE hyperimmunized mice. These results coincide with the findings of Fahey (26, 27) and of Uhr (76). The detection of anti-WEE antibody formation by the RIP test shows that antibody level becomes detectable 4 days after antigenic challenge. This level reaches the peak 8 days after injection, then starts to level off after 10 days. Compared with the literature value on a similar experiment (2), it is conclusive

that the result represents a typical primary IgM response curve.

Study of this model through computer simulation leads to the conclusion that the simulated and experimental data are closely paralled to each other in both primary and secondary responses under the following defined conditions:

1. The latent period for ICC to become IAC is 20 hr.
2. The latent period for IAC to become ABFC is 20 hr.
3. The life span of ABFC is 48 hr.
4. The maximum number of generations that a precursor cell would undergo is 9 generations.
5. The effective portion of a given dose of antigen varies with the concentration of the antigen but is always less than 1%.
6. The elimination rate of this effective portion of a given dose of antigen is very slow and is found to be about 1.2 %/hr.
7. Optimal dosage for immunization is found to be in the range of 1.0×10^7 to 1.0×10^8 pfu of virus.
8. The number of IgG precursors in a primary response is 1/30 of the number of IgM ABFC at the peak of antibody production.

The uniqueness of this model is that it embodies a lot of information concerning an immunological response. This model simulates a whole series of events starting from the animal host itself and describes in full detail the various components and steps involved in an immune response. As in any simulation models, the conditions predicted may and may not be true but it provides a way to acquire

information that could not be obtained otherwise. No model is perfect in itself and both the numbers and the value of the standard conditions should be changed if new evidence arises and new values are available in the future.

APPENDIX

Table 1. COULTER COUNTER PROGRAM

```
10 COM A,Z,S,D$[32],DS[3,50]
20 REM: COULTER COUNTER PROGRAM
30 DIM TS[9,50],CS[3,50],MS[3],SS[3]
40 DIM A$[5],C$[5],Q$[110],P$[110]
50 DIM T$[160],H$[100],B$[3]
60 REM: RUN SECTION
70 REM
80 X=0
90 C$="12345"
100 FOR I=1 TO 110
110 Q$[I,I]=" "
120 NEXT I
130 Q$[,1]="+"
140 DISP "ENTER TITLE: 5 LINES <=32 SPACES";
150 FOR I=1 TO 5
160 INPUT T$[I*32-31,I*32]
170 NEXT I
180 DISP "ENTER # OF DATA SETS: <=5  ";
90 INPUT N
200 DISP "DO YOU WANT CHANNEL DIFFERENCES";
20 INPUT B$
220 DISP "ENTER HEADINGS: <=20 SPACES  ";
230 FOR I=1 TO N
240 INPUT H$[I*20-19,I*20]
250 NEXT I
260 DISP "ENTER FIRST AND LAST THRESHOLD #   ";
270 INPUT A0,Z0
280 DISP "ENTER APERTURE SETTING  ";
290 INPUT A8
300 DISP "ENTER ATTENUATION SETTING  ";
310 INPUT A9
320 C4=0
330 DISP "DO YOU WISH TO SET THE SCALE ";
340 INPUT A$
350 IF A$="NO" THEN 420
360 C4=1
370 DISP "ENTER YMAX FOR CHANNEL PLOT ";
380 INPUT Y
390 IF B$="NO" THEN 420
400 DISP "ENTER YMIN,YMAX FOR DIFF. PLOT ";
410 INPUT Y0,Y9
420 FOR I= TO N
430 DISP "ENTER FIL # FOR DATA SET #";I;
440 INPUT S[I]
450 NEXT I
460 FOR I= TO N
470 LOAD  DATA S[I]
```

COULTER COUNTER PROGRAM (Cont')

```
480 J=0
490 J9=(A0-A)/S
500 FOR J0=A0 TO Z0 STEP S
510 J=J+1
520 J9=J9+1
530 FOR K=1 TO 3
540 T[3*I-+K,J]=D[K,J9]
550 NEXT K
560 NEXT J0
570 NEXT I
580 REM
590 REM COMPUTE CHANNEL COUNTS
600 REM
610 A=A0
620 Z=Z0
630 X=0
640 FOR I= TO N
650 T=0
660 FOR T0=A TO Z-1 STEP S
670 T=T+1
680 M1=(T[3*I-2,T]+T[3*I-1,T]+T[3*I,T])/3
690 M2=(T[3*I-2,T+1]+T[3*I-1,T+1]+T[3*I,T+1])/3
700 C[I,T]=M1-M2
710 IF X >= C[I,T] THEN 730
720 X=C[I,T]
730 NXT T0
740 NEXT I
750 REM
760 RM PRINT DATA
770 C=0
780 FOR C0=A TO Z STEP S
790 C=C+1
800 IF (C-)/12=INT((C-)/2) THEN 820
810 GOTO 840
820 GOSUB 2360
830 PRINT H$,LIN1
840 K=
850 FOR I= TO N
860 C1=T[K,C]
870 C2=T[K+1,C]
880 C3=T[K+2,C]
890 M[I]=(C1+C2+C3)/3
900 S[I]=(((C1-M[I])^2+(C2-M[I])^2+(C-M[I])^2)/2)^0.5
910 K=K+3
920 NEXT I
930 FOR I=1 TO N
940 WRITE (15,950)C0,T[3*I-2,C],M[I];
```

```
950 FORMAT F4.0,X,2F6.0,3X
960 NEXT I
970 PRINT
980 FOR I=1 TO N
990 WRITE (15,1000)T[*I-1,C],S[I];
1000 FORMAT 5X,F6.0,F6.,3X
1010 NEXT I
1020 PRINT
1030 FOR I=1 TO N
1040 IF M[I]=0 THEN 1070
1050 S1=00*S[I]/M[I]
1060 GOTO 1080
1070 S1=0
1080 WRITE (15,1090)T[3*I,C],S;
1090 FORMAT 5X,F6.0,F5.1,"%",X
1100 NEXT I
1110 PRINT
1120 IF C0=Z THEN 1230
1130 FOR I=1 TO N
1140 IF I= THEN 1190
1150 IF D$= NO" THEN 190
1160 WRITE (15,1170)C[I,C],C[I,C]-C[,C];
1170 FORMAT 2X,2F6.0,6X
180 GOTO 1210
190 WRITE (15,1200)C[I,C];
1200 FORMAT 2X,F6.0,12X
1210 NEXT I
1220 PRINT
1230 NEXT C0
1240 REM
1250 REM PLOT CHANNEL COUNTS
1260 REM
270 GOSUB 2360
1280 PRINT LIN3
1290 IF C4=1 THEN 1310
1300 Y=X
1310 Y=Y/100
1320 PRINT TAB15,"0";
1330 FOR J=1 TO 10
1340 WRITE (15,1350)J*Y*10;
1350 FORMAT 2X,F8.0
1360 NEXT J
1370 PRINT
1380 WAIT 333
1390 PRINT TAB15,"+";
1400 FOR I= TO 10
1410 WRITE (15,1420)"---------+";
```

```
1420 FORMAT F1.0
1430 NEXT I
1440 PRINT
1450 C=0
1460 FOR C0=A TO (Z-1) STEP S
1470 C=C+
1480 P$=Q$
1490 M=0
1500 FOR I= TO N
1510 P=C[I,C]/Y+
1520 IF P >= 1 THEN 1540
1530 P=1
1540 P$[P,P]=C$[I,I]
1550 IF M>P THEN 1570
1560 M=P
1570 NEXT I
1580 V=C0*A8*A9*0.09
1590 D=((6*V)/PI)^(1/3)
1600 WRITE (15,1610)D,V
1610 FORMAT F7.2,F7.1,1X,"+"
1620 WRITE (15,1630)C0,P$[I,M]
1630 FORMAT 6X,F3.0,6X,F1.0
1640 NEXT C0
1650 V=C0*A8*A9*0.09
1660 D=((6*V)/PI)^(/3)
1670 WRITE (15,1610)D,V
1680 IF B$="NO" THEN 2350
1690 REM
1700 REM FIND DIFFERENCS FROM CONTROL
1710 X=Y=0
1720 FOR I=2 TO N
1730 C=0
1740 FOR C0=A TO (Z-1) STEP S
1750 C=C+1
1760 C[I,C]=C[I,C]-C[1,C]
1770 NEXT C0
1780 NEXT I
1790 FOR I= TO (N-1)
1800 C=0
1810 FOR C0=A TO (Z-1) STEP S
1820 C=C+1
1830 C[I,C]=C[I+1,C]
1840 IF X >= C[I,C] THEN 1860
1850 X=C[I,C]
1860 IF Y <= C[I,C] THEN 1880
1870 Y=C[I,C]
1880 NEXT C0
```

```
1890 NEXT I
1900 IF C4=1 THEN 1930
190 Y0=Y
1920 Y9=X
1930 S1=(Y9-Y0)/100
1940 REM
1950 REM PLOT DATA
1960 REM
1970 GOSUB 2360
980 PRINT LIN3
1990 Q=ABS(Y0/S1)+1
2000 Q$[1,1]="+"
2010 Q$[Q,Q]="+"
2020 PRINT TAB6;
2030 FOR J=0 TO 100 STEP 10
2040 WRITE (15,2050)Y0+J*S;
2050 FORMAT 2X,F3.0
2060 NEXT J
2070 PRINT
2080 PRINT TAB14,"+";
2090 FOR I=1 TO 10
2100 WRITE (5,2110)"---------+";
2110 FORMAT F1.0
2120 NEXT I
2130 PRINT
240 C=0
2150 FOR C0=A TO (Z-1) STEP S
2160 C=C+1
2170 P$=Q$
2180 M=Q
2190 FOR I= TO (N-1)
2200 P=(C[I,C]/S1)+Q
2210 P$[P,P]=C$[I,I]
2220 IF M>P THEN 2240
2230 M=P
2240 NEXT I
2250 V=C0*A8*A9*0.09
2260 D=((6*V)/PI)^(1/3)
2270 WRITE (15,2280)D,V
2280 FORMAT F7.2,F7.1,1X,"+"
2290 WRITE (15,2300)C0,P$[,M]
2300 FORMAT 6X,F3.0,6X,F1.0
2310 NEXT C0
2320 V=C0*A8*A9*0.09
2330 D=((6*V)/PI)^(1/3)
2340 WRITE (15,2280)D,V
2350 END
```

COULTER COUNTER PROGRAM (Cont')

```
2360 PRINT WBYTE12
270 WAIT 3333
2380 PRINT LIN3
2390 FOR I=1 TO 5
2400 PRINT SPA5,T$[I*32-31,I*32]
2410 NEXT I
2420 PRINT
2430 RETURN
```

DATA STORAGE

```
10 COM A,Z,S,D$[2],DS[3,50]
20 DIM A$[5]
30 DISP " ENTER OR LIST     ";
40 INPUT A$
50 IF A$="ENTER" THEN 80
60 IF A$="LIST" THEN 340
70 GOTO 30
80 MAT D=ZER
90 DISP "ENTER FILE FOR DATA STORAGE ";
100 INPUT F
110 DISP "ENTER DATA DESCRIPTION <= 32CHAR";
120 INPUT D$
130 DISP "ENTER FIRST AND LAST THRESHOLD ";
140 INPUT A,Z
150 DISP " ENTER THRESHOLD STEP ";
60 INPUT S
170 T0=1
180 FOR T=A TO Z STEP S
190 DISP "ENTER 3 COUNTS FOR T#";T;
200 INPUT D[1,T0],D[2,T0],D[,T0]
20 T0=T0+1
220 NEXT T
230 DISP " ENTER # OF CORRECTIONS ";
240 INPUT C
250 FOR I=1 TO C
260 DISP "INPUT T#, READING#, & COUNT ";
270 INPUT T,C,D[C,T/S]
280 NEXT I
290 STORE  DATA F
300 END
310 REM
320 REM: LISTING SECTION
330 REM
340 DISP "LIST DATA ALSO ";
350 INPUT A$
360 C1=0
370 IF A$="NO" THEN 390
380 C1=1
390 DISP "NTER FIRST & LAST FILE FOR LIST";
```

```
400 INPUT F0,F9
410 L=60
420 FOR I=F0 TO F9
430 LOAD  DATA I
440 L0=5+C1*(1+4*(INT((Z-A-1)/0)+1))
450 L=L+L0
460 IF L<60 THEN 510
470 L=L0
480 PRINT WBYTE12
490 WAIT 1234
500 PRINT LIN2
50 PRINT LIN2,SPA5,"FILE #";I
520 PRINT SPA5,D$
530 WRITE (15,540)A,Z
540 FORMAT 5X,"THRESHOLD",F3.0," TO",F3.0
550 IF C1=0 THEN 760
560 PRINT
570 T=A
580 PRINT TAB7;
590 FOR K=T TO T+10
600 WRITE (15,610)K;
610 FORMAT F6.0
620 IF K=Z THEN 640
630 NEXT K
640 PRINT
650 FOR J= TO 3
660 PRINT TAB7;
670 FOR K=T TO T+10
680 WRITE (15,690)D[J,K];
690 FORMAT F6.0
700 IF K=Z THEN 720
710 NEXT K
720 PRINT
730 NEXT J
740 T=T+11
750 IF T <= Z THEN 580
760 NEXT I
770 END
```

Table 2. HISTOGRAM PROGRAM

START KEY # 0

```
10 DIM A[50]
20 FOR I=1 TO 50
30 A[I]=0
40 NEXT I
45 PRINT "HISTOGRAM"
50 S1=S2=S3=S4=N=R3=R4=R5=T1=0
60 R1=1E+99
70 R2=-R1
80 DISP "ENT 1 FOR HISTOGRAM";
90 INPUT S5
100 IF S5#1 THEN 165
110 DISP "OFFSET =";
120 INPUT O
121 PRINT "OFFSET= "O
130 DISP "CELL WIDTH";
140 INPUT C
145 PRINT "CELL WIDTH = "C
160 B=50
165 DISP "ENT 1 TO PRINT DATA";
170 INPUT D
180 IF D=0 THEN 200
190 PRINT "DATA"
200 DISP "PRESS DATA ENTRY KEY";
210 END
```

DATA ENTRY KEY # 1

```
10 DISP "X("N+1")=";
20 INPUT X
50 Z=FNX(1)
60 GOTO 10
70 END
```

DELETE KEY # 2

```
10 DISP "DELETE X =";
20 INPUT X
30 PRINT "DELETE:";
41 T1=1
50 Y=FNX(-1)
60 END
```

BASIC STATISTICS KEY # 5

```
10 M=S1/N
20 S=SQR((S2-M*M*N)/(N-1))
30 M3=S3/N-3*M*S2/N+2*M^3
40 M4=S4/N-4*M*S3/N+6*(M^2)*S2/N
50 M4=M4-3*M^4
60 FORMAT F12.4,/,F12.4,/,F12.4,/,F12.4
65 PRINT
70 PRINT "N="N
80 WRITE (15,60)"MEAN="M,"STD.DEV="S,"SKEWNESS="M3/S^3
111 IF T1=0 THEN 120
112 PRINT "MIN,MAX,RANGE MAY BE INCORRECT"
120 WRITE (15,60)"XMIN="R1,"XMAX="R2,"RANGE="R2-R1
150 IF R3=0 THEN 170
160 PRINT "NO. TOO SMALL="R3
170 IF R4=0 THEN 190
180 PRINT "NO. TOO LARGE="R4
190 FOR J=1 TO 10
200 PRINT
210 NEXT J
220 END
```

HISTOGRAM KEY # 6

```
10 P=1
20 W=FNY (1)
30 END
```

HISTOGRAM/PLOT KEY # 7

```
10 P=1
20 W=FNY(1)
30 END
```

HISTOGRAM PROGRAM (Cont')

BASIC STATISTICS KEY # 5

```
10 M=S1/N
20 S=SQR((S2-M*M*N)/(N-1))
30 M3=S3/N-3*M*S2/N+2*M^3
40 M4=S4/N-4*M*S3/N+6*(M^2)*S2/N
50 M4=M4-3*M^4
60 FORMAT F12.4,/,F12.4,/,F12.4,/,F12.4
65 PRINT
70 PRINT "N="N
80 WRITE (15,60)"MEAN="M,"STD.DEV="S,"SKEWNESS="M3/S^3
111 IF T1=0 THEN 120
112 PRINT "MIN,MAX,RANGE MAY BE INCORRECT"
120 WRITE (15,60)"XMIN="R1,"XMAX="R2,"RANGE="R2-R1
150 IF R3=0 THEN 170
160 PRINT "NO. TOO SMALL="R3
170 IF R4=0 THEN 190
180 PRINT "NO. TOO LARGE="R4
190 FOR J=1 TO 10
200 PRINT
210 NEXT J
220 END
```

HISTOGRAM KEY # 6

```
10 P=1
20 W=FNY (1)
30 END
```

HISTOGRAM/PLOT KEY # 7

```
10 P=1
20 W=FNY(1)
30 END
```

CELL STATISTICS KEY # 8

```
10 PRINT
11 FORMAT F5.0,F12.4,F11.0,F17.5
12 PRINT "CELL#";"   LOWER LIMIT";
13 PRINT TAB18;"   NO. OF OBS";"  %RELATIVE FREQ"
30 Y=FNC(1)
40 FOR I=1 TO B
45 WRITE (15,11)I,O+(I-1.5)*C,A[I],100*A[I]/N
50 NEXT I
60 FOR J=1 TO 10
70 PRINT
80 NEXT J
90 END
```

(FNX) KEY # 13

```
180 DEF FNX(Z)
182 IF D#1 THEN 190
183 WRITE (15,184)X
184 FORMAT F12.4
190 IF X>R1 THEN 210
200 R1=X
210 IF X<R2 THEN 230
220 R2=X
230 N=N+Z
240 S1=S1+X*Z
250 Y=X*X
260 S2=S2+Y*Z
270 Y=Y*X
280 S3=S3+Y*Z
290 Y=Y*X
300 S4=S4+Y*Z
310 IF S5#1 THEN 400
320 Y=INT((X-O)/C+1.5)
330 IF Y<1 THEN 370
340 IF Y>B THEN 390
350 A[Y]=A[Y]+Z
360 GOTO 400
370 R3=R3+Z
380 GOTO 400
390 R4=R4+Z
400 RETURN 0
```

(FNY) KEY # 15

```
 10 DEF FNY(X)
 11 FOR I=1 TO 50
 12 IF R5>A[I] THEN 14
 13 R5=A[I]
 14 NEXT I
 20 W=2.5*R5/N
 30 U=(N*C/(2.5066*S))*(40/R5)
 40 FORMAT 2F5.2
 45 PRINT
 46 PRINT
 50 WRITE (15,40)"EACH X ="W;"  PERCENT"
 60 PRINT
 70 PRINT
 75 Y=FNC(1)
 80 FOR I=1 TO B+1
 90 Y=O+(I-1.5)*C
100 FORMAT 2F12.4
110 WRITE (15,100)Y" .";
120 IF P=0 THEN 140
130 Z=FNZ(Y)
140 PRINT
145 IF I=B+1 THEN 190
150 Y=Y+0.5*C
160 PRINT TAB13;".";
170 Z=FNP(Y)
180 NEXT I
190 FOR J=1 TO"10
191 PRINT
192 NEXT J
193 END
```

(FNC) KEY # 15

```
 10 DEF FNC(Y)
 20 J=50
 30 IF A[J]#0 THEN 70
 40 J=J-1
 50 GOTO 30
 70 B=J*(J<B)+B*(J >= B)
 80 RETURN 0
```

Table 3. IMMUNE RESPONSE MODEL PROGRAM

```
10 RMARK: IMMUNE RESPONSE MODEL: DATA INPUT & CALC, FILE#0
20 DIM DS[150,12],PI[6],P5[6],G5[11],O5[02],Q5[02],H5[07],XI[6]
30 DIM AI[3,2]
40 MAT D=ZER
50 A[1,1]=0
60 A[1,2]=A[2,]=1
70 A[2,2]=A[3,1]=6
80 A[3,2]=7
90 GOTO 840
100 REM: MEAN ABFC
110 DEF FNZ(T)
120 G3=(G-1)*T8
130 G4=G*T8
140 IF T >= T3+G THEN 160
150 RETURN 0
160 G1=XP(L*G3)
170 G2=EXP(L*G4)
180 Q1=-1/E1*(1-1/G1)
190 Q2=-1/*(1-/G2)
200 U1=+G1*3
210 U2=1+G2*E3
220 Z0=2^(G-)*EXP(-A)
230 IF G=G9 THEN 280
240 IF T3+G3 <= T AND T<T3+G4 THEN 310
250 IF T3+G4 <= T AND T<T3+T9+G THEN 70
260 IF T3+T9+G3 <= T AND T<T3+T9+G4 THEN 440
270 GOTO 50
280 IF T3+G3 <= T AND T<T3+T9+G3 THEN 30
290 GOTO 620
300 RM: PART 1 & 5
310 Z1=XP(A1*Q)/Q1
320 Z2=EXP(A1*U1*E0)/U1
330 Z3=EXP(A1*(E2+E0))
340 Z=Z0*(Z1+/E2*(Z2-Z3))
350 RETURN Z
360 RM: PART 2
370 Z1=EXP(A1*Q1)/Q
380 Z2=EXP(A1*Q2)/Q2
390 Z3=EXP(A1*U*E0)/U1
400 Z4=EXP(A1*U2*E0)/U2
410 Z=Z0*(Z1-Z2+/E2*(Z3-Z4))
420 RETURN Z
430 REM: PART 3
440 Z1=/U1
450 Z2=EXP(A1*U1*E0)
460 Z3=EXP(A1*U1*E4)
470 Z4=EXP(A1*(E2+E4))
```

```
450 Z5=XP(A1*U2*E0)/J2
490 Z6=XP(A1*Q2)/Q2
500 Z=Z0 (1/Q2*(Z1*(Z2-Z3)+Z4-Z5)-Z6)
510 RETURN Z
520 REM: PART 4
530 Z1=1/J1
540 Z2=EXP(A1*U1*0)
550 Z=EXP(A1*U1*E4)
560 Z4=1/J2
570 Z5=XP(A1*U2*E0)
580 Z6=EXP(A1*U2*E4)
590 Z=Z0/Q2*(Z1*(Z2-Z3)-Z4*(Z5-Z6))
600 RETURN Z
60 REM: PART 5
620 Z1=EXP(A1*E2)/E2
630 Z2=EXP(A1*E4)-EXP(A1*0)
640 Z3=/(E2*U1)
650 Z4=EXP(A*(1+G*E3*E0))
660 Z5=EXP(A*(1+G1*E3*E4))
670 Z=Z0*(Z1*Z2+Z3*(Z5-Z4))
680 RETURN Z
690 RM: FRACTION
700 DEF FNF(I)
70 Y=0
720 FOR D=A[I,1] TO A[I,2]
730 Y=Y+EXP(-R)*R^D/FNV(D)
740 NEXT D
750 RETURN Y
760 REM: FACTORIAL
770 DF FNV(X)
780 F=1
790 FOR I=1 TO X
800 F=I*F
80 NEXT I
820 RETURN F
830 REM: ENTRY
840 DISP " JEIGHT OF MOUSE IN GRAMS ";
850 INPJT W
860 DISP "LYMPH. RADIUS(U), DENSITY(G/ML)";
870 INPJT R1,D6
880 DISP " 1ST ANTIGEN DOSE (PFU) ";
890 INPUT D0
900 DISP " 2ND ANTIGEN DOSE (PFU) ";
910 INPUT D9
920 DISP "ANTIGEN ELIMINATION RATE (/HOUR)";
930 INPUT L
940 L=0.0012*L
```

```
950 DISP "LATENT PHASE (HOURS) FOR ICC TO BECOME IAC";
960 INPUT T5
970 DISP "LATENT PERIOD  (HOURS) FOR IAC TO BECOME ABFC";
980 INPUT T2
990 DISP "CELL GENERATION TIME (HOURS) ";
1000 INPUT T8
100 DISP " ABFC AB-PRODUCTION (HOURS) ";
020 INPUT T9
1030 DISP " MAX. NO. CELL DIVISIONS";
1040 INPUT G5
1050 DISP "INPUT TIME OF SECOND INJECTION";
1060 INPUT X1
1070 DISP " STEP TIM (HOURS) ";
1080 INPUT H0
090 DISP " LENGTH OF RUN (HOURS) ";
1100 INPUT T7
1110 IF T7 >= 624 THEN 150
1120 DISP "RE-ENTER: MIN. LNGTH 624 HOURS ",
130 GOTO 100
1140 REM: ICC CALC
150 L1=0.02*W
1160 L2=0.02*L1
170 L3=L2/(4.1888*R1^*D6)*E+2
1180 L4=0.0778*W
1190 L5=5.5E+07*L4
1200 V4=0.8*L5
120 B4=0.2*L5
220 C1=0.7*L3
1230 C2=C3=0.5*L3
240 V1=B1=0.5*C1
1250 V2=0.8*C2
1260 B2=0.2*C2
1270 V3=0.9*C3
1280 B3=0.*C3
1290 V=V+V2+V3
100 V5=V+V4
130 B=B1+B2+B3
1320 B5=B+B4
1330 S1=-04*V
1340 S2=E-04*V4
1350 S3=1E-04*B
1360 S4=1E-04*B4
1370 S=S1+S2+S3+S4
1380 REM: FRACT STIM ABFC
1390 IF D0 <= 5E+09 AND D0 >= E+08 THEN 1490
1400 IF D0 <= 1+08 AND D0 >= 1E+07 THEN 1470
1410 IF D0 <= 1E+07 AND D0 >= 1E+06 THEN 1450
```

```
1410 IF D0 <= 1E+06 AND D0 >= 1E+05 THEN 430
1420 F7=0.1*D0
1430 GOTO 500
1440 F7=0.015*D0
1450 GOTO 1500
1460 F7=0.002*D0
1470 GOTO 1500
430 F7=0.00025*D0
1500 R=F7/S
1510 F0=EXP(-R)
1520 F1=FNF1
1530 F2=FNF2
1540 F3=FNF3
1550 F4=F0+F1+F2+F3
1560 M0=(F0/F4)*S
1570 S5=(S3+S4)*((S3+S4)/(S1+S2))
1580 A0=INT((F2/F4)*S5+0.5)
1590 REM: IG-M VS T
1600 T1=T5
1610 G9=G5
1620 H0=0.5*A0
1630 A=0.0025
1640 A1=A/L
1650 I=EXP(L*T)
1660 S2=I-/E1
1670 S=S1-
1680 T3=T1+T2
1690 M0=N=0
1700 FOR T=0 TO 576 STEP H0
1710 E0=EXP(-L*(T-T2))
1720 E4=EXP(-L*(T-T2-T9))
1730 N=N+1
1740 Y=0
1750 FOR G=1 TO G9
1760 Y=Y+FNZ(T)*0.99
1770 NEXT G
780 D[N,1]=T
1790 D[N,2]=Y*A0
1800 IF D[N,2] <= 1 THEN 1820
180 D[N,3]=LGT(D[N,2])
1820 D[N,4]=M0=M0+H0*(2.52E+06*D[N,2]-M0*0.03)
1830 IF D[N,4] <= 1 THEN 1850
1840 D[N,5]=LGT(D[N,4])
1850 NEXT T
1860 A2=A0*D[102/H0,2]*1/0
1870 REM
1880 REM: IG-G VS T
```

IMMUNE RESPONSE MODEL PROGRAM (Con't)

```
1890 T1=T5
1900 G9=G5
190 E=EXP(L*T1)
1920 2=-/E1
1930 E3=E1-
1940 T3=T1+T2
1950 N=INT(96/H0)
1960 FOR T=0 TO 720 STP H0
1970 E0=EXP(-L*(T-T2))
1980 E4=EXP(-L*(T-T2-T9))
1990 N=N+1
2000 Y=0
200 FOR G=1 TO G9
2020 Y=Y+FNZ(T)
2030 NEXT G
2040 D[N,6]=A2*Y
2050 IF D[N,6] <= 1 THEN 2070
2060 D[N,7]=LGT(D[N,6])
2070 D[N,8]=M0=M0+H0*(2.52E+06*D[N,6]-M0*0.02)
2080 IF D[N,8] <=  THEN 2100
2090 D[N,9]=LGT(D[N,8])
2100 NEXT T
2110 REM
220 REM: SECONDARY RESPONSE
210 M7=D[180/H0,2]
2140 M8=M8+M7
2150 W8=(A0+M7)*5
2160 IF D9 <= 1E+07 AND D9 >= E+06 THEN 2190
2170 IF D9 <= 1E+06 AND D9 >= 1E+05 THEN 2210
2180 IF D9 <= 1E+05 AND D9 >= 1E+04 THEN 2230
2190 F8=D9*0.004
2200 GOTO 2240
220 F8=D9*0.03
2220 GOTO 2240
2230 F8=D9*0.1
2240 R=F8/M8
2250 K0=EXP(-R)
2260 K1=FNF1
2270 K2=FNF2
2280 K3=FNF3
2290 K4=K0+K1+K2+K3
2300 A3=(K2/K4)*W8
20 T1=T5
2302 G9=G5
2303 E1=EXP(L*T1)
2304 E2=-1/E1
2305 E3=E1-
```

IMMUNE RESPONSE MODEL PROGRAM (Con't)

```
2306 T3=T+T2
230 N=INT(X1/H0)
2320 FOR T=X1 TO T7 STEP H0
2330 N=N+1
2331 Y=0
2332 FOR G= TO G9
2333 Y=Y+FNZ(T)*0.99
2334 NEXT G
2340 D[N,6]=(A3+A2)*Y
2360 IF D[N,6] <= 1 THEN 2380
2370 D[N,7]=LGT(D[N,6])
2380 D[N,8]=M0=M0+1.2E+0+H0*(2.52E+06*D[N,6]-M0*0.02)
2390 IF D[N,8] <= 1 THEN 240
2400 D[N,9]=LGT(D[N,8])
2410 NEXT T
2420 LINK 1
2430 END
```

IMMUNE RESPONSE MODEL PROGRAM -RESULT SECTION

```
10 REMARK: IMMUNE RESPONSE MODEL: RESULTS, FILE#1
20 H$="IMMUNE RSPONSE MODEL     "
30 DISP "   ENTER DESCRIPTIVE HEADING.    ",
40 INPUT H$[27]
50 DISP SPA5"READY PRINTER, REPLY 0.    ",
60 INPUT K
70 REM ***************************
80 REM  *** WRITE INPUT DATA ***
90 REM ***************************
100 IF K THEN 130
110 PRINT LIN1,WBYTE12
120 WAIT 1000
130 WRITE (15,730)H$
140 PRINT LIN3"MOUSE WEIGHT (GRAMS) ="W
150 PRINT "LYMPHOCYTE RADIUS (MICRONS) ="R"DENSITY (G/ML) ="D6
160 WRITE (15,70)"1ST ANTIGEN DOSE (PFU) ="D0
170 FORMAT E10.2
180 WRITE (15,170)"2ND ANTIGEN DOSE (PFU) ="D9
190 PRINT LIN1"PROPORTIONALITY CONSTANT AG/CELL  ="A
200 PRINT "ELIMINATION RATE & PER HOUR  ="00*L
210 PRINT "  LATENT PHASE (HOURS) FOR ICC TO BECOME IAC ="T5
230 PRINT "  LATENT PHASE (HOURS) FOR IAC TO BECOME ABFC="T2
240 PRINT "CELL GENERATION TIME (HOURS) ="T8
250 PRINT "ABFC LIFE SPAN (HOURS) ="T9
260 PRINT "MAXIMUM NO. CELL DIVISIONS ="G5
270 REM ********************
280 REM  *** ICC TABLE ***
290 REM ********************
300 PRINT LIN4"ESTIMATED NO. OF ICC"
310 WRITE (15,320)"TISSUES          BLOOD          TOTAL"
320 FORMAT /,/,28X,"LYMPHOID",5X,"PERIPHERAL",/,29X,F.0
330 WRITE (15,340)L1
340 FORMAT /,"WIGHT (GRAMS)",F22.3,10X,"-",2X,"-"
350 WRITE (15,360)L4
360 FORMAT "VOLUME (ML)",22X,"-",F15.3,10X,"-"
370 WRITE (15,380)L3,L5,L3+L5
380 FORMAT "NO. LYMPHOCYTES",10X,3E13.4
390 WRITE (15,400)V,V4,V5
400 FORMAT "NO. T-CELLS",14X,3E13.4
410 WRITE (15,420)B,B4,B+B4
420 FORMAT "NO. B-CELLS",14X,3E13.4
430 WRITE (15,440)S1,S2,S+S2
440 FORMAT "NO. WEE SPECIFIC T-CELLS ",E13.4
450 WRITE (15,460)S3,S4,S3+S4
460 FORMAT "NO. WEE SPECIFIC B-CELLS ",3E13.4
470 WRITE (15,480)S
```

```
480 FORMAT /,29X,"TOTAL T & B SPECIFIC ICC",E13.4
490 REM ************************
500 REM  *** FRACTION DATA ***
510 REM ************************
520 PRINT LIN4"FRACTION VIRGIN CELLS ="F0
530 PRINT "FRACTION LOW-ZONE TOLERANCE ="F1
540 PRINT "FRACTION AB-FORMING CELLS ="F2
550 PRINT "FRACTION HIGH-DOSE PARALYSIS ="F3
560 PRINT LIN1"Ig-M PRECURSORS AT TIME ZERO="A0
570 PRINT " PRIMARY Ig-G PRECURORS  ="A2
580 PRINT "SECONDARY Ig-G PRECURORS  ="A3
590 RM **********************
600 REM  *** RESULT DATA ***
610 REM **********************
620 PRINT LIN1,WBYTE12
630 WAIT 1000
640 WRITE (15,730)H$
650 WRITE (15,660)"=========== IG-G ==========="
660 FORMAT /,/,14X,"=========== IG-M ==========",8X,F.0
670 WAIT 150
680 WRITE (15,690)"ABFC       AB MOL.  NANOGRAMS"
690 FORMAT "  HOURS        ABFC       AB MOL.  NANOGRAMS",8X,F1.0
700 PRINT
710 FOR J=1 TO N
720 WRITE (15,730)D[J,1],D[J,2],D[J,4],.49427E-09*D[J,4];
730 FORMAT F6.0,2F12.3,E12.3
740 WRITE (15,750)D[J,6],D[J,8],2.6565E-10*D[J,8]
750 FORMAT 2F12.3,E12.3
760 WAIT 150
770 NEXT J
780 REM ******************
790 RM  *** GRAPHING ***
800 REM ******************
810 REM: MIN, MAX
820 Y0=Y9=D[,3]
830 FOR J=1 TO N
840 FOR K=3 TO 9 STEP 2
850 IF D[J,K] >= Y0 THEN 870
860 Y0=D[J,K]
870 IF D[J,K] <= Y9 THEN 890
880 Y9=D[J,K]
890 NEXT K
900 NEXT J
910 REM: SCALING FACTOR
920 IF Y0=Y9 THEN 1120
930 S=FNP(Y9-Y0)
940 IF S<4 THEN 970
950 S=INT(S+0.995)*0^(P0-2)
```

```
960 GOTO 980
970 S=INT(2.5*S+0.9875)/2.5*10^(P0-2)
980 A1=Y9-00.5*S
990 A9=Y0+0.5*S
1000 I=0
1010 IF A1<0 AND A9>0 THEN 160
1020 P[1]=10
1030 P[2]=5
1040 P[3]=2
1050 FOR D1=1 TO 3
1060 FOR R0=1 TO 3
1070 K=INT(FNP(0.5*(A1+A9))*10^(D1+)/P[R0]+0.5)
1080 I=K*P[R0]*10^(P0-D1-1)
1090 IF I>A1 AND I<A9 THEN 1160
1100 NEXT R0
1110 NEXT D1
1120 PRINT LIN1"GRAPH SKIPPED: NOT SCALEABLE"
1130 STOP
1140 REM: GRAPH HEADINGS
1150 FORMAT F14.3,4F25.3
1160 PRINT LIN1,WBYTE12
1170 WAIT 1000
1180 WRITE (15,1150)H$
1190 WRITE (15,1200)"G-AB MOL. = D"
1200 FORMAT /,"M-ABFC = A, M-AB MOL. = B, G-ABFC = C, ",F.0
1210 PRINT LIN1;SPA54"LOG10 SCALE"
1220 WRITE (15,1150)I,25*S+I,50*S+I,75*S+I,00*S+I
1230 REM: GRAPH INIT
1240 P$="ABCDEF"
1250 FOR K=1 TO 76 STEP 25
1260 O$[K]="."
1270 NEXT K
1280 FOR K=1 TO 81 STEP 20
1290 Q$[K]="- - - - - - - - - - - - - "
300 NEXT K
1310 REM: WORKING GRAPH SECTION
1320 L1=9
1330 FOR L=1 TO N
1340 L1=L1+1
1350 GOTO L1-9 OF 1380
1360 G$=O$
1370 GOTO 1410
1380 L1=0
1390 G$=Q$
1400 REM: DTERMINE GRAPH-PTS
1410 FOR J=1 TO 4
1420 P[J]=(D[L,2*J+1]-I)/S+1
```

```
1430 NEXT J
1440 REM: FIX GRAPH-PTS
1450 P9=102
1460 FOR K=1 TO 4
1470 IF P[K]=0 THEN 1640
1480 FOR J=K TO 4
1490 IF P[J]#P[K] THEN 1620
1500 IF J=K THEN 1610
1510 GOTO D1 OF 1550
1520 P9=P9+1
1530 G$[P9,P9]=P$[K,K]
1540 P9=P9+1
550 G$[P9,P9]=P$[J,J]
1560 P[J]=0
1570 P9=P9+1
1580 G$[P9,P9]=","
1590 D1=1
1600 GOTO 1620
1610 D1=0
1620 NEXT J
1630 G$[P[K],P[K]]=P$[K]
1640 NEXT K
1650 WRITE (15,1670)D[L,1],G$[,P9-1]
1660 NEXT L
1670 FORMAT F9.2,1X,F1.0
1680 DISP " END"
1690 STOP
1700 REMARK: POWER FUNCTION
1710 DEF FNP(X)
1720 P0=0
1730 S9=SGNX
1740 X=ABSX
1750 IF X<1 THEN 1800
1760 IF X<0 THEN 1830
1770 X=X/10
1780 P0=P0+1
1790 GOTO 1760
1800 X=X*10
1810 P0=P0-
1820 IF X<1 THEN 1800
1830 RETURN S9*X
1840 END
```

LITERATURE CITED

1. Adams, R. B., W. H. Voelker and E. C. Gregg. 1967. Electrical counting and sizing of mammalian cells in suspension: An experimental evaluation. Phys. Med. Biol. 12:79-92.

2. Adler, W. H. and S. G. Rabinowitz. 1973. Host defenses during primary Venezuelan equine encephalomyelitis virus infection in mice. II. In vitro method for the measurement and quantitation of the immune response. J. Immunol. 110:1354-1362.

3. Altman, P. L. and D. S. Dittmer. 1964. Biology data book, pp. 270-274. Federation of American Societies for Experimental Biology, Washington, D. C.

4. Arquilla, E. R. and J. Finn. 1963. Genetic differences in antibody production to determinant groups of insulin. Science. 142:400-401.

5. Bell, G. I. 1971. Mathematical model of clonal selection and antibody production, II. J. Theor. Biol. 33:339-378.

6. Bell, G. I. 1971. Mathematical model of clonal selection and antibody production. III. The cellular basis of immunological paralysis. J. Theor. Biol. 33:379-398.

7. Biozzi, G., C. Stiffel, D. Mouton, Y. Bouthillier and C. Decreusefond. 1968. A kinetic study of antibody producing cells in the spleen of mice immunized intravenously with sheep erythrocytes. Immunol. 14:7-20.

8. Black, J. S. and C. J. Inchley. 1974. Characteristics of immunological memory in mice. I. Separate early generation of cells mediating of IgM and IgG memory to sheep erythrocytes. J. Exp. Med. 140:333-346.

9. Boyum, A. 1968. Isolation of mononuclear cells and granulocytes from human blood. Scand. J. Clin. Lab. Invest. 21:77-79.

10. Burnett, M. 1962. The thymus gland. Sci. Am. 138:2-9.

11. Cardiff, R. D., W. E. Bradt, T. C. McCloud, S. Shapiro and P. K. Russel. 1971. Immunological and biophysical separation of Dengue 2 antigen. J. Virol. 7:15-23.

12. Chappell, W. A., M. A. Bucca, L. A. White and W. C. Gamble. 1972. Production manual: viral, rickettsial, chlamydial, mycoplasmal reagents, pp. 4-10. U. S. Department of Health, Education and Welfare, Atlanta, Georgia.

13. Claman, H. N., E. A Chaperon and R. F. Triplett. 1966. Immunocompetence of transferred thymus-marrow cell combination. J. Immunol. 97:828-832.

14. Cohen, M. and P. A. Bretscher. 1968. Minimal model for the mechanism of antibody induction and paralysis by antigen. Nature. 220:44-448.

15. Cohen, S. 1970. A model for the mechanism of antibody induction and tolerance with specific attention to the affinity characteristics of antibodies produced during the immune response. Biol. 27:19-29.

16. Cohen, S. 1971. Receptor theory and antibody formation, pp. 132-139. In O. Makela, A. Cross and T. U. Konsunen (eds.). Cellular interactions in the immune response. Karger, Basel.

17. Cohen, S. and M. Milgram. 1971. Proliferation of maximally activated antigen-primed cells: A computer simulation. J. Immunol. 107:115-122.

18. Conrad, R. E. and J. S. Ingraham. 1974. Rate of hemolytic antibody production by single cells in vivo in rabbits. J. Immunol. 112:17-25.

19. Cooke, R. A. and A. Van der Veer. 1916. Human sensitization. J. Immunol. 1:201-305.

20. Cooper, M. D. and A. R. Lawton. 1974. The development of the immune system. Sci. Am. 231:58-72.

21. Craddock, C. G., R. Longmire and R. McMillon. 1973. Lymphocytes and the immune response I. New England J. Med. 285:324-329.

22. Craddock, C. G., R. Longmire and R. McMillon. 1973. Lymphocytes and the immune response II. New England J. Med. 285:378-384.

23. Dalrymple, J. M., A. Y. Teramoto, R. D. Cardiff and P. K. Russel. 1971. Radioimmune precipitation of group A arbovirus antigens. Walter Reed Army Institute of Research, Washington, D. C. (Personal communication).

24. Diener, E. and W. D. Armstrong. 1967. Induction of antibody formation and tolerance in vitro to a purified protein antigen. The Lancet II. pp. 1281-1285.

25. Edelman, G. M. 1970. The structure and function of antibodies. Sci. Am. 232:34-42.

26. Fahey, J. L. and A. G. Robinson. 1966. Factors controlling serum gamma globulin concentration. J. Exp. Med. 118:845-867.

27. Fahey, J. L. and S. Sell. 1966. The immunoglobulins of mice. V. The metabolic (catabolic) properties of five immunoglobulin classes. J. Exp. Med. 122:41-58.

28. Fink, M. A. and V. A. Quinn. 1953. Antibody production in inbred strains of mice. J. Immunol. 70:61-67.

29. Friedman, H. 1973. RNA in the immune response. Ann. N. Y. Acad. Sci. 249:18-48.

30. Gerloff, R. K., B. H. Hoyer and L. C. McLaren. 1962. Precipitation of radiolabeled poliovirus with specific antibody and antiglobulin. J. Immunol. 89:559-565.

31. Green, L., L. Ellman, W. J. Martin and B. Benacerraf. 1971. Genetic control of specific immune responses in guinea pigs, pp. 76-82. In O. Makela, A. Cross and T. U. Konsunen (eds.). Cell interaction and receptor antibodies in immune response. Academic Press, London, New York.

32. Hege, J. S. and L. J. Cole. 1966. A mathematical model relating circulating antibody and antibody-forming cells. J. Immunol. 97:34-40.

33. Herbert, G. A. and B. Pittman. 1965. Factors affecting removal of $(NH_4)_2SO_4$ from salt fractionated serum globulins employing a spectrophotometric procedure for determination of sulfate. Health Lab. Sci. 2:48-53.

34. Herbert, G. A., P. L. Pelham and B. Pittman. 1973. Determination of the optimal ammonium sulfate concentration for the fractionation of rabbit, sheep, horse and goat antiserum. Appl. Microbiol. 25:26-36.

35. Hiramoto, R. M., V. K. Ghanta, J. R. McGhee and N. M. Hamlin. 1973. A mathematical model for the quantitation of tumor and antibody-forming cell populations within an animal's body. J. Immunol. 111:1546-1553.

36. Hoskin, J. M. 1971. Virological Procedures, pp. 18-93. Butterworth, Inc., Washington, D. C.

37. Jerne, N. K. 1955. The natural selection theory of antibody formation. Proc. Nat. Acad. Sci., U. S. A. 41:849-858.

38. Jerne, N. K. 1971. The somatic generation of immune recognition. Europe J. Immunol. 1:1-9.

39. Jerne, N. K. 1973. The immune system. Sci. Am. 229:52-60.

40. Jerne, N. K., A. A. Nordin and C. Henry. 1962. The agar plaque technique for recognizing antibody-producing cells, pp. 109-122. In B. Amos and K. Koprowski (eds.). Cell bound antibody. Wistar Institute Press, Philadelphia.

41. Jilek, M. and J. Sterzl. 1970. Modeling of the immune processes, pp. 335-345. In I. Riha and J. Sterzl (eds.). Developmental aspects of antibody formation and structure. Academia, Prague and Academic Press, New York.

42. Jilek, M. and Z. Urisinyova. 1970. The probability of contact between the immunocompetent cell and antigen. Folia Microbiol. 15:294-302.

43. Kappler, J. W., P. C. Hunter, D. Jacobs and E. Lord. 1974. Functional heterogeneity among the T-derived lymphocytes of the mouse. I. Analysis by adult thymectomy. J. Immunol. 113:27-38.

44. Kubitschek, H. E. 1969. Counting and sizing microorganisms with the Coulter Counter, pp. 593-610. In J. R. Norris and D. W. Ribbons (eds.). Methods in Microbiology, Academic Press, New York.

45. Kubitschek, H. E., H. E. Bendigkeit and M. R. Loken. 1967. Onset of DNA synthesis during the cell cycle in chemostat cultures. Proc. Natl. Acad. Sci. 57:1611-1617.

46. Lerner, R. A. and F. J. Dixon. 1973. The human lymphocyte as an experimental animal. Sci. Am. 228:82-91.

47. Marchalonis, J. J. and V. X. Gledhill. 1968. Elementary stochastic model for the induction of immunity and tolerance. Nature. 220:608-611.

48. Mayerson, H. S. 1963. The lymphatic system. Sci. Am. 158:2-12.

49. McDevitt, H. O. and A. Chinitz. 1969. Genetic control of the antibody response: Relationship between immune response and histocompatibility (H-2) type. Science. 163:1207-1208.

50. Meyer, P. L. 1970. Introducing probability and statistical applications, pp. 1-5. Addison-Wesley Co. Inc., Mass.

51. Miller, J. F. A. P. 1961. Immunological function of the thymus. The Lancet II. pp. 748-749.

52. Miller, J. F. A. P. and G. F. Mitchell. 1969. Thymus and antigen reactive cells. Transplant Rev. 1:3-42.

53. Mitchison, N. A. 1964. Induction of immunological paralysis in two zones of dosage. Proc. Roy. Soc. B. 161:275-292.

54. Mitchison, N. A. 1966. Recognition of antigen by cells. Progr. Biophys. Molec. Biol. 16:1-14.

55. Monath, T. P. C. 1971. Neutralizing antibody responses in the major immunoglobulin classes to yellow fever 17D vaccination of humans. Amer. J. of Epidemiol. 93:122-129.

56. Mozes, E. and G. Shearer. 1972. Genetic control of immune responses, pp. 167-195. In H. Kopvowski (ed.). Current topics in microbiology and immunology, Vol. 59. Springer-Verlag, New York.

57. Nossal, G. J. V. 1964. How cells make antibodies. Sci. Am. 199:2-10.

58. Nossal, G. J. V., M. L. Warmer, H. Lewis and J. Sprent. 1972. Quantitative features of a sandwich radioimmunolabelling technique for lymphocyte surface receptors. J. Exp. Med. 135:405-428.

59. Nota, N. R., M. Liacopoules-Briot, C. Stiffed and G. Biozzi. 1964. L' immuno-cyto-adherence: une methode simple et quantitative pour letude in vitro des cellules productrices d' anticorp. C. R. Acad Sci. (Paris). 259:1277-1280.

60. Paulovsky, S., J. L. Binet, C. Dereusefond and Y. Biozzi. 1970. Etude de la response immunologique an niverau cellulaire. I. Identification des cellules formatrices de rosettes eu microscopie optique et electronizue. Ann. Inst. Pasteur. 119:63-75.

61. Porter, R. R. 1967. The structure of antibodies. Sci. Am. 217:81-90.

62. Rabellino, E., S. Colon, H. M. Grey and E. R. Unanne. 1971. Immunoglobulins on the surface of lymphocytes. I. Distribution and quantitation. J. Exp. Med. 121:156-167.

63. Raff, M. C. 1970. The use of surface antigenic markers to define different populations of lymphocytes in the mouse, pp. 83-90. In O. Makela, A. Cross and T. U. Konsuner. (eds.). Cell interactions and receptor antibodies in immune responses. Academic Press, London, New York.

64. Ratz, P. H. and D. Y. E. Perey. 1973. Lymphocytes in Peyer's pathches of the mouse: Analysis of the constituent cells in terms of their capacities to mediate functions of mature T and B lymphocytes. J. Immunol. 113:1507-1512.

65. Richards, F. F., W. H. Konigsberg, R. W. Rosenstein and J. M. Varga. 1975. On the specificity of antibodies. Science. 187:130-137.

66. Roelants, G. 1972. Antigen recognition by B and T lymphocytes. Cur. Topics in Microbiol. and Immunol. 59:135-165.

67. Ross, S. M. 1972. Introduction to probability models, pp. 115-132. Academic Press, New York, London.

68. Scheibel, I. F. 1963. Heredity differences in the capacity of guinea pigs for production of diphtheria antitoxin. Acta Path. Microbiol. Scand. 20:464-484.

69. Shellam, G. R. 1969. Mechanism of induction of immunological tolerance. V. Priming and tolerance with small doses of polymerized flagellin. Immunol. 16:45-56.

70. Shellam, G. R. and G. J. V. Nossal. 1968. Mechanism of induction of immunological tolerance. IV. The effects of ultra-low doses of flagellin. Immunol. 14:273-284.

71. Sonada, S., M. Shurro and M. Schlamowitz. 1970. Studies of I-125 trace labeling of immunoglobulin G by chloramine-T. Immunochemistry. 7:885-898.

72. Stahl, W. R. 1967. The role of models in theoretical biology, pp. 166-210. In Progress in theoretical biology I. Academic Press, New York, London.

73. Sterzl, J. and A. Nordin. 1971. The common cell precursor for cells producing different immunoglobulins, pp. 213-230. In Cell interaction and receptor antibodies in immune response. Academic Press, London, New York.

74. Tsokos, C. P. 1972. Probability distribution: An introduction to probability theory with applications, pp. 37-41. Wadsworth Publishing Co. Inc., California.

75. Tyan, M. L., H. O. McDevitt and L. A. Herzenberg. 1969. Genetic control of the antibody response to a synthetic polypeptide: Transfer of response with spleen cells or lymphoid precursors. Transplant Proc. 1:548-550.

76. Uhr, J. W. and J. B. Baumann. 1961. *Antibody formation. I. The* supression of antibody formation by passively administered antibody. J. Exp. Med. 113:935-937.

77. Uhr, J. W. M. S. Finkelstein and J. B. Baumann. 1962. Antibody formation. III. The primary and secondary antibody response to bacteriophage Ø X 174 in guinea pigs. J. Exp. Med. 115:655-669.

78. Uhr, J. W., M. S. Finkelstein. 1963. Antibody formation. IV. Formation of rapidly and slowly sedimenting antibodies and immunological memory to bacteriophage Ø X 174. J. Exp. Med. 117:457-477.

79. Vaz, N. M. and B. B. Levine. 1970. Immune responses of inbred mice to repeated doses of antigen: Relationship to histocompatibility (H-2) type. Science. 168:852-854.

80. White, A. 1975. Nature and biological activities of thymus hormones: Prospects for the future. Ann. N. Y. Acad. Sci. 2:523-530.

81. Wilson, J. D. 1971. The relationship of antibody-forming cells to rosette-forming cells. Immunol. 21:233-245.

82. Wilson, J. D. and J. F. A. P. Miller. 1971. T and B rosette-forming cells. Europ. J. Immunol. 1:501-503.

83. Yoffey, J. M. and F. C. Courtice. 1970. Lymphatics, lymph and the lymphomyloid complex, p. 48. Academic Press, London.

APPLICATION OF THE IMMUNE RESPONSE MODEL

The simulation of this computer model is to provide basic information that is required for the future development of the in vivo CLAM detection system.

This model conveys the necessary material that allows the following studies:

1. The various components of the immune system of an animal that are actively involved in an immune response.

2. The interaction of these components and their relationships to one another.

3. The kinetics of a humoral antibody response in both active and passive immunity. Of special interest in this area is the early antibody formation.

4. The quantitative study of circulating antibody level that marks the limitation and availability of various detection methods and specifies the level of sensitivity that the in vivo CLAM system should arrive at.

5. The theoretical minimum time lapse between an antigenic challenge and the initiation of an immune response (either humoral or cellular).

6. The quantitative study of the distribution of immunocompetent cells and level of antibody in major lymphoid organs. This provides an alternative to the detection of early infection at a tissue rather than the circulatory level, if the former is found to be more advantageous.

7. The relationship between the body weight and the extent of an immune expression of an animal under the same immunological and physiological conditions.

8. The effect of antigenic dosage on the immunological responsiveness (activated or tolerant) of the immuno-competent cell population of an animal.

9. The catabolic rate of the immunogenic determinants of a given dose of virus that specifies the extension of continuous antigenic challenge and the duration of immunity.

10. This model provides a framework for future modeling effort which is needed to diversify the application of the in vivo CLAM system to areas (e.g. air pollution or the detection of) an antigen of interest.

11. The possibility of studying the various proposed immune mechanisms (e.g. in T and B cell interaction) by the modeling approach.

RECOMMENDATION

(A) In vivo CLAM system

Serum albumins microsphere (Nuclear Product Division. The 3M Co. Minn.) which would be labeled with either ^{130}I, ^{51}Cr, ^{113m}In or ^{99m}Ic have been used extensively for the study of regional blood flow of the various organs of an animal; kinetics of phagocytosis and the detection of peripherol vacular diseases such as cirrhosis.

Tc labeled serum albumin microsphere has often been used in lung scanning and liver scanning to review pathological abnormality, and is widely applicable in the studies of pulmonary embolic disease. ^{46}Sc-labeled microsphere has been used to study the blood supply to hepatic V-2 carcinoma implants. Serum albumin micropheres are basically nontoxic to an animal from which the sum is derived. The LD_{50} of human serum albumin to mice is 72.2 mg/kg and 43.8 mg/kg in rats. Both dogs and monkeys have survived doses as high as 68.1 mg/kg. An animal could stand serial injections with albumin microsphere without any apparent physiological disturbance.

Other microspheres such as aggregates of Sr Co_3 labeled with ^{87m}Sr. ^{85}Sr and $^{11}C^{60}$ and ^{99}Tc-labeled gelatin and amylose microspheres. These microspheres have the same advantages as that of serum albumin microspheres but have a longer biological half life and are non-proteinnacious material.

Non-metabolizable microspheres such as the radioactive $^{24}Na^{52}$ glass microspheres, ^{46}Sc.^{203} Hg ceramic microspheres, latex microspheres labeled with 27 different radionuclides, ^{32}p labeled carnaubal wax microsphere, is often used for the studies of (1) Measurement of regional blood flow, (2) Cardiac output, (3) Fractional shunting of blood through arteriovenous anastomoses, (4) The treatment of malignant neoplasm, (5) To irradiate a particular organ without diffusion of the radioactivity through the body. Other inert particles that could be used to study blood flow rate and phagocytosis are carbon, thorium dioxide, saccharide iron oxide, chromic phosphate and colloidal gold. These particles could persist in some phagocytic cells at the site of removal from the circulation almost indefinitely.

Another potential soluble immunoadsorbent that could be used in the vivo CLAM system is the formaldehyde or glutaraldchyde treated erythrocytes as the antigen carriers. These treated cells are resistant to lysis and could be used to study the antigenic stimulation of lymphocytes and the detection of corresponding antibody. Chemicals such as dinitrodiflworobenzene, bisdiazotized benzidinc, toluene diisocyanate could be used as coupling agents which link the antigen covalently to the erythrocyte carrier.

(B) Modeling

Future work should be done on the kinetics of phagocytosis which can field important information such as the duration and extent of continuous antigenic stimulation that is due to the continuous release of immunogenic fragments of antigens from phagocytic cells. This study could be done by the use of the in vivo CLAM system. The number of phagocytic cells in an animal could be evaluated by the detection of radioactive microsphere that are phagocytized by these cells. The rate of release of antigenic fragments can be estimated by the tissue culture technique. A new sector in the immune response model should be added that accounts for the multiplication rate of viruses in an infected animal. This sector should include the burst size of viral infected cells. The level and duration of the viremia in an infected animal (if any); the distribution of these viruses in the various lymphoid organs; the threshold of virus that could cause an infection, the probability of the number of cells that would be infected; and the rate of removal of infected virus. This information is of great value in the diagnosis of viral infection under natural conditions.

CONCLUSIONS

Based upon the experimental data found which is presented in this final technical report and previous annual and status reports, the following conclusions have been reached in the process of the Coated Latex Adsorption Method (CLAM) as an effective method of virus detection and identification.

1. Polyvinyl toluene latex particles of 2.02 μm diameter are relatively inert and exhibit excellent virus adsorption properties.

2. Major latex-virus aggregates may be demonstrated directly with light microscopy and indirectly by Coulter Counter volume profile analysis.

3. Two major groups of adsorption have been defined - non-agglutination (NAGG) adsorption and agglutination (AGG) adsorption. Agglutination has been further defined as ultramicro adsorption agglutination, micro adsorption agglutination and macro adsorption agglutination. Each group represents a greater or lesser degree of reaction and therefore may be correlated with the degree of sensitivity of the system.

4. The CLAM system has been effectively used to detect Western equine encephalitis (WEE), Eastern equine encephalitis (EEE), St. Louis encephalitis (SLE), influenza Hong Kong/A_2 Strain, and hog cholera virus in addition to WEE and SLE antibody, Concanavalin A, Salmonella bacteria, and Staphylococcus toxin. There is no reason not to assume that the process may be effectively applied to other viruses, antisera, bacteria, and other latex-adsorbing substances (i.e. hormones, enzymes, most other proteins, pesticides, etc.)

5. Computerization of the data analysis has decreased significantly the total time required for characterization of the process, and therefore permits complete analysis in less than 15 minutes.

6. Image analysis of virus-induced latex aggregates has been devloped which permits characterization of aggregates by type and number. Thus the method may be used to provide a scan of virus-reacted latex particles which may be used independently to characterize the virus-induced effect upon latex, or may be used in conjunction with the Coulter Counter method as a preliminary rough screening process.

7. Automation of the process appears to be quite feasible with the major biological steps well defined in terms of procedures, reaction times, limits of sensitivity, and fundamental operational requirements. Limits of engineering design and operation are apparently the only parameters which need further investigation.

RECOMMENDATIONS

Based upon the progress of research accomplished on the Office of Naval Research Contract, the following recommendations are submitted:

1. CLAM Process

    a. instrument modifications - sample rate, nosepiece designs
    b. procedural changes - choice of fixatives
    c. data analysis - adaptation of modeling to system
    d. new experiments - application to food and water

2. Simulated projections, correlations, modeling
    - assay of viruses, antibodies, virus infected cells, toxin, bacteria

3. Biophysical markers for detection
    - fluorescence tagging, enzyme markers, protein markers, tritiated water, electron dense material (i.e. phosphotungstic acid), DNA and/or RNA stains

4. Mathematical treatment for analysis
    - derive equations, values

5. Applications and Modifications
    - signal amplification
    - sample recovery, continuous sampling
    - low level counts vs. detection efficiency
    - automation
    - multichannel analysis (up to 1000 channels)
    - kinetic methanisms

INSTRUMENT AND LATEX PARTICLE STANDARDIZATION

Because a major goal involved in this process is that of universal adsorption detection, a full understanding of the operating and functioning characteristics of the test components and instruments used has been of necessity. To determine those parameters unique to latex dilution or count and Coulter Counter efficiency, an extensive examination of latex counts and instrument operating properties was performed. Dilutions of 10% solids, 2.02 um diameter polyvinyltoluene latex in Isoton (Coulter Electronics, Hialeah, Florida) were prepared from 1:10,000 to 1:100,000. Three counts of 0.050 ml sample each were obtained at thresholds 3, 4, and 5 on a Coulter Counter model F (Coulter Electronics, Hialeah, Florida) equipped with a 70 um aperture tube and set at: Attenuation 1, Aperture 8, Sample size 50 . These channels were chosen because they represented the total number of instrument-detected latex particles within the latex suspension and yet were sufficiently selective enough and eliminated any normal background counts. Additionally, the theoretical number of latex in each sampled dilution from 1:10,000 to 1:100,000 was calculated based on an original 10% solids latex count of 1.128×10^9 latex/0.050 ml. Interpolated values were calculated for the experimentally derived threshold counts in channels 3, 4 and 5 (Table 59). When plotted (Fig. 34) the correlation of theoretical to experimental counts indicated an excellent fitting especially in dilutions 1:30,000 and greater. Thus, the counts in any dilution of latex may be more critically accepted as to their accuracy and without accounting for any apparent coincidence correction. In those dilutions less than 1:30,000, the discrepancies may be corrected by applying a simple instrument efficiency factor.

To analyze further the relationship of latex counts and instrument efficiency, a linear regression was performed on all experimental values. The statistics for each data set were also calculated and the equation was defined for each straight line (Table 60). When plotted (Fig. 35) a distinction was seen between the data points and the straight line function. It would appear that a 1:60,000 dilution of latex might be the optimum dilution at which theoretical and experimental counts overlap. However, the graph must be viewed carefully and the tremendous effect of theoretical low dilution counts should be noted.

Table 59 Theoretical, Experimental, and Interpolated Counts for Latex Dilutions of 1:10,000 to 1:100,000 in Thresholds 3, 4, and 5

THEORETICAL LATEX COUNT				EXPERIMENTAL THRESHOLD 3 LATEX COUNT			
*** INTERPOLATED ***		****** GIVEN ******		*** INTERPOLATED ***		****** GIVEN ******	
X	Y	X	Y	X	Y	X	Y
10.00	112800.0000	10.00	112800.0000	10.00	50395.9000	10.00	50396.0000
11.00	103353.0000			11.00	49548.5000		
12.00	94977.6000			12.00	49212.6000		
13.00	87509.2000			13.00	48501.4000		
14.00	81103.2000			14.00	47729.5000		
15.00	75435.1000			15.00	46910.9000		
16.00	70500.0000	16.00	70500.0000	16.00	46059.9000	16.00	46060.0000
17.00	66213.6000			17.00	45190.7000		
18.00	62491.6000			18.00	44317.3000		
19.00	59246.2000			19.00	43454.0000		
20.00	56400.0000	20.00	56400.0000	20.00	42614.9000	20.00	42615.0000
21.00	53874.0000			21.00	41792.3000		
22.00	51211.2000			22.00	41206.7000		
23.00	48953.4000			23.00	40548.7000		
24.00	46962.4000			24.00	39909.2000		
25.00	45120.0000	25.00	45120.0000	25.00	39279.0000	25.00	39279.0000
26.00	43365.2000			26.00	38686.7000		
27.00	41748.6000			27.00	37900.6000		
28.00	40257.0000			28.00	37226.9000		
29.00	38878.4000			29.00	36572.0000		
30.00	37600.0000	30.00	37600.0000	30.00	35942.0000	30.00	35942.0000
31.00	36377.9000			31.00	35437.9000		
32.00	35225.2000			32.00	34958.6000		
33.00	34165.6000			33.00	34491.3000		
34.00	33162.9000			34.00	34023.5000		
35.00	32220.7000			35.00	33542.2000		
36.00	31332.9000	36.00	31333.0000	36.00	33034.9000	36.00	33035.0000
37.00	30493.5000			37.00	32364.3000		
38.00	29680.8000			38.00	31701.4000		
39.00	28920.0000			39.00	31069.4000		
40.00	28200.0000	40.00	28200.0000	40.00	30491.0000	40.00	30491.0000
41.00	27510.7000			41.00	30199.4000		
42.00	26854.9000			42.00	29963.2000		
43.00	26230.4000			43.00	29748.2000		
44.00	25635.1000			44.00	29508.2000		
45.00	25067.0000	45.00	25067.0000	45.00	29205.0000	45.00	29205.0000
46.00	24526.8000			46.00	28559.0000		
47.00	23995.4000			47.00	27829.2000		
48.00	23496.3000			48.00	27035.4000		
49.00	23019.3000			49.00	26197.1000		
50.00	22560.0000	50.00	22560.0000	50.00	25333.9000	50.00	25334.0000
51.00	22116.0000			51.00	24441.9000		
52.00	21691.0000			52.00	23567.5000		
53.00	21281.6000			53.00	22735.1000		
54.00	20887.7000			54.00	21969.1000		
55.00	20508.5000			55.00	21293.9000		
56.00	20143.0000	56.00	20143.0000	56.00	20734.0000	56.00	20734.0000
57.00	19789.1000			57.00	20465.4000		
58.00	19447.7000			58.00	20288.6000		
59.00	19118.2000			59.00	20184.4000		

Table 59 (cont)

THEORETICAL LATEX COUNT				EXPERIMENTAL THRESHOLD 3 LATEX COUNT			
*** INTERPOLATED ***		****** GIVEN ******		*** INTERPOLATED ***		****** GIVEN ******	
X	Y	X	Y	X	Y	X	Y
60.00	16800.0000	60.00	16800.0000	60.00	20133.9000	60.00	20134.0000
61.00	16491.0000			61.00	19967.1000		
62.00	16192.1000			62.00	19838.5000		
63.00	15902.8000			63.00	19666.5000		
64.00	15622.7000			64.00	19529.8000		
65.00	15351.4000			65.00	19366.7000		
66.00	15088.5000			66.00	19195.7000		
67.00	14833.7000			67.00	19015.4000		
68.00	14586.6000			68.00	18824.2000		
69.00	14346.8000			69.00	18620.5000		
70.00	14113.9000	70.00	14114.0000	70.00	18402.9000	70.00	18403.0000
71.00	13886.8000			71.00	18060.2000		
72.00	13666.1000			72.00	17740.4000		
73.00	13451.6000			73.00	17457.0000		
74.00	13242.9000			74.00	17223.4000		
75.00	13040.0000	75.00	13040.0000	75.00	17053.0000	75.00	17053.0000
76.00	12841.9000			76.00	17055.1000		
77.00	12649.0000			77.00	17123.3000		
78.00	12461.1000			78.00	17247.2000		
79.00	12278.2000			79.00	17416.3000		
80.00	12099.9000	80.00	12100.0000	80.00	17619.9000	80.00	17620.0000
81.00	11923.4000			81.00	17646.1000		
82.00	11750.7000			82.00	17643.4000		
83.00	11581.8000			83.00	17611.9000		
84.00	11416.7000			84.00	17551.8000		
85.00	11255.4000			85.00	17463.1000		
86.00	11097.8000			86.00	17345.9000		
87.00	10943.9000			87.00	17200.3000		
88.00	10793.8000			88.00	17026.4000		
89.00	10647.4000			89.00	16824.3000		
90.00	10504.8000			90.00	16594.1000		
91.00	10365.8000			91.00	16335.9000		
92.00	10230.5000			92.00	16049.8000		
93.00	10099.0000			93.00	15735.8000		
94.00	9971.0000			94.00	15394.1000		
95.00	9846.8000			95.00	15024.8000		
96.00	9726.2000			96.00	14628.0000		
97.00	9609.2000			97.00	14203.6000		
98.00	9495.8000			98.00	13752.0000		
99.00	9386.1000			99.00	13273.0000		
100.00	9279.9000	100.00	9280.0000	100.00	12766.9000	100.00	12767.0000

Table 59 (cont)

EXPERIMENTAL THRESHOLD 4 LATEX COUNT				EXPERIMENTAL THRESHOLD 5 LATEX COUNT			
*** INTERPOLATED ***		****** GIVEN ******		*** INTERPOLATED ***		****** GIVEN ******	
X	Y	X	Y	X	Y	X	Y
10.00	51534.9000	10.00	51535.0000	10.00	51337.9000	10.00	51338.0000
11.00	50724.3000			11.00	50468.1000		
12.00	49894.1000			12.00	49586.0000		
13.00	49049.5000			13.00	48695.9000		
14.00	48195.5000			14.00	47801.9000		
15.00	47337.3000			15.00	46908.2000		
16.00	46479.9000	16.00	46480.0000	16.00	46018.9000	16.00	46019.0000
17.00	45628.5000			17.00	45138.3000		
18.00	44788.2000			18.00	44270.5000		
19.00	43963.9000			19.00	43419.7000		
20.00	43160.9000	20.00	43161.0000	20.00	42589.9000	20.00	42590.0000
21.00	42417.2000			21.00	41814.8000		
22.00	41698.2000			22.00	41063.3000		
23.00	40999.4000			23.00	40330.7000		
24.00	40315.9000			24.00	39612.5000		
25.00	39643.0000	25.00	39643.0000	25.00	38904.0000	25.00	38904.0000
26.00	38922.6000			26.00	38135.6000		
27.00	38216.6000			27.00	37363.9000		
28.00	37533.5000			28.00	36600.5000		
29.00	36881.7000			29.00	35977.0000		
30.00	36269.9000	30.00	36270.0000	30.00	35344.9000	30.00	35345.0000
31.00	35695.3000			31.00	35003.6000		
32.00	35552.4000			32.00	34706.6000		
33.00	35212.3000			33.00	34420.1000		
34.00	34945.6000			34.00	34110.0000		
35.00	34423.2000			35.00	33742.6000		
36.00	33915.9000	36.00	33916.0000	36.00	33283.9000	36.00	33284.0000
37.00	33031.0000			37.00	32421.0000		
38.00	32128.2000			38.00	31531.9000		
39.00	31253.9000			39.00	30662.2000		
40.00	30454.0000	40.00	30454.0000	40.00	29858.0000	40.00	29858.0000
41.00	30097.1000			41.00	29454.1000		
42.00	29842.5000			42.00	29149.3000		
43.00	29639.5000			43.00	28902.7000		
44.00	29437.6000			44.00	28673.2000		
45.00	29185.9000	45.00	29186.0000	45.00	28420.0000	45.00	28420.0000
46.00	28557.7000			46.00	27918.4000		
47.00	27847.7000			47.00	27357.0000		
48.00	27074.4000			48.00	26740.5000		
49.00	26256.3000			49.00	26073.9000		
50.00	25412.0000	50.00	25412.0000	50.00	25361.9000	50.00	25362.0000
51.00	24526.9000			51.00	24452.0000		
52.00	23656.9000			52.00	23527.5000		
53.00	22827.1000			53.00	22624.9000		
54.00	22062.4000			54.00	21780.7000		
55.00	21366.0000			55.00	21031.2000		
56.00	20829.0000	56.00	20829.0000	56.00	20413.0000	56.00	20413.0000
57.00	20567.2000			57.00	20171.8000		
58.00	20396.1000			58.00	20034.9000		
59.00	20295.9000			59.00	19978.7000		

Table 59 (cont)

EXPERIMENTAL THRESHOLD 4 LATEX COUNT				EXPERIMENTAL THRESHOLD 5 LATEX COUNT			
*** INTERPOLATED ***		****** GIVEN ******		*** INTERPOLATED ***		****** GIVEN ******	
X	Y	X	Y	X	Y	X	Y
60.00	20247.0000	60.00	20247.0000	60.00	19979.9000	60.00	19980.0000
61.00	20074.0000			61.00	19826.8000		
62.00	19892.0000			62.00	19658.9000		
63.00	19701.9000			63.00	19478.1000		
64.00	19504.4000			64.00	19285.6000		
65.00	19301.7000			65.00	19083.9000		
66.00	19091.6000			66.00	18874.0000		
67.00	18875.0000			67.00	18657.7000		
68.00	18661.0000			68.00	18436.6000		
69.00	18441.3000			69.00	18212.5000		
70.00	18219.9000	70.00	18220.0000	70.00	17986.9000	70.00	17987.0000
71.00	17932.6000			71.00	17696.4000		
72.00	17659.3000			72.00	17431.5000		
73.00	17439.6000			73.00	17202.8000		
74.00	17253.6000			74.00	17020.7000		
75.00	17121.0000	75.00	17121.0000	75.00	16896.0000	75.00	16896.0000
76.00	17127.3000			76.00	16920.1000		
77.00	17157.7000			77.00	17002.3000		
78.00	17293.2000			78.00	17132.8000		
79.00	17434.6000			79.00	17301.9000		
80.00	17603.0000	80.00	17603.0000	80.00	17500.0000	80.00	17500.0000
81.00	17614.5000			81.00	17530.4000		
82.00	17597.9000			82.00	17531.0000		
83.00	17553.4000			83.00	17501.8000		
84.00	17490.9000			84.00	17442.9000		
85.00	17380.7000			85.00	17354.5000		
86.00	17252.7000			86.00	17236.5000		
87.00	17097.2000			87.00	17089.2000		
88.00	16914.1000			88.00	16912.5000		
89.00	16703.5000			89.00	16706.7000		
90.00	16465.6000			90.00	16471.7000		
91.00	16200.5000			91.00	16207.7000		
92.00	15909.2000			92.00	15914.9000		
93.00	15588.8000			93.00	15593.2000		
94.00	15242.5000			94.00	15242.8000		
95.00	14869.2000			95.00	14863.6000		
96.00	14469.2000			96.00	14456.3000		
97.00	14042.5000			97.00	14020.3000		
98.00	13589.1000			98.00	13556.1000		
99.00	13109.2000			99.00	13063.6000		
100.00	12602.9000	100.00	12603.0000	100.00	12542.9000	100.00	12543.0000

Figure 34 Theoretical, experimental, and interpolated counts for latex dilutions of 1:10,000 to 1:100,000 in threcholds 3,4, and 5

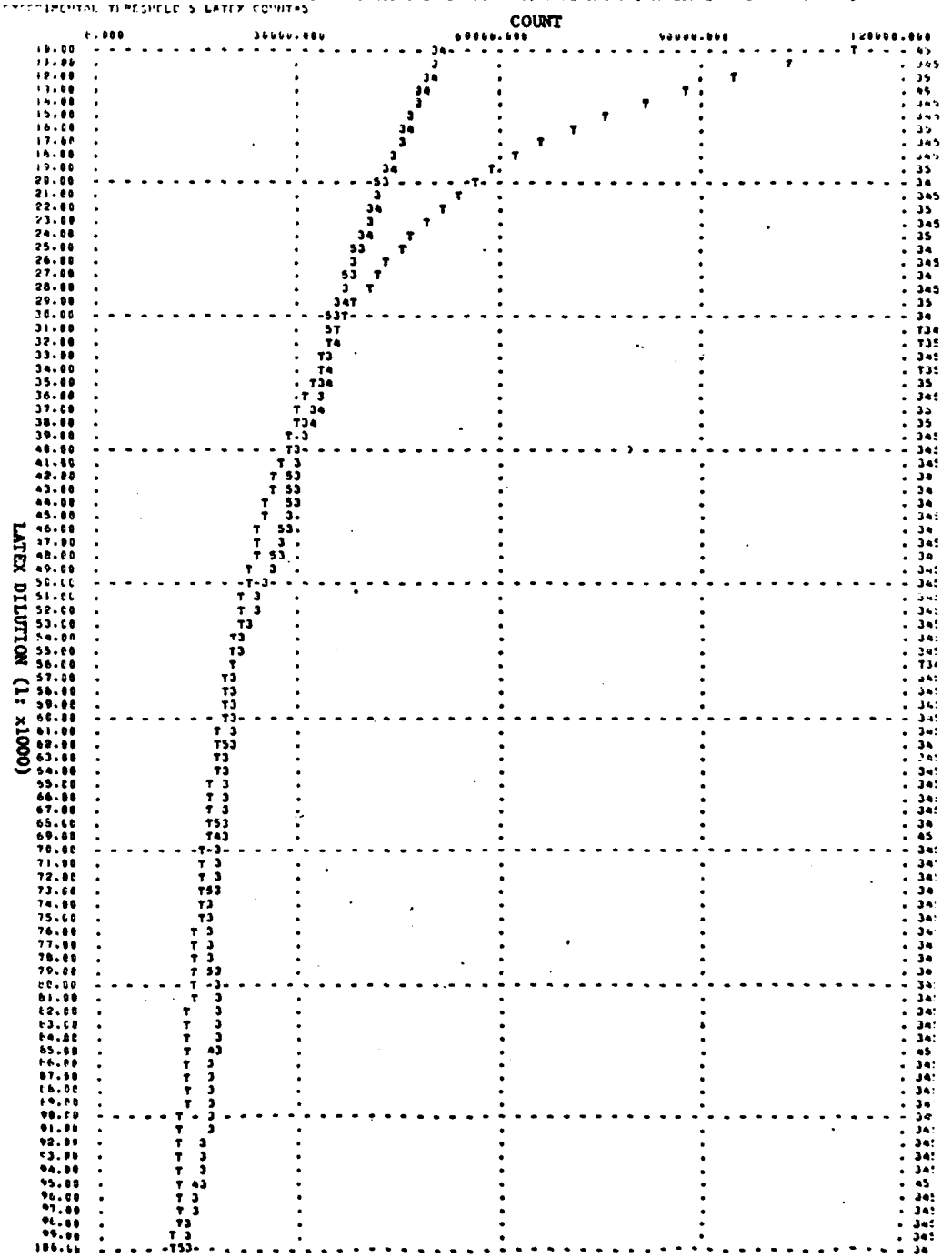

Table 60 Linear regression of theoretical and experimental threshold counts

DATA SET # 1 (THEORETICAL COUNT)

DATA SET # 2 (THRESHOLD 3 COUNT)

DATA SET # 3 (THRESHOLD 4 COUNT)

DATA SET # 4 (THRESHOLD 5 COUNT)

THEORETICAL COUNT		THRESHOLD 3 COUNT		THRESHOLD 4 COUNT		THRESHOLD 5 COUNT	
10.00	112000.00	10.00	50396.00	10.00	51535.00	10.00	51336.00
15.00	75500.00	15.00	46060.00	15.00	46480.00	15.00	46019.00
20.00	56500.00	20.00	42615.00	20.00	43161.00	20.00	42590.00
25.00	45120.00	25.00	39279.00	25.00	39643.00	25.00	38904.00
30.00	37600.00	30.00	35942.00	30.00	36270.00	30.00	35345.00
35.00	31333.00	35.00	33035.00	35.00	33916.00	35.00	33264.00
40.00	28200.00	40.00	30491.00	40.00	30454.00	40.00	29858.00
45.00	25067.00	45.00	29305.00	45.00	29156.00	45.00	28420.00
50.00	22560.00	50.00	25334.00	50.00	25412.00	50.00	25362.00
55.00	20143.00	55.00	20734.00	55.00	20829.00	55.00	20413.00
60.00	18800.00	60.00	20134.00	60.00	20247.00	60.00	19980.00
70.00	16114.00	70.00	18403.00	70.00	18220.00	70.00	17987.00
75.00	15040.00	75.00	17053.00	75.00	17121.00	75.00	16896.00
80.00	14100.00	80.00	17620.00	80.00	17603.00	80.00	17500.00
100.00	11280.00	100.00	12767.00	100.00	12603.00	100.00	12543.00

DATA SET #	1	2	3	4
# OF DATA POINTS	15.00	15.00	15.00	15.00
MEAN OF X	47.53	47.53	47.53	47.53
ST. DEV. OF X	26.01	26.01	26.01	26.01
MEAN OF Y	35003.50	29271.20	29512.00	29095.93
ST. DEV. OF Y	27296.04	11692.20	11996.27	11852.60
REGRESSION COEF.	-846.60	-433.34	-444.30	-436.03
STANDARD ERROR	16664.61	3226.01	3340.03	3426.60
CORRELATION COEF.	-0.81	-0.96	-0.96	-0.96
X-INTERCEPT	88.78	115.08	113.96	113.96
Y-INTERCEPT	75340.61	49869.17	50630.93	49916.96

EQUATION # 1: Y = (75340.614) + (-846.601) * X

EQUATION # 2: Y = (49869.173) + (-433.337) * X

EQUATION # 3: Y = (50630.934) + (-444.297) * X

EQUATION # 4: Y = (49916.965) + (-436.030) * X

Table 60 (cont)

EQUATION # 1: Y = (75340.614) + (-840.601) * X

FOR	X=	10.00	Y=	66854.61	FOR	X=	56.00	Y=	27818.98
FOR	X=	11.00	Y=	66014.01	FOR	X=	57.00	Y=	26970.38
FOR	X=	12.00	Y=	65157.41	FOR	X=	58.00	Y=	26121.78
FOR	X=	13.00	Y=	64308.81	FOR	X=	59.00	Y=	25273.18
FOR	X=	14.00	Y=	63460.21	FOR	X=	60.00	Y=	24424.58
FOR	X=	15.00	Y=	62611.61	FOR	X=	61.00	Y=	23575.98
FOR	X=	16.00	Y=	61763.00	FOR	X=	62.00	Y=	22727.38
FOR	X=	17.00	Y=	60914.40	FOR	X=	63.00	Y=	21878.78
FOR	X=	18.00	Y=	60065.80	FOR	X=	64.00	Y=	21030.18
FOR	X=	19.00	Y=	59217.20	FOR	X=	65.00	Y=	20181.58
FOR	X=	20.00	Y=	58368.60	FOR	X=	66.00	Y=	19332.98
FOR	X=	21.00	Y=	57520.00	FOR	X=	67.00	Y=	18484.38
FOR	X=	22.00	Y=	56671.40	FOR	X=	68.00	Y=	17635.77
FOR	X=	23.00	Y=	55822.80	FOR	X=	69.00	Y=	16787.17
FOR	X=	24.00	Y=	54974.20	FOR	X=	70.00	Y=	15938.57
FOR	X=	25.00	Y=	54125.60	FOR	X=	71.00	Y=	15089.97
FOR	X=	26.00	Y=	53277.00	FOR	X=	72.00	Y=	14241.37
FOR	X=	27.00	Y=	52428.40	FOR	X=	73.00	Y=	13392.77
FOR	X=	28.00	Y=	51579.80	FOR	X=	74.00	Y=	12544.17
FOR	X=	29.00	Y=	50731.20	FOR	X=	75.00	Y=	11695.57
FOR	X=	30.00	Y=	49882.60	FOR	X=	76.00	Y=	10846.97
FOR	X=	31.00	Y=	49034.00	FOR	X=	77.00	Y=	9998.37
FOR	X=	32.00	Y=	48185.40	FOR	X=	78.00	Y=	9149.77
FOR	X=	33.00	Y=	47336.80	FOR	X=	79.00	Y=	8301.17
FOR	X=	34.00	Y=	46488.19	FOR	X=	80.00	Y=	7452.57
FOR	X=	35.00	Y=	45639.59	FOR	X=	81.00	Y=	6603.97
FOR	X=	36.00	Y=	44790.99	FOR	X=	82.00	Y=	5755.37
FOR	X=	37.00	Y=	43942.39	FOR	X=	83.00	Y=	4906.77
FOR	X=	38.00	Y=	43093.79	FOR	X=	84.00	Y=	4058.17
FOR	X=	39.00	Y=	42245.19	FOR	X=	85.00	Y=	3209.56
FOR	X=	40.00	Y=	41396.59	FOR	X=	86.00	Y=	2360.96
FOR	X=	41.00	Y=	40547.99	FOR	X=	87.00	Y=	1512.36
FOR	X=	42.00	Y=	39699.39	FOR	X=	88.00	Y=	663.76
FOR	X=	43.00	Y=	38850.79	FOR	X=	89.00	Y=	-184.84
FOR	X=	44.00	Y=	38002.19	FOR	X=	90.00	Y=	-1033.44
FOR	X=	45.00	Y=	37153.59	FOR	X=	91.00	Y=	-1882.04
FOR	X=	46.00	Y=	36304.99	FOR	X=	92.00	Y=	-2730.64
FOR	X=	47.00	Y=	35456.39	FOR	X=	93.00	Y=	-3579.24
FOR	X=	48.00	Y=	34607.79	FOR	X=	94.00	Y=	-4427.84
FOR	X=	49.00	Y=	33759.19	FOR	X=	95.00	Y=	-5276.44
FOR	X=	50.00	Y=	32910.59	FOR	X=	96.00	Y=	-6125.04
FOR	X=	51.00	Y=	32061.98	FOR	X=	97.00	Y=	-6973.64
FOR	X=	52.00	Y=	31213.38	FOR	X=	98.00	Y=	-7822.24
FOR	X=	53.00	Y=	30364.78	FOR	X=	99.00	Y=	-8670.84
FOR	X=	54.00	Y=	29516.18	FOR	X=	100.00	Y=	-9519.44
FOR	X=	55.00	Y=	28667.58					

Table 60 (cont)

EQUATION # 2: Y = (49669.173) + (-433.337) * X

FOR	X=	10.00	Y=	45535.80	FOR	X=	56.00	Y=	25602.28
FOR	X=	11.00	Y=	45102.46	FOR	X=	57.00	Y=	25168.94
FOR	X=	12.00	Y=	44669.12	FOR	X=	58.00	Y=	24735.60
FOR	X=	13.00	Y=	44235.79	FOR	X=	59.00	Y=	24302.26
FOR	X=	14.00	Y=	43802.45	FOR	X=	60.00	Y=	23868.93
FOR	X=	15.00	Y=	43369.11	FOR	X=	61.00	Y=	23435.59
FOR	X=	16.00	Y=	42935.77	FOR	X=	62.00	Y=	23002.25
FOR	X=	17.00	Y=	42502.44	FOR	X=	63.00	Y=	22568.91
FOR	X=	18.00	Y=	42069.10	FOR	X=	64.00	Y=	22135.58
FOR	X=	19.00	Y=	41635.76	FOR	X=	65.00	Y=	21702.24
FOR	X=	20.00	Y=	41202.42	FOR	X=	66.00	Y=	21268.90
FOR	X=	21.00	Y=	40769.09	FOR	X=	67.00	Y=	20835.56
FOR	X=	22.00	Y=	40335.75	FOR	X=	68.00	Y=	20402.23
FOR	X=	23.00	Y=	39902.41	FOR	X=	69.00	Y=	19968.89
FOR	X=	24.00	Y=	39469.07	FOR	X=	70.00	Y=	19535.55
FOR	X=	25.00	Y=	39035.74	FOR	X=	71.00	Y=	19102.21
FOR	X=	26.00	Y=	38602.40	FOR	X=	72.00	Y=	18668.88
FOR	X=	27.00	Y=	38169.06	FOR	X=	73.00	Y=	18235.54
FOR	X=	28.00	Y=	37735.72	FOR	X=	74.00	Y=	17802.20
FOR	X=	29.00	Y=	37302.39	FOR	X=	75.00	Y=	17368.87
FOR	X=	30.00	Y=	36869.05	FOR	X=	76.00	Y=	16935.53
FOR	X=	31.00	Y=	36435.71	FOR	X=	77.00	Y=	16502.19
FOR	X=	32.00	Y=	36002.37	FOR	X=	78.00	Y=	16068.85
FOR	X=	33.00	Y=	35569.04	FOR	X=	79.00	Y=	15635.52
FOR	X=	34.00	Y=	35135.70	FOR	X=	80.00	Y=	15202.18
FOR	X=	35.00	Y=	34702.36	FOR	X=	81.00	Y=	14768.84
FOR	X=	36.00	Y=	34269.03	FOR	X=	82.00	Y=	14335.50
FOR	X=	37.00	Y=	33835.69	FOR	X=	83.00	Y=	13902.17
FOR	X=	38.00	Y=	33402.35	FOR	X=	84.00	Y=	13468.83
FOR	X=	39.00	Y=	32969.01	FOR	X=	85.00	Y=	13035.49
FOR	X=	40.00	Y=	32535.68	FOR	X=	86.00	Y=	12602.15
FOR	X=	41.00	Y=	32102.34	FOR	X=	87.00	Y=	12168.82
FOR	X=	42.00	Y=	31669.00	FOR	X=	88.00	Y=	11735.48
FOR	X=	43.00	Y=	31235.66	FOR	X=	89.00	Y=	11302.14
FOR	X=	44.00	Y=	30802.33	FOR	X=	90.00	Y=	10868.80
FOR	X=	45.00	Y=	30368.99	FOR	X=	91.00	Y=	10435.47
FOR	X=	46.00	Y=	29935.65	FOR	X=	92.00	Y=	10002.13
FOR	X=	47.00	Y=	29502.31	FOR	X=	93.00	Y=	9568.79
FOR	X=	48.00	Y=	29068.98	FOR	X=	94.00	Y=	9135.45
FOR	X=	49.00	Y=	28635.64	FOR	X=	95.00	Y=	8702.12
FOR	X=	50.00	Y=	28202.30	FOR	X=	96.00	Y=	8268.78
FOR	X=	51.00	Y=	27768.96	FOR	X=	97.00	Y=	7835.44
FOR	X=	52.00	Y=	27335.63	FOR	X=	98.00	Y=	7402.10
FOR	X=	53.00	Y=	26902.29	FOR	X=	99.00	Y=	6968.77
FOR	X=	54.00	Y=	26468.95	FOR	X=	100.00	Y=	6535.43
FOR	X=	55.00	Y=	26035.61					

Table 60 (cont)

EQUATION # 3: Y = (50630.934) + (-444.297) * X

FOR	X=	10.00	Y=	46187.96	FOR	X=	56.00	Y=	25750.28
FOR	X=	11.00	Y=	45743.66	FOR	X=	57.00	Y=	25305.99
FOR	X=	12.00	Y=	45299.37	FOR	X=	58.00	Y=	24861.69
FOR	X=	13.00	Y=	44855.07	FOR	X=	59.00	Y=	24417.39
FOR	X=	14.00	Y=	44410.77	FOR	X=	60.00	Y=	23973.09
FOR	X=	15.00	Y=	43966.47	FOR	X=	61.00	Y=	23528.80
FOR	X=	16.00	Y=	43522.18	FOR	X=	62.00	Y=	23084.50
FOR	X=	17.00	Y=	43077.88	FOR	X=	63.00	Y=	22640.20
FOR	X=	18.00	Y=	42633.58	FOR	X=	64.00	Y=	22195.90
FOR	X=	19.00	Y=	42189.28	FOR	X=	65.00	Y=	21751.61
FOR	X=	20.00	Y=	41744.99	FOR	X=	66.00	Y=	21307.31
FOR	X=	21.00	Y=	41300.69	FOR	X=	67.00	Y=	20863.01
FOR	X=	22.00	Y=	40856.39	FOR	X=	68.00	Y=	20418.71
FOR	X=	23.00	Y=	40412.09	FOR	X=	69.00	Y=	19974.42
FOR	X=	24.00	Y=	39967.80	FOR	X=	70.00	Y=	19530.12
FOR	X=	25.00	Y=	39523.50	FOR	X=	71.00	Y=	19085.82
FOR	X=	26.00	Y=	39079.20	FOR	X=	72.00	Y=	18641.52
FOR	X=	27.00	Y=	38634.91	FOR	X=	73.00	Y=	18197.23
FOR	X=	28.00	Y=	38190.61	FOR	X=	74.00	Y=	17752.93
FOR	X=	29.00	Y=	37746.31	FOR	X=	75.00	Y=	17308.63
FOR	X=	30.00	Y=	37302.01	FOR	X=	76.00	Y=	16864.34
FOR	X=	31.00	Y=	36857.72	FOR	X=	77.00	Y=	16420.04
FOR	X=	32.00	Y=	36413.42	FOR	X=	78.00	Y=	15975.74
FOR	X=	33.00	Y=	35969.12	FOR	X=	79.00	Y=	15531.44
FOR	X=	34.00	Y=	35524.82	FOR	X=	80.00	Y=	15087.15
FOR	X=	35.00	Y=	35080.53	FOR	X=	81.00	Y=	14642.85
FOR	X=	36.00	Y=	34636.23	FOR	X=	82.00	Y=	14198.55
FOR	X=	37.00	Y=	34191.93	FOR	X=	83.00	Y=	13754.25
FOR	X=	38.00	Y=	33747.63	FOR	X=	84.00	Y=	13309.96
FOR	X=	39.00	Y=	33303.34	FOR	X=	85.00	Y=	12865.66
FOR	X=	40.00	Y=	32859.04	FOR	X=	86.00	Y=	12421.36
FOR	X=	41.00	Y=	32414.74	FOR	X=	87.00	Y=	11977.06
FOR	X=	42.00	Y=	31970.45	FOR	X=	88.00	Y=	11532.77
FOR	X=	43.00	Y=	31526.15	FOR	X=	89.00	Y=	11088.47
FOR	X=	44.00	Y=	31081.85	FOR	X=	90.00	Y=	10644.17
FOR	X=	45.00	Y=	30637.55	FOR	X=	91.00	Y=	10199.88
FOR	X=	46.00	Y=	30193.26	FOR	X=	92.00	Y=	9755.58
FOR	X=	47.00	Y=	29748.96	FOR	X=	93.00	Y=	9311.28
FOR	X=	48.00	Y=	29304.66	FOR	X=	94.00	Y=	8866.98
FOR	X=	49.00	Y=	28860.36	FOR	X=	95.00	Y=	8422.69
FOR	X=	50.00	Y=	28416.07	FOR	X=	96.00	Y=	7978.39
FOR	X=	51.00	Y=	27971.77	FOR	X=	97.00	Y=	7534.09
FOR	X=	52.00	Y=	27527.47	FOR	X=	98.00	Y=	7089.79
FOR	X=	53.00	Y=	27083.17	FOR	X=	99.00	Y=	6645.50
FOR	X=	54.00	Y=	26638.88	FOR	X=	100.00	Y=	6201.20
FOR	X=	55.00	Y=	26194.58					

Table 60 (cont)

EQUATION # 4: Y = (49916.965) + (-533.030) * X

FOR	X=	10.00	Y= 45536.66	FOR	X=	56.00	Y= 25367.28
FOR	X=	11.00	Y= 45096.63	FOR	X=	57.00	Y= 24949.25
FOR	X=	12.00	Y= 44660.60	FOR	X=	58.00	Y= 24511.22
FOR	X=	13.00	Y= 44082.57	FOR	X=	59.00	Y= 24073.19
FOR	X=	14.00	Y= 43764.54	FOR	X=	60.00	Y= 23635.16
FOR	X=	15.00	Y= 43346.51	FOR	X=	61.00	Y= 23197.13
FOR	X=	16.00	Y= 42908.48	FOR	X=	62.00	Y= 22759.10
FOR	X=	17.00	Y= 42470.45	FOR	X=	63.00	Y= 22321.07
FOR	X=	18.00	Y= 42032.42	FOR	X=	64.00	Y= 21883.04
FOR	X=	19.00	Y= 41594.39	FOR	X=	65.00	Y= 21445.01
FOR	X=	20.00	Y= 41156.36	FOR	X=	66.00	Y= 21006.98
FOR	X=	21.00	Y= 40718.33	FOR	X=	67.00	Y= 20568.95
FOR	X=	22.00	Y= 40280.30	FOR	X=	68.00	Y= 20130.92
FOR	X=	23.00	Y= 39842.27	FOR	X=	69.00	Y= 19692.89
FOR	X=	24.00	Y= 39404.24	FOR	X=	70.00	Y= 19254.86
FOR	X=	25.00	Y= 38966.21	FOR	X=	71.00	Y= 18816.83
FOR	X=	26.00	Y= 38528.18	FOR	X=	72.00	Y= 18378.80
FOR	X=	27.00	Y= 38090.15	FOR	X=	73.00	Y= 17940.77
FOR	X=	28.00	Y= 37652.12	FOR	X=	74.00	Y= 17502.74
FOR	X=	29.00	Y= 37214.09	FOR	X=	75.00	Y= 17064.71
FOR	X=	30.00	Y= 36776.06	FOR	X=	76.00	Y= 16626.68
FOR	X=	31.00	Y= 36338.03	FOR	X=	77.00	Y= 16188.65
FOR	X=	32.00	Y= 35900.00	FOR	X=	78.00	Y= 15750.62
FOR	X=	33.00	Y= 35461.97	FOR	X=	79.00	Y= 15312.59
FOR	X=	34.00	Y= 35023.94	FOR	X=	80.00	Y= 14874.56
FOR	X=	35.00	Y= 34585.91	FOR	X=	81.00	Y= 14436.53
FOR	X=	36.00	Y= 34147.88	FOR	X=	82.00	Y= 13998.50
FOR	X=	37.00	Y= 33709.85	FOR	X=	83.00	Y= 13560.47
FOR	X=	38.00	Y= 33271.82	FOR	X=	84.00	Y= 13122.44
FOR	X=	39.00	Y= 32833.79	FOR	X=	85.00	Y= 12684.40
FOR	X=	40.00	Y= 32395.76	FOR	X=	86.00	Y= 12246.37
FOR	X=	41.00	Y= 31957.73	FOR	X=	87.00	Y= 11808.34
FOR	X=	42.00	Y= 31519.70	FOR	X=	88.00	Y= 11370.31
FOR	X=	43.00	Y= 31081.67	FOR	X=	89.00	Y= 10932.28
FOR	X=	44.00	Y= 30643.64	FOR	X=	90.00	Y= 10494.25
FOR	X=	45.00	Y= 30205.61	FOR	X=	91.00	Y= 10056.22
FOR	X=	46.00	Y= 29767.58	FOR	X=	92.00	Y= 9618.19
FOR	X=	47.00	Y= 29329.55	FOR	X=	93.00	Y= 9180.16
FOR	X=	48.00	Y= 28891.52	FOR	X=	94.00	Y= 8742.13
FOR	X=	49.00	Y= 28453.49	FOR	X=	95.00	Y= 8304.10
FOR	X=	50.00	Y= 28015.46	FOR	X=	96.00	Y= 7866.07
FOR	X=	51.00	Y= 27577.43	FOR	X=	97.00	Y= 7428.04
FOR	X=	52.00	Y= 27139.40	FOR	X=	98.00	Y= 6990.01
FOR	X=	53.00	Y= 26701.37	FOR	X=	99.00	Y= 6551.98
FOR	X=	54.00	Y= 26263.34	FOR	X=	100.00	Y= 6113.95
FOR	X=	55.00	Y= 25825.31				

Figure 35 Linear regression of theoretical and experimental threshold counts

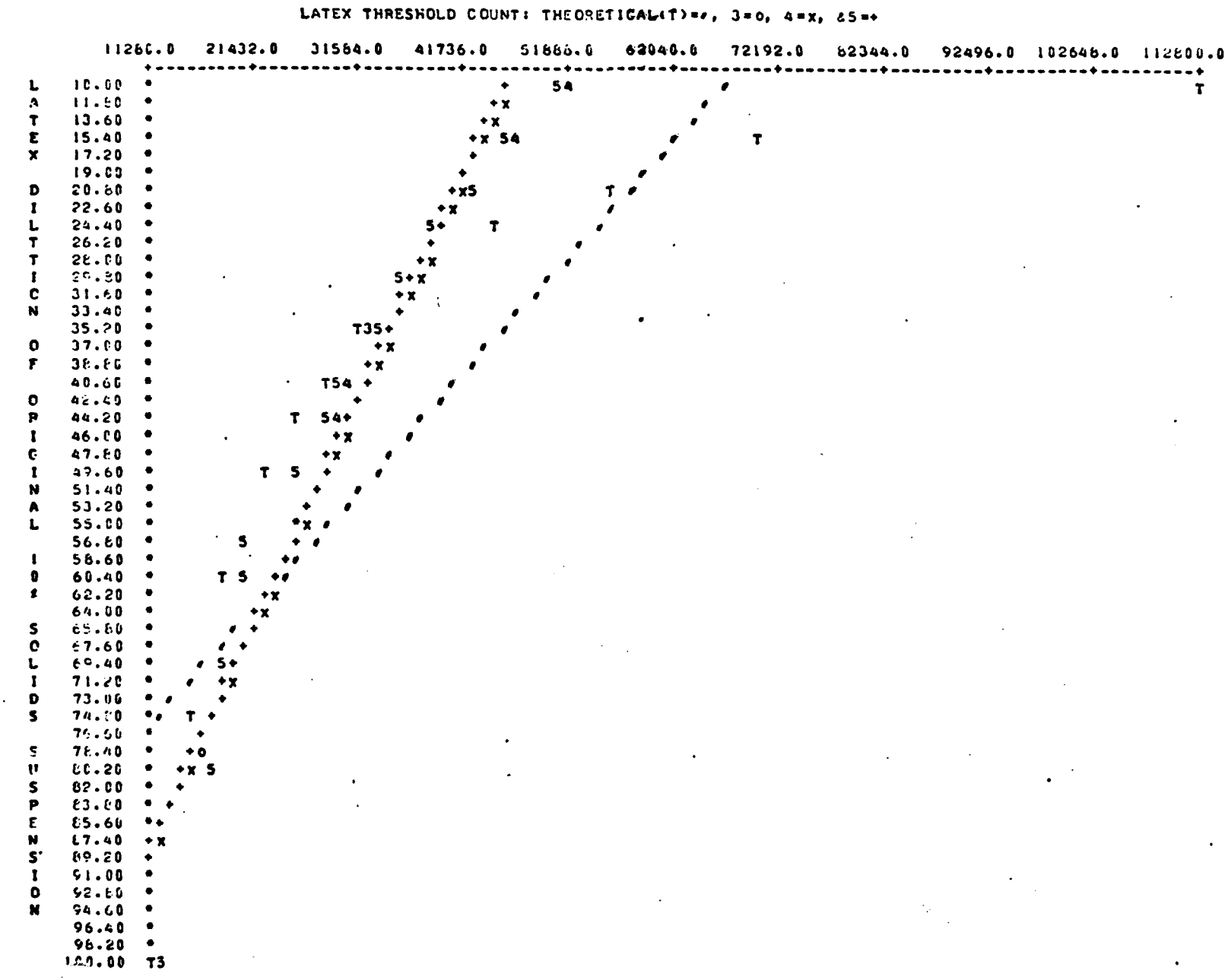

Table 61 Latex Counts in Channels 2-32 for Attenuations 1, .707, and .500

[illegible] ... ITL.

ATTENUATIONS 1,.707,.500
[illegible] SIZE [illegible] LATEX
[illegible] 7 [illegible]
[illegible] 1-1, 1-[illegible], 1-[illegible]

ATTENUATION 1			ATTENUATION .707			ATTENUATION .500		
2	[illegible]	[illegible]	2	11379	11437	2	[illegible]	12671
	[illegible]	[illegible]		11213	10[illegible].83		12726	94.35
	[illegible]	[illegible]		[illegible]	0.[illegible]%		12731	0.75%
	[illegible]			[illegible]			1112	
3	[illegible]	[illegible]	3	11017	1117[illegible]	3	11585	11559
	[illegible]	[illegible].92		11[illegible]	93.77		11413	134.45
	[illegible]	[illegible]%		11[illegible]	0.84%		11678	1.16%
	37			54			340	
4	[illegible]	11187	4	11109	11112	4	11336	11219
	[illegible]	13[illegible].25		11129	15.[illegible]		11213	114.61
	11078	1.19%		11099	0.14%		11107	1.02%
	149			-1			2	
5	[illegible]	10938	5	11103	11113	5	11146	11217
	[illegible]	57.30		11105	16.20		11191	35.04
	11[illegible]4	[illegible].52%		11132	0.15%		11312	0.76%
	[illegible]			-13			-11	
6	[illegible]	10543	6	11[illegible]	11127	6	11202	11226
	[illegible]	[illegible]		110[illegible]	105.[illegible]		11242	22.54
	[illegible]44	[illegible]%		11[illegible]	0.96%		11240	0.20%
	[illegible]71[illegible]			165			117	
7	[illegible]76	[illegible]	7	10918	10[illegible]	7	10908	11111
	[illegible]	[illegible]		11[illegible]	76.21		11[illegible]	179.72
	[illegible]	[illegible]		10[illegible]	0.70%		11[illegible]	1.[illegible]
	[illegible]			192			[illegible]4	
8	[illegible]	[illegible]	8	1[illegible]	10770	8	10992	11058
	[illegible]	[illegible]		1[illegible]	87.1[illegible]		111[illegible]	[illegible].76
	[illegible]	1.14%		10777	0.25%		11029	0.76%
	[illegible]			[illegible]			-33	
9	[illegible]	4[illegible]	9	10315	10[illegible]	9	111[illegible]	11[illegible]
	[illegible]	[illegible]		10191	1[illegible]		10[illegible]	1[illegible].93
	[illegible]	1.51%		[illegible]	1.5[illegible]%		11187	1.21%
	[illegible]			[illegible]			-419	
10	[illegible]	[illegible]	10	[illegible]	[illegible]	10	1[illegible]	11510
	[illegible]	[illegible]		[illegible]	[illegible]		11[illegible]	[illegible].27
	[illegible]	[illegible]		[illegible]	1.[illegible]		11[illegible]	4.[illegible]%
	[illegible]			[illegible]			[illegible]7[illegible]	
11	[illegible]	[illegible]	11	[illegible]	[illegible]	11	10[illegible]	10[illegible]
	[illegible]	[illegible]		[illegible]	177.[illegible]		10[illegible]	[illegible]
	[illegible]	[illegible]		[illegible]	[illegible]		10[illegible]	[illegible]
	[illegible]			[illegible]			[illegible]	
12	[illegible]	[illegible]	12	[illegible]	[illegible]	12	10[illegible]77	10720
	[illegible]	[illegible]		[illegible]	[illegible]		[illegible]	[illegible]
	[illegible]	[illegible]		[illegible]	[illegible]		[illegible]	1.[illegible]
	[illegible]			[illegible]			[illegible]79	
13	[illegible]	[illegible]	13	[illegible]	[illegible]	13	10[illegible]	10[illegible]7
	[illegible]	[illegible]		[illegible]	[illegible]		[illegible]	[illegible]
	[illegible]	[illegible]		[illegible]	1.[illegible]		[illegible]	[illegible]
	[illegible]			[illegible]			[illegible]	
14	[illegible]	[illegible]	14	[illegible]	[illegible]	14	[illegible]	[illegible]
	[illegible]	[illegible]		[illegible]	[illegible]		[illegible]71	17[illegible]
	[illegible]	[illegible]		[illegible]	1.7[illegible]		[illegible]	[illegible]

Table 61 (cont)

15	1373	1410	15	2943	2868	15	7288	7353
	1427	31.77		2804	70.15		7454	88.46
	1429	2.25%		2857	2.45%		7318	1.20%
	194			249			925	
16	1145	1215	16	2700	2619	16	6394	6429
	1196	81.73		2574	70.04		6393	60.91
	1305	6.73%		2584	2.67%		6499	0.95%
	92			225			824	
17	1090	1123	17	2398	2394	17	5583	5605
	1162	36.30		2421	29.21		5760	86.13
	1118	3.23%		2363	1.22%		5532	1.54%
	126			273			865	
18	975	997	18	2096	2121	18	4661	4740
	1027	26.77		2084	54.03		4663	123.81
	990	2.68%		2183	2.55%		4677	2.61%
	141			238			751	
19	857	856	19	1830	1883	19	4045	3989
	895	39.01		1946	58.56		3841	129.79
	817	4.56%		1874	3.11%		4082	3.25%
	98			162			464	
20	784	758	20	1704	1721	20	3592	3526
	785	47.06		1707	27.47		3455	68.60
	786	6.21%		1753	1.60%		3530	1.95%
	91			166			388	
21	674	668	21	1550	1556	21	3162	3138
	643	22.19		1562	6.04		3144	27.50
	686	3.32%		1555	0.39%		3108	0.86%
	59			223			265	
22	585	609	22	1365	1333	22	2820	2873
	614	21.93		1256	67.00		2860	61.10
	628	3.60%		1378	5.03%		2940	2.13%
	56			121			171	
23	564	553	23	1197	1212	23	2720	2702
	522	27.60		1251	34.43		2676	23.25
	574	4.99%		1187	2.84%		2711	0.86%
	48			54			239	
24	498	505	24	1173	1157	24	2505	2464
	512	7.00		1162	18.45		2471	46.44
	505	1.39%		1137	1.59%		2414	1.88%
	54			101			225	
25	423	451	25	1055	1056	25	2314	2239
	454	30.81		1071	14.53		2172	71.34
	446	6.83%		1042	1.38%		2231	3.19%
	29			74			190	
26	391	422	26	956	982	26	2038	2049
	457	33.18		989	22.90		2070	17.93
	418	7.86%		1000	2.33%		2040	0.88%
	24			118			175	
27	384	398	27	867	864	27	1873	1875
	412	14.02		884	22.19		1853	22.55
	399	3.52%		840	2.57%		1898	1.20%
	42			79			70	

Table 61(cont)

28	359	356	28	753	785	28	1804	1805
	348	7.38		839	47.27		1852	46.51
	362	2.07%		762	6.02%		1759	2.58%
	4			28			199	
29	355	352	29	757	756	29	1602	1606
	354	4.36		761	5.05		1600	9.30
	347	1.24%		751	0.67%		1617	0.58%
	25			38			-25	
30	308	327	30	717	718	30	1667	1631
	322	22.48		773	54.51		1602	33.06
	352	6.88%		664	7.59%		1624	2.03%
	37			56			143	
31	281	290	31	675	662	31	1501	1488
	306	13.66		635	23.10		1464	20.55
	284	4.71%		675	3.49%		1498	1.38%
	12			52			111	
32	268	279	32	620	610	32	1462	1377
	298	16.78		635	31.22		1292	85.00
	270	6.01%		575	5.12%		1376	6.17%
	-52			38			121	
33	251	330	33	565	572	33	1296	1256
	360	69.43		526	49.34		1276	53.48
	380	21.04%		624	8.63%		1195	4.26%

Table 62 CENTROID LOCATION SHIFT AS A FUNCTION OF ATTENUATION SETTING (X-AXIS)

CENTROID LOCATION (CHANNEL)			
=== INTERPOLATED ===		====== GIVEN ======	
X	Y	X	Y
0.50	17.9521	0.50	18.0388
0.51	17.7390		
0.52	17.5311		
0.53	17.3281		
0.54	17.1300		
0.55	16.9366		
0.56	16.7479		
0.57	16.5635		
0.58	16.3836		
0.59	16.2079		
0.60	16.0363		
0.61	15.8686		
0.62	15.7048		
0.63	15.5448		
0.64	15.3884		
0.65	15.2354		
0.66	15.0859		
0.67	14.9395		
0.68	14.7963		
0.69	14.6561		
0.70	14.5187		
0.71	14.3841	0.71	14.4781
0.72	14.2304		
0.73	14.0880		
0.74	13.9478		
0.75	13.8100		
0.76	13.6746		
0.77	13.5416		
0.78	13.4108		
0.79	13.2825		
0.80	13.1565		
0.81	13.0328		
0.82	12.9115		
0.83	12.7925		
0.84	12.6759		
0.85	12.5617		
0.86	12.4498		
0.87	12.3402		
0.88	12.2330		
0.89	12.1282		
0.90	12.0257		
0.91	11.9255		
0.92	11.8277		
0.93	11.7323		
0.94	11.6392		
0.95	11.5485		
0.96	11.4601		
0.97	11.3740		
0.98	11.2904		
0.99	11.2090		
1.00	11.1300	1.00	11.1614

Figure 36 CENTROID LOCATION SHIFT AS A FUNCTION OF ATTENUATION SETTING (X-AXIS)

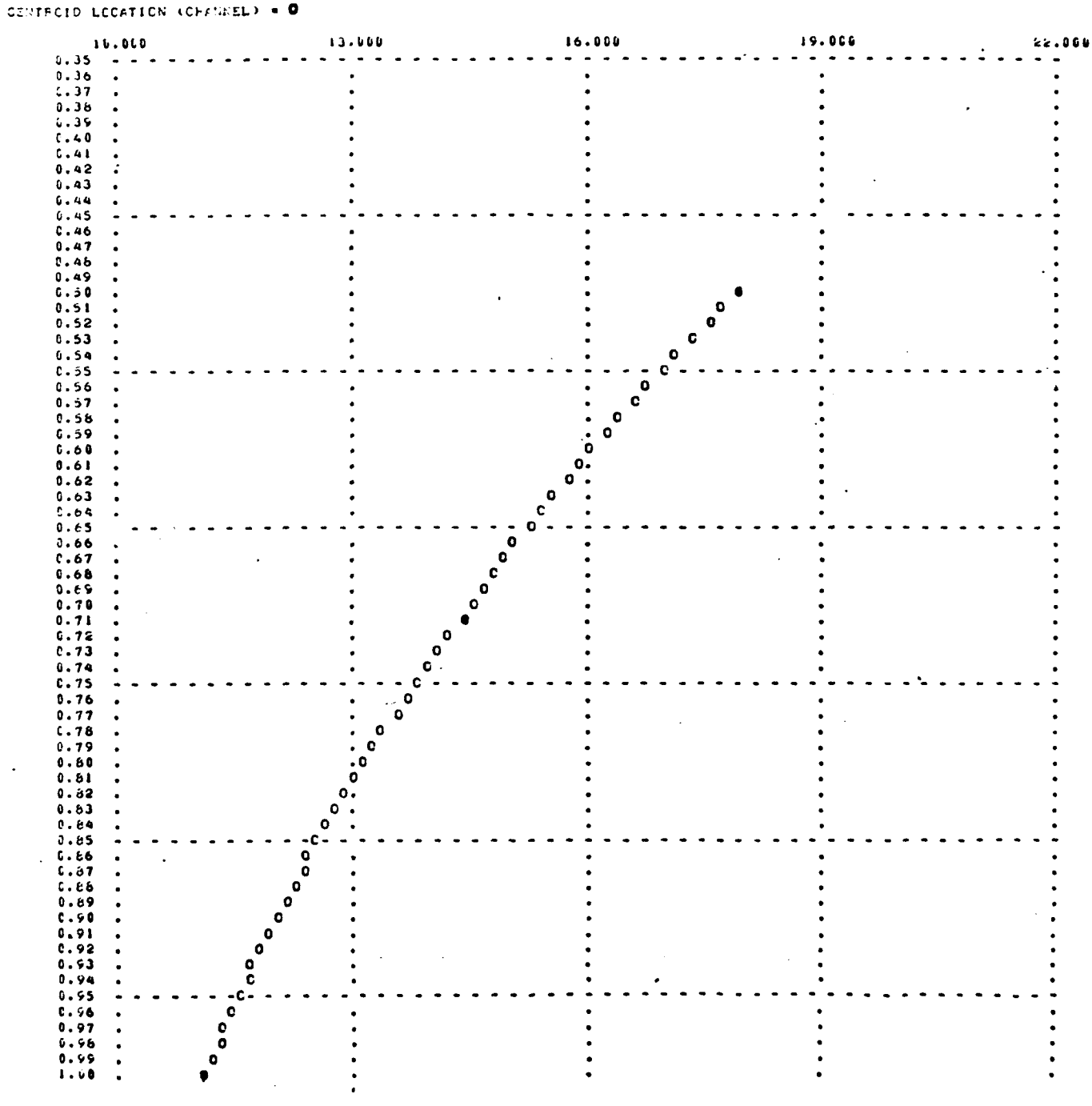

CHANNEL RESOLUTION FOR COULTER COUNTER MODEL F

By using a computer program, the attenuation for a given series of apertures, thresholds, and volumes was calculated by the following equation:

$$B = (V) \quad (I) \; / \; (K) \; (T)$$

where B is the attenuation, V is the volume of displacement, I is the aperture current, K is a constant equal to 5.3949×10^{-4} when a 70 um aperture tube is used, and T is the channel interval or threshold setting.

Table 63 indicates the resolution attained by all combinations of aperture and attenuation settings. From the table, the resolution in each channel may therefore be determined, and in effect, the sensitivity of each process (single channel shift, multiple channel shift, or centroid analysis) may be regulated to suit the requirements of the detection instrument operator. For example, at aperture 8 and attenuation 1, each channel can resolve 0.722 um^3. Therefore, the 2.02 um polyvinyltoluene particle (volume = 4.315931 um^3) would be detected in channel 5.977744. This agrees with experimental values which indicate that channel 6 contains single latex particles. The discrepancy may be due, in part, to instrument limits which prohibit any greater selectivity channel than 0.1. At aperture 16 and attenuation 1, each channel can resolve 1.444 um^3. A particle of 4.315931 um^3 volume would then be detected in channel 2.988872. This also agrees with the experimental value of channel 3.

Determining the resolution in each channel allows the operator to increase or decrease the sensitivity of the process which he is using. It also permits expansion of the processes beyond the latex-adsorbent complex. Wide application of single channel shift, multiple channel shift, or centroid analysis in the detection of enlarged tissue culture cells; bacteria adsorbing latex; particle kinetics; immunological testing and diagnostics; land, air, and water pollution detection, etc. are conceivable possibilities which must not be ignored.

Table 63 Resolution (μ^3/channel) at All Aperture and Attenuation Combinations

Attenuation	Aperture 1	2	4	8	16	32	64	128	256	512
0.125	0.0112	0.0225	0.0448	0.0896	0.1792	0.359	0.718	1.436	2.872	5.777
0.177	0.0159	0.0319	0.0638	0.1273	0.254	0.509	1.018	2.036	4.072	8.144
0.250	0.0225	0.0448	0.0897	0.1795	0.3590	0.7184	1.436	2.873	5.777	11.55
0.354	0.0317	0.0638	0.1273	0.2545	0.5090	1.0180	2.036	4.072	8.144	16.28
0.500	0.0449	0.0899	0.180	0.360	0.720	1.444	2.888	5.777	11.55	23.10
0.707	0.0635	0.1273	0.2545	0.500	1.0180	2.036	4.072	8.144	16.288	32.56
1.0	0.0909	0.1803	0.360	0.722	1.444	2.888	5.777	11.55	23.10	46.36
2.0	0.1818	0.3600	0.7200	1.444	2.888	5.777	11.55	23.10	46.20	92.40
4.0	0.360	0.820	1.4545	2.8750	5.777	11.55	23.10	46.25	92.92	185.00
8.0	0.720	1.444	2.888	5.777	11.55	23.10	46.00	92.00	184.00	368.10

COULTER COUNTER PARTICLE HISTORY

It would be of interest to know the origin of the particles counted in a specified channel. For example, what percentage of the count measured in channel 12 was the result of 2 particles from channel 6 combining; what percentage is the result of a channel 4 particle and a channel 8 particle combining? Since there are about 100 channels that can be utilized on the Coulter Counter, the number of combinations in any of the higher-numbered channels is monumental. The problem can be reduced somewhat by limiting the number of channels to be considered to the first 30. Little activity takes place above the 30th channel, so this simplification is justified. But there are still a staggering number of combinations to consider.

Let:

i = channel number
C_i = control count (before addition of virus) in channel i
C_i' = experimental count (after addition of virus) in channel i
E_i = number particles that entered channel i
L_i = number particles that left channel i

Then the basic relationship that holds is:

$$C_i' - C_i = E_i - L_i.$$

In other words, the net change equals the net change.

Since the different sizes of particles are homogenously mixed in solution, it is apparent that they should all have an equal chance to interact with each other. It will further be assumed that once particles combine, they can not dissociate again, that the process is irreversible.

Suppose, for simplicity, that only the first four channels 1, 2, 3, 4, are being considered. Expanding the basic relationship for each channel:

$$C'_1 - C_1 = -(2f_{1,1}E_2 + f_{1,2}E_3 + f_{1,3}E_4)$$

$$C'_2 - C_2 = f_{1,1}L_1 - (f_{2,1}E_3 + f_{2,2}E_4)$$

$$C'_3 - C_3 = \tfrac{1}{2}f_{1,2}L_1 + \tfrac{1}{2}f_{2,1}L_2 - (f_{3,1}E_4)$$

$$C'_4 - C_4 = \tfrac{1}{2}f_{1,3}L_1 + f_{2,2}L_2 + \tfrac{1}{2}f_{3,1}L_3$$

Where $f_{i,j}$ = the fraction of channel i particles combining with j particles. Note that $f_{i,j} \neq f_{j,i}$.

In channel one, the number of particles entering that channel, E must equal zero, since there are no lower channels to contribute to this one. $L_1 = 2f_{1,1}E_2 + f_{1,2}E_3 + f_{1,3}E_4$, in terms of E. Each term can be described as "the subset of particles leaving channel i is the fraction of particles entering channel $i+j$ due to particles in channels i and j combining". The "2" in the first term is to balance the equation, since two particles from channel one had to combine to form one particle entering channel two. In each of the other terms, only

one particle from channel one is required to form a particle in the entering channel, so no balancing is needed. Simular explanations can be given for each of the terms in the remaining equations. In channel 3, the ½'s in front of the E terms ($\frac{1}{2}f_{1,2}L_1 + \frac{1}{2}f_{2,1}L_2$) are needed to also balance the equations. Only one-half of the particles leaving channel i come from channels i and j combining; the other half is leaving from channel j due to j and i particles combining.

Now, in order to solve this system of equations, we must either express E in terms of L or vice versa. In the example, substitution would be reasonable, since we know

$$E = 0$$

$$E = f_{1,1}L_1$$

$$E = \tfrac{1}{2}f_{1,2}L_1 + \tfrac{1}{2}f_{2,1}L_2$$

$$E = \tfrac{1}{2}f_{1,3}L_1 + f_{2,2}L_2 + \tfrac{1}{2}f_{3,1}L_3$$

and everything could be expressed in terms of L. But for larger systems, such as n=24, substitution becomes impractical. Matrix manipulation is the method needed.

Using matrix notation, the equations can be rewritten:

$$A\text{-}L - B\text{-}E = C''$$

where A_{nxn} is the matrix of L_{nx1} co-efficients (subscripts demoting matrix size), B_{nxn} is the matrix of E_{nx1} co-efficients, and $C''_{nx1} = C'_{nx1} - C_{nx1}$.

From the basic relationship:

$$C'' = E\text{-}L \text{ or } L = E - C''$$

Substituting:

$$A\cdot(E\text{-}C'') - B\cdot E = C''$$

Solving for E:

$$E = (A\text{-}B)\text{-}1\ (A+I)\ C''$$

Where I is the identity matrix. These manipulations may now be easily performed on a computer.

The only perplexing problem left is how to assign values to the assumed fractions. There is no way to determine experimentally the fraction of particles that will leave or enter a particular channel, so theoretical values must be assumed. One of the first assumptions made was that little or no activity takes place in the higher channels. If it is assumed that no activity takes place

outside of the range being considered, then the fraction data may be extracted from the equations. All the fractions of particles leaving channel 1 must add up to 1; likewise, all the fractions of particles entering the other channels from channel 1 must add up to one. It happens that the fractions involved in both cases are the same (as it should be). Thus, in the example:

$$f_{1,1} + f_{1,2} + f_{1,3} = 1$$

$$f_{2,1} + f_{2,2} = 1$$

$$f_{3,1} = 1$$

If equal probability is assigned to each possible combination (for lack of a better assignment), then:

$$f_{1,1} = f_{1,2} = f_{1,3} = 1/3$$

$$f_{2,1} = f_{2,2} = 1/2$$

$$f_{3,1} = 1$$

In general:

$$f_{i,j} = \frac{1}{n-i}$$

where n is the total number of channels being considered.

Thus numerical values are now assigned to the matrices, and therefore can be solved for E. One E is known, L is also known from the relationship L = E + C".

Experimentally, the results have not been tested enough to validate this treatment. In fact, preliminary trials have tended to show some serious defects. But this is a good basis on which to develop refinements, and, perhaps, completely new theory.

CODE SHEET FOR REPORTS

(7-1-73 - 9-30-74)	(Cumulative Status Report No. A001AK, Office of Naval Research Contract N00014-73-C-0084, Task No. NR 136-952, July 1, 1973 - September 30, 1974)
(7-1-72 - 9-30-73)	(Annual Technical Report No. 1 Office of Naval Research Contract N00014-73-C-0084, Task No. NR 136-952, July 1, 1972 - September 30, 1973)
(9-1-67 - 6-30-73)	(Final Technical Report, Naval Weapons Laboratory Contract N00178-70-C-0160, September 1, 1967 - June 30, 1973)
(2-1-70 - 1-31-71)	(Annual Technical Report Naval Weapons Laboratory Contract N00178-70-C-0160, February 1, 1970 - January 31, 1971)
(2-1-71 - 1-31-72)	(Annual Technical Report, Naval Weapons Laboratory Contract N00178-70-C-0160, February 1, 1971 - January 31, 1972)
(2-1-72 - 6-30-72)	(Annual Technical Report, Naval Weapons Laboratory Contract N00178-70-C-0160, February 1, 1972 - June 30, 1972)

OFFICE OF NAVAL RESEARCH
BIOLOGICAL & MEDICAL SCIENCES DIVISION
MICROBIOLOGY PROGRAM, Code 443
DISTRIBUTION LIST FOR TECHNICAL, ANNUAL AND FINAL REPORTS

Number of Copies

(12) Administrator, Defense Documentation Center
Cameron Station
Alexandria, Virginia 22314

(6) Director, Naval Research Laboratory
Attention: Technical Information Division
Code 2027
Washington, D. C. 20390

(6) Director, Naval Research Laboratory
Attention: Library Code 2029 (ONRL)
Washington, D. C. 20390

(3) Office of Naval Research
Department of the Navy
Microbiology Program Director (Code 443)
Arlington, Virginia 22217

(2) Director, Research Division (Code 71)
Bureau of Medicine and Surgery
Department of the Navy
Washington, D. C. 20390

(2) Technical Reference Library
Naval Medical Research Institute
National Naval Medical Center
Bethesda, Maryland 20014

(1) Office of Naval Research Branch Office
495 Summer Street
Boston, Massachusetts 02100

(1) Office of Naval Research Branch Office
536 South Clark Street
Chicago, Illinois 60605

(1) Office of Naval Research Branch Office
1030 East Green Street
Pasadena, California 91101

(1) Office of Naval Research
Contract Administrator - Southeastern Area
2110 G Street, NW
Washington, D. C. 20007

Number of Copies

(1) Commanding Officer
U. S. Naval Medical Research Unit No. 2
Box 14
APO San Francisco 96263

(1) Commanding Officer
U. S. Naval Medical Research Unit No. 3
FPO New York 09527

(1) Officer in Charge
U. S. Naval Medical Research Unit No. 4
U. S. Naval Hospital
Great Lakes, Illinois 60088

(1) Officer in Charge
Submarine Medical Research Laboratory
U. S. Naval Submarine Base, New London
Groton, Connecticut 06342

(1) Scientific Library
U. S. Naval Medical Field Research Laboratory
Camp Lejeune, North Caroline 28542

(1) Scientific Library
Naval Biomedical Research Laboratory
Naval Supply Center
Oakland, California 94625

(1) Scientific Library
Naval Aerospace Medical Research Institute
Naval Aerospace Medical Center
Pensacola, Florida 32512

(1) Commanding Officer
U. S. Naval Air Development Center
Attn: Aerospace Medical Research Department
Johnsville, Warminster, Pennsylvania 18974

(1) Commanding Officer
U. S. Naval Unit
Fort Detrick
Frederick, Maryland 21701

(1) Commanding General
U. S. Army Medical Research & Development Command
Forrestal Building
Washington, D. C. 20314
ATTN: MEDDH-SR

Number of Copies

(1) Life Sciences Division
Army Research Office
3045 Columbia Pike
Arlington, Virginia 22204

(1) Life Sciences Division
Air Force Office of Scientific Research
1400 Wilson Boulevard
Arlington, Virginia 22207

(1) STIC-22
4301 Suitland Road
Washington, D. C. 20390

(1) Director
Walter Reed Army Institute of Research
Walter Reed Army Medical Center
Washington, D. C. 20012